THE MOLECULAR GENETICS OF HUMAN RENAL TRACT MALFORMATIONS

Thesis submitted by

Sally Anne Feather

For the degree of Doctor of Philosophy
at The University of London

September 1999
Molecular Genetics Unit
Institute of Child Health
30 Guilford Street
London WC1N 1EH.

This thesis is dedicated with love and gratitude to my parents and Mark.

ABSTRACT

This thesis describes work in two contrasting renal tract malformations: the oral-facial-digital syndrome type 1 (OFD1) and primary vesicoureteric reflux (VUR).

I mapped OFD1 to an 18cM interval on the short arm of the X chromosome between the telomeric marker *DXS996* and the centromeric marker *DXS7105,* using samples from two pedigrees with five affected females with OFD1, with a lod score of 3.32 at an intragenic polymorphic marker at *KAL.* Microsatellite marker analysis of three additional pedigrees with OFD1 did not narrow the region further. I examined the expression of candidate genes KAL, APXL, FXY and calbindin in human fetal tissue using reverse transcription. I performed mutation screening by SSCP on the candidate genes *KAL, APXL, CLC4, FXY, ARHGAP6, GRPR, SCML1, RAIR2* and *STK9* and excluded them as candidates for OFD1. I performed histological studies on renal tissue from an affected female with OFD1 to characterise the origin of the renal cysts as glomerulocystic in the polycystic renal disease in OFD1.

I performed a collaborative genome wide scan in seven pedigrees with VUR and reflux nephropathy (RN) and analysed the results using GENEHUNTER parametric and non-parametric linkage (NPL) analysis. The analysis was performed separately for analysis V (individuals with VUR only), analysis R (individuals with RN only) and analysis T (individuals with either VUR or RN). The results revealed a major locus on chromosome one between the markers *D1S1613* and *D1S1653* with a maximum NPL score of 5.48 and a p value of 0.0002. The results suggested genetic heterogeneity with additional loci on chromosomes 3, 8 and 20. The candidate regions chromosomes 6p and 10q did not reach significance in this analysis but a region on the X chromosome reached significance with a NPL score of 0.58 and a p value of 0.04.

ACKNOWLEDGEMENTS

I wish to acknowledge the assistance of a large number of people in this thesis.

I would like to thank my collaborators. Collaborators in OFD1: Professor D Donnai for sharing samples in OFD1 pedigree two, Brunella Franco, TIGEM, Milan, Huda Zoghbi, Baylor Institute, Texas, USA, Alan Ashworth and Jo Perry, Institute of Cancer Research, London, UK and Dorothy Trump, Cambridge University UK for sharing information on candidate genes in the OFD1 region, Dr S Dodd, Royal London Hospital, London, UK for providing autopsy material from individual II.2 in pedigree one with OFD1, Dr D Kernohan, Belfast University, N. Ireland, UK for assisting me in my visit to collect samples from pedigree five. Collaborators in VUR: Koen Devriendt, Leuven University, Belgium for providing samples from VUR pedigrees six and seven, Judith Goodship, Tim Goodship and Paul Warwicker, Newcastle University, UK for sharing samples from VUR pedigree two and Joan Carter, Newcastle University, UK for performing half the genome wide analysis in VUR, Chris Reid, Guys Hospital, London, UK for providing me with details of pedigrees 3,4, and 5 so that I could collect samples from them and Kathryn Lewis, Guys Hospital, for advice on the interpretation of GENEHUNTER results.

I wish to thank a number of individuals at the Institute of Child Health and Great Ormond Street Hospital. In the Molecular Genetics Unit, Victoria Wright and Diana Blaydon who worked with me to perform half the genome wide analysis in VUR, and all other colleagues in the laboratory for molecular genetics and computing advice. In the Developmental Biology Unit, Paul Winyard for assistance with histological techniques, Veronique Duke for assistance with reverse transcription experiments and Jennifer Allison for assistance with ascertaining pedigrees with VUR. I wish to thank

all the consultants on the renal unit at Great Ormond Street Hospital for referring families to me with VUR and OFD1.

I particularly wish to thank all the families and individuals with VUR and OFD1 who gave me blood samples and clinical details so that this work would be possible.

I wish to thank Sue Malcom and Adrian Woolf who supervised this thesis and Robin Winter for invaluable advice at my thesis committee.

I am grateful to Action Research for providing me with a research training fellowship, the National Kidney Research fund for financing the VUR project with consummables and a research assistant's salary. I thank the Kidney Research Aid Fund for financing some consummables.

Chapter One INTRODUCTION

1.1. Overview

It has been estimated that 5% of the population have renal tract (i.e. kidneys, ureter and bladder) malformations but the majority are of little clinical significance (Woolf and Winyard, 1998). At the severe end of the spectrum, malformations of the renal tract account for up to 40% of children in end stage renal failure (Ehrich et al, 1992; McEnery et al, 1992). Renal tract malformations encompass a wide spectrum of disorders including renal dysplasia (undifferentiated kidneys), renal hypoplasia (small kidneys), renal agenesis (absent kidneys), duplications of the kidney and ureters, vesicoureteric reflux (VUR) (the retrograde passage of urine from the bladder to the ureter and sometimes the kidney) and obstruction at various sites including the pelvi-ureteric junction (PUJ obstruction) and the urethra (posterior urethral valves) (Woolf and Winyard, 1998). Malformations can occur throughout the renal tract and constitute defects in early organogenesis. However, in this thesis I also include work on polycystic kidney disease, a disorder of terminal differentiation of the renal epithelia. Overall, the aetiology of renal tract malformations is postulated to be multifactorial including genetic factors, teratogens and obstruction. Progress has been made towards understanding the pathogenesis of some renal tract malformations but much remains to be discovered.

This thesis describes a molecular genetics approach to investigating the aetiology of two contrasting disorders of developmental differentiation of the human renal tract. The first is the oral-facial-digital syndrome type 1 (OFD1), a rare disorder in which characteristic malformations of the face, oral cavity and digits occur in

association with polycystic renal disease. The second disorder is primary, non-syndromic vesicoureteric reflux (VUR), a very common disorder in which the mode of inheritance is complex. My hypotheses, which I set out to prove in this thesis, are:

1. OFD1 is an X-linked dominant disorder;

2. Genes play a major role in the pathogenesis of VUR and it will be possible to define susceptibility loci genome-wide.

1.2. The anatomy of development of the human renal tract

A description of the normal development of the renal tract will lead to an appreciation of the anatomical locations where malformations arise and hence their pathogenesis. The human renal tract is derived from intermediate mesoderm on the dorsal body wall and develops sequentially through three stages in fetal life in a cranial to caudal progression: the pronephros, the mesonephros and the metanephros (Larsen, 1993). The pronephros and mesonephros degenerate during human fetal development and it is the metanephros which becomes the post-natal kidney.

1.2.1.The pronephros

The pronephric duct, which is the most cranial portion of the nephrogenic cord, can first be visualised on day 22 of gestation just ventral to the seventh and 14th anterior somites and develops from intermediate mesoderm (Gilbert, 1994). The cells of the pronephric duct migrate caudally. Anteriorly, the pronephric duct induces the adjacent mesenchyme to undergo mesenchymal to epithelial transformation to form the pronephric kidney tubules which open proximally to

the coelomic cavity by nephrostomes and coalesce distally to join the pronephric duct which grows caudally towards the cloaca. The pronephric tubules are not considered to contribute to excretion in mammals. In mammals, the pronephric tubules and the anterior portion of the pronephric duct degenerate by day 24 of gestation but the more caudal parts of the pronephric duct persist as the Wolffian or mesonephric duct (Saxen, 1987).

1.2.2. The mesonephros

The mesonephros includes the mesonephric duct and adjacent mesonephric tubules. The mesonephros develops from the dorsolumbar segments of the nephrogenic cord below the pronephros to form the urogenital ridge. As the pronephric tubules disappear, the mesonephric duct initiates the development of approximately 30 new kidney tubules in the adjacent mesenchyme which appear at day 25. The mesonephric duct is initially a solid column of cells in which a lumen appears in a caudocranial direction after fusion with the cloaca at approximately 4 weeks gestation. Approximately 40 mesonephric tubules are produced. The cranial tubules regress as the caudal tubules are forming so there are never more than 30 pairs at any time (Larsen, 1993). A mesonephric tubule consists of a glomerulus and a more lateral tubule with thicker walled proximal and thinner walled distal segments which connects to the mesonephric duct. These nephrons transiently produce relatively small quantities of urine between weeks 6-10 of gestation (Moore, 1988) which drain via the mesonephric duct.

The glomeruli of the mesonephros involute completely by 16 weeks of gestation. However, other mesonephric structures persist. In males some of the mesonephric tubules persist as the vas deferens and efferent ducts of the testes (Moore 1988)

and the mesonephric duct forms the duct of the epididymis, the seminal vesicle and the ejaculatory duct. In the female, only a few vestigial structures persist to form the epoophorn, the paraoophoron and Gartner's duct and otherwise the whole mesonephros degenerates.

1.2.3. The metanephros

Formation of the human metanephros commences at day 28 after fertilisation when the ureteric bud sprouts from the distal part of the mesonephric duct (Figure 1.1.) opposite the 28th somite where it curves medially to form the cloaca (Larsen, 1993).

The proximal end of the ureteric bud, the ampulla, penetrates the metanephric blastema which then begins to condense around the tip. The first glomeruli can be detected at 9 weeks of gestation in humans and nephrogenesis is complete by weeks 34-36 of gestation. Subsequently, further growth of the kidney continues by lengthening of the proximal tubules, loops of Henle and collecting ducts.

The metanephros is the precursor of the human adult kidney. It consists of two main cell types: epithelial cells of the ureteric bud and the mesenchymal cells of the metanephric mesenchyme (Figure 1.2.). These two tissues send chemical messages to each other during development to induce the growth of the other and it has been shown in organ culture (Grobstein, 1953a and b) that if the signals sent by one tissue are absent the other tissue fails to develop normally. The ureteric bud undergoes serial branching to form the ureter, renal pelvis and collecting ducts and the mesenchyme undergoes an epithelial conversion to form the proximal nephrons from the glomerulus to the distal tubule.

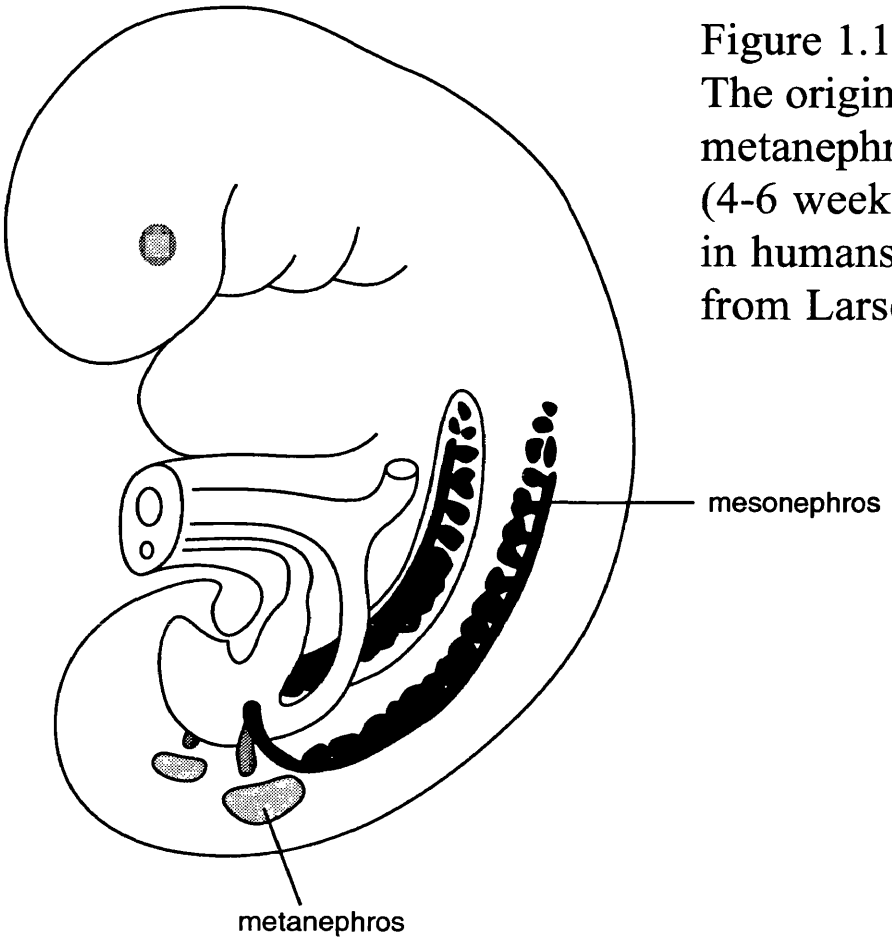

Figure 1.1
The origin of the metanephric kidney (4-6 weeks gestation in humans) (adapted from Larsen, 1993)

Figure 1.2
Cell lineages in the metanephros (adapted from Hardman et al, 1994)

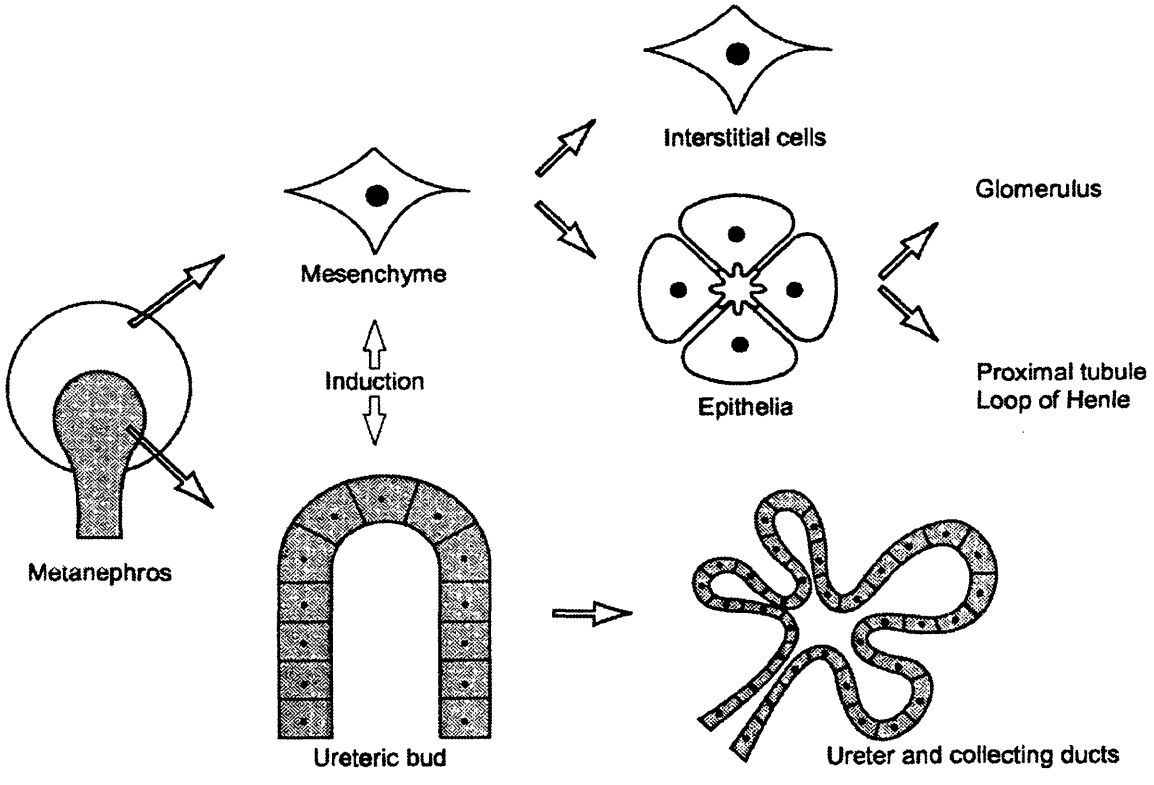

1.2.3.1. Differentiation of the mesenchyme and derivatives

The mesenchyme is initially loosely arranged around the penetrating ureteric bud. The first step is for the mesenchyme to condense around the tip of the ureteric bud. The condensed mesenchymal cells undergo a mesenchymal to epithelial conversion to become the renal vesicle. The renal vesicle elongates to form a comma shape which folds back on itself to form an S-shaped body. The tubule continues to elongate and differentiate giving rise to the proximal convoluted tubule, the descending and ascending limbs of the loop of Henle and the distal convoluted tubule. The distal convoluted tubule fuses with the collecting duct of the ureteric bud to form a continuous functioning unit.

1.2.3.2. Glomerulus

The proximal end of the S-shaped body invaginates into a cup shape and forms Bowman's capsule which encases a tuft of capillaries to form the glomerulus. The glomerulus produces an ultrafiltrate because of the hydrostatic pressure generated in its capillaries by afferent and efferent arterioles. This ultrafiltrate is modified and reabsorbed by down-stream segments of the nephron. Four main types of cells are found in the fully developed glomerulus: podocytes (visceral epithelia), parietal epithelia, mesangial cells and endothelial cells. Podocytes have foot processes which are in intimate contact with the glomerular basement membrane and are essential for protein size restriction during the ultrafiltration of urine. The parietal epithelia forms Bowman's capsule. Mesangial cells are embedded in extracellular matrix and have multiple roles including physical support for glomerular capillary loops and modualtion of both matrix production and degradation. It is in the glomerulus that the majority of cysts in OFD1 are located

(Bernstein, 1993).

1.2.3.3. Proximal convoluted tubule

The proximal tubule derives from the mid-portion of the S-shaped body and is a direct continuum of the parietal epithelium of Bowman's capsule. The main role of the proximal tubular cells is to reabsorb minerals, ions, water and organic solutes such as glucose and amino acids. Approximately two thirds of the ultrafiltrate of the glomerulus is reabsorbed here. The epithelial cells of the proximal convoluted tubule have a well developed brush border to increase their surface area for reabsorption and numerous mitochondria and lysosomes that reflect their high metabolic rate.

1.2.3.4. Loop of Henle

The loop of Henle consists of three parts: the distal straight portion of the proximal tubule, the thin descending limb and the thick ascending limb. The thick and thin limbs of the Loop of Henle form a loop that descends deep into the medulla and generate the osmotic gradient which permits the reabsorption of water by the collecting ducts. Maturation of the loops occurs post-natally.

1.2.3.5. Distal tubule

This comprises the thick ascending loop of Henle and the distal convoluted tubule. The thick ascending loop actively transports ions. The macula densa lies adjacent to the glomerulus and monitors sodium delivered to the distal tubule and modifies the secretion of renin from the juxtaglomerular apparatus accordingly.

1.2.3.6. Connecting tubule

The connecting duct is a short segment that attaches the mesenchymally derived distal tubule to the ureteric bud derived collecting duct and was originally thought to be mesenchymal in origin. The connecting duct is now thought to be derived from the ureteric bud (Howie et al, 1993).

1.2.3.7. Differentiation of the ureteric bud and derivatives

As the ureteric bud grows into the metanephric blastema, the ampulla begins to divide. The process of growth and branching continues during nephrogenesis, mainly in the outer or nephrogenic cortex which lead to an arborised collecting duct system connected to nephrons which have formed in parallel from mesenchyme. At first, a single nephron is associated with a single ureteric bud branch, which will form its collecting duct. Subsequently, arcades of nephrons are formed resulting in up to seven nephrons being attached to a single collecting duct. New nephrons are attached to the proximal part of the ampulla, whilst older nephrons shift their attachment to the connecting piece of the new nephron (Potter, 1972). Approximately twenty generations of branching have occurred to form the one million nephrons present in each human kidney (Ekblom, 1994).

1.2.3.8. Renal pelvis and collecting ducts

The collecting ducts of the adult kidney drain a variable number of calyces which together compromise the renal pelvis, and the renal pelvis drains into the ureter. The pelvis and major calyces are formed by the coalescence of the first three to six generations of branches of the ureteric bud at its point of entry in to the metanephric mesenchyme. The minor calyces form the subsequent generation of branches. Nephrons attached to these early ureteric bud branches transfer to a later

branch or degenerate (Potter, 1972)

1.2.3.9. Development of the bladder, ureter and vesicoureteric junction

Between 4 –6 weeks gestation the urorectal septum splits the cloaca (hind gut derivative) into the primitive urogenital sinus anteriorly and the rectum posteriorly (Figure 1.3.). The superior part of the primitive urogenital sinus, which is continuous with the allantois, forms the bladder. The constricted pelvic urethra at the base of the bladder forms the membranous urethra in females and the prostatic and membranous urethra in males (Larsen, 1993)

At the same time, the distal portions of the mesonephric ducts and attached ureteric ducts become incorporated into the posterior wall of the bladder (Figure 1.4.). The mouths of the mesonephric ducts flare into trumpet shaped structures that begin to expand, flatten and blend into the bladder wall. The superior portion of the trumpet shaped structures expand and flatten more rapidly than the inferior part. Therefore, the mouth of the narrow portion of the mesonephric duct appears to migrate inferiorly along the posterior bladder wall. This incorporates the distal ureters into the wall of the bladder and causes the mouths of the narrow part of the mesonephric ducts to migrate inferiorly until they open into the pelvic urethra just below the neck of the bladder. The bladder trigone is the triangular area of exstrophied mesonephric duct wall on the inferior wall of the bladder. The mesodermal tissue of the trigone is later overgrown by the endoderm to form the bladder wall (Larsen, 1993).

Figure 1.3
Development of the primitive urogenital sinus (4-6 weeks gestation in humans) (adapted from Larssen 1993)

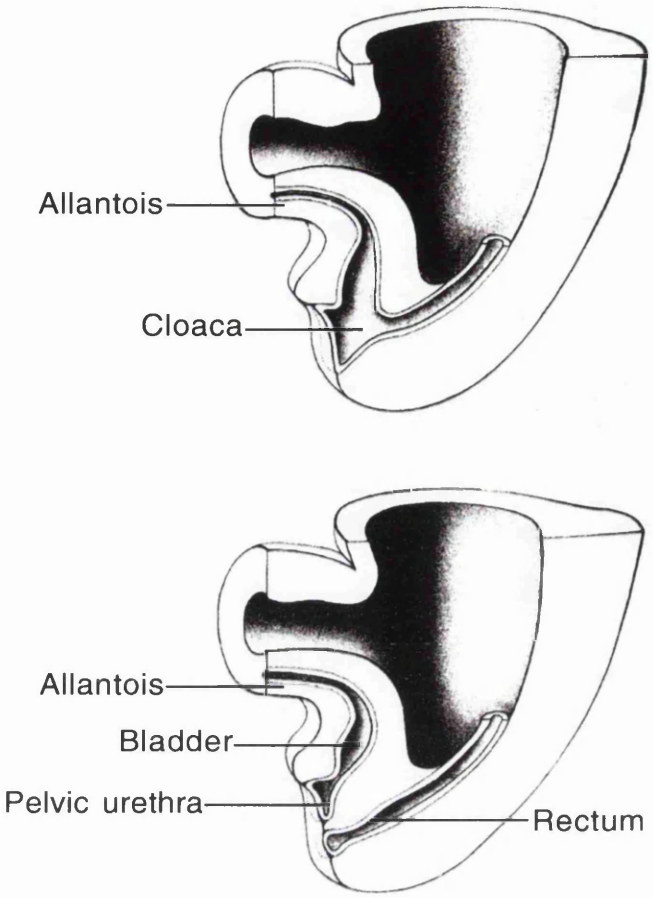

Figure 1.4
Exstrophy of the mesonephric ducts and ureters into the posterior wall of the bladder (4-6 weeks gestation in humans) (adapted from Larssen 1993)

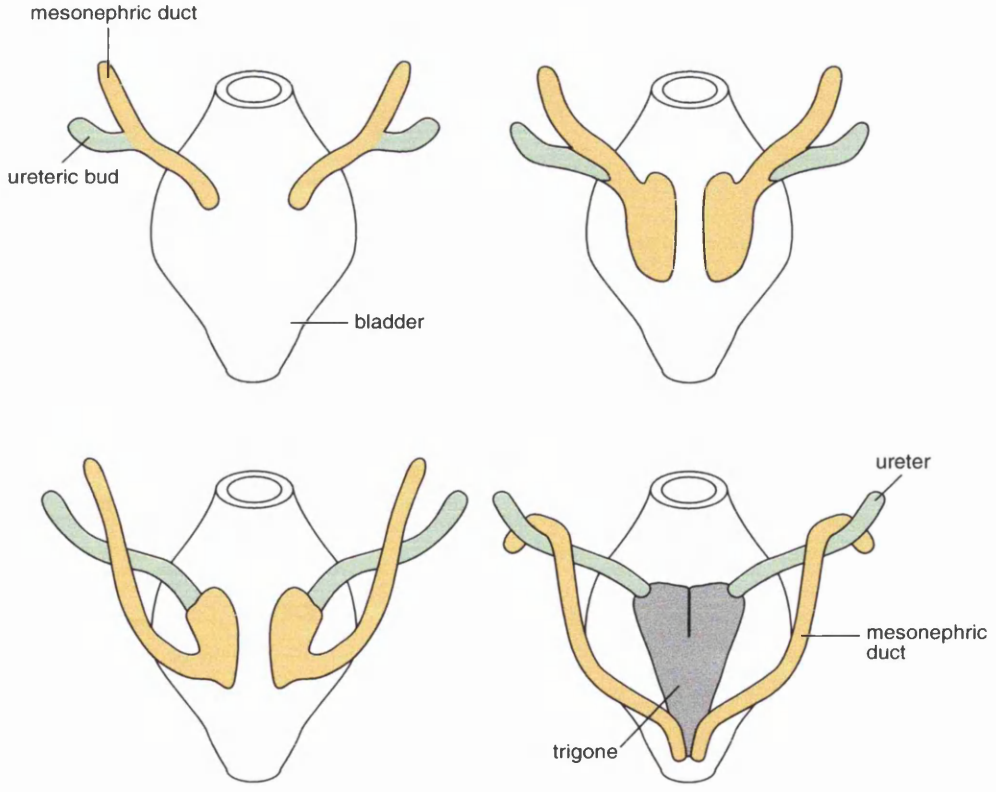

Figure 1.5
The vesicoureteric junction

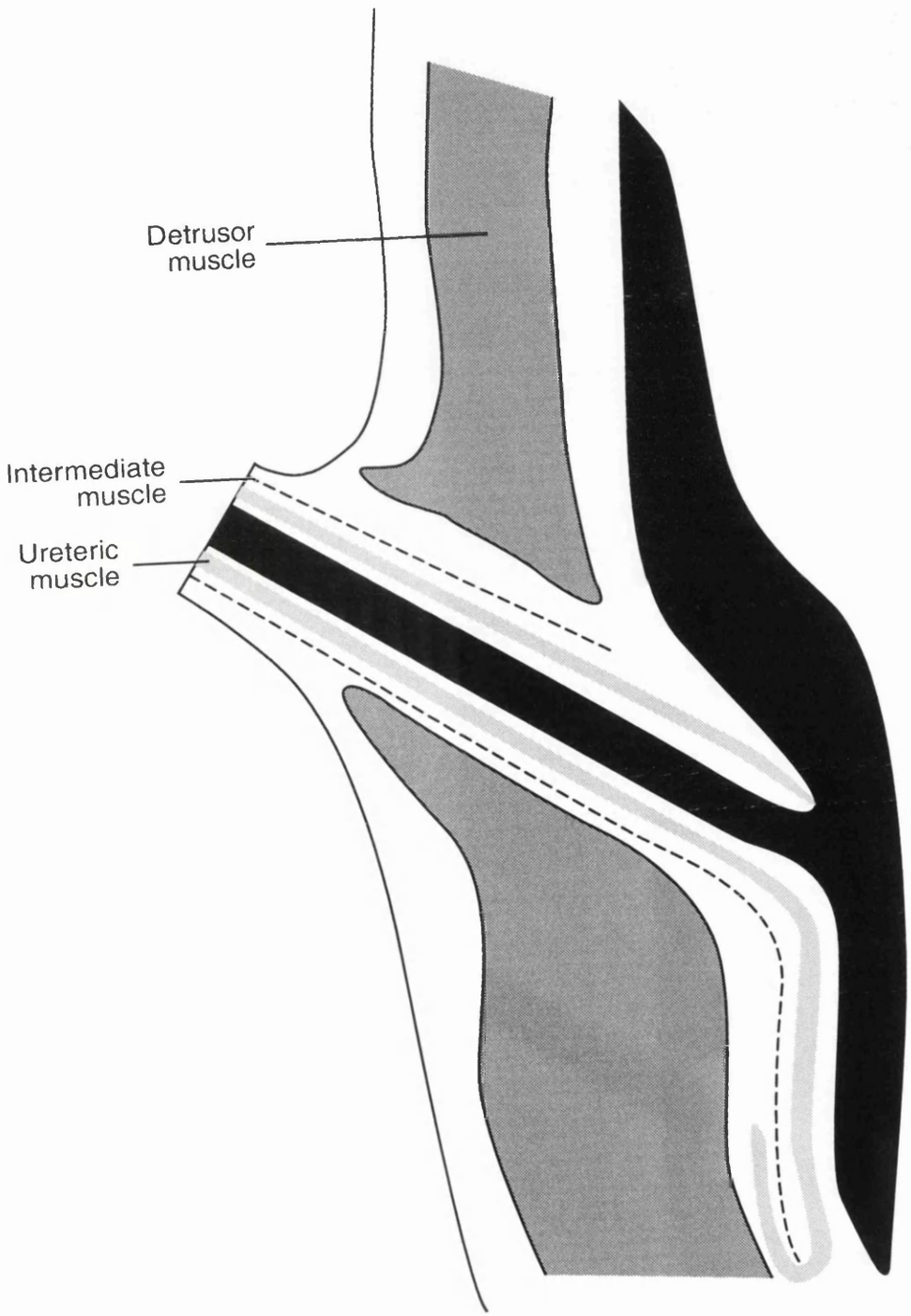

1.2.3.10. The anatomy of the vesicoureteric junction

The vesico-ureteric junction (VUJ) is the site where the ureter meets the bladder (Figure 1.5.) and within the VUJ the ureter traverses the bladder and there are three layers of muscle in the VUJ: ureteric, intermediate and detrusor muscle (Waldeyer et al, 1882).

The integrity of the VUJ is established during human fetal life (Matsuno et al, 1984; Lyon et al, 1969). Normally, the VUJ is competent in preventing VUR, and this is considered to be due to its comparatively long intramural segment which passes obliquely through the bladder wall and is effectively compressed and sealed by contraction of the bladder during micturition (Sampson, 1903). This is in contrast to other animals such as the rabbit in which the intramural segment is short and readily permits VUR.

VUR, the second renal tract malformation to be discussed in this thesis, is caused by a defect in the competency of the VUJ.

1.3. Genes and the development of the renal tract.

1.3.1. Molecular mechanisms in normal renal tract development

The normal development of a complex system such as the renal tract is likely to require the co-ordinated activity of a large number of genes. The key processes involved in development of the renal tract include cell proliferation (Winyard et al, 1996a), apoptosis (Coles et al, 1993), differentiation, morphogenesis and migration. Published work describing the expression patterns of over 200 genes in the development of the renal tract have been summarised in a systematic manner and are available on the database: mbsig2.sbc.man.ac.uk/kidbase/kidhome.html. It

is to be anticipated that the expression and function of many more molecules will be documented in the future.

Genes that are important in the development of the renal tract can be placed in a number of categories.

1. Transcription factors are proteins that bind DNA and regulate the expression of other genes: i.e. they enhance or switch off the transcription of mRNA and examples include PAX2 (Torres et al, 1995), WT-1 (Kreidberg et al, 1993).

2. Growth factors produced by the metanephros bind to cell surface receptors either of the cell producing the growth factor (autocrine), adjacent (juxtacrine) or more distant cells. The largest group of cell surface receptors for growth factors are tyrosine kinases. When the ligand has bound the receptor tyrosine kinases dimerize, are autophosphorylated and transduce signals into the cell. Growth factors influence cell division, cell survival, apoptosis, differentiation and morphogenesis. Examples of growth factors include glial cell derived neurotrophic factor (GDNF) (ligand), RET (its receptor tyrosine kinase) and GDNFα (an accessory receptor) (Jing et al, 1996; Pachnis et al, 1993)

3. Adhesion molecules are of two types, molecules that mediate the attachment of cells to one another (cell-cell adhesion molecules) and cells that mediate the attachment of cells to the surrounding matrix (cell-matrix adhesion molecules). An example of an adhesion molecules is KAL, a protein mutated in Kallmann's syndrome (Legouis et al, 1993; Duke et al, 1995).

4. Cell survival factors influence proliferation and apoptosis and are proto-oncogenes. An example is BCL2 (LeBrun et al, 1993).

Disruption of these categories of genes have been shown to cause renal tract malformations in mice and men as will be discussed in the next two sections and

these categories of genes could be considered to be candidates for renal tract malformations.

1.3.2. Mouse mutants with renal tract malformation as a phenotype

There are numerous mouse mutants with a renal malformation due to mutations. Such mice can give clues to genes that may be important in human renal tract malformations. Table 1 shows examples of the renal phenotype in mice which are null mutants for important genes in the development of the renal tract. In some cases, there are different effects in homozygous and heterozygous mouse mutants. For example the majority of *GDNF* -/- mutants have a renal phenotype (renal agenesis) whereas only a minority of +/- mice have small or absent kidneys (Moore et al, 1996; Pichel et al, 1996). The *PAX2* null mutant mouse has renal agenesis and mullerian defects (absent fallopian tubes) whereas the heterozygotes have hypoplastic kidneys (Torres et al, 1995). There are two other heterozygote mouse models; the *Krd* mouse which has kidney and retinal defects and is caused by a transgenic insertion of mouse chromosome 19 which deletes part of the chromosome including *PAX2* (Keller et al, 1994) and a mouse with defects of the brain, ear, eye and kidney due to a mutation in *PAX2* identical to the mutation in a case of human renal-coloboma syndrome (Favor et al, 1996).

However, when some other genes thought to be important in renal development by experiments in vitro are disrupted in the mouse there is no renal phenotype e.g. null mutants of hepatocyte growth factor (*HGF)* (Schmidt et al, 1995; Uehara et al, 1995), *MET* (Bladt et al, 1995), *ROS* (Sonnenberg et al, 1996), transforming growth factor (*TGFβ-1*) (Shull et al, 1992; Letterio et al, 1994), *PAX8* (Mansouri et al, 1998). This would suggest there may be other genes that can rescue the lack

of a particular gene product in renal tract development in the mouse.

When a null mutant mouse for a particular gene is created in different mouse strains different renal phenotypes can occur. For example, null mutants for *BCL2* can have either hyperproliferation of epithelial elements in the kidney with consequent cystic dilatation of proximal and distal tubules (Veis et al, 1994) or a total arrest of renal development (Sorenson et al, 1995). The mice also develop cysts but in all segments of the tubules associated with a secondary upregulation of proliferation (Sorenson et al; 1996). Mice with homozygous null mutations of the *EGF* receptor have collecting duct dilatation and renal failure and the severity depends on the strain of mice suggesting the presence of modifying genes (Threadgill et al; 1995).

Table 1.1: Null mutant mice with renal malformations

Transcription factors

BF2 (small,fused and undifferentiated kidneys) (Hatini et al, 1996)

HOXa11/HOXd11 (small or absent kidneys) (Davis et al, 1995)

Lim1 (absent kidneys) (Shawlot et al, 1995)

N-MYC (poorly developed mesonephric kidneys) (Stanton et al, 1992)

PAX2 (small or absent kidneys) (Torres et al, 1995)

WT1 (absent kidneys) (Kreidberg et al, 1993)

Growth factors and receptors

EGF receptor (cystic collecting duct) (Threadgill et al, 1995)

BMP7 (undifferentiated kidneys) (Dudley et al, 1995)

RET (small or absent kidneys) (Schuchardt et al, 1994)

PDGF B chain (absent mesangial cells) (Leveen et al, 1994)

WNT4 (undifferentiated kidneys) (Stark et al, 1994)

Adhesion molecules and receptors

α3 integrin (decreased collecting duct branching) (Kreidberg et al, 1996)

α8 integrin (impaired ureteric bud branching and nephron formation) (Muller et al, 1997)

Other molecules

BCL2 (small kidneys) (Veis et al, 1994)

Formin (absent kidneys) (Mass et al, 1990)

COX2 (small kidneys) (Morham et al, 1995)

RAR αγ/αβ2 (small or absent kidneys) (Mendelsohn et al, 1994)

1.3.3. Mutations of genes that cause renal tract malformations in humans

1.3.3.1. Renal tract malformations as part of complex syndromes

Malformations of the renal tract can occur as part of complex syndromes with other features such as external malformations and some examples are shown in Table 1.2. As of 1998, there were 435 syndromes recorded which include renal malformations (Winter and Baraitser, 1998). There are specific malformations which occur as part of syndromes e.g. renal agenesis in Kallmann's syndrome (Duke et al, 1998). The oral-facial-digital syndrome type 1 described in this thesis is another example in which the specific disease is renal cysts. Sometimes a wide range of renal phenotypes occur as part of a syndrome e.g. Branchio-oto-renal syndrome (Melnick et al, 1976).

Table 1.2: Examples of genetic mutations that cause human renal tract malformation syndromes (modified from Woolf and Winyard, 1998)

Apert's syndrome (*FGFR2* mutation-growth factor receptor) (Wilkie et al, 1995) Hydronephrosis and duplicated renal pelvis (Cohen et al, 1993)

Branchio-oto-renal syndrome (*EYA1* mutation-transcription factor) (Abdelhak et al, 1997) Renal agenesis and dysplasia (Melnick et al,1976)

Campomelic dysplasia (*SOX9* mutation-transcription factor) (Wagner et al, 1994) Diverse renal tract malformations (Houston et al, 1983)

Denys Drash syndrome (*WT1* mutations-transcription factor) (Coppes et al, 1993) Calyceal defects (Jadresic et al, 1990)

Fanconi's anaemia (*FAA* mutation-DNA repair defect)(Lo Ten Fo et al, 1996) Renal agenesis, dysplasia and VUR

Kallmann's syndrome (*KAL* mutation-cell signalling molecule) (Franco et al, 1991) Renal agenesis (Duke et al, 1998)

Renal-coloboma syndrome (*PAX2* mutation-transcription factor) (Sanyanusin et al, 1995) Renal hypoplasia and VUR (Sanyanusin et al,1995)

Simpson-Golabi-Behmel syndrome (*GPC3* mutation-proteoglycan) (Pilia et al, 1996) Renal overgrowth and dysplasia (Hughes-Benzie et al, 1996)

1.3.3.2. Non-syndromic renal tract malformations

Not all renal tract malformations occur as part of complex syndromes. In 1974, Cain et al cited 12 reports of familial renal tract malformations and described a kindred with two siblings, the first with bilateral renal agenesis and the second with unilateral renal agenesis and contralateral dysplasia. Others have suggested a ten fold higher incidence of solitary kidney in first degree relatives of patients with bilateral agenesis compared with control subjects (Roodhoft et al, 1984). A further kindred has been described with non-syndromic renal dysplasia and aplasia in a single kindred in a probable autosomal dominant fashion (McPherson et al, 1987). Others have described kindreds with congenital single kidney with probable autosomal dominant inheritance (Murugasu et al, 1991, Arfeen et al, 1993). Primary non-syndromic VUR is a further example of an isolated renal tract malformation and is discussed in section 1.6. The genetic bases of most isolated renal tract malformations are as yet undefined. However, the genes *CDC5L* and *USF2* are disrupted by a translocation t(6;19)(p21;q13.1) in an individual with isolated multicystic renal dysplasia (Groenen et al, 1996; Groenen et al, 1998) and polymorphisms in the angiotensin type 2 (*AT2*) receptor gene are associated with isolated congenital anomalies of the kidney and urinary tract (Nishimura et al, 1999).

1.4. Non-genetic causes of renal tract malformations

Renal tract malformations can also be caused by non-genetic causes including obstruction and teratogens.

1.4.1. Teratogens and malformations of the renal tract

Many agents have been described as causing teratogenesis of the developing urinary tract (Brown et al, 1997). Teratogens implicated in renal tract malformations include vitamin A (Rothman et al, 1995), ethanol (Gage et al, 1991), glucose (Novak et al, 1994) and angiotensin converting enzyme inhibitors (Brown et al, 1997).

1.4.2. Obstruction of the urinary tract in development

Obstruction of the urinary tract at the level of the pelviureteric junction, the vesicoureteric junction, the ureter or the urethra is associated with renal tract malformations. If the obstruction occurs early in development the kidney is typically dysplastic; in later development there is typically hydronephrosis, subcortical cysts and reduced renal parenchymal growth (Potter, 1972; Bernstein et al, 1988; Thorner et al, 1995). If the urinary tract is obstructed experimentally increased apoptosis occurs as well as increased expression of BCL2, TGF-β, angiotensin II and EGF (Chevalier et al, 1996; Attar et al, 1998).

1.5. The oral-facial-digital syndrome type 1 (OFD1). OMIM 311200

1.5.1.Definition and classification

The oral-facial-digital syndrome was first defined in 1962 and was called orofaciodigital dysostosis (Gorlin, 1962). OFD1 is a complex disorder in which affected females have characteristic malformations of the face, oral cavity and digits in association with polycystic kidney disease. The condition is rare with an incidence of 1 in 250,000 and it occurs in diverse racial backgrounds (Salinas et

al, 1991). The facial features include facial asymmetry, frontal bossing, hypertelorism, broad nasal bridge, long philtrum which may be cleft, micrognathia and facial milia. Patchy alopecia also occurs. The oral cavity is affected with tongue tethering, oral frenulae and hamartomata which may be present in any part of the oral cavity or the upper respiratory tract and may be multiple. The teeth may be overcrowded; some teeth may be absent or extra teeth may be present. Digital features are present in 50-70% and include pre- and post-axial polydactyly, syndactyly, clinodactyly and brachydactyly (Toriello et al, 1993).

Polycystic kidney disease has been reported in the literature and renal failure necessitating dialysis and transplantation in either childhood or adulthood can dominate the clinical picture (Connacher et al, 1987; Donnai et al, 1987). Cysts can occur in other organs including the pancreas. Malformations of the central nervous system occur in as many as 40% of cases including agenesis of the corpus callosum, hydrocephalus, cerebellar anomalies and cystic changes. Learning difficulties are common. (Connacher et al, 1987). The dysmorphic features can be very variable and the renal status even within a family can be very variable (Toriello et al, 1988). There are eight other oral-facial-digital syndromes with features that subtly overlap with each other (Table 4.1.) (Toriello et al, 1993).

1.5.2. Polycystic kidney disease in OFD1

The renal cystic disease in OFD1 is predominantly glomerulocystic which is a histopathological pattern in which the majority of the cysts are found in the glomerulus (Bernstein et al, 1993). This is in contrast with autosomal dominant polycystic kidney disease (ADPKD) in which the renal cysts in the adult arise

throughout the nephron, although neonates with ADPKD may have glomerular cysts (Fellows et al, 1976; Ross et al, 1975). According to Bernstein (1993), glomerular cysts are present in three different clinical contexts; glomerulocystic kidney disease (GCKD) which can be sporadic or autosomal dominant, associated with multiple malformation syndromes including Zellweger, tuberous sclerosis, OFD1 and finally glomerular cysts can be present in dysplastic kidneys.

The genes mutated in some polycystic renal diseases are already known and might give clues to the gene responsible for OFD1. *PKD1* and *PKD2* are two genes known to be mutated in ADPKD. *PKD1* codes for a protein which may be involved in cell-cell matrix interactions with additional ion channel functions (The European Polycystic Kidney Disease Consortium, 1994; Hughes et al, 1995) and *PKD2* codes for a protein with putative ion channel functions (Mochizuki et al, 1996). Furthermore, these genes have been shown to interact with each other through a probable coiled-coil domain (Qian et al, 1997). One of the genes mutated in tuberous sclerosis, *TSC2*, codes for a protein with GTPase activating function (Wienecke et al, 1995).

A number of processses have been shown to operate in renal cyst formation; tubular cell hyperplasia (Welling et al, 1988), tubular fluid accumulation (Avner et al, 1992; Wilson et al, 1991) and abnormalities in extracellular matrix (Wilson et al, 1992; Calvet et al, 1993). These aberrations of cell biology and physiology need to be understood in the light of advances in the genetics of polycystic renal disease which suggested that a two-hit mechanism (as in some inherited cancer syndromes) may be operating in the cysts.

It has been postulated that a genetic two-hit mechanism operates in ADPKD as it has been shown that PKD1 is recessive at the cellular level. The epithelia in a

single cyst is usually clonal (Qian et al, 1996) but with somatic loss of heterozygosity or an additional mutation present in up to 24% of cysts inactivating the normal polycystin allele (Qian et al, 1996; Brasier and Henske, 1997). However, the majority of cysts do not have loss of polycystin staining (Geng et al, 1997) which might argue against this mechanism.

1.5.3. Genetics of OFD1

Considerable evidence exists that OFD1 is an X-linked dominant, male lethal, disorder (Doege et al, 1964; Wettke-Schafer et al, 1983). Firstly, OFD1 occurs almost exclusively in females with only one report of an affected male. He survived and died in the immediate post natal period with polycystic kidney disease and pulmonary hypoplasia presumably related to intrauterine oligohydramnios (Gillerot et al, 1993). A case of Klinefleter syndrome (XXY) has been reported with OFD1 with a phenotype very similar to affected females (Wahrman et al, 1966). Secondly, there is typically a strong history of miscarriage in affected families which is presumed to be due to loss of affected hemizygous males. Thirdly, in considering the siblings of patients affected with OFD1 there is an increased number of females compared with males.

A previous report of an insertion of an extra segment in chromosome 1 has yet to be substantiated with modern cytogenetic techniques (Ruess et al, 1962). This mode of inheritance contrasts with the other oral-facial-digital syndromes which are autosomal recessive (Toriello et al, 1993), apart from OFD VIII which is X-linked recessive, (Edwards et al, 1988) and also with autosomal dominant polycystic kidney disease.

1.5.4. The approach taken towards identifying the gene for OFD1 in this thesis.

I took a conventional approach in this study. This involved testing for linkage in OFD1 on the X chromosome. Once linkage was established, in the absence of chromosomal aberrations to pinpoint the location of the gene, databases were examined and collaborations with individuals working on the X chromosome were used to select positional candidate genes within the candidate region.

1.5.4.1. Principles of linkage studies

A chromosomal marker and a disease trait cosegregate together at meiosis more often than would be expected by chance if they are in close physical proximity on a chromosome. The null hypothesis, which a linkage study sets out to prove or refute, is that a disease trait and a chromosomal region is not linked in a series of meiotic events. As the distance between the disease gene and the chromosomal region under investigation increases then recombination in meiosis occurs more often than when the gene is located very close to the region. If the two loci are unlinked this could be expected by chance to occur in half of the meioses (Ott, 1991).

The recombination fraction (θ) is the measurement of genetic linkage and this is the probability that a parent will produce a recombinant offspring. Recombination occurs when homologous chromosomes cross over in meiosis. Theta ranges from 0 for loci that are very tightly linked to 0.5 for loci that are unlinked or on different chromosomes. CentiMorgans (cM) are the units in which the genetic distance of two loci are usually defined. Two loci are 1cM apart if they show recombination once in 100 meioses.

The lod score defined by Morton (1955) is the logarithm of the odds for linkage. The likelihood (L) of observing a particular configuration of a disease and a marker locus in a family is calculated assuming no linkage ($\theta = 0.5$). This likelihood is then compared with the likelihood of observing the same configuration of the two loci within the same family, assuming varying degrees of linkage over a selected range of recombination fractions (θ ranges from 0.0 to 0.5). Log_{10} of the ratio of these likelihoods is then determined for each value of θ within the range and each of the resulting numbers is referred to as a lod score, z(x), where x represents a particular value of θ within the range of recombination fractions.

$$Z(x) = \log_{10} \frac{L \text{ (pedigree given } \theta = x)}{L \text{ (pedigree given } \theta = 0.5)}$$

The value z(x) is referred to as the two-point lod score, since it involves linkage between only two loci (i.e. the disease locus and a marker locus). Calculation of lod scores is facilitated by the used of computer programmes such as the LINKAGE package (Lathrop and Lalouel, 1984).

The most likely recombination fraction θ(max) is the value of θ which give the highest lod score (Zmax). Positive lod scores favour linkage and negative lod scores make linkage unlikely. A lod score of 3.0 or more which represents an odds ratio of 1000:1 in favour of linkage is taken as evidence that two loci are linked. This allows for a prior probability of linkage of 1 in 50 and has been used in practice has been found to be a good indicator of linkage. A lod score of –2.0 is taken as evidence of non-linkage (Ott, 1991).

Multipoint linkage analysis can be used to maximize linkage information and/or to localise the disease gene more precisely on a map of markers. The most likely position is estimated by comparisons of logarithms of the likelihoods for the gene being at different positions on the genetic map.

1.5.4.2. Polymorphic markers used in linkage studies

Microsatellite markers were used in this study and are runs of repeating base pairs (Weber and May, 1989; Litt and Luty, 1989). Primers are designed to anneal to single copy DNA which flanks the repeats. A marker typically has several alleles with known sizes. The number of times the length of the repeat varies differs between different chromosomes and different individuals. PCR products of different size are then resolved by gel electrophoresis. Microsatellite include dinucleotides (two repeating base pairs), trinucleotide (three repeating base pairs) and tetranucleotide (four repeating base pairs).

Microsatellite markers have been placed on a number chromosomal maps which aim to position the markers correctly in order along the chromosome e.g. Genethon and The Location Database which were used in this study.

1.5.4.3. Strategies once the region of linkage is established

OFD1 is a rare disorder and once the disease gene was mapped to an 8 cM region on the short arm of the X chromosome it was not possible to obtain additional families with a large number of meioses to narrow the region further.

Analysis of a number of gross chromosomal rearrangements involving the X chromosome have been used to locate disease genes. In Duchenne muscular dystrophy the presence of X-autosome translocations in females with muscular

dystrophy, allowed the disease to be located on Xp21 (Greenstein et al, 1977; Lindenbaum et al, 1979). Deletions involving the X chromosome have been used to map Kallmann's syndrome in which the disease was placed proximal to the steroid sulphatase locus (Ballabio et al, 1987) and the locus narrowed to 350kB (Petit et al, 1990). Despite karyotyping affected individuals with OFD1 in my thesis no gross chromosomal aberrations were found nor were there any literature reports of OFD1 in association with chromosomal aberrations.

The region to which I initially mapped OFD1 was 19.8 cM. It was then reduced to 9.8 cM which is so large a candidate gene approach had to be taken. A candidate gene approach which involves choosing a gene based on its expression pattern, function or similarity to another disease gene. Genes which have been successfully discovered in this way include *FGFR3* which was chosen as the candidate gene for achondroplasia as it was expressed in cartilage (Rousseau et al, 1994).

Initially, my strategy was to consider all known genes within the region based on the knowledge available about their expression and function. A gene was considered to be a good candidate if it was expressed in the face, hands, feet and kidneys in fetal development or in the kidney postnatally. Expression studies were performed in these organs in some candidate genes. If the function of the gene could be developmental or if the function of the gene related to the function of other genes causing polycystic renal disease as mentioned in section 1.5.2., it was also considered to be a candidate. Genes considered to be candidates included *APXL* (Apical Protein Xenopus Laevis like) which codes for a protein which may modulate the activity of amiloride sensitive sodium channels and in the adult was shown to be expressed in the lung, brain, kidney and pancreas (Schiaffino et al,

1995) and *KAL* which codes for a putative cell adhesion molecule and is the gene responsible for X-linked recessive Kallmann's syndrome (Franco et al, 1991) in which affected males have similar phenotypic defects to OFD1; midline defects and renal agenesis. Once the known candidate genes in the region had been excluded, I turned my search turned to the potential discovery of novel genes within the region.

During this part of my thesis work I had to establish collaborations with other groups actively searching for novel genes using techniques such as the analysis of direct sequence data generated from this region by the Sanger Centre, (Cambridge, UK) as used to find the gene for X-linked retinoschisis (Sauer et al, 1997) and further analysis of the expressed sequences mapped to this region (Boguski and Schuler, 1995). This lead to the examination of further genes within the region as candidates.

1.6. Vesicoureteric reflux (VUR) and Reflux nephropathy (RN) (OMIM 193000)

1.6.1. Definition and classification

VUR is the retrograde passage of urine from the bladder to the ureters and, depending on the degree of reflux, to the kidneys. Primary VUR, which is the focus of this thesis is VUR in the absence of secondary causes such as a neuropathic bladder or obstruction to bladder outflow. RN is defined as the renal parenchymal disease associated with VUR and includes three types of disease: focal renal scarring associated with urinary tract infection, a developmental defect affecting both the kidney and ureter and focal segmental glomerulosclerosis in the

kidney with renal impairment. In the work to be described in this thesis, renal histology was not available and RN therefore theoretically could include any of these three parenchymal diseases. RN accounts for approximately 10% of adults in renal failure (Bailey, 1991).

1.6.2. Diagnosis of VUR and RN

In this thesis the diagnosis of VUR and RN was made radiologically. VUR was defined as the presence of reflux on a cystogram study which could be direct (Figure 1.6.) (contrast or radioisotope introduced directly into the bladder by a catheter) or indirect (Figure 1.7.) (radioisotope excreted through the kidneys). The severity of VUR can be graded (Figure 1.8.). Cystography is a reliable technique as in individual patients variability in demonstrating VUR on consecutive occasions has only been shown in less than 4% of cases and with low grades of VUR (Jequier et al, 1989). In addition, there is little variation in the reporting of VUR on individual cystograms between paediatric radiologists regarding the diagnosis of VUR (Craig et al, 1997).

In this study, RN was defined as the presence of parenchymal disease on an intravenous pyelogram (Figure 1.9.) or an isotope renogram (Figure 1.10.). RN is not reliably detected with an ultrasound scan (Smellie et al, 1995). The radioisotope scan is generally considered to be more sensitive than the intravenous pyelogram in the detection of renal scarring (Merrick et al, 1980; Goldraich et al, 1989; Mansour et al, 1987). The intravenous pyelogram typically shows blunted calyces with overlying parenchymal thinning and each modality may also show a small smooth kidney which is more likely to be a congenital malformation.

Figure 1.6
Contrast cystogram showing bilateral severe VUR

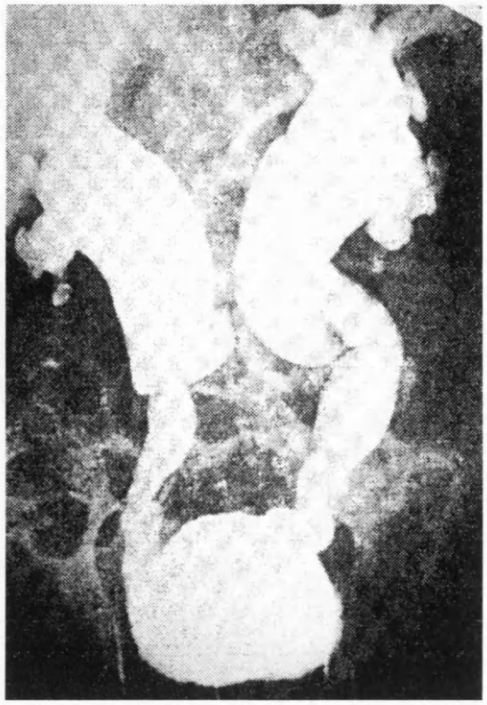

Figure 1.7
Direct radionuclide cystogram showing Left VUR (indicated by arrow)

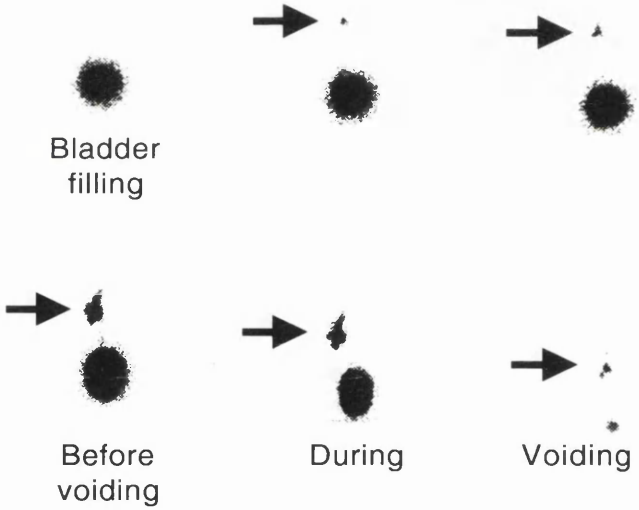

Figure 1.8
International classification of VUR

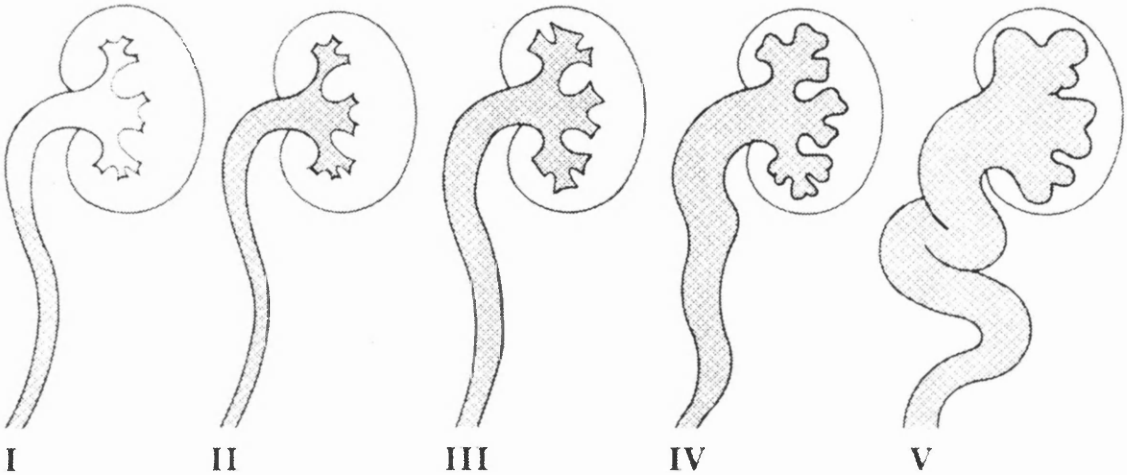

Figure 1.9
Intravenous urogram showing bilateral renal scanning

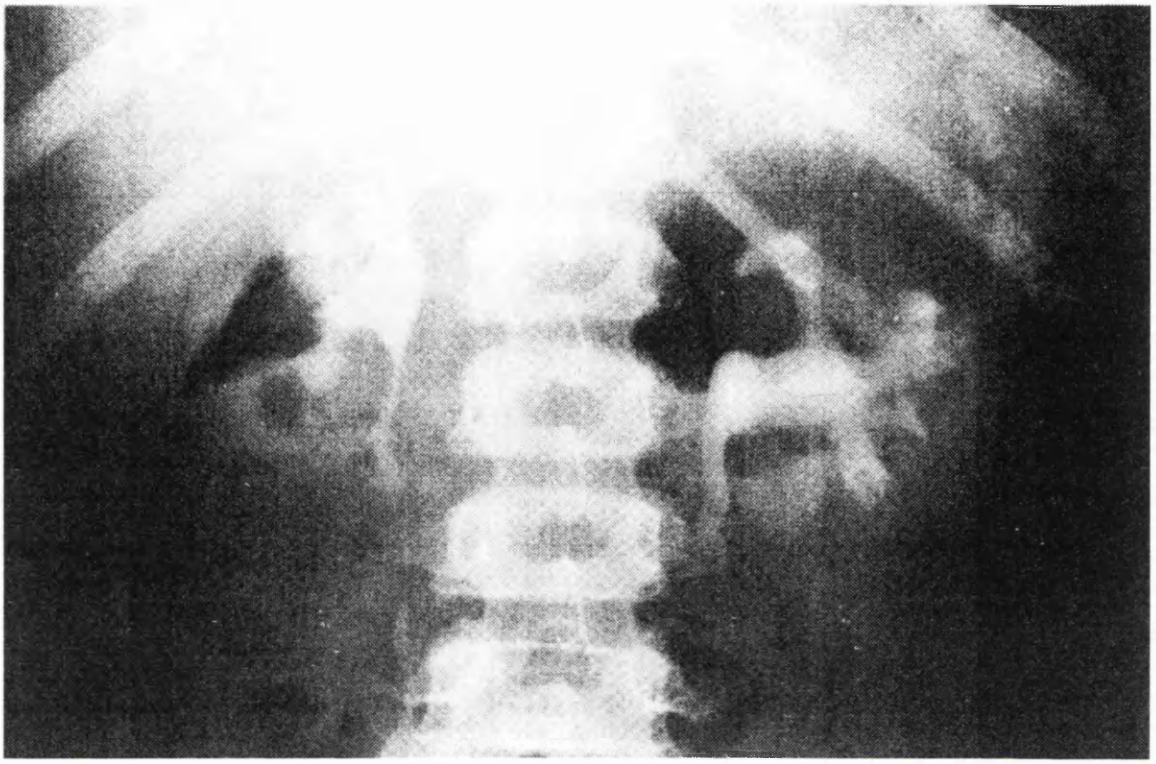

Figure 1.10
DMSA scan, with impaired function of the right kidney (R=25%, L=75%) and focal defects of the left kidney

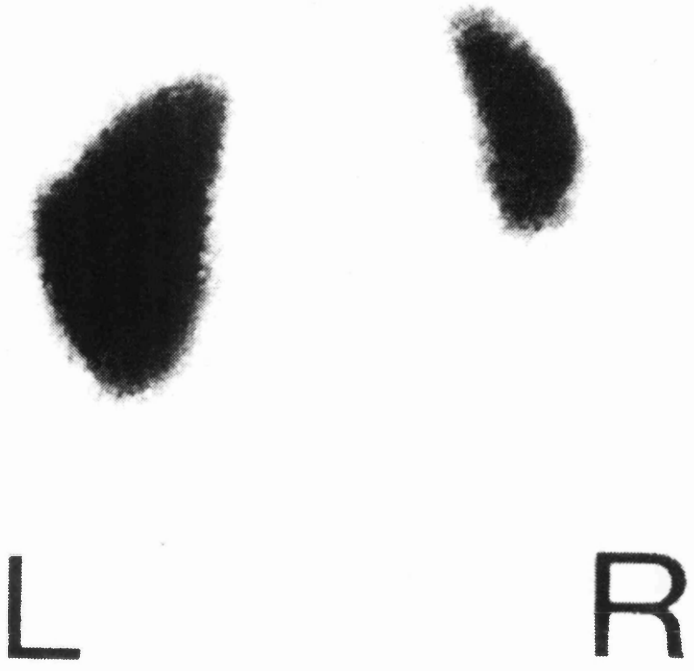

1.6.3. Pathogenesis of primary VUR

The nature of the defect in primary VUR is debated, which will be important in considering potential candidate genes in VUR.

1. A more lateral and oblique insertion of the ureter into the bladder wall leading to a shorter length of intramural ureter which is unable to be squeezed closed during bladder contraction has been postulated to cause VUR (Figure 1.11.) and also an abnormally shaped ureteric orifice (Mackie et al, 1975a and b; Tanagho et al, 1969).

2. Abnormal innervation of the vesicoureteric junction has also been suggested as a mechanism for VUR (Dixon et al, 1998).

3. An increase in collagen in refluxing compared with normal ureters has been reported (Lee et al, 1992). Another study reported the reduced muscle in the lower ureters in neonates compared with adults and this constitutes a possible mechanism for the regression of VUR with age (Cussen et al, 1967).

4. More recently, voiding dysfunction has been suggested as a mechanism for VUR in apparently primary cases (Koff et al, 1992). It has been postulated that dysfunctional bladder contraction might alter the anatomy of the bladder wall and the VUJ allowing VUR to occur. In addition increased bladder pressures might occur forcing urine back across the VUJ (Allen et al, 1979, Allen et al, 1992, Koff et al; 1992).

Figure 1.11
Anatomical features of the non-refluxing and refluxing ureter (adapted from Eccles 1996)

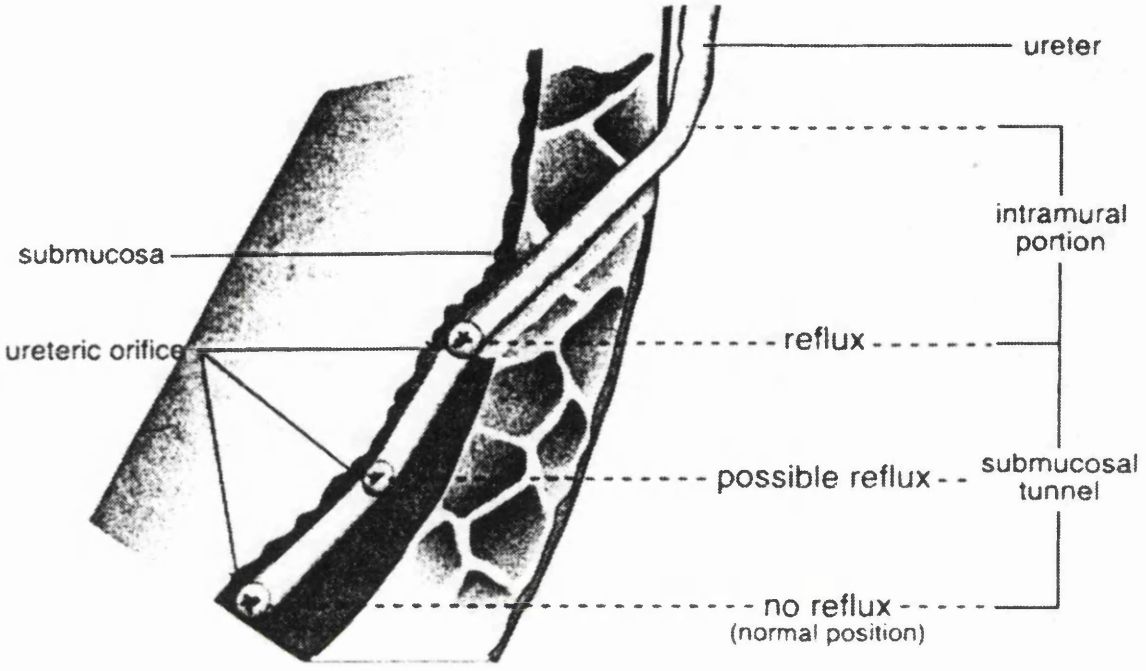

1.6.4. Pathogenesis of RN

There are three different types of RN between which it has not been possible to differentiate in this study.

1. RN due to inflammation and scarring caused intrarenal reflux (IRR) of infected urine. This has been demonstrated in pig models (Ransley and Risdon, 1975a; Ransley and Risdon, 1978b). IRR has only been shown to occur in compound papillae at the poles of the kidney in some individuals (Ransley et al, 1979) which might suggest that some individuals are genetically predisposed to RN in the presence of VUR. However non-refluxing papillae have been shown to transform into refluxing papillae in the same individual (Ransley and Risdon, 1978b).

2. RN has also been shown to be a developmental defect of renal tissue such as dysplasia (undifferentiated renal tissue) especially in male infants with VUR (Risdon, 1971a and b; Risdon et al, 1975). Developmentally abormal renal tissue has also been found in foci in the non-scarred areas of renal parenchyma in kidneys thought to be damaged by IRR of infected urine (Hinchcliffe et al, 1992: Risdon et al, 1993). Here it could be postulated that the same mutation causes two related ureteric bud defects simultaneously, RN and VUR.

3. Once renal damage has occurred in RN superimposed focal and segemental glomerulosclerosis can occur which is present in 90-100% of patients with end stage renal failure and RN (Zimmerman et al, 1973; Torres et al, 1980a) and it is possible that separate genetic mechanisms influence the rate of progression to end stage renal failure in RN.

1.6.5. Incidence of VUR in the normal population

The overall incidence of VUR in the infant and child population is estimated to be 1-2% based on two types of study. The first type of study investigated the presence of VUR in asymptomatic children by cystogram. In studies on healthy children with no apparent abnormalities of the urinary tract, VUR was found in less than 1-2% on infants (Campbell et al, 1930; Kjellberg et al, 1957; Jones et al, 1958; Hodson et al, 1960).

The second type of study to investigate the incidence of screened infants and children for asymptomatic bacteriuria and screened those found to be positive with cystograms. Again the incidence of VUR was found to be 1-2% (Abbott et al, 1972; Kunin et al, 1960 and Meadow et al, 1969). However, these studies may underestimate the incidence of VUR as children without bacteriuria are not screened. Two reviewers of the published data on incidence of VUR concluded that the incidence is 1.8% (Ransley et al, 1978a) and between 0.4-1.8% (Bailey, 1979). In this thesis I assume an incidence of 1%.

The incidence of VUR has been shown to be significantly lower in Afro-Caribbean children compared with Caucasian children (Askari et al, 1982; Booth, et al, 1975; Kunin et al, 1960 and Skoog et al, 1991) suggesting a genetic effect.

VUR is reported with greater frequency in females in older children (Baker et al, 1966; MacGregor et al, 1975). However, in children who present with UTI, VUR is found with a similar frequency in the two sexes (Kjellberg et al, 1957; Kelais et al, 1971; Baker , 1966). In contrast, in the prenatal diagnosis of infants with VUR and dysplasia male infants are more commonly found than females (Yeung et al, 1997).

1.6.6. Twin studies in VUR and Reflux Nephropathy

Estimating and comparing the concordance rates for monzygotic (MZ) and dizygotic (DZ) twins for a disorder (i.e. when both members of the pair are affected) can give insight into the role of genetic factors in the aetiology of the disorder (Allen et al, 1967). If the concordance is 100% in MZ twins and between 25% and 50% in DZ twins, it may be concluded that the disorder is strictly genetic and probably due to either a single recessive (DZ concordance 25%) or dominant gene (DZ concordance 50%). For a disorder in which genetic factors are important in the aetiology, but not the sole factor, the concordance rate for MZ twins will still be greater than for DZ twins and the concordance rate for MZ twins reared apart will be the same as for MZ twins reared together. For example, in insulin dependent diabetes mellitus, the MZ concordance is 30% and the DZ concordance 6-10%.

In VUR, there are 11 reports in the literature of MZ twins which are concordant for VUR (Stephens et al, 1955; Mebust et al, 1972; Atwell et al, 1974; Pochackveski et al, 1974; Hampel et al, 1975; Redman et al, 1976; De Vargas et al, 1978; Kerr et al, 1983; Sirota et al, 1986; Heale et al, 1997; Winnearls et al, 1983). There is only one report of DZ twins which are discordant for VUR published (Stephens et al, 1955). It is difficult to claim a greater incidence in MZ compared with DZ twins based on these findings as isolated reports of concordance in MZ twins are subject to ascertainment bias. A statistically significant difference was reported between the incidence of VUR of 75% in 9/12 MZ twin pairs (average age when studied = 4.4 years) compared with 40% in 7/15 pairs of DZ twins (average age when studied = 2.3 years) (Curran et al, 1998). This study suggests a strong role for genetic factors in the pathogenesis of primary

VUR.

It is interesting to note that two of the MZ twin pairs are non-concordant for RN (Kerr et al, 1983; Stephens et al, 1955) which suggests that environmental factors also play a role in the pathogenesis of RN. In summary, twin studies suggest that genetic factors play a role in the aetiology of VUR.

1.6.7. Familial aggregation studies in VUR

There are numerous reports of families with more than one affected individual with VUR and there are many different relationships of affected relatives reported (Tobenkin et al, 1964; Simpson et al, 1970; Burger et al, 1972; Schmidt et al, 1972; Miller et al, 1972; Mobley et al, 1973; Middleton et al, 1975; Lewy et al, 1975; Fried et al, 1975; Uehling et al, 1992; Heale et al, 1997).

A more accurate approach to assessing the genetic contribution to VUR is achieved by systematic screening studies of relatives of index cases with VUR (Table 1.3.). The incidence in relatives can then be compared with the incidence in the general population

First Author (date)	Type of screening method	Number screened and ages (if known)	Incidence of VUR and/or RN
Bois (1975)	Medical history only	First degree relatives of 436 index patients	4% VUR
Dwoskin (1976)	Cystogram screening	204 siblings (0-21 years)	22% VUR
Jerkins (1982)	Cystogram screening	104 siblings (3months-16 years)	32% VUR
Van den Abbeele (1987)	Cystogram screening	60 siblings	45% VUR
Kenda (1992)	Cystogram and isotope renogram screening	105 siblings (4 months-6.3 years)	45% VUR 25% RN
Connolly (1997)	Cystogram screening	482 siblings (2 weeks-12.8 years)	37% VUR (46% under 2 years)
Noe (1992a)	Cystogram screening	36 offspring (2months-9 years)	66% VUR
Noe (1992b)	Cystogram screening	354 siblings	34%VUR (46% under 18 months)
Scott (1997)	Cystogram screening	Neonates in families with a history of VUR	31% VUR
DeVargas (1975)	Cystogram screening if positive medical history	First degree relatives	30% VUR

Table 1.3: Systematic screening studies of relatives of index cases with VUR

Overall, systematic cystogram screening studies have suggested an incidence of VUR in first degree relatives of between 26-66%. The only study which is much lower is that of Bois et al (1975). This probably underestimated the incidence of VUR as it relied entirely on incidence of VUR in relatives as reported by medical history. DeVargas et al (1975) only screened individuals with cystograms if they had a positive history of urinary tract symptoms which again would underestimate the incidence. In the study of Scott et al (1997) the neonates screened may have been a more distant relative to the index case with VUR which might underestimate the incidence in first degree relatives. Finally, a much higher incidence of VUR is noted if the relatives screened are under two years of age (Noe et al, 1992; Connolly et al, 1997). This is to be expected if VUR regresses with age as was discussed in section 1.6.3. Furthermore Connolly et al (1996) showed that in the follow-up of asymptomatic siblings who were screened with cystograms, 52.8% of cases of VUR identified at a mean age of 21 months had resolved.

1.6.8. Recurrence risks to siblings of index cases with VUR

Collectively, the screening studies described in section 1.6.7. demonstrate that there is an increased incidence of VUR in first degree relatives of index cases with VUR than in the general population as described in section 1.6.5. The recurrence risk to siblings of probands compared with the general population risk (λs) is 20-30. This relative risk is similar to other complex disorders in which genetics plays an important role in the pathogenesis such as insulin dependent diabetes mellitus (IDDM) ($\lambda s=15$), but is much less than in a Mendelian recessive trait such as cystic fibrosis ($\lambda s=500$) or a Mendelian dominant trait such as Huntingdon disease

(λs=5,000) (Farrer and Cupples, 1998).

1.6.9. Segregation studies in VUR

Segregation analysis aims to determine the transmission pattern of the trait within families and to test this pattern against predictions from specific genetic models to determine which model best fits the data. A segregation analysis using 88 families containing at least one individual with VUR has been performed (Chapman et al, 1985) using the POINTER epidemiology software package (Lalouel and Morton, 1981) which calculates maximum likelihood estimates for different genetic models. The authors suggest that a single major locus was the most likely mode of inheritance for VUR.

1.6.10. Candidate loci for VUR and RN

A number of candidate regions for VUR and RN have already been suggested by previous authors.

1.6.6.10.1. Chromosome 6p

Some studies have found positive associations between VUR, RN and particular HLA types and are summarised in Table 5. The HLA locus is on the short arm of chromosome 6. It is possible that differences in immune response associated with HLA type could predispose to increased renal impairment in RN (Kincaid-Smith, 1975). It is also known that components of the immune system are important in the normal development of the renal tract (Cale et al, 1998) and abnormalities could cause VUR and RN. An alternative explanation could be that a functional change in a developmental gene in close proximity to the HLA locus on

chromosome 6 could be in linkage disequilbrium with the HLA locus.

Using a different approach, Mackintosh et al (1989) used HLA-type as a genetic marker for the short arm of chromosome 6, the location of the major histocompatibility antigens. They used data from six families with recurrent UTI and VUR, two reported in their own paper and four previously reported by Sengar et al (1979). They calculated a lod score of 3.326 with a recombination fraction $\theta = 0.05$ for the HLA locus which suggests significance but they have also included data on individuals without VUR in the families who should actually be classified as unknown. If the unaffected individuals were classified as unknown the significance of this lod score would be diminished.

Table 1.4: Studies reporting associations between HLA types, VUR and RN

Author (year)	HLA type	Type of patient
Bailey and Wallace (1978)	HLA-B12 positive association	CRF due to RN compared with other causes
McDonald et al (1976)	HLA-A3 positive association	CRF due to RN compared with other causes
Torres et al (1980b)	HLA-B12 positive association in female patients HLA-B8 with HLA-A9 or HLA-Bw15-positive association in male patients HLA-Bw15 – positive association in both sexes.	ESRF due to RN compared with other causes
Sengar et al (1978)	HLA- Aw32-positive association	VUR

1.6.10.2. Chromosome 10q

The long arm of chromosome 10 is another potential candidate region for VUR and RN as three key nephrogenesis genes *RET, FGFR2* and *PAX2* are located there. *PAX2* is a transcription factor mutated in the renal-coloboma syndrome in which affected individuals have VUR associated with renal hypoplasia and visual defects (Sanyanusin et al, 1995). In addition, a number of mutant mice for *PAX2* have a renal phenotype as discussed in section 1.3.2. *FGFR2* is mutated in Apert syndrome (Wilkie et al, 1995) and up to 10% of individuals have hydronephrosis and a duplicated renal pelvis (Cohen et al, 1993). Null mutant mice for *RET* have

abnormal development of the urinary tract (Schuchardt et al, 1994).

1.6.10.3. The X chromosome

A number of authors have suggested that VUR may be X-linked in certain kindreds (Middleton et al, 1975; Lewy et al, 1975; Miller et al, 1972). In addition, VUR associated with RN, in which the renal parenchymal disease is a developmental defect, occurs more commonly in males, suggesting the X chromosome may be a candidate locus for VUR and RN (Risdon et al, 1993). In addition, Nishimura et al (1999) reported an association between a polymorphism of the *AT2* receptor on the long arm of the X chromosome and male infants with diverse malformations of the renal tract including VUR.

1.6.10.4. The renin-angiotensin system

In addition to the study of Nishimura et al (1999), the relationship has been examined between severity of reflux nephropathy and polymorphisms of the renin-angiotensin system. Ozen et al (1997) have demonstrated an association between the severity of RN and the DD intronic polymorphism of *angiotensinogen* which has been shown to be related to functional differences in angiotensinogen activity.

1.6.11. Approaches taken in identifying susceptibility loci in VUR and RN

VUR and RN are likely to be genetically heterogeneous occurring in isolation or as part of complex syndromes such as the renal-coloboma syndrome (Sanyanusin et al, 1995) caused by mutations in the *PAX2* gene. VUR and RN have been reported to occur in apparently dominant families (Heale et al, 1997; Burger et al,

1972; Chapman et al, 1985) and these are the type of large families that have been collected in this study. An analogy can be drawn with early onset breast cancer in which, although the disease is polygenic overall, a small subset of families with early onset as a distinguishing feature appeared to have a dominant Mendelian mode of inheritance and analysis of these families led to the mapping and isolation of *BRAC1* on chromosome 17q21 (Hall et al, 1990). An alternative approach would have been to study large numbers of affected sibling pairs to look for susceptibility loci as in insulin dependent diabetes mellitus (IDDM) (Davies et al, 1994) and multiple sclerosis (Ebers et al, 1996; Haines et al, 1996 and Sawcer et al, 1996) but much larger kindreds were available for study in VUR and RN. As the families collected in my thesis were large dominant looking families I elected to perform two different simultaneous analyses 1. Parametric analysis (model dependent analysis) using an autosomal dominant model for VUR with variable penetrance and expression. 2. Non-parameteric (model free analysis) using an affected relative pair method as the genetic model for VUR is not yet known.

VUR regresses with age (Tamminem-Mobius et al, 1992) and so individuals who are older at investigation may be falsely labelled as unaffected. In addition, the diagnosis is made by invasive radiological investigation as stated in section 1.6.2. and some individuals may not have had the appropriate investigations. For these reasons, I only labelled individuals with VUR on cystogram or RN on intravenous pyelogram or isotope renogram affected and everyone else was unknown. Specifically, I did not include individuals with symptoms such as hypertension and history only of renal disease as definite positive cases of VUR and/or RN. Although essential given the natural history of VUR and the limitations of full diagnostic work ups on all individuals, these stringent criteria reduce the power of

the families under investigation.

The question arises "Are VUR and RN caused by the same genes?" As discussed in section 1.6.5. there are at least three different types of RN which it has not been possible to separate in this study. VUR and RN could either be seen as developmental manifestations of the same genetic defect or RN could be caused by IRR of infected urine in which case it could be postulated that separate genes predispose to the renal disease. To attempt to address these question the analysis performed in this study analysed individuals with VUR only, individuals with RN only and also individuals with either VUR or RN in three separate analyses.

At the commencement of this work, two regions, chromosome 6p and chromosome 10q, were good candidates for VUR and RN as discussed in sections 1.6.10.1. and 1.6.10.2. respectively. These regions were the first to be examined and microsatellite markers from these regions were used. Another approach would have been to examine individual candidate genes on chromosome 10q but this was not undertaken as the linkage data was not suggestive and a large number of potential other candidate genes are known to be important in nephrogenesis as discussed in section 1.3.1. 2. The pathogenesis of VUR is not entirely understood, as discussed in section 1.6.3, which might make candidate genes difficult to predict. Therefore a genome wide scan was embarked upon using microsatellite markers as discussed in section 1.5.4.3.

The linkage analysis in the genome-wide scan in VUR and RN was performed using GENEHUNTER package (Kruglyak et al, 1996). This programme simultaneously calculates a parametric (model dependent) linkage analysis and a non-parametric (NPL)(model independent) linkage analysis. NPL analysis is less powerful than parametric analysis but more accurate if the genetic model is

misspecified. NPL methods are based on the extent to which affected relatives share alleles at the locus under investigation. GENEHUNTER uses identical by descent (IBD) allele sharing in which the common allele shared between two affected individuals in a family must have been inherited from a common ancestor. NPL is calculated using a pairwise approach between individuals and is extended to simultaneously compare allele sharing in all affected individuals in a pedigree and is suitable for the family sizes used in this study. The analysis used by the programme is multipoint.

The significance of the NPL results from the genome-wide scan have been assessed using the criteria of Lander and Kryglyak, 1995 reporting a p value of less than 0.05 as suggestive of linkage.

Diseases in which similar approaches have been taken include IDDM and inflammatory bowel disease (IBD). In IDDM, there are currently 17 different loci mapped genome wide. The two major loci are considered to be *IDDM1* and *IDDM2* (Vyse and Todd, 1996). *IDDM1* is the HLA region on chromosome 6 (Clerget-Darpoux et al, 1980; Spielman et al, 1980) and the second locus (*IDDM2*) is the insulin gene on chromsome 11 (Spielman et al, 1993; Bennett et al, 1995). The other loci are as yet undefined. In IBD, a number of genome wide scans have been performed. Hugot et al (1996) found two loci for Crohn disease on chromosomes 16 and 1. The locus on chromosome 16 has been confirmed by other authors (Ohmen et al, 1996; Parkes et al, 1996; Cavanaugh et al, 1998; Cho et al, 1998). Additional loci on chromosomes 3,12 and 7 were found by Satasangi et al (1996).

1.7.1. Experimental strategy

In my thesis I investigated two renal tract malformations, OFD1 and VUR.

In OFD1, I set out to prove the hypothesis that the disorder mapped to the X chromosome using microsatellite markers and a linkage approach. Having proved this, I examined a number of candidate genes in the region of linkage; both expression patterns and mutation screening. I also performed histological studies on post mortem renal tissue from an affected female with OFD1.

In VUR, I set out to find susceptiblity loci genome wide using a microsatellite markers along all the chromosomes and performed a combined non-parametric and parametric analysis of the data using GENEHUNTER.

Chapter Two MATERIALS AND METHODS

2.1 MATERIALS

2.1.1. General reagants

The following chemicals were supplied by Sigma Chemicals Company (Poole, Dorset, UK): ammonium acetate, ammonium persulphate (APS), bovine serum albumin (BSA), bromophenol blue, diaminobenzadine tetrahydrochlorodihydrate (DAB), diethylprocarbonate (DEPC), deoxyribonuclease 1 amplification grade (Dnase), ethylene-diamine-tetra-acetic acid (EDTA), ethidium bromide, fetal calf serum (FCS), hydrogen peroxide, mineral oil, nonidet P-40 (NP40), orange G, paraformaldehyde (PFA), chlorinated organopolysiloxane in heptane (sigmacote), silver nitrate, sodium dodecyl sulphate (SDS), sterile tissue culture water, N,N,N',N', tetramethylethylenediamine (TEMED), xylene cyanol.

The following reagants were supplied by BDH Ltd (Poole, Dorset, UK): chloroform, formaldehyde solution (40%), glacial acetic acid, nitric acid, orange G, proteinase K, propan-2-ol, sodium carbonate (anhydrous), sodium chloride, sucrose, TRIS (tris(hydoxymethyl)aminomethane), urea.

Other companies supplied the following: ABC kit (Dako, High Wycombe, Bucks, UK), Citifluor TM (Chemical Labs, High Wycombe, Bucks, UK), ^{32P} dCTP (ICN Biomedicals Limited, Thame, Oxfordshire, UK), dNTPs (Pharmacia Biotech, Uppsala, Sweden), Dyna-M-280 beads (Dynal UK, Ltd), Ethanol (Hayman Limited, Witham, Essex, UK), Formamide (ACS grade) (Scientific Imaging Systems, Rochester, USA), Histoclear (National Diagnostics, Atlanta, Georgia, USA),

Leibovitz 15 (L-15) media (Gibco BRL, Paisley, UK), Phenol (liquified and washed in tris buffer (Life Science,Merck Ltd, Poole, Dorset, UK), Phosphate buffered saline (PBS)(Gibco BRL, Paisley, UK), Proteinase K solution (Boehringer Mannheim, Mannheim, Germany), RNase (Boehringer Mannheim, Mannheim, Germany), T7 sequenase version 2.0 sequencing kit (United States Biochemicals), Taq polymerase, 10x ammonium (NH_4) buffer and 50mM $MgCl_2$ (Bioline, London, UK), TRIS-Borate buffer (TBE) (0.9 M TRIS, 20mM EDTA (pH 8.0), 0.9 M Boric Acid) (Amresco, Solon, Ohio, USA), TRI REAGANT^{TM} (Molecular Research Centre, Inc,), Xylene (Merck Limited, Poole, UK), Wizard minicolumns (Promega,).

2.1.2. Photography, autoradiography and blotting

The X ray film used was Kodak X-OMAT AR. Cassettes were supplied by Genetic Research Instrumentation and 3MM chromatography paper (Whatman Ltd, Maidstone, Kent, UK)

2.1.3. Gel electrophoresis

The following supplied the reagants for gel electrophoresis: agarose (Life technologies, Gibco BRL, Paisley, UK), Polyacrylamide Easigel: Acrylamide, bis-acrylamide, 7M urea, 1 x TBE, 6% w/v-1315 w/v, ratio detection 19: 1 (Scotlab, Strathyclyde, UK), mutation detection enhancement gel (MDE)(FMC Bioproducts, Rockland, USA), plates for polyacrylamide gel electrophoresis, spacers and combs (Gibco BRL, Paisley, UK).

The gel used for the genome scan was Sequagel (National Diagnostics, Atlanta,

Georgia, USA). The genome scan was performed on an ABI 377 sequencer (Perkin Elmer Applied Biosytems, Foster City, Ca, USA) and the software used in analysis was Genescan version 2.0 and Genotyper version 2.0 (Perkin Elmer Applied Biosytems, Foster City, Ca, USA). The 36 cm well to read distance plates for the ABI sequencer, 36 well shark tooth combs and 0.2 mm spacers were supplied by Perkin Elmer Applied Biosytems (Foster City, Ca, USA).

2.1.4. Molecular size markers

1 kb and 100 bp ladders for agarose gel electrophoresis were supplied by Life technologies (Gibco BRL, Paisley, UK). 300 and 500 TAMRA size markers for the ABI sequencer (Perkin Elmer Applied Biosytems, Foster City, Ca, USA).

2.1.5. Microscopy

Light and fluorescent microscopy was performed on a Zeiss Axiophot microscope (Carl Zeiss, Oberkochen, Germany) using lenses of 10x, 20x, 40x and 63x (oil immersion) magnification. Specimens were photographed using Fuji Super G 100 colour negative or Kodak Ektachrome 64 colour positive film. Confocal fluorescent microscopy used a Leica Aristoplan microscope and computer confocal laser scanning system (Arsitoplan-Leica, Heidelberg, Germany) with oil immersion lenses of 10x, 25x, 40x, 63x and 100x and software interpolation of intermediate magnifications. Images were saved as tagged label format (TIF) and imported for labelling into Adobe Photoshop (Version 3; Adobe Systems Europe, Edinburgh, UK) or Microsoft Powerpoint (Version 4; Microsoft Corporation, Seattle, USA).

2.1.6. Oligonucleotides

The size of the polymerase chain reaction (PCR) product is the first number in bold. The conditions of the PCR reaction are given in brackets. The first number is the annealing temperature. All PCR reactions were carried out under the following conditions: initial denaturation 95^0C for 5 minutes and then 30 cycles 95^0C for 1 minute, annealing temperature for 1 minute and extension for 1 minute 72^0C, followed by a 10 minute extension step at 72^0C. All were performed at 1.5 mM magnesium concentrations unless otherwise stated. The upper primer of a pair is the forward (sense) primer and the lower primer is the reverse (antisense) primer.

Unless otherwise stated, the primers were supplied by Genosys Biotechnologies (Europe) Ltd, Pampisford, Cambs, UK.

2.1.6.1. Microsatellite markers

The primers sets used for linkage analysis were supplied by Research Genetics (Huntsville, USA). Set 6.0 were used for the X chromosome in OFD1 and for chromosomes 2, 4, 5, 6, 7, 11, 12, 15, 17, 18, 19, 20 and X in the genome scan in pedigrees 1-5. The remainder of the genome scan in pedigrees 1-5 and the whole genome scan in pedigrees 6-7 was performed with fluorescently labelled primers of set 8.0 supplied by Research Genetics. This set of markers was designed by the Co-operative Human Linkage Centre (CHLC) (http://www.chlc.org) and was supplied by Research Genetics. This set contains 387 markers with an average heterozygosity of 0.76, an average spacing of 10 cM and 89 % tri or tetranucleotide repeats.

The markers are arranged into panels, which are made up of between 4 and 17

primers pairs that can generate PCR products which can be loaded in to a single gel lane, with overlapping-sized alleles differentiated by use of different coloured fluorescent dyes. One of three dyes were used: HEX (4,7,2',4',5',7'-hexachloro-6-carboxyfluorescein) is displayed as green, TET (4,7,2',7'-tetrachloro-6-carboxyfluorescein) is displayed as yellow and FAM (6'carboxyfluorescein) is displayed as blue. The dye is attached to the 5' end of the forward primer and is therefore incorporated in to the PCR product. The conditions for these primers were provided by Research Genetics.

The following primers on the X chromosome were supplied by Genosys who provided the annealing temperatures (*DXS996, KAL, DXS1223, DXS8051, DXS7108, DXS8022, DXS987, DXS8036, DXS7105*). The sequences are available through The Genome Database (http://www.hgmp.mrc.ac.uk).

2.1.6.2. Single strand conformation polymorphism analysis and heteroduplex screening

The primers used in this thesis were either published primers in which case the reference is given or designed using sequence information available through The Genome Database (http://www.hgmp.mrc.ac.uk/gdb/gdbtop.html) or provided without sequence information as part of collaborations. Unless otherwise stated, they include intronic sequence adjacent to introns.

Primers used to screen *KAL* have been described in Hardelin et al 1993.

Primers used to screen *CLC4*

There was no intronic sequence available and these primers were designed in exonic

sequence

Exon 1 **139** (57^0C)

5'GGTCACTCCTCTCAAATTTG3'

5'CTCCGGGCTGAAATCGACAT3'

Exon 2 **240** (60^0C)

5'CGCCCACCTGGACAGCAT3'

5'GGATTTCTCCTCCTGTGGTGTTG3'

Exon 4 **118** (60^0C)

5'GGTGCCAGTGCTTACATTCTG3'

5'CTCTGGTATGCCAGAGCCACA3'

Exon 5 **201** (55^0C)

5'ATAAAGACCATTTTGAGCGGC3'

5'GCCTCTTGCCCTCATTCTT3'

Exon 6 **80** (58^0C)

5'GTGCTTTCAGCTGCAGCG3'

5'CTCTTCTAGACTGAAAAGCAC3'

Exon 7 **272** and **330** (57^0C and 57^0C)

5'GTCAGTTACTACTTTCCCCTG3'

5'CTCCAGCACCGGGTACTT3'

5'ATCGCCTGGTGCAGGAGG3'

5'CTTCATGCCAAAGGTAAATATGGT3'

Exon 8 **185** (62^0C)

5'ATCCCGTCGGGCCTCTTCATC3'

5'GAGGCAGGCCGCAGCTCC3'

Exon 9 **260** and **195** (60^0C and 62^0C)

5'GGAGTTACCAGGATGACGGTG

5'GGTGAGCACCGACAGTGG3'

5'ACACTGGCCACCGACGTCATG3'

5'TATTGCGAGAATCAGTTGGCCCT3'

Exon 10 **192** (62^0C)

5'AACGCCAGACAGAGGCAGGAG3'

5'GCTCCGCGTCACCAGGCA3'

Exon 11 **326** and **277** (55^0C and 53^0C)

5'AGACTTCTTGGCATCATCACA3'

5'CAAACTCATTAGGAAACACAG3'

5'GGCATTTTATAGCTTTAACCC3'

5'AATTTAATTTCTTTTTCTTTTTCAACA3'

Primers used to screen *APXL* have been described in Schiaffino et al 1995

Primers used to screen *GRPR*

Exon 1 **360, 380** and **330** (52^0C, 55^0C and 50^0C)

5'GAAAGACGCTGTGGGAAAATAG3'

5'CACCTAAAAGTTCCCTTAGATG3'

5'CATAGATCTTATCTTCATCTTCAC3'

5'GCATCCACTGGAGCACACG3'

5'GTTCATTTCCAGTCTGGCTTTG3'

5'CAATATGTTACACTCAAGAAGTC3'

Exon 2 **350** (52^0C)

5'CCTCCTTTAAATATTGTACGCC3'

5'TGCAGATTCAAGTGTCATGGC3'

Exon 3 **550** (52^0C)

5'GTGAACTCCTCTATTGCCC3'

5'CTGAAGGCTCTTTGGAGG3'

Primers used to screen *HSCALDK9*

Exon 1 **142** (53^0C)

5'GTGGCGTGCCCGTAA3'

5'AATGCAAACAGAAGGAGCT3'

Exon 2 **228** (52^0C)

5'ACAAAACTGTACTTCAGCTTT3'

5'CCCATTAAGTGGGCTCT3'

Exon 3 **224** (52^0C)

5'GGAGAAGTTAGTTTTGAAGAA3'

5'TCACGTATTATGTTATGAGG3'

Primers used to screen *ARHGAP6*

The primers for the 12 exons of this gene were provided without sequence information as part of a collaboration with Dr H.Zoghbi (Baylor Institute, Texas, USA) and primer sequence is not detailed in this thesis.

Primers used to screen *HCCS*

The primers for the 7 exons of this gene were provided without sequence information as part of a collaboration with Dr H.Zoghbi (Baylor Institute, Texas, USA) and

primer sequence information is not detailed in this thesis.

Primers used to screen *SCML1*

The primers for the 6 exons of this gene were provided without sequence information as part of a collaboration with Dr D Trump (Cambridge University, Cambridge, UK) and primer sequence information is not detailed in this thesis.

Primers used to screen *MID1/FXY*

The primers for the 12 exons of this gene were provided without sequence information as part of a collaboration with Dr B Franco (TIGEM, Milan, Italy) and Professor A Ashworth (ICR, London, UK) and primer sequence is not detailed in this thesis.

Primers used to screen *STK9*

The primers for the exons of this gene were provided without sequence information as part of a collaboration with Dr B Franco (TIGEM, Milan, Italy) and the primer sequence is not detailed in this thesis.

2.1.6.3. Reverse Transcription

APXL **543** (55^0C) (corresponding to nucleotides 4044-4587)

(Schiaffiano et al 1995)

5'GCCAGGGAGATCGTGGGGAAG3'

5'GTTCACCACTTTGTCCAGGTC3'

FXY **800** (52^0C) (corresponding to nucleotides 166-935) (Perry et al 1998)

5'ACAGCCTCTGCTTCAACTGC3'

5'TTGGTTCCAATAATCTGTCG3'

β-actin **838** (60^0C) (corresponding to nucleotides 610-1383)

5'ATCTGGCACCACACCTTCTACAATGAGCTGCG3'

5'CGTCATACTCCTGCTTGCTGATCCACATCTGC3'

GRPR **350** (52^0C)

5'CCTCATTGGCAACATCACT3'

5'CTGCTTCTTGACATGTATATTC3'

KAL **295** (55^0C) (corresponding to nucleotides 123-394) (Duke et al 1995)

5'GCTGGACGAGTCGCTGTCTGCCGG3'

5'CCCCCTGCTTCACCAACAGCATGT3'

2.1.7. Sources of human fetuses

Human tissues were provided by the Medical Research Council-funded Human Embryo Bank maintained at the Institute of Child Health, London, UK from embryonic and fetal collections made under local research ethical committee permission. Three normal human fetuses were collected from chemically-induced (RU486) and surgically induced terminations perfomed at 8-9 weeks after fertilisation as described (Duke et al 1995). The stage of gestation was determined by standard criteria from examination of external morphology (Larsen, 1993) and the organs dissected by Dr AS Woolf in ice-cold L15 media and then snap-frozen in liquid nitrogen prior to RNA extraction.

2.1.8. Antibodies

Primary antibodies raised against the following molecules were used in this thesis.

The concentration of the antibodies used in immunohistochemistry is given in brackets at the end.

WT-1

(C-19, Santa Cruz Biotechnology Ltd, Santa Cruz, CA, USA). This is an affinity purified rabbit polyclonal antibody raised against an 18 amino acid peptide mapping at the carboxy terminus of the human WT-1 protein which is conserved in all 4 isoforms of the protein. This antibody has been found by both the manufacturer and other groups to specifically recognise the WT-1 transcription/splicing factor protein on Western blot (Larsson et al, 1995; Winyard et al, 1996a) (1:50).

PAX2

A gift from Dr Greg Dressler (Howard Hughes Institute, Ann Arbour, Michigan, USA). This rabbit polyclonal antibody was raised against amino acids 188-385 in the carboxy terminus of PAX2 (Dressler et al; 1992). This sequence does not include the highly conserved paired domain which is located in the amino terminal region of the full length PAX2 protein (Dressler et al; 1990). Using cells transfected with PAX2, 5 and 8 there is only appreciable activity with PAX2 and, using deletion mutants of PAX2, this antibody recognises major epitopes between amino acids 270-338 (Phelps and Dressler, 1996) (1:50)

PCNA

(Ab-1; Oncogene Science, Cambridge, Massachussets, USA). This antibody is mouse

monoclonal (IgG2) to the human DNA-polymerase delta associated protein which is expressed at high levels during S phase (Bravo et al 1987). This gene is highly conserved across different species (Suzuka et al 1989) and it has been recently shown that this antibody detects a single band in the developing sheep (Attar et al 1998). Secondary biotinylated antibodies which combined anti mouse/ anti rabbit IgG was derived from the ABC kit (DAKO, High Wycombe, Bucks, UK).

2.1.9. Lectins

FITC and TRITC conjugated lectins were obtained from Sigma (Poole, Dorset, UK). Lectins are proteins or glycoproteins often derived from natural sourced such as plants, which bind to specific carbohydrate residues. The specificities of lectins used in this thesis were: *Arachis hypogaea* (peanut)(β-gal(1-3)galNAc) and *Tetragonolobus lotus purpureas* (asparagus pea)(α-L-fuc). In the kidney, lectins can be used to identify different parts of the mature nephron (Holthofer et al, 1981 and 1984; Verani et al, 1989). *Tetragonolobus lotus purpurae* binds to the proximal tubules and *Arachis hypogaea* binds to the collecting ducts.

2.2. METHODS

2.2.1. DNA Extraction from blood

The ammonium acetate protein precipitation method was used to extract DNA from blood samples which involves three stages. On each occasion that samples were transferred to different containers great care was taken not to confuse the specimens.

1. Cell Lysis

EDTA tubes containing 5-10 mls of frozen blood were uncapped and inverted over 50 ml plastic Falcon tubes and thawed at room temperature (approximately 45 minutes). Ice-cold water was added to give a final volume of 50 mls.The falcon tubes were inverted to mix well and lyse the red blood cells. The tubes were centrifuged for 20 minutes at 4^0C. The supernatant was discarded leaving a white pellet. 25mls of 0.1% NP40 (0.1mls of NP40 in 100 mls of water) was added to each tube to wash the nuclear pellet and the tubes were vortexed to break up the nuclear pellet. The samples were then centrifuged for 20 minutes at 4^0C and 2300 rpm and the supernatant discarded.

2. Nuclei Lysis and Protein Degradation

Three mls of nuclei lysis buffer (10mM TRIS/ 400mM NaCl/ 2mM Na-EDTA) was added to the tubes and they were vortexed to resuspend the nuclear pellet completely. Two hundred µl of 10% SDS and 600 µl proteinase K solution (2 mg/ml of proteinase K buffer (2mM Na-EDTA/1% SDS)) were added. The tube contents were mixed by

inversion. The samples were then incubated at 60^0C for 1 hour (or overnight at 37^0C) shaking occasionally. One ml of saturated ammonium acetate (148g NH4 acetate in 100 mls of water) which precipitates protein was added. The samples were shaken vigorously for 15 seconds. They were then allowed to stand at room temperature for 10-15 minutes and spun for 15 minutes at room temperature at 2300 rpm.

3. DNA precipitation

The supernatant was transferred to a separate tube using a plastic pastette and 2 volumes of absolute ethanol (approximately 10 mls) were added. The tubes were gently mixed by inversion and DNA threads were spooled out on the tip of a sealed glass pasteur pipette without allowing the DNA to dry. The DNA was then placed in 500 µl of TE (10 mM TRIS (tris(hydoxymethyl)aminomethane)1 mM EDTA pH adjusted to 8.0 with HCl) overnight on a rotator at room temperature.

The quantity and quality of DNA was then measured spectrophotometrically (OD 260 and 280 nm).

2.2.2. DNA Extraction from histological sections

DNA was extracted from paraffin embedded histological tissue from kidney and spleen post mortem samples.

1. Dissolving paraffin and cleaning the tissue

Small pieces of tissue (approximately 5-10 mg) were removed from the block and placed in a clean 1.5 ml eppendorf using a 20 µl pipette tip. The eppendorf was then

filled with clean 1.2 mls Xylene to dissolve paraffin. Once the paraffin had dissolved completely the eppendorf was spun at 14,000 rpm for 10 minutes. The Xylene was removed carefully from the pellet and the eppendorf was filled with 1.2 mls 100 % alcohol and shaken gently. The eppendorf was then spun again at 14,000 rpm for 10 minutes. The alcohol was removed carefully. The eppendorf was then placed upside down in a culture hood to dessicate.

2. Nuclei Lysis and Protein Degradation

DNA extraction solution was then made up freshly (100mM Tris HCl and 4mM EDTA (pH 8.0): 2 mls of solution contained 200 µl 1M Tris-HCl pH 8.0 and 16 µl 0.5M EDTA pH 8.0 and 1744 µl sterile tissue culture water. Proteinase K 40 µl (Proteinase K solution 18.6 mg/ml) was added to the DNA extraction solution.Two hundred and fifty µl of solution were added to each tube. The eppendorf was wrapped in paraffin wax to reduce evaporation and left at 37^0C overnight. The paraffin wax was then removed and the sample vortexed briefly to dislodge the tissue from the bottom. The eppendorf was then boiled for 7 minutes, ensuring that the lids were tightly on and the samples were immersed and then centrifuged at 14,000 rpm.

3. DNA precipitation

A phenol-chloroform extraction was then performed. Equal volumes of phenol/chloroform were added to the sample (approximately 300 µl). If the sample was small 50-100 µl was added to increase output. The sample was then vortexed

briefly to avoid shearing and was then spun at 14,000 rpm for 5 minutes. The supernatant was then removed and 200 µl of neat chloroform was added. Three times volume of 100% ethanol (room temperature) and 3M NaOA (pH 8) at 1/10th vol were added. The samples were then at -70^0C overnight and then spun at 4^0C for at least 0.5 - 1 hr. The supernatant was then removed and sample left to dry in culture hood for 20-30 minutes. The pellet was then resusupended in sterile water and the DNA content tested spectrophotmetrically.

2.2.3. RNA Extraction from human fetal tissue

1. Preparation of equipment and solutions

Gloves were worn at all times and efforts were made to ensure that the working area was dust free. All solutions for RNA work were made, where possible from solids which were kept separate from general chemicals in the laboratory. Where handling was essential, chemicals were weighed out using spatulas that were baked. The solutions were then treated with 0.1% diethylypyrocarbonate (DEPC) at room temperature overnight and autoclaved. DEPC is a potent inhibitor of ribonuclease (Rnase) and is broken down to ethanol and carbon dioxide by autoclaving (Fedorcsak and Ehrenberg, 1966). The only aqueous solutions which were not DEPC-treated were those which could not be autoclaved. These solutions were made up in bottles which had been DEPC treated, autoclaved and baked. Organic solvents were filtered where possible. If this was not possible, for example with phenol containing liquids,

then aliquots were kept which were only used for RNA work. All glassware, spatulas and homogenisers were baked overnight at 200^0C before use. The DEPC solution was then poured off, the plasticware was autoclaved and baked dry at 80 0C. Sterile plasticware was assumed to be RNase-free.

2. Total RNA extraction using TRI REAGANT ™

Total RNA was extracted from human fetal tissue which had been dissected using TRI REAGANT ™. This method is based on thiocyanate/phenol methodology of RNA extraction of Chomczynski and Sacchi (1987).

TRI REAGANT ™ promotes formation of RNA complexes with guanidium and water molecules and inhibits hydrophilic interactions of DNA and proteins. As a consequence, DNA and proteins are excluded from the aqueous phase leaving the RNA which can be purified. The RNA is high quality and contains the whole range of cellular RNA molecules.

Tissues for RNA extraction were either freshly dissected or previously stored in liquid nitrogen. RNA was extracted from samples as follows. Tissues were homogenised in 1ml TRI REAGANT ™ per 100mg tissue by passing sequentially through 19, 21, 23 and 25 gauge needles on a 1 ml syringe. Homogenates were left at room temperature for 5 minutes to permit the complete dissociation of nucleoprotein complexes.

Next, 0.2ml choroform/1 ml TRI REAGENT TM was added to the homogenate and they were vigorously shaken for 15 seconds before being left to stand at room

temperature for 10 minutes. The samples were centrifuged at 12,000 rpm at 4^0C for 15 minutes. The homogenate separates out into two phases; an upper clear aqueous phase containing the RNA, and a lower red coloured phase containing the DNA and protein, separated by a thick interface of cellular debris and protein.

The upper aqueous phase was removed, taking care not to take any of the interface and mixed with 0.5ml of propan-2-ol. Samples were vortexed and left to stand at room temperature for 10 minutes to precipitate the RNA. The samples were again centrifuged at 12,000 rpm at 4^0C for 15 minutes. The RNA formed a white pellet at the bottom of the tube. The supernatant was discarded and the pellet washed in ice cold 75% ethanol before respinning at the same speed for 5 minutes. The pellet was air-dried and resuspended in DEPC water, the amount depended on the size of the pellet. The RNA was measured spectrophotometrically at 260nm and stored at -70^0C until used.

2.2.4. The polymerase chain reaction (PCR)

PCR reactions are reliant on the specific binding of the primers to the homologous regions of cDNA. Within the PCR reaction several reaction several factors influence the binding specificity. Annealing temperature will affect the stringency of the reaction. The theoretical annealing temperature is dependent on the nucleotide content and can be calculated from the formula: Annealing temperature in ^{0}C = 4(G + C) + 2 (A+T) – 5. This temperature was not always optimal but was used as the mid-point for optimisation. Alternatively, the annealing temperature for a set of primers was provided by the manufacturer. It was necessary, on occasions, to further optimise

the annealing temperature for the reaction. Similarly, magnesium chloride ($MgCl_2$) concentrations needed for each set of primers were optimised to give maximum yield and minimum spurious amplification although the starting point for was 1.5mM $MgCl_2$. The volumes of the total reaction and contents are described in each case. Thermocycling conditions were as follows: Denaturation 95^0C for 5 minutes followed by 30 X cycle which consisted of 1 minute 95^0C (denaturation), 1 minute at annealing temperature and 1 minute at 72^0C (elongation) and finishing with 10 minutes at 72^0C (elongation).

2.2.5. Agarose gel electrophoresis

All PCR products were visualised by electrophoresis on agarose gel. The agarose gel was prepared by dissolving 2 g of agarose in 100mls 1x TBE and heating in the microwave at 700 watts until the agarose had dissolved. The gel was then left until hand hot and then 10 µl of ethidium bromide solution added and the gel poured.

Five µl of PCR product and 5 µl of loading dye (50% glycerol, 10mM EDTA, 0.05% bromophenol blue, 0.05% xylene cyanol) were loaded into each well and an appropriate size marker loaded into another lane. The gel was electrophoresed at 75 volts for 30 minutes – 1 hour, depending on the size of the product, and then the DNA bands visualised in ultraviolet light.

2.2.6. Reverse transcription

Reverse transcription (RT) comprises the production of complementary double

stranded DNA (cDNA) using single stranded RNA molecules as a template. The process uses a reverse transcription enzyme derived from a retrovirus. Reverse transcription can be performed using specific or random primers. The latter allows polymerase chain reactions (PCR) for different cDNAs to be performed using the products of a single RT reaction and is also more economical in terms of RNA usage. Random priming was used.

PCR allows the selective amplification of target DNA sequences (Erlich, 1989). This process required the oligonucleotide primers, one for each strand of DNA on either side of the region to be amplified. PCR relies on cycles of denaturation of the double stranded DNA to give single strands, primer annealing to their complementary sequences and synthesis of new strands from the primers by DNA polymerase. Successive repetition of this process results in the specific amplification of the region bounded by the primers.

Combination of these two techniques allows highly specific and sensitive amplification of a specific mRNA species. It is especially useful for the detection of mRNA molecules at low copy number that cannot be detected by other techniques, such as northern analysis and in very small samples such as embryonic organs. The integrity of the RNA used in each RT rection was verified by amplification of β-actin, which is expressed in all cells.

1. Removal of contaminating genomic DNA

Contaminating genomic DNA was removed from RNA samples by incubation for exactly 15 minutes at room temperature of 300ng total RNA with 1μl

deoxyribonuclease (DNase) I reaction buffer, 1 μl DNase I, (1U/l (l Amp Grade) and DEPC water to a total volume of 10 μl. The DNAse I was inactivated by adding 1 μl 20mM (EDTA) to the reaction mixture and heating to 65^0C for 10 minutes.

2. Non-specific priming technique

RNA was diluted to 0.5 μg per μl and 1 μl of this added to 1 μl of 1:15 dilution of hexamers and made up with 10 μl with DEPC water. This was heated to 70^0C for 6 minutes. The reaction mixture was cooled to 37^0C and 10 μl of a premix (4 μl 5x first strand buffer, 0.5 μl RNase inhibitor, 2 μl 2.5 mM dNTPs, 2μl 0.1M DTT and 1 μl RT). This was incubated at 37^0C for 1 hour. Tubes were heated to 95^0C for 5 minutes to destroy the RT enzyme, 80 μl of DEPC water were added and then snap chilled on ice. Five -10 μl were used in subsequent PCR reactions and the remainder stored at -70^0C.

3. PCR of reverse transcription products

Primers were designed so they crossed introns. Thus, the expected product sizes for genomic DNA and cDNA differed and contamination with genomic DNA could be detected. A number of negative controls were also used, including omission of the RT enzyme and substitution of water for the RNA or DNA (depending on the stage of the reaction).

5-10 μl of the randomly primed RT product was used for each reaction. A pre-mix was made for each sample containing: 2.5 μl 10x NH_4 reaction buffer, 1.5 μl 50 mM $MgCl_2$, 2 μl 5mM dNTPs, 0.5 μl 3' primer (100ng/ml). 0.5 μl 5' primer (100ng/ml), 1

unit of Taq polymerase and DEPC water to make a total volume of 25 µl. Primer sequences used are shown in section 2.1.6.3. To prevent evaporation, mineral oil was layered over each sample. The PCR products were then visualised on a 1% agarose gel.

2.2.7. Microsatellite markers labelled with α32dCTP

1. Polymerase chain reaction

One µl of DNA samples were aliquoted into clean eppendorfs and a master mix for the PCR reaction made which contained 1µl DNA, 1.25 µl 10x NH_4 buffer, 1.25 µl dNTPs, 0.375 µl $MgCl_2$, 1 unit of Taq polymerase and distilled water to make up to a final volume of 25 µl. The master mix was made up times the number of samples plus one to account for pipetting errors. Then 1 1 µl of α32P dCTP (3000 Ci/mmol) per ml of reaction mix was added. The mix was then aliquoted between each eppendorf. The thermal cycling conditions are described in section 2.2.4. The annealing temperatures for the individual markers was supplied by Research Genetics. The PCR products were visualised electrophoretically on agarose gel as described in section 2.2.5.

2. Gel preparation

The plates were cleaned and rinsed and dried and then cleaned with 95 % ethanol and again dried. The smaller plate was then coated with sigmacote. The plates were

allowed to dry and then assembled with spacers in between held in place by bull-dog clips.

The gel mix was made as follows: 80 mls Easigel polyacrylamide gel mix 19:1, 350 µl 10% APS and 80 µl TEMED. The gel was poured horizontally using a 50 ml plastic syringe and then the toothed combs were placed upside down in the top of the gel and also clamped in place. The gel was then left to dry for 1 hour.

The gel was then placed in gel tank with 500 mls 1x TBE in the upper and lower chambers. The combs were removed and the top of the gel cleaned with TBE and the combs were then carefully placed in to the gel so the teeth were 4mm into the gel and the gel was pre-run for 1 hour at 65 Watts.

3. Loading mix

Three µl of PCR product were added to 3 µl of Formamide loading dye (95% formamide, 20mM EDTA, 0.05% bromophenol blue) in a clean eppendorf. The samples were denatured at 95^0C for 2 minutes and 3 µl were then loaded on to the polyacrylamide gel. The gel was then run for approximately 2.5 hours.

4. Disassembling the gel

The gel plates were then carefully separated leaving the gel adhering to the lower, larger plate. The gel was then blotted on to 3MM Whatmann paper. The gel was then covered with cling film and dried on the gel drier. The gel was then placed in a cassette with an undeveloped photographic film in the dark room and left for 24 hours to develop. The film was then developed and the alleles were visualised as dark bands

on the photographic film.

2.2.8. Microsatellite markers labelled with fluorescent dyes

1. Polymerase chain reactions

The polymerase chain reactions were performed in 6.25 μl volume containing 1 μl DNA, 0.625 μl 10x NH_4 buffer, 0.625 μl dNTPs, 0.1875 μl 50mM $MgCl_2$, 0.3125 μl forward primer, 0.3125 μl reverse primer, 0.08 μl Taq polymerase and made up to 6.25 μl with distilled water.

A master mix containing the above solutions times the number of DNA samples to be analysed + 5 to allow for pipetting discrepancies was made up initially for each microtitre plate. The DNA was titrated in to a 96-well microtitre plate. Each sample was given a grid location. Then 5.25 μl of the master mix was aliquotted in to each well containing DNA using a multichannel pipette. A drop of mineral oil was place on the solution to prevent evaporation during thermal cycling and a lid was placed on the plate. The PCR reactions were carried out using the thermocyler as described in section 2.2.4. The annealing temperatures for the individual markers were supplied by Research Genetics.

2. Pooling of PCR products

Once the PCR reactions for a panel of primers were complete, the PCR products for each sample of DNA were pooled together so that they could be run out and detected in a single gel lane. The samples for each were pooled to give a total of 30 μl

volume. One μl of each FAM labelled PCR product, 1 μl of each TET labelled PCR product and 2 μl of each HEX labelled PCR product were added to the corresponding well of a fresh 96 well microtitre plate and distilled water added to give a final volume of 30 μl.

An internal size standard is required to accurately measure the allele sizes of the markers. Genescan TAMRA-350 or TAMRA-500 (if the PCR products to be run were larger than 300 bp in size) internal lane standard kit was used. This contains loading buffer (blue dextran, 50 mg/ml; 25 mM EDTA) and TAMRA (red) (which is prepared by Pst 1 digestion of plasmid DNA, followed by ligation of a TAMRA-labelled 22-mer oligodeoxynucleotide to the cut ends and a subsequent enzyme digestion with BstU 1 which yields 16 single stranded fragments which range from 35-500 bases in size in the case of TAMRA-500 or 35-350 bases in size in the case of TAMRA-350). The size standard fragments are uniformly spaced to allow accurate base size labelling.

A master loading buffer mix of 20 μl loading buffer, 25 μl TAMRA standard and 80 μl of Formamide (ACS grade) all stored at 4^0C was made freshly. Three μl of the loading buffer mix was aliquoted into each well of the 96 well plates and

2 μl of the pooled PCR product mix for each lane aliquoted into the corresponding well. The samples were then denatured at 95^0C for 2 minutes and placed on slushy ice. Three μl was then loaded in to the 24 lane polyacrylamide gels and electrophoresed on an ABI 377 analyser.

3. Polyacrylamide gel electrophoresis on the ABI 377 sequencer

The ABI 377 sequencer used with the Genescan and Genotyper software programmes is capable of simultaneously processing PCR fragment information from many markers for many DNA samples. Automated fluorescent scanning detection of DNA fragments allows measurement of the fragment molecular length based on its mobility and quantity, enabling accurate and efficient genotyping to be carried out. PCR products for a particular DNA sample, which differ in either size or dye label can be pooled together and electrophoresed simultaneously in a single gel lane together with an internal size standard. The internal size standard comprises specific double stranded DNA fragments of known sizes which are labelled with fluorescent dye TAMRA (red) and used to create a calibration curve within each gel.

The length of each PCR product within the lane is determined by comparison with the calibration curve. The width of the gel is scanned 600 times per hour by a laser fixed at a height of 15 cm from the bottom of the gel. Each scan consists of four passes, once through each of the four different colour filters. When a DNA fragment migrates into the laser scanning region a photomultiplier tube detects fluorescent light and converts it into an electrical signal. These results are transmitted to the computer and stored. Results can be viewed as electropherograms, as a reconstructed gel image or in the form of a table.

4. Gel preparation

Thirty six cm glass plates designed for the ABI 377 sequencer were used. The glass plates were cleaned thoroughly and rinsed with milli-rho distilled water and allowed to dry. They were then assembled and clamped into place in the ABI gel plate

cassette with spacers between the plates.

Five % polyacrylamide gels were prepared using ultra-pure sequagel sequencing system: 37 mls of diluent, 8 mls of concentrate and 5 mls of buffer. To this mix was added 400 µl of 10% APS and 20 µl of TEMED.

The gel was then poured using a 50 ml plastic syringe and once this was completed the toothed comb was then inserted upside down into the upper gel and this was then clamped. The gel was allowed to set for a minimum of 1 hour. Once the gel was set a 36 well toothed comb was inserted so that the teeth entered into the gel to a distance of approximately 4mm.

5. Assembly of the ABI 377 sequencer

The cassette containing the gel plates was then clamped into position in the gel chamber. Five hundred mls of 1x TBE buffer was poured in to the upper and lower buffer chambers and the electrodes attached. The plate was scanned to ensure the cleanliness of the plates and purity of the gel. The gel was then allowed to pre-run for approximately one hour until the gel temperature reached 48-52^{0}C and electric current reached the desired steady state before the samples were loaded.

6. Genescan

The information is initally stored by the ABI 377 in a gel file which stores raw data and tracking information for the entire run. Genescan is the software programme used to collect and analyse the raw data from the gel. There are two steps to the Genescan analysis. The processing step collects electrical signals from the scanner and creates

Sample files from the Gel file. The analysis step creates a project, adds sample file references and analyses the sample files one at a time. Gel processing parameters including the selection of the sample sheet to be used, the scan range and whether the lanes are automatically tracked and extracted can be set up as required. The analysis step also depends on the gel type, minimum peak heights, sizes of the peaks to be analysed, the well-to-read distance and the size-calling methods. The file name for the collected data file and the length of the electrophoresis are defined.

The identity of the individuals whose samples were to be analysed were entered on to the sample sheet. The colours of the dyes used to label the PCR products were defined.

7. Genotyper

Genotyper is a software programmed designed to analyse Genescan results files, creating genotyping data suitable for linkage analysis. Genotyper filters out peaks or bands caused by stutter, peaks or bands are arranged into groups and categories depending on the colour and size and the allele sizes are called. The functions of Genotyper were saved as a macro and the Genescan file was imported and the macro run. The results were viewed as a plot window or as a table. The results were all individually checked to ensure that the correct peaks had been assigned and the table updated accordingly.

2.2.9. Linkage analysis

2.2.9.1. Linkage analysis in VUR

1. Pedigree files

Pedigree files for each chromosome were created in the Exel package of Microsoft office for windows version 5.0 (Microsoft Corporation, Seattle, USA) and imported to be incorporated into linkage programmes at the Human Genome Mapping Project (http://www.hgmp.mrc.ac.uk). Individuals were only classified as affected if they had 1. VUR demonstrated on a cystogram (analysis V) 2. RN on an intravenous pyelogram or radio-isotope scan (analysis r) 3. VUR and/or RN (analysis T).

2. Data files

Data files were created in the preplink programme function of FASTLINK (Terwilliger and Ott, 1994) at the Human Genome Mapping Project (http:// hgmp.mrc.ac.uk). The disease parameters used were: Gene frequency 0.01, phenocopy 0.1, autosomal dominant with penetrance 75%.

The published allele frequencies for each microsatellite marker were obtained from the Co-operative human linkage centre web site and used wherever possible. If the frequencies were unavailable or there was an additional allele to published frequencies the frequencies were estimated from the founder individuals in the pedigrees.

Marker distances and orders used were supplied by with the Research Genetics sets 6.0 and 8.0 and the two maps were integrated using these distances.

3. GENEHUNTER analysis

GENEHUNTER analysis was used to analyse the genome wide scan results in VUR. GENEHUNTER is a software package that allows for rapid and complete single point or multipoint parametric and nonparametric linkage analysis from pedigrees of moderate size (Kruglyak et al, 1996) and is discussed in Section 1.6.11. GENEHUNTER is one of a number of linkage programmes available at the Human Genome Mapping Project (http://www.hgmp.mrc.ac.uk).

The pedigrees files and the data files were entered into the GENEHUNTER programme and specifications given as to the size of intervals down each chromosome the results should be computed. The results were computed at 1 cM intervals along the chromosome.

2.2.9.2. Linkage analysis in OFD1

1. Pedigree files

Pedigree files for families 1 and 2 were created manually. The affectation status of affected females and unaffected males were marked as known but apparently unaffected females were marked as unknown affectation status in view of the wide range of phenotype in OFD1.

2. Data files

Data files were created in the preplink function of LINKAGE.

Disease frequency was 0.001 the disorder was X linked dominant and the penetrance

100 %. Allele frequencies were obtained from the Genome database (www. gdb.org) and distances were calculated from the Genethon map.

3. MLINK and LINKMAP analysis

The pedigree and data files were analysed in the parametric MLINK programme of LINKAGE. MLINK computes two-point lod scores at a user-defined set of recombination fractions in this case 0.0, 0.01, 0.05, 0.1, 0.2, 0.3 and 0.4.

Multipoint analysis was performed using the LINKMAP version of the LINKAGE package (Terwilliger and Ott, 1994)

2.2.10. Single strand conformation polymorphism analysis (SSCP)

SSCP (Orita, 1989) is a commonly used initial test for mutations and several samples of either different patients or different gene areas can be tested at once. A region of DNA, optimally 200-300 bp in length is amplified by PCR in both a mutant and wild type control sample. The products are then denatured and electrophoresed through a non-denaturing polyacrylamide gel. The single stranded molecules in each product fold into a three dimensional conformation which is dependent on nucleotide sequence. Different conformations migrate differently through the gel; hence a mutation including insertions, deletions and base changes would lead to an altered migration pattern when compared with the wild type. This can be detected as a band shift visualised either by radioactive labelling of the PCR product or silver staining (Ainsworth, et al 1991) Approximately 84% of mutations are thought to be detectable

by SSCP (Jordanova et al, 1997). Detection levels can be optimized by varying different conditions such as running temperature and the glycerol concentration in the gel.

1. PCR reactions

PCR was performed using DNA from affected individuals and unaffected family members as described in Section 2.2.4.

2. Gel preparation and loading

The plates were cleaned and rinsed and dried and then cleaned with 95 % ethanol and again dried. The smaller plate was then coated with sigmacote. This was allowed to dry and the plates were assembled with 0.4 mm spacers in between and held in place by bull-dog clips. The gel mix for SSCP was: 26 mls MDE gel, 30 mls distilled water, 6mls 5x TBE, 300 µl 10% APS and 30 µl TEMED.

The gel was poured horizontally using a 50 ml plastic syringe and then the toothed combs were placed upside down in the top of the gel and also clamped in place.

The gel was then left to dry for 1 hour. The gel was then placed in gel tank with 500 mls 0.5x TBE in the upper and lower chambers. The combs were removed and the top of the gel cleaned with TBE and the combs were then carefully placed in to the gel so the teeth were 4mm into the gel and the gel was pre-run for 1 hour at 15 Watts.

Three µl of DNA product and 3 µl of Formamide dye were mixed and denatured at 95^0C for 2 minutes. The gel was run for 4 hours at 45 Watts at room temperature or overnight at 15 Watts.

3. Gel development

The gel plates were carefully prised apart and the gel blotted on to 3MM Whatman paper and then floated gel down on the surface of a tray which contained 500 mls of 10% ethanol solution and then 500 mls more of 10% ethanol solution were poured on top and the paper peeled away from the gel. This stage fixes the gel. The ethanol was then replaced by 1 litre of 1% nitric acid and this oxidation stage took 3 minutes. The nitric acid was then removed and the gel washed with 1 litre of water before impregnating it with silver by soaking it in 0.012M silver nitrate solution for 20 minutes and then rinsing down again with water for a few seconds. Bands were visualised by addition of a 0.28M sodium carbonate and 0.019 M formaldehyde solution. The development was stopped by soaking the gel in 10% acetic acid and rinsing again with water. The gel was then shrunk by immersing it in 50% ethanol for up to 30 minutes. Finally, the gel was blotted on to 3MM Whatman paper and dried at 80^0C for one hour.

2.2.11. Heteroduplex analysis

The principle of this technique is that a mutant strand will form a heteroduplex with a wild type strand and the heteroduplex will migrate at a different rate from homoduplex. It is used for samples larger than 300 base pairs in size (too large for SSCP analysis).

PCR was performed as in SSCP section. Gel plates were prepared as in the SSCP section with the exception that 1mm spacers were used and the plates were sealed

with masking tape along the bottom and sides.

Gel mix consisted of 75 mls MDE, 18 mls 5X TBE and 22.5g urea made up to a final volume of 150 mls with distilled water. To this was added 600 µl 10% APS and 60 µl TEMED. The gel was then poured using a 50 ml syringe with the plates horizontal.

Four µl PCR product was loaded with 1 µl of sucrose loading dye (50% sucrose, 0.2% bromophenol blue and 0.3% xylene cyanol). The product was then denatured under the following conditions: 95^0C for 5 minutes, 75^0C for 5 minutes, 55^0C for 5 minutes and held at 37^0C until loading. This allows the strands to separate and reanneal slowly to form heteroduplexes. Gels were electrophoresed in 0.6x TBE at 700 volts for 16 hours. The gels were then stained with 0.012M silver nitrate solution as described in the SSCP section.

2.1.12. Sequencing

1. PCR templates for direct sequencing

The region to be sequenced was amplified in a PCR reaction. One of the pairs of primers was biotinylated at the 5' end. Each reaction contained 1 µl DNA, 5 µl 10x NH_4 buffer, 3 µl $MgCl_2$, 5 µl dNTPs, 1 µl 3' primer (100ng/ml), 1 µl 5'primer (100ng/ml), 1 unit Taq polymerase and distilled water to make a total volume of 50 µl. Samples were cycled as on the thermocycler as described in section 2.2.4. and the PCR products visualised electrophoretically on agarose gel as described in section 2.2.5.

2. Obtaining a single stranded product

To obtain a single stranded PCR product for direct sequencing Dyna-M-280 Streptavidin beads were used. Dynabeads are magnetic polystyrene beads which have streptavidin covalently attached to the surface. The procedure involves the beads binding to the biotinylated strand of the PCR product (at the 5' end of the biotinylated primer). The product is then denatured and placed in a rack next to a magnet. The magnetic beads and the bound PCR strand are drawn to the side of the tube next to the magnet and the rest of the PCR mix can be removed, including the unbound other strand. Hence only one strand of DNA is left in the tube.

Thirty μl of Dynabeads were prewashed with 100μl TES (10 mM TRIS, 1 mM EDTA, 100 mM NaCl) twice. Each time, after gently resuspending the beads in TES by gentle pipetting, the tube was placed in the magnetic rack which drew the beads to the side of the tube, allowing the TES to be removed after 30 seconds. Forty three μl of PCR product was then added to the prewashed Dynabeads and mixed by pipetting. The tube was left on the bench for 5 minutes to allow the DNA to bind to the beads. The tube was tapped occasionally to keep the beads suspended. The tube was placed in the magnetic rack and the supernatant was removed. The beads plus bound PCR product were washed twice with 100μl TES as before. One hundred μl of 0.15M NaOH was then added to denature the product. This was mixed gently by pipetting, and left on the bench for 5 minutes. The tube was placed on the magnetic rack and the supernatant (NaOH plus the nonbiotinylated strand) was removed. The Dynabeads

were washed once with 100 µl TES. Then once with 100 µl distilled water. Finally, the beads were resuspended in 5 µl distilled water.

3. Sequencing reaction

The first step is to anneal the DNA template to the primer. After adding 5 µl distilled water to the Dynabeads plus bound DNA, the total volume was 7 µl (allowing for residual distilled water after washing). The 7 µl volume plus 2 µl (5pm) of the non-biotinylated PCR primer and 2 µl reaction buffer (5x) were added to a clean eppendorf tube. The mixture was warmed at 65^0C for 2 minutes, then cooled on the bench for 30 minutes.

4. Labelling reaction

To the template, the following were added: 1 µl DTT, 2 µl labelling mix (diluted 1 in 10), 1 µl α-^{35}S dATP and 2 µl sequenase V2.0 (diluted 1 in 8 in enzyme dilution buffer). The mixture was left to stand at room temperature for 4 minutes.

5. Termination reaction

Three and a half µl of the labelling reaction was added to each of four tubes (prewarmed at 42^0C for 3 minutes) containing 2.5 µl of one of ddGTP, ddATP, ddTTP or ddCTP. The tubes were placed at 42^0C for 5 minutes. 4 µl of stop solution was then added to each tube. Samples were electrophoresed within 5 days.

6. Polyacrylamide gel electrophoresis

The plates were prepared and gel mixed and poured as described in section 2.2.7. The reactions were denatured at 94^0C for 4 minutes, put on ice and 3 μl of the reactions (including stop solution dye) were loaded in each well. The four termination tubes of each reaction were run adjacently. The electrophoresis was performed at 65 Watts for approximately 2.5 hours. The gel was dissembled and developed as described in section 2.2.7.

2.2.13. Histological studies

2.2.13.1. Immunohistochemistry

Immunohistochemistry was developed by Coons et al (1955) and has become a routine histochemical technique. It involves the identification of molecules in situ by means of a specific antigen-antibody reaction associated together with a means of visualisation.

For conventional immunohistochemistry using tissue sections, tissues are first fixed to preserve morphology, then dehydrated, embedded in a wax block and cut in to thin (3-6 μm slices). The slices are placed on a glass slide which has been pre-coated to facilitate adhesion. Sections are then rehydrated, may be pre-treated to increase penetration of the antibodies as necessary and then blocked with serum and/or albumin. Serum or albumin prevents non-specific antibody binding. Optimal blocking would be provided by using serum of the same species but in this case fetal calf serum was used. Primary antibodies are then applied. In this thesis indirect

immunohistochemistry is performed in which the primary antibody is unconjugated and detected by a conjugated antibody raised to the species of the primary antibody. Renal tissue was obtained from the index case at autopsy and were fixed in 4% paraformaldehyde and embedded in paraffin wax in the pathology department at the Royal London Hospital, London, UK.

1. Rehydration and pretreatment

Ten μm sections were placed on glass slides and were dewaxed through Histoclear twice for 5 minutes and then stepwise through 95%, 90%. 75%, 50% and 30% alcohol for 3 minutes each. Finally, they were soaked in distilled water for 5 minutes. After washing in phosphate buffered saline (PBS, pH 7.4) for 5 minutes and tap water for 10 minutes they were immersed in citric acid buffer (2.1 g/l, pH 6.0) and boiled in the microwave at 700 W for 8 minutes. They were allowed to cool in a container surrounded by running tap water, washed in tap water, deionised water and then PBS.

2. Blocking steps

The avidin-biotin peroxidase technique detects peroxidase activity and therefore endogenous peroxidase must be blocked. Slides were immersed in 3% hydrogen peroxide in PBS for 10 minutes and then washed twice in deionised water for 5 minutes. Non-specific antibody binding was blocked by preincubation of the slides with fetal calf serum (10% volume/volume in PBS).

3. Primary antibody

Primary antibodies used were PAX2, WT1 and PCNA antibodies.

Excess blocking solution was carefully wiped from the slides. 100 µl of antibody diluted in blocking solution was carefully pipetted over the sections. Slides were covered with a plastic cover slip to ensure even distribution of the antibody and placed in a humid chamber. This was prepared by lining a surgical instrument tray with PBS soaked tissues. Slides were incubated at 37^0C for 1 hour or 4^0C overnight depending on the antibody and then washed three times in PBS.

4. Detection, counterstaining and mounting

A commercially available avidin-biotin peroxidase (ABC) kit was used. This is based on the ability of the egg white glycoprotein avidin to non-immunologically bind four molecules of the vitamin biotin. Multiple copies of the biotinylated secondary antibody bind with unlabelled primary antibody (bound to the tissue antigen of choice). The section is then treated with the avidin-biotin peroxidase complex (ABC). This binds to multiple sites so that the signal is greatly amplified. Primary antibodies can therefore be used at a higher dilution using this technique resulting in the lowering of spurious staining. Peroxidase activity is then detected by colour changes in DAB (diaminobenzadine tetrahydrochlorodihydrate). A brown precipitate is produced by the peroxidase in the streptavidin-biotin mixture and this can be monitored by direct vision or microscopically. Slides can then be counterstained to allow histological detection of structure and to aid localisation of the antibody.

Species appropriate biotinylated antibody at a dilution of 1:100 in TBS was pipetted

carefully over sections. Slides were covered, placed in the humid chamber and incubated for 30 minutes at room temperature. At the same time the streptavidin-biotin mixture was made from 1:100 dilutions of the two reagants and kept at room temperature during the incubation period of the secondary antibody.

Slides were rinsed and washed in TBS and then the streptavidin mixture applied. Slides were again incubated for 20-30 minutes at room temperature. After washing well in TBS, with a final rinse in water, slides were immersed in 0.5mg/ml DAB with 0.03% hydrogen peroxide. Slides were allowed to develop for 1-10 minutes and, depending on the intensity of the reaction.

Methyl green stains nuclei blue and is therefore an appropriate contrast with the brown of DAB. Sections were immersed in 0.5% methylgreen in 0.1M sodium acetate (pH 4.0) for 5-10 minutes. The slides were then washed three times in deionised water by dipping them 10 times in the first and second wash and then 30 seconds in the third. This procedure was repeated with three changes of butan-1-ol.

The slides were then immersed in histoclear for 10 minutes and allowed to dry and were then mounted in dextropopoxyphene (DPX) and left to dry overnight.

The slides were then examined on a Zeiss Axiophot microscope.

2.2.13.2. Lectin staining

Sections were prepared as decribed for immunohistochemistry rehydration and pretreatment.

After washing in PBS for 5 mins, sections were incubated in propidium iodide (PI) with RNase A in PBS at 370C for 30 mins, and then counterstained with FITC-

conjugated *Tetragonolobus lotus* (pea Asparagus) or *Arachis hypogaea* (peanut) lectins at 1 in 50 dilution of PBS in a humid chamber at room temperature for 1-4 hours or overnight at 4^0C. These lectins bind to proximal tubules and distal segments (distal tubule and collecting ducts) respectively. The sections were then washed three times in PBS. Sections were mounted in Citifluor^{TM} examined under fluorescence (wavelength 488 nm for FITC and 568 nm for PI) on a Leica confocal laser scanning microscope.

2.2.14. Ascertainment of patients studied

Ethical permission had been granted by the Institute of Child Health, London UK for this study and families were supplied with an information sheet about the study. The families were visited and detailed clinical histories were taken. Radiological data was confirmed by contacting clinicians responsible for their care wherever possible.

Peripheral venous blood samples were obtained from family members (10-20mls) into EDTA tubes for DNA extraction. Two mls sample in a lithium heparin tube was taken from an affected individual in each pedigree was sent for a basic chromosome karyogram at the regional cytogenetics centre and a 10 mls EDTA sample was sent to European Collection of Cell Cultures, CAMR, Salisbury, Wiltshire, UK for transformation into immortalised cell lines by EBV. Samples from pedigree 2 (VUR) were provided by Dr JA Goodship (Newcastle University, Newcastle, UK) pedigrees 6 and 7 (VUR) by Dr K Devriendt (University of Leuven, Leuven, Belgium) and pedigree 2 (OFD1) by Professor D Donnai (University of Manchester, Manchester, UK).

Renal ultrasound scans were performed on cases of OFD1 who had not had renal scans before or only when they were very young as the polycystic renal disease may develop later. Apparently unaffected females with OFD1 in the pedigrees were assessed clinically and with renal ultrasound scans when possible.

3.1 Oral-facial-digital syndrome type 1

3.1.1. Clinical features

A positive diagnosis of OFD1 was made based on a combination of 1. Facial features including facial asymmetry, facial milia and hypertelorism 2. Oral features including cleft lip and palate, tethered or cleft tongue, hamartomata, skin tags and a range of dental abnormalities 3. Digital features which included brachydactyly, syndactyly and polydactyly. Additional features including polycystic renal disease, cysts in other organs, multiple miscarriages and central nervous system abnormalities were also noted.

In total, I ascertained and analysed five pedigrees and fifteen sporadic cases of OFD1. The pedigrees are shown in figures 3.1 – 3.5 and the typical clinical details are summarised in tables 3.1- 3.5. The typical clinical details of the sporadic cases are summarised in table 3.6. Figure 3.6 illustrates some of the typical dysmorphic features in affected individuals in pedigree one. Figure 3.7 shows renal and pancreas ultrasound scans in individuals III.1 and III.2 in pedigree one. Figure 3.8 shows dysmorphic features in pedigree five and Figure 3.9 shows dysmorphic features in sporadic cases 2, 3 and 4.

The pedigrees are consistent with X-linked dominant inheritance. With the exception of pedigree three, in which an affected male died soon after birth, all affected individuals are female. In all the pedigrees multiple first trimester miscarriages were noted in affected females which were considered to be

consistent with miscarriage of affected male infants. This was not the case in the mothers of the sporadic cases.

A wide range of age of onset and severity of polycystic renal disease was noted. Pedigrees one, two and four had polycystic renal disease as the presenting clinical feature. In pedigree two, renal ultrasound scans have all been reported as normal but the age at which the ultrasounds were performed is not clear. In pedigree four, renal ultrasound scans were requested but the family declined further investigation. Six out of fifteen sporadic cases have polycystic renal disease; one individual has chronic renal failure and four are in end stage renal failure. Sporadic case S1 had a normal renal ultrasound as a neonate but bilateral polycystic renal disease by seven years of age. In pedigree one there is a wide range of severity of polycystic renal disease. III.1 and III.2 have bilateral polycystic renal disease and III.1 was in end stage renal failure in her late teens. I.2 was in end stage renal failure in the 5^{th} decade of life whereas II.2 and II.4 have normal renal function as assessed by plasma creatinine in the 3^{rd} decade of life, II.2 has unilateral renal cysts and II.4 has bilateral renal cysts. In view of the wide range of first documentation of renal polycystic disease (neonatal to 5^{th} decade) and unknown rate of deterioration in renal function, it is difficult to predict the occurrence and evolution of kidney disease in an individual case of OFD1.

The dysmorphic features are very variable between affected individuals in a single pedigrees and between pedigrees and sporadic cases. The digital features are asymmetrical in most individuals. Learning difficulties are common. Most individuals have not had cerebral imaging but in the two cases that have had

cerebral imaging cerebral cysts were noted. In addition, cysts were present in the pancreas in individuals in pedigrees 1 and 5.

As part of the clinical assessment, a chromosome karyotype analysis was performed in all sporadic cases and in an affected individual in each pedigree. No gross chromosomal aberrations were noted. This excludes unbalanced translocation as the alternative explanation for the high incidence of recurrent miscarriage in affected females.

Figure 3.1. Pedigree One OFD1

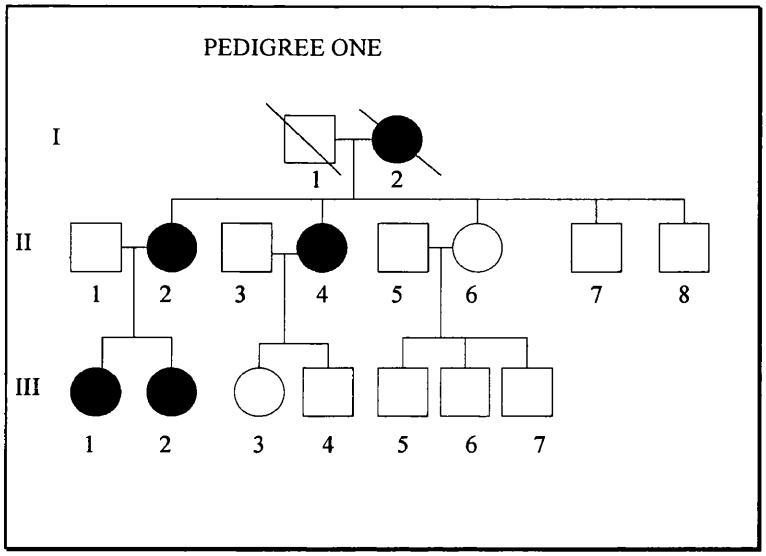

Table 3.1. Clinical details of pedigree One OFD1

Individual	Renal ultrasound scan	Renal function	Oral and facial features	Digital features	Other
I.2	Bilateral polycystic kidneys	End stage renal failure (5th decade) Renal transplant	'Characteristic face'	Not documented	Learning difficulties Multiple miscarriages
II.2	Unilateral polycystic kidney	Normal plasma creatinine (3rd decade)	Hypertelorism Pseudocleft upper lip Tongue hamartoma	Not documented	Learning difficulties Multiple miscarriages
II.4	Bilateral polycystic kidneys	Plasma creatinine 104μM (3rd decade)	Hypertelorism Pseudocleft upper lip Tethered tongue Cleft palate	Syndactyly middle and index finger left hand Left hallux varus and duplication	Learning difficulties Multiple miscarriages
III.1	Bilateral polycystic kidneys	End stage renal failure aged 15 years Renal Transplant	Hypertelorism Pseudocleft upper lip High arched palate Oral frenulae, absent canines	Brachydactyly left index finger and 4th toes	Learning difficulties Pancreatic cysts
III.2	Bilateral polycystic kidneys	Plasma creatinine 54μM (2nd decade)	Pseudocleft upper lip Hypertelorism High arched palate,tethered and cleft tongue	Brachydactyly 4th toes	Learning difficulties

Figure 3.2
Radiological features of pedigree one (OFD1)

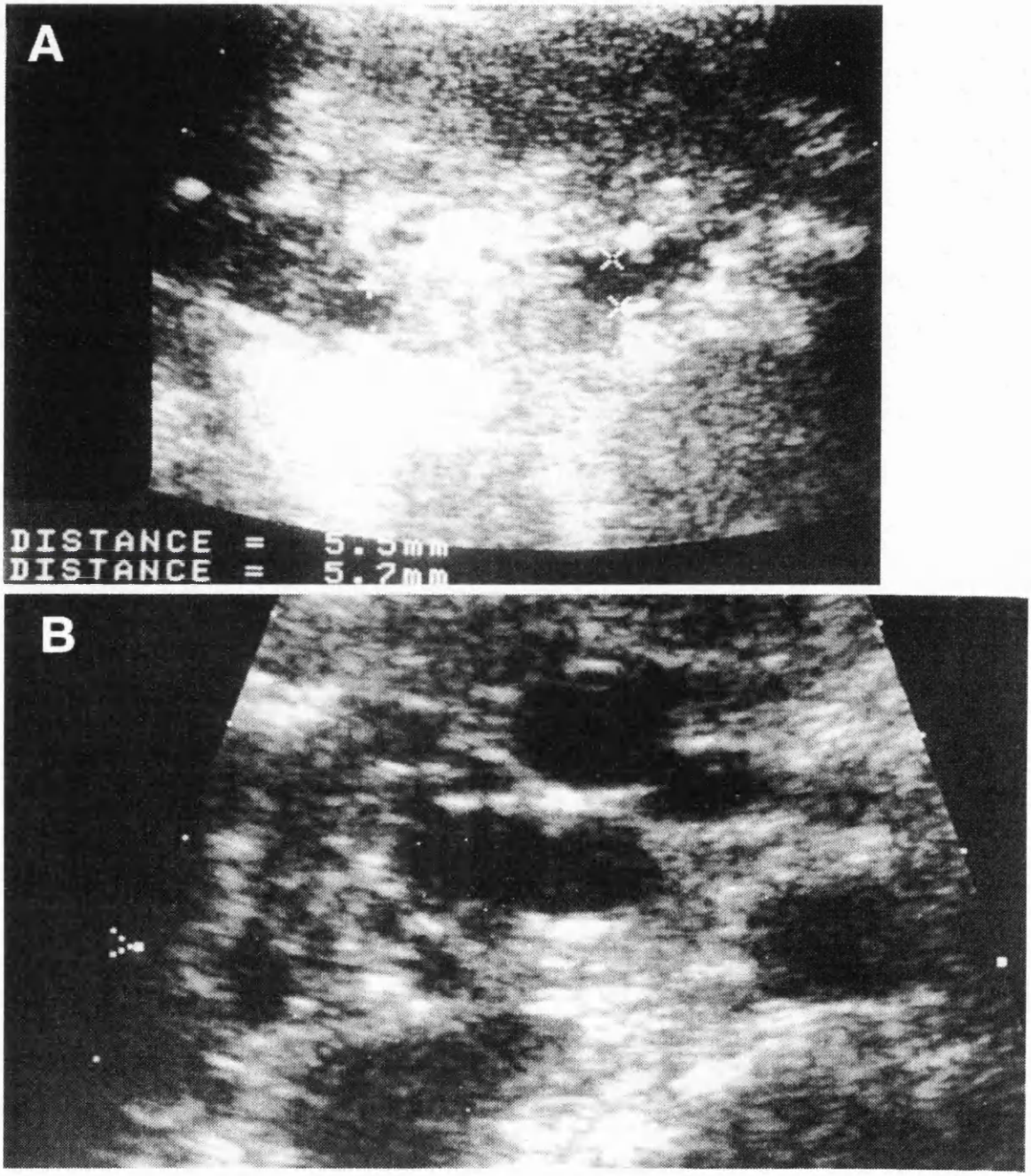

A. Ultrasound scan of kidney of III.2 showing multiple cysts up to 5mm in diameter
B. Ultrasound scan of pancreas of III.1 showing multiple cysts.

Figure 3.3
Dysmorphic features of pedigree one (OFD1)

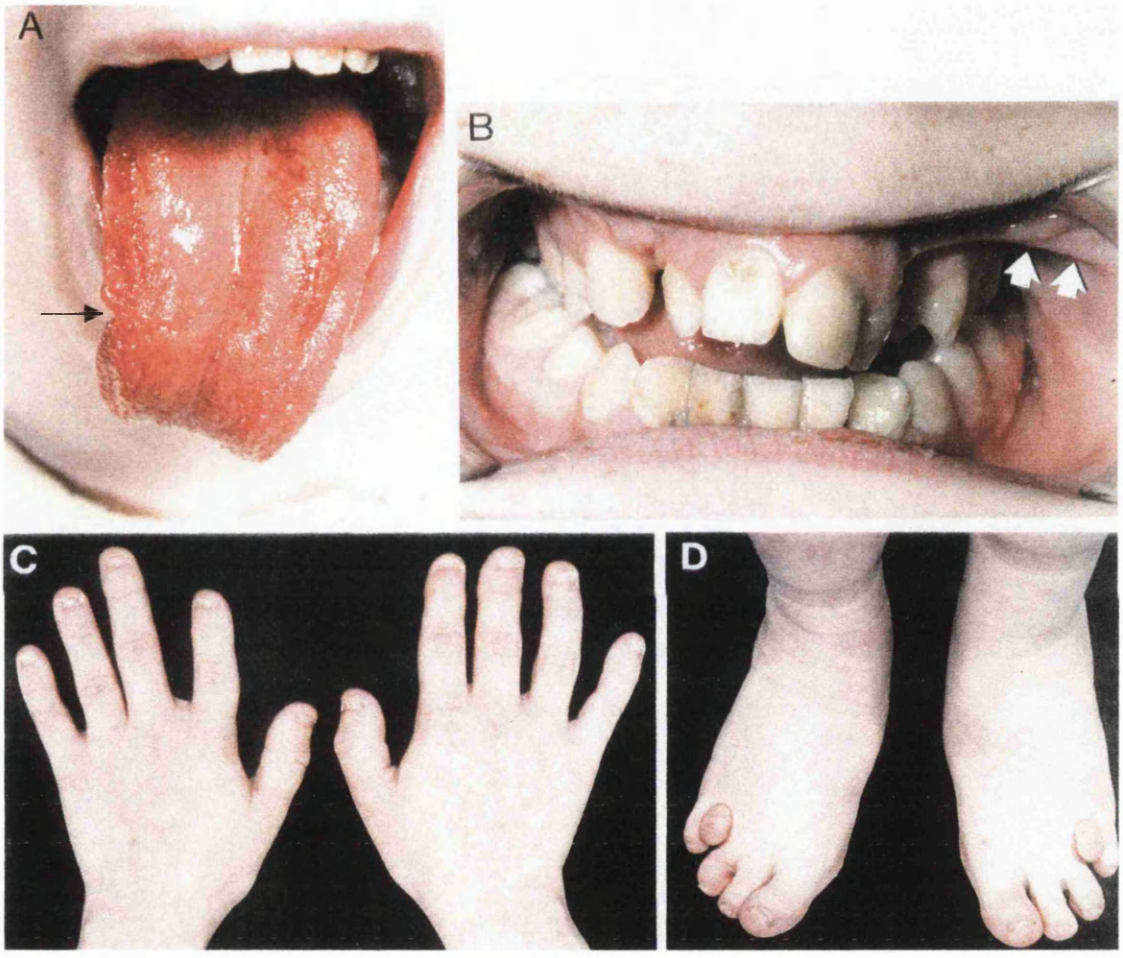

A. Individual III.1 – Cleft of the tongue
B. Individual III.1 – Abnormal dentition - absent canine teeth and oral frenulum
C. Individual III.1 – Brachydactyly of index finger of the left hand.
D. Individual III.1 – Brachydactyly of 4th toes in both feet.

Figure 3.4. Pedigree Two

Pedigree two is also described by Donnai et al, 1987

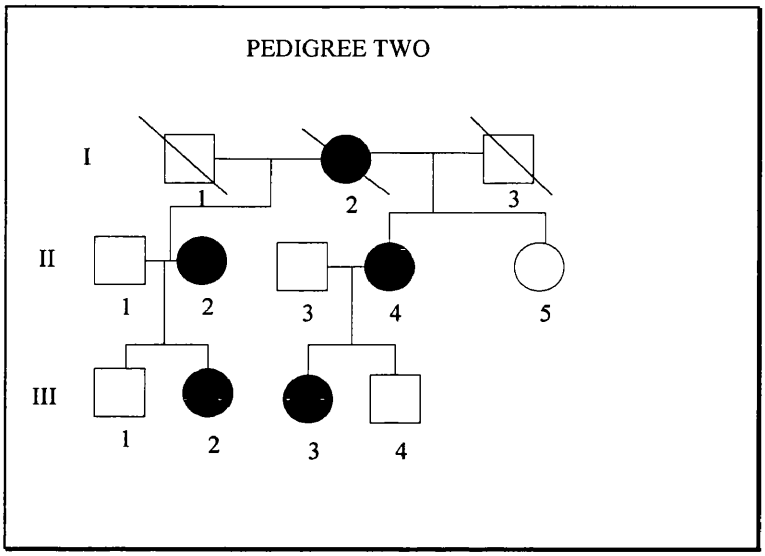

Table 3.2. Clinical details of pedigree Two OFD1

Individual	Renal ultrasound scan	Renal function	Facial and oral features	Digital features	Other
I.2	Bilateral polycystic kidneys	End stage renal failure (5th decade)	Oral frenulae	Brachydactyly	Not documented
II.1	Bilateral polycystic kidneys	End stage renal failure (6th decade)	Not documented	Brachydactyly and 'curved fingers'	Not documented
II.4	Bilateral polycystic kidneys	Chronic renal failure	Irregular lip margin Bilateral jaw cleft Oral frenulae	Brachydactyly	Not documented
III.2	Bilateral polycystic kidneys	Not documented	Facial asymmetry Anti-mongoloid slant Facial milia Cleft lip Oral frenulae Irregular tongue	Brachydactyly Cutaneous syndactyly Pre axial polydactyly right foot Broad halluces	Learning difficulties
III.3	Unilateral renal cysts	Not documented	Facial milia Irregular lips Oral frenulae Cleft jaw Irregular tongue	Brachydactyly Clinodactyly of 4th and 5th fingers	Tremor of hands

Figure 3.5. Pedigree Three OFD1
Pedigree Three is also described by Goodship et al, 1991

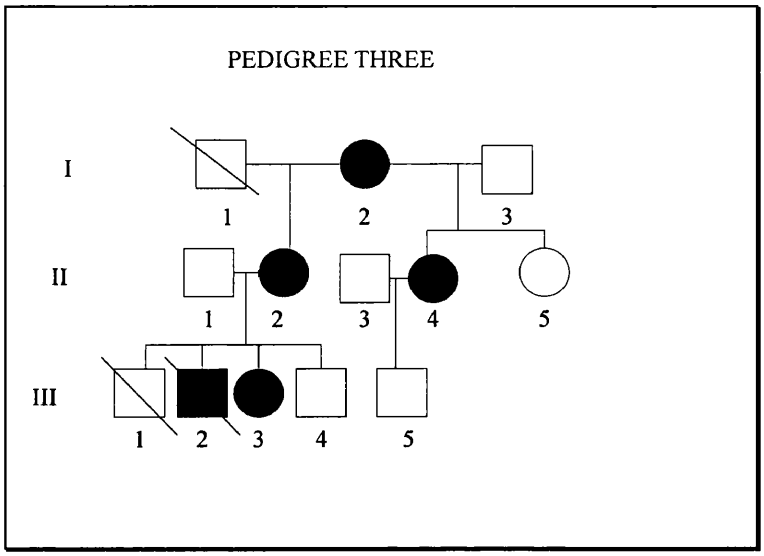

Table 3.3. Clinical details of pedigree 3 OFD1

Individual	Renal ultrasound scan	Renal function	Facial and oral features	Digital features	Other
I.2	Normal	Not measured	Bifid tongue Multiple oral frenulae	Not described	Not recorded
II.2	Normal	Not measured	Pseudocleft upper lip Lobulated tongue Oral frenulae	Short fifth metacarpals	Two first trimester miscarriages
II.4	Normal	Not measured	Multiple oral frenulae Lobulated tongue	Not described	Not recorded
III. 2	Normal	Not measured	Midline pseudocleft upper lip Cleft soft palate Hypertelorism	Bifid halluces with varus Bifid toe right foot	Cardiac defect died as neonate due to cardiac failure
III.3	Not done	Not measured	Multiple oral frenulae Cleft lip and palate	Not described	Not recorded

III.1 died of Sudden Infant Death syndrome in the first year of life. He was reported to have no dysmorphic features.

Figure 3.6. Pedigree Four OFD1
Pedigree Four is also described in Scolari et al, 1997

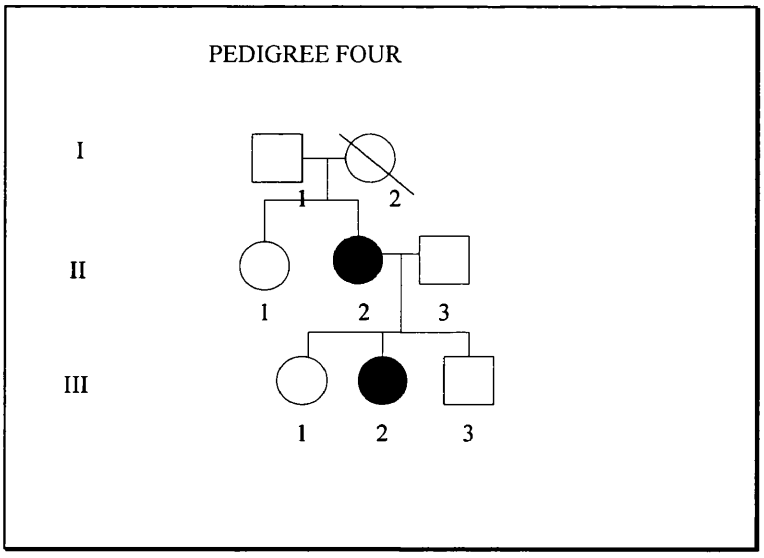

Table 3.4. Clinical details of Pedigree Four OFD1

Individual	Renal ultrasound scan	Renal function	Facial and oral features	Digital features	Other
II.2	Bilateral polycystic kidney disease	Chronic renal failure (5^{th} decade)	Cleft palate Characteristic face Patchy alopecia	Clinodactyly of fingers	Miscarriage
III.2	Bilateral polycystic kidney disease	End stage renal failure (16 years) Renal transplant	Facial asymmetry Cleft palate Cleft lip	Clinodactyly of fingers and toes. Syndactyly of fingers	Liver and pancreatic cysts Cerebral atrophy and learning difficulties

Figure 3.5. Pedigree Five OFD1
Pedigree Five is also described by Kernohan and Dodge, 1969

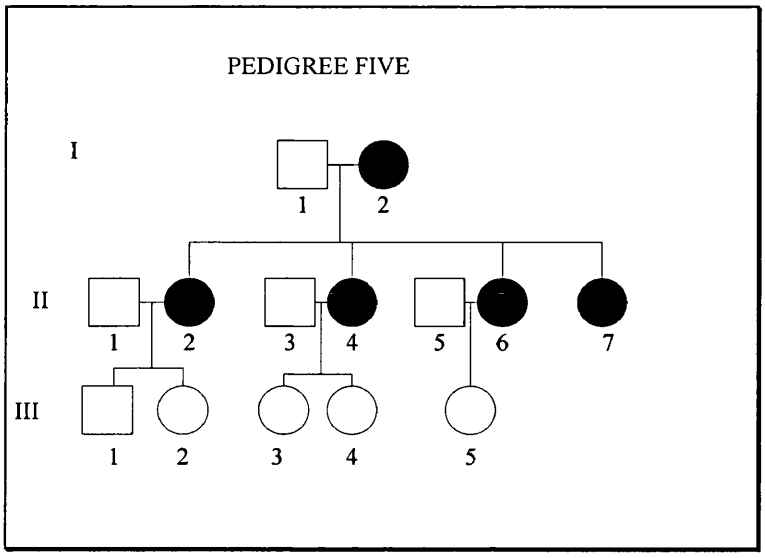

Table 3.5. Clinical details of pedigree Five OFD1

Individual	Renal Ultrasound	Renal function	Facial and oral features	Digital features	Other
I.2	Not performed	Not measured	Hypertelorism Extra teeth Hamartoma Oral frenulae	Not documented	Not documented
II.2	Not performed	Not measured	Hypertelorism Tongue tie Absent lower incisors Oral frenulae	Syndactyly middle and ring finger left hand	Three first trimester miscarriages
II.4	Not performed	Not measured	Oral hamartoma Bifid tongue Oral frenulae	Clinodactyly	First trimester miscarriage
II.6	Not performed	Not measured	Hamartoma on tongue	Not documented	Not documented
II.7	Not performed	Not measured	Facial milia Lobulated and tied tongue Hamartoma	Brachydactyly and syndactyly	Learning difficulties

It has not been possible to examine any individuals in generation III.

Figure 3.8
Dysmorphic features of pedigree five (OFD1)

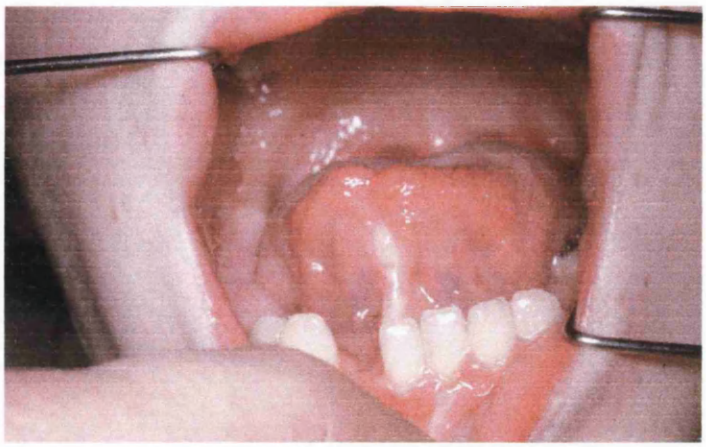

A. Individual II.1 – hypertrophied frenulum, bifid tongue and absent incisor

B. Individual II.2 – cleft tongue and hamatomata

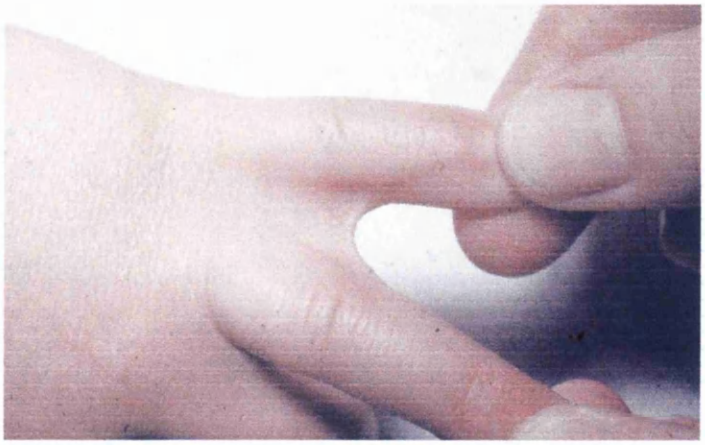

C. Individual II.1 – syndactyly left hand

Table 3.6. Clinical details of sporadic cases of OFD1

Individual	Renal ultrasound scan	Renal function	Facial and oral features	Digital features	Other
S1	Bilateral polycystic renal disease aged 7 years.	Not known	Hypertelorism Absent teeth Dental cysts Tongue tie Cleft palate	Brachydactyly	Learning difficulties Poor coordination
S2	Bilateral polycystic renal disease aged 15years	Chronic renal failure	Hypertelorism Facial milia Cleft lip Nasal cyst Cleft palate Overcrowded teeth	Bilateral poly syndactyly	Learning difficulties
S3	Normal renal ultrasound aged 20years	Normal aged 20 years	Cleft lip Facial milia Overcrowded teeth Oral frenulae Patchy alopecia	Brachydactyly all digits	Learning difficulties
S4	Bilateral polycystic renal disease aged 17years	End stage renal failure	Hypertelorism Facial milia Tongue tie Cleft palate Overcrowded teeth	Not documented	Learning difficulties
S5	Not performed	Not known	Hypertelorism Irregular lip margin Overcrowded teeth Oral frenulae Cleft lip and palate Hypoplastic tongue	Syndactyly left index and middle finger Pre-axial polydactyly left foot Syndactyly left foot	Learning difficulties
S6	Normal renal ultrasound aged 4 years	Normal	Cleft palate Tongue tie Absent teeth Hamartomata	Syndactyly fingers bilaterally Brachydactyly	Learning difficulties
S7	Normal renal ultrasound aged 15 years	Normal	Cleft lip and palate Tongue tie Lobulated tongue Extra teeth Hamartoma	Right hanad and foot brachydactyly	Learning difficulties
S8	Not performed	Not measured	Facial milia Tongue tie Hamartoma High palate Absent molars	Syndactyly Clinodactyly little fingers Pre-axial polydactyly right foot	Learning difficulties
S9	Normal renal ultrasound aged 3 years	Normal	Cleft lip High arched and cleft palate Delayed dental eruption Alopecia Facial milia	Brachydactyly Pre-axial polydactyly Syndactyly right foot	Learning difficulties Absent corpus callosum with large cyst
S10	Bilateral polycystic renal disease	End stage renal failure	Hamartoma Oral frenulae dental abnormalities	Polydactyly Clinodactyly Bony syndactyly	Not documented
S11	Not performed	Not measured	Bilobed tongue Oral frenulae Irregular teeth	Clinodactyly 5th toes	Not documented
S12	Bilateral polycystic kidneys as a neonate	End stage renal failure as a neonate	Cleft lip and palate Hypertelorism	Pre-axial polydactyly both hands	Not documented
S13	Bilateral polycystic kidneys	End stage renal failure	Asymmetrical face Facial milia	Brachydactyly	Not documented
S14	Not performed	Not measured	Oral frenulae	Polydactyly and syndactyly	Learning difficulties
S15	Not performed	Not measured	Cleft lip and palate	Brachydactyly	-

Figure 3.9
Dysmorphic features of sporadic cases of OFD1

A. Sporadic case 2
– hypertelorism, asymmetrical face

B. Sporadic case 4
– clefting of the lip

C. Sporadic case 3
– cleft lip

3.1.2. Histological studies in OFD1

Histological studies were performed on renal autopsy tissue from individual I.2 in pedigree 1 as shown in Figures 3.10 and 3.11 The kidneys contained multiple cysts. As expected for an end-stage kidney, there was marked fibrosis between cysts (Figure 3.10 A and B). Most cysts were lined by flat epithelial cells and were enclosed by fibrotic walls. In approximately 5-10% of such structures in any section, a single glomerular tuft was seen to be attached to the cyst lining (Figure 3.10 A and B). A subset of nuclei in these tufts stained with antibody to WT-1, consistent with identities as podocytes (Figure 3.10 C) and many tufts within the cysts contained open capillary loops. Other glomeruli had mildly dilated Bowman's spaces and a minor population of glomerular tufts were sclerosed. Up to 50% of the nuclei in the tufts of cystic glomeruli stained with antibody to PCNA (Figure 3.10 D), suggesting proliferation. The majority (> 90%) of cysts failed to stain with either FITC conjugated *Tetragonolobus lotus* and *Arachis hypogaea* lectins (Figure 3.11 A) meaning that they did not orginate from the proximal or distal convoluted tubules respectively. Mildly dilated tubules were also noted (Figure 3.10 G and H) of up to 100-200 μm. These stained with *Arachis hypogaea* lectin (Figure 3.11 B) and never contained glomerular tufts suggesting a distal tubule rather than glomerular origin. The epithelial cells which lined the distal tubule cysts stained with PAX2 antibody (Figure 3.10 G and H). Glomerular cysts did not express PAX2 (Figure 3.10 E and G). Dilated distal tubules showed no immunoreactivity with WT-1 antibody (data not shown). Up to 50% of nuclei in dilated distal tubules stained with PCNA antibody (data not shown).

The majority of cysts failed to stain with lectins that bind to proximal and distal tubules and some contained tufts with capillary loops surrounded by cells staining for WT-1, a protein expressed by podocytes in the postnatal kidney. These data demonstrate that these cysts are of glomerular origin. However, a minority of smaller cysts stained with *Arachis hypogaea* lectin, indicating an origin in distal tubules. These data demonstrate that these cysts are of glomerular origin.

Normally, less than 1% of nuclei in normal postnatal glomeruli are PCNA positive but in this tissue proliferation was noted in approximately 50% of cells within glomerular tufts attached to OFD1 cyst walls. Deregulated proliferation might therefore be important in the genesis of OFD1 renal cysts.

Figure 3.10
Histology slides in OFD1 – individual I.2 in pedigree one

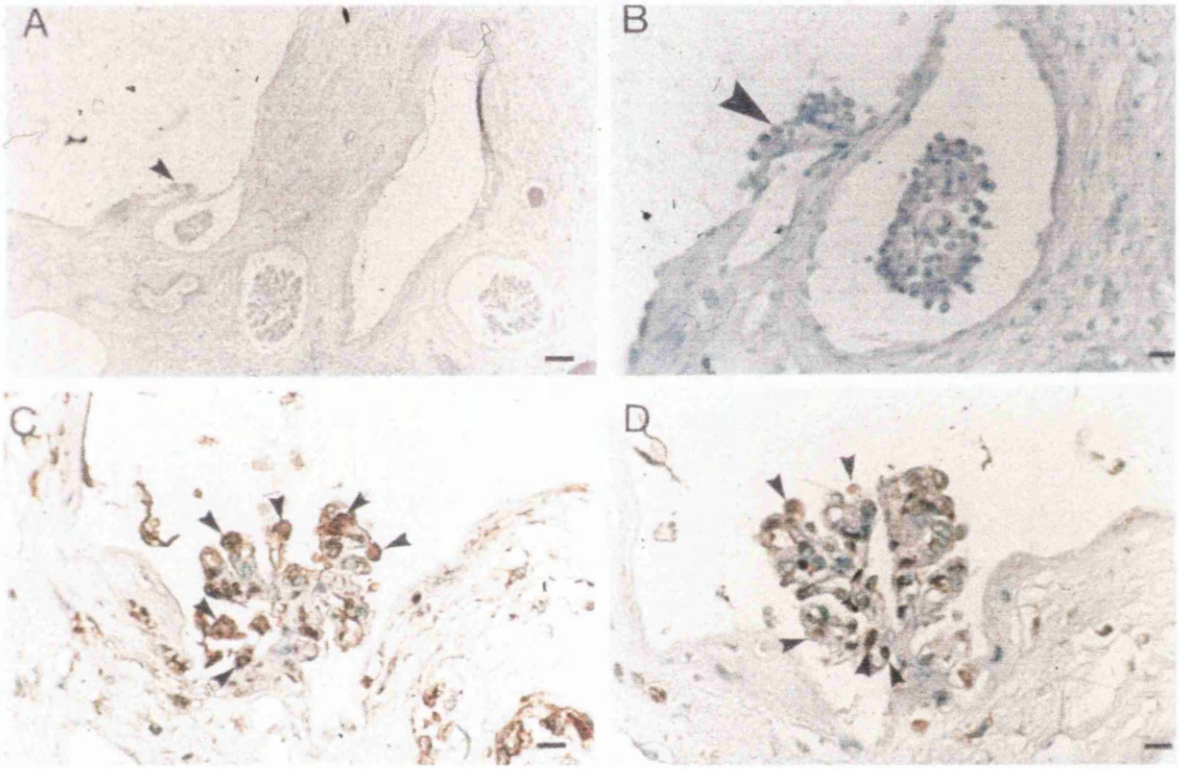

A. Low power of renal tissue showing cysts of varying diameter
B. Higher power demonstartes glomeruli with mildly dilated Bauman's spaces as well as larger glomerular cysts.
C. Podocytes (arrowheads) in a glomerular cyst stained with WT-1 antibody.
D. PCNA-staining nuclei (arrowheads) in the tuft of a cystic glomerulus.

All nuclei in the panel were counterstained with methyl, green, while positive immunohistochemical signals appear brown.
Bars are 60μm in A, 15μm in B and G and 10μm in other frames.

Figure 3.10
Histology slides in OFD1 – individual I.2 in pedigree one

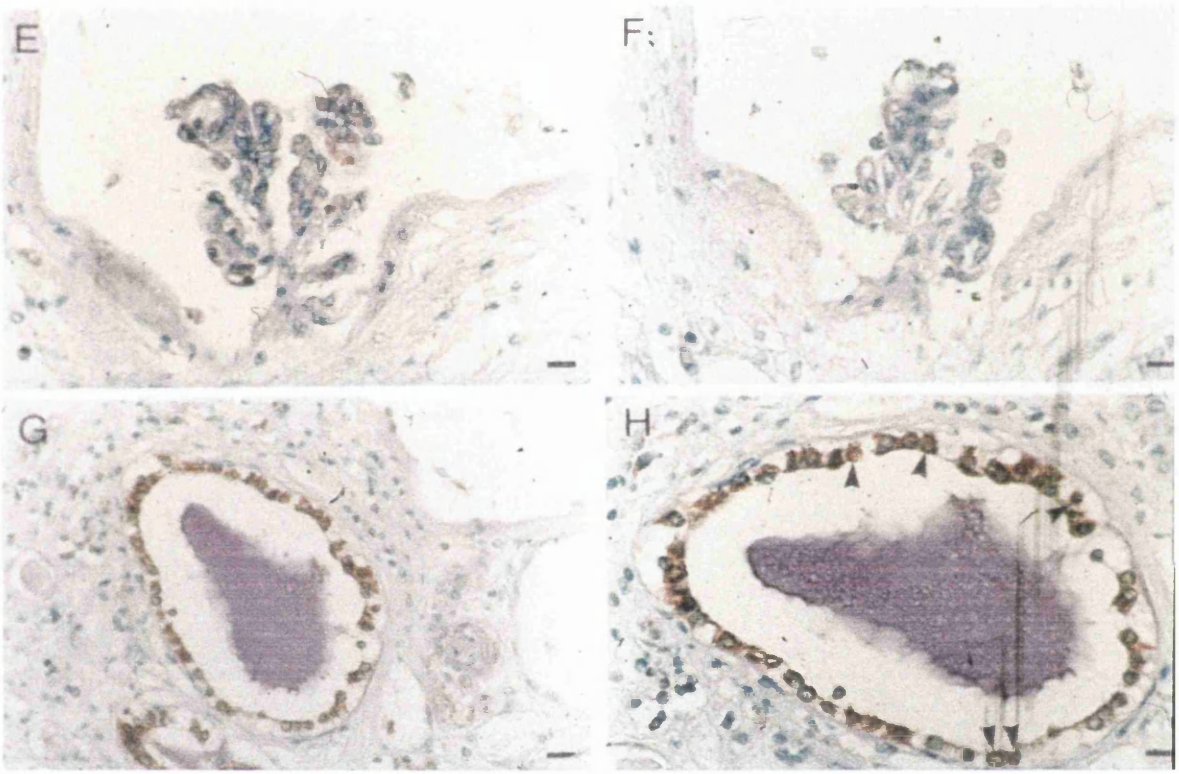

E. Absence of PAX2 protein nuclear staining in a glomerular cyst.
F. Representative lack of staining when first antibodies are omitted.
G. A cystic distal tubule epithelium stained with antibody to PAX2; two cysts on the right were negative for PAX2 and were presumably of glomerular origin.
H. High-power view of distal cyst depicted in G. In some cells PAX2 staining in clearly localised to nuclei (arrowheads).

All nuclei in the panel were counterstained with methyl, green, while positive immunohistochemical signals appear brown.
Bars are 60μm in A, 15μm in B and G and 10μm in other frames.

Figure 3.11
Lectin histochemistry in OFD1 kidney – individual I.2 in pedigree one

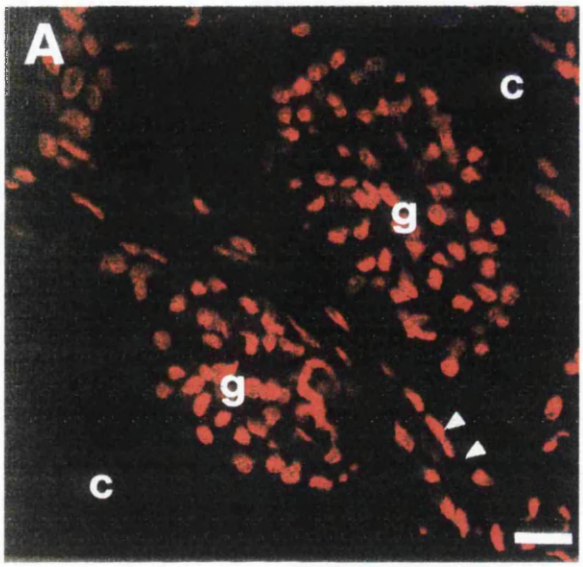

A. Parietal epithelium (arrowheads) of two glomerular cysts (c) showed no rectivity with FITC-conjugated *Arachis hypogaea lectin*. Glomerular tufts are also indicated (g). Lack of staining was also noted with *Tetragonolobus Lotus lectin* (not shown)

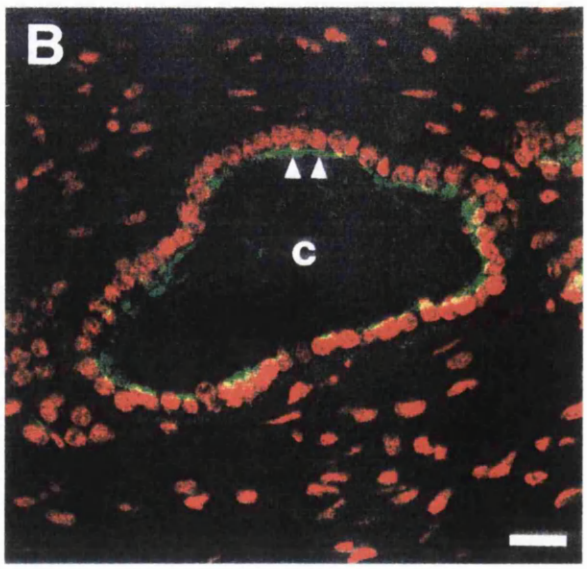

B. Epithelial cells (arrowheads) lining a tubule stained positively with FITC-conjugated *Arachis hypogaea* (green) suggesting a distal tubule origin. All nuclei are stained red with propodium iodide (PI). Bars are 20mm

3.1.3. Mapping OFD1 to the short arm of the X chromosome

3.1.3.1. Microsatellite marker analysis

A set of sixteen microsatellite markers spaced down the X chromosome at an average of 10.75 centiMorgan intervals (Research Genetics set 6.0) were amplified as an initial screen to find the location of the gene for OFD1 using samples from pedigrees 1 and 2. The markers used were *DXS6807, DXS987, DXS989, DXS1068, DXS6810, DXS1003, DXS7132, DXS6800, DXS6789, DXS6799, DXS6797, DXS6804, DXS1001, DXS1047, GATA31E08* and *DXS1193*. Further markers were chosen from the Genethon map. The only marker in which recombinations did not occur in affected females in the two pedigrees was *DXS987*. Additional microsatellite markers for finer mapping were chosen from the Genethon map and the region was narrowed to a 19.8 centiMorgan interval on Xp22.2-22.3 between the telomeric marker *DXS996* and the centromeric marker *DXS7105* (Figure 3.12 shows affected females in pedigree 1 sharing the same allele of *DXS8022* and figure 3.13 shows affected females in pedigree 2 sharing the same allele of an intragenic polymorphic marker for *KAL*; both markers are within the region).

The haplotypes for the two pedigrees for this region are shown in Figure 3.14 The region is large but was not narrowed further as it was not possible to be sure whether apparently unaffected females had OFD1 or not. In affected males, the phenotype would be predicted to be very severe and so unaffected males were labelled as definitely unaffected. In pedigree one II.6 is an apparently unaffected female as she has none of the dysmorphic features of her

Figure 3.12
Polymorphic marker *DXS8022* in OFD1 pedigree one

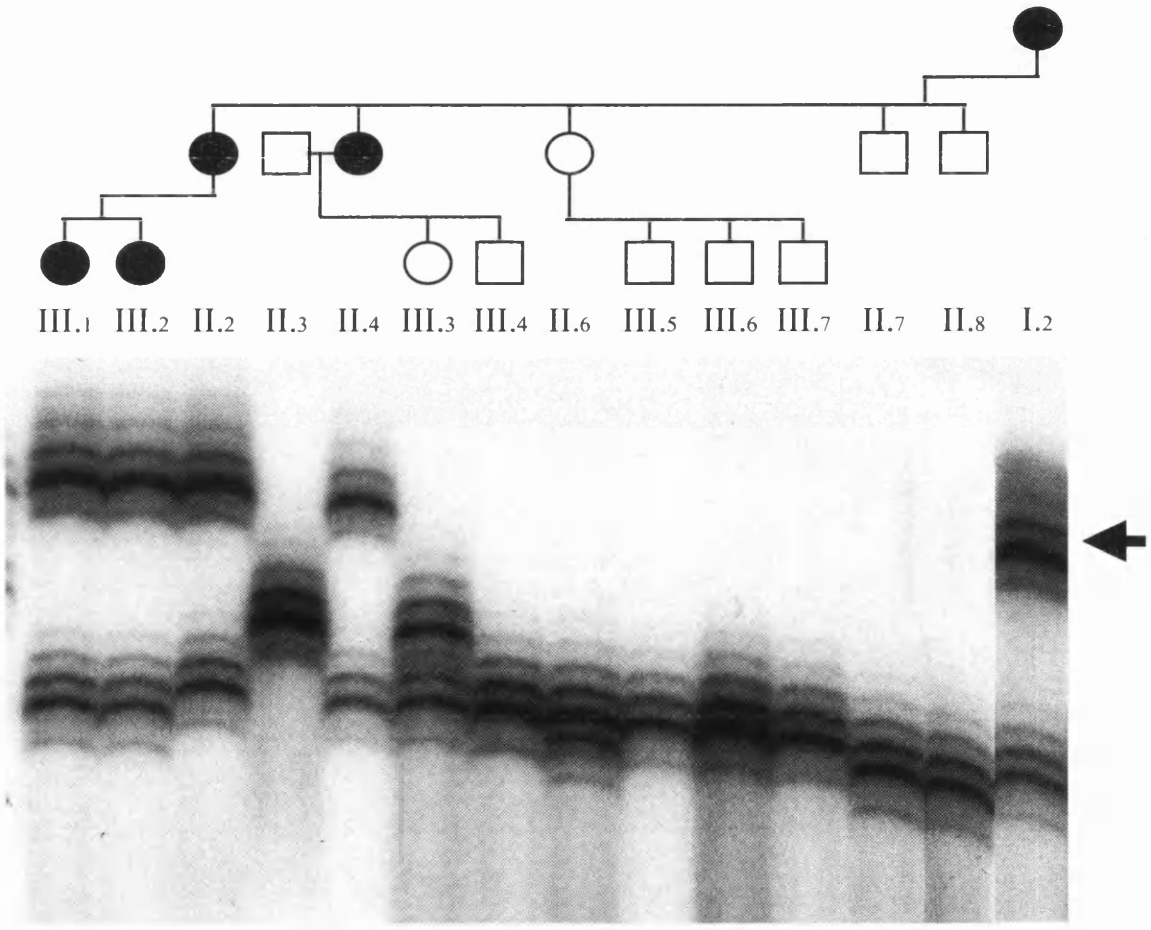

Note: ⟶ Allele shared by all affected females in pedigree one

Figure 3.13
Polymorphic marker *KAL* in OFD1 pedigree two

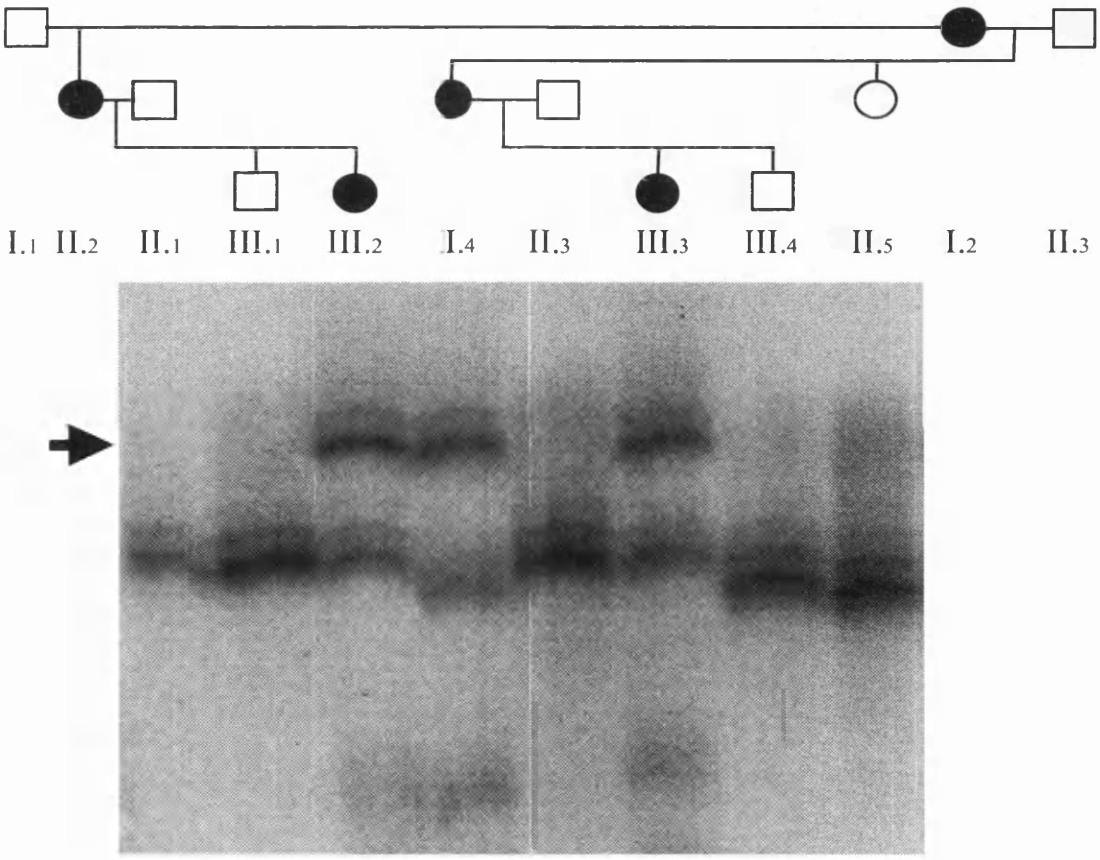

Note: ⟶ Allele shared by all affected females in pedigree two

Figure 3.14
Haplotype results for pedigrees one and two used in mapping OFD1

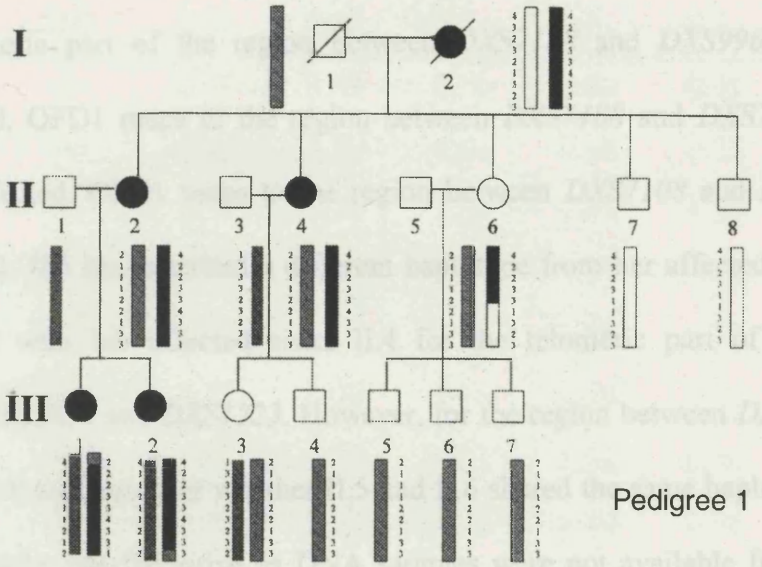

Pedigree 1

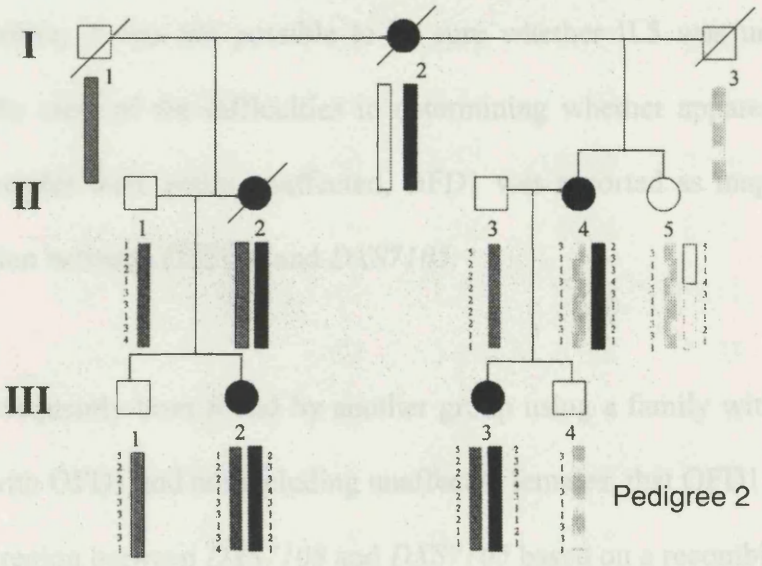

Pedigree 2

Family trees used in the analysis. The shaded circles represent affected individuals. The order of markers displayed is *DXS996, KAL, DXS1223, DXS8051, DXS7108, DXS8022, DXS987, DXS8036, and DXS7105.* The bars indicate the most likely haplotypes. The affected haplotype is indicated by the solid black bars and the unaffected haplotype by the solid white bars. In pedigree one, the haplotype of I-1 is indicated by the diagonal shaded bars. In pedigree two, the haplotype of I-1 is indicated by diagonal shaded bars and I-3 by light grey bars. In pedigree two, the haplotype of II-5, which could either be affected or unaffected, is indicated by a dotted outline. In both pedigrees, additional male haplotypes that have been introduced are indicated by the dark grey bars.

affected relatives. However, II.6 has a history of miscarriage and has passed on the unaffected haplotype from I.1 to all her three normal sons III.5, III.6 and III.7. II.6 has inherited the same haplotype as her affected sisters II.2 and II.4 for the telomeric part of the region between *DXS7108* and *DXS996.* If II.6 is unaffected, OFD1 maps to the region between *DXS7108* and *DXS7105,* but if II.6 is affected, OFD1 maps to the region between *DXS7108* and *DXS996.* In pedigree 2, II.5 has inherited a different haplotype from her affected mother I.2 compared with her affected sister II.4 for the telomeric part of the region between *DXS996* and *DXS1223.* However, for the region between *DXS8051* and *DXS7105* it was not clear whether II.5 and II.6 shared the same haplotype or the markers were uninformative as DNA samples were not available from I.2 and I.3. As before, it was not possible to be sure whether II.5 was unaffected or affected. In view of the difficulties in determining whether apparently normal normal females were really unaffected, OFD1 was reported as mapping to the wider region between *DXS996* and *DXS7105.*

It has subsequently been found by another group using a family with 5 affected females with OFD1 and not including unaffected females, that OFD1 maps to the narrower region between *DXS7108* and *DXS7105* based on a recombination in an affected female at *DXS7108* and a lod score of 2.11 (Gedeon et al, 1999).

3.1.3.2. Linkage results

Two-point analysis of Pedigrees one and two (Table 3.7) using a 100% penetrance gave a maximum two-point lod score of 2.67 at $\theta = 0.0$ with the

Table 3.7
Linkage results for pedigrees one and two for OFD1

Marker	Recombination fractions (θ)						
	0.0	0.01	0.05	0.1	0.2	0.3	0.4
DXS996	$-\infty$	0.16	0.68	0.76	0.62	0.39	0.19
	$-\infty$	0.24	0.30	0.41	0.36	0.25	0.14
KAL	$-\infty$	1.90	2.34	2.29	1.85	1.25	0.60
	3.32	3.25	2.97	2.61	1.89	1.19	0.54
DXS1223	**2.67**	2.62	2.43	2.18	1.66	1.11	0.54
	2.32	2.27	2.09	1.86	1.40	0.94	0.47
DXS8051	1.83	1.81	1.73	1.61	1.32	0.96	0.51
	2.24	2.20	2.03	1.82	1.40	0.96	0.49
DXS7108	$-\infty$	–0.30	0.51	0.82	0.92	0.71	0.37
	2.13	2.11	2.02	1.83	1.37	0.86	0.37
DXS8022	**2.52**	2.50	2.41	2.24	1.79	1.23	0.59
	2.84	2.79	2.60	2.35	1.80	1.19	0.55
DXS987	1.05	1.06	1.08	1.06	0.94	0.71	0.40
	1.49	1.48	1.40	1.29	1.02	0.71	0.37
DXS8036	1.76	1.74	1.67	1.54	1.19	0.75	0.29
	2.32	2.27	2.10	1.87	1.38	0.84	0.32
DXS7105	$-\infty$	0.20	0.78	0.93	0.87	0.62	0.28
	$-\infty$	–0.00	0.58	0.72	0.68	0.47	0.20

For each marker, the upper line of figures indicates the two-point lod score for all family members using 100% penetrance, and the lower line indicates the score for affected females and unaffected males only. The maximum lod scores are highlighted in bold in each case.

marker *DXS1223* and a slightly lower lod score (2.52 at $\theta = 0$) with the more proximal marker *DXS8022.* An 'affecteds only' analysis, using affected females and unaffected males only, gave a maximum lod score of 3.32 at $\theta = 0.0$ with *KAL* and a lod of 2.84 at $\theta = 0.0$ with *DXS8022.* The higher lod score in the 'affecteds only' analysis was due to the elimination of individual II.6 in pedigree 1. As discussed in section 3.1.3.1, II.6 in pedigree 1 and II.5 in pedigree 2 could represent cases of incomplete penetrance. A lod score of 3.0 or above represents a significant score. An 'affecteds only' multipoint analysis gave a maximum lod score of 3.56 at *KAL* but also a lod score of 3.56 between *DXS987* and *DXS8036* (data not shown).

3.1.4. Microsatellite analysis of pedigree three between *DXS7108* and *DXS7105* supports a diagnosis of OFD1 in pedigree three

Figure 3.15 Microsatellite marker analysis for OFD1 pedigree three between *DXS7108* and *DXS7105*.

The marker order is *DXS7108, DXS8022, DXS987, DXS8036, DXS999, DXS7105*

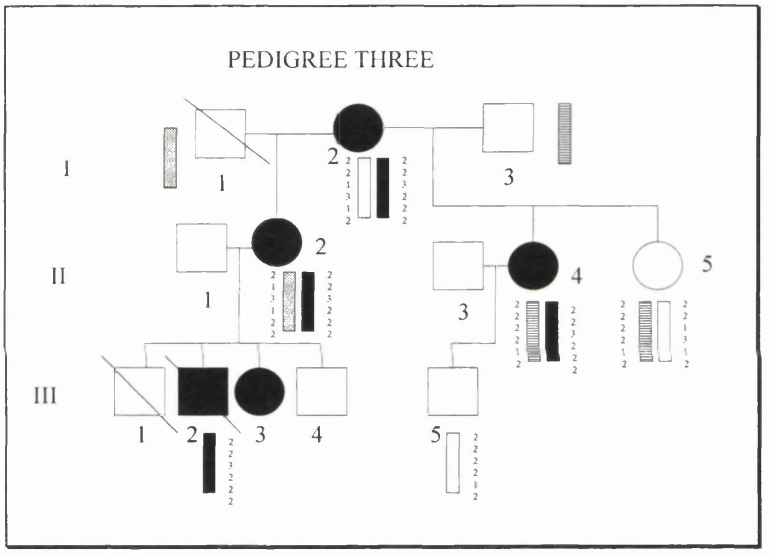

As shown in Figure 3.15, all affected individuals share the same haplotype (shown in black) between *DXS7108* and *DXS7105*. The original authors of this paper questioned whether pedigree 3 had OFD1 or OFD2, all affected individuals do share the same haplotype across the OFD1 region, suggesting this pedigree represents OFD1 or could be allelic with OFD1.

3.1.5. Microsatellite analysis of pedigrees four and five between *DXS7108* and *DXS7105* does not narrow the candidate region further

Figure 3.16 Microsatellite marker analysis for OFD1 Pedigree Four between *DXS7108* and *DXS7105*.

The marker order is *DXS7108, DXS8022, DXS987, DXS8036, DXS999, DXS7105*

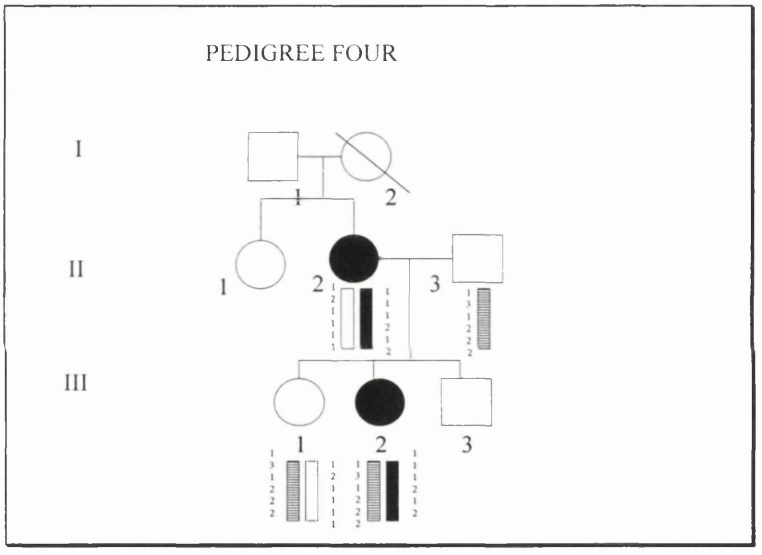

Haplotype analysis across the OFD1 region shows that the affected individual III.2 has inherited a different haplotype (shown in black) than her unaffected sister III.1 from their affected mother II.2. Unfortunately, no DNA sample was available from III.3. Little can be concluded from these results as there are no recombinants within the OFD1 region but even if there were it would be difficult to assign the affectation status of III.1 as discussed in section 3.1.1. The results of the microsatellite marker *DXS8022* is shown in Figure 3.17.

Figure 3.17
Marker *DXS 8022* Pedigree four

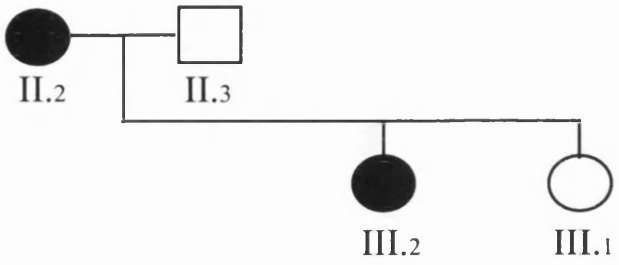

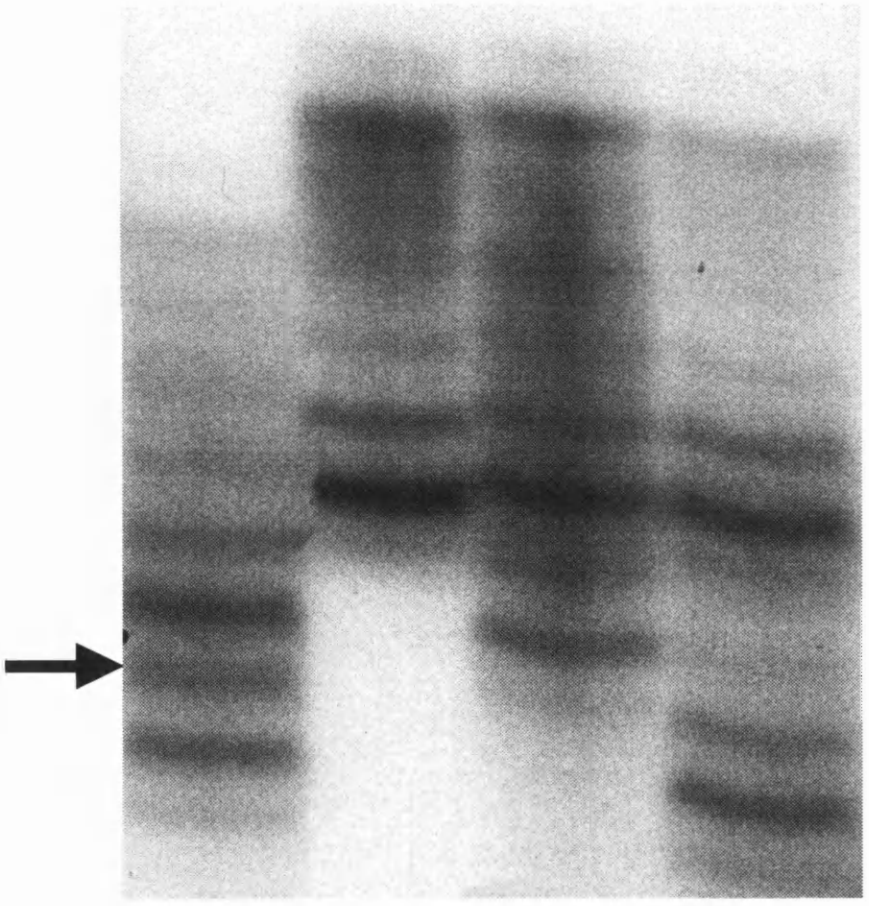

Note ⟶ allele has been passed from affected II.2 to affected III.2 but not unaffected III.1

Figure 3.18. Microsatellite marker analysis for OFD1 Pedigree Five between *DXS7108* and *DXS7105*.

The marker order is *DXS7108, DXS8022, DXS987, DXS8036, DXS999, DXS7105*

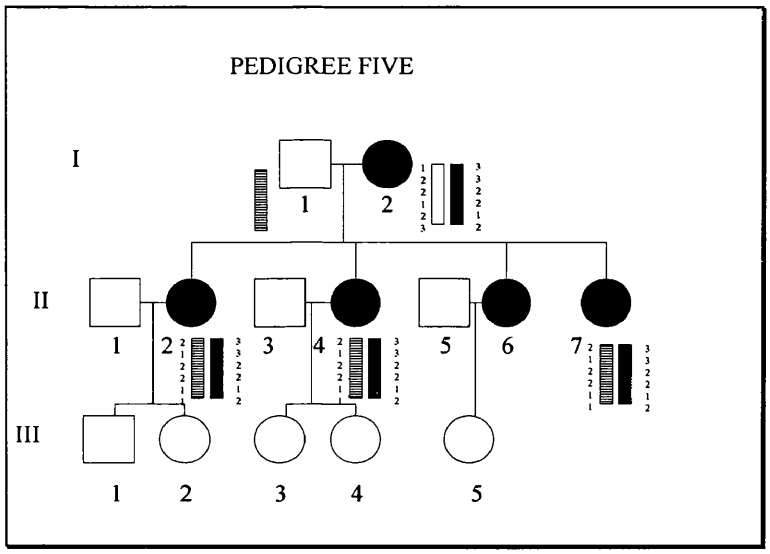

Haplotype analysis between *DXS7108* and *DXS7105* showed that all affected females in generation II for whom DNA samples were available, had all inherited the same haplotype (shown in black) from their affected mother. The results of the microsatellite marker *DXS999* in Pedigree Five is shown in Figure 3.19.

To summarise, I found that OFD1 maps to a 19.8 centiMorgan interval between *DXS7108* and *DXS7105*. This was subsequently narrowed by another group to a 9.8cM interval between *DXS85* and *DXS7105* (Gedeon et al, 1999). The available data in five pedigrees has not made it possible to narrow the region further.

Figure 3.19
Marker DXS 999 pedigree five

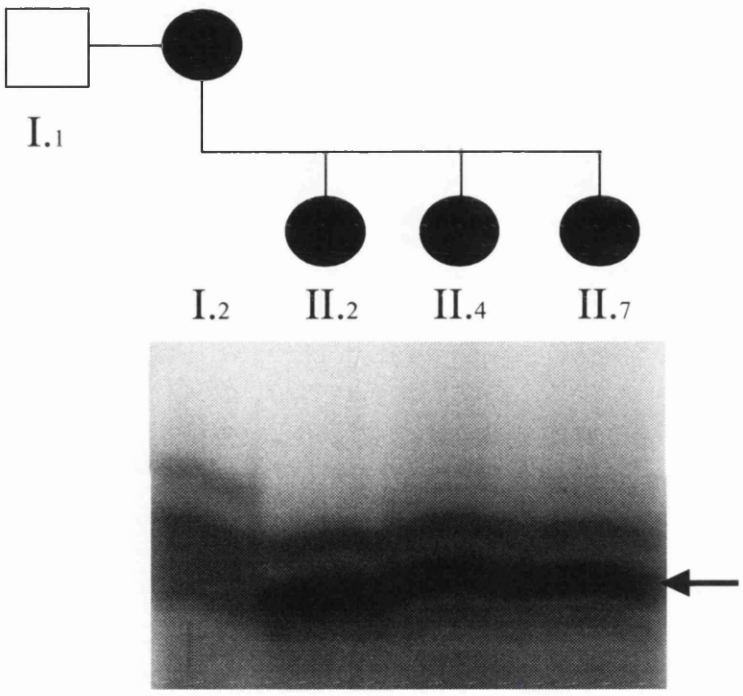

Note ⟶ allele is shared by all affected offspring

3.1.6. Examination of candidate genes in the OFD1 region

At the time I began the analysis of candidate genes in the OFD1 region, the gene for OFD1 was thought to be located between *DXS996* to *DXS7105*. Subsequently, it became apparent as discussed in section 3.1.3. that OFD1 mapped to a narrower region between *DXS7108* and *DXS7105* and the genes *KAL, APXL, FXY* and *CLC4*, included in this section, were outside the critical region.

3.1.6.1. Expression of candidate genes using reverse transcription

In order to be considered a candidate for OFD1, a gene should be expressed in early human fetal face, feet, hands and kidney. Expression of the genes *KAL, FXY* (finger on X and Y)*/MID1*(Midline 1), *APXL* (Apical protein *Xenopus laevis* Like) and *GRPR* (Gastrin-releasing peptide receptor) as demonstrated by reverse transcription in 8 week and 9 week gestation human fetal tissue is shown in figure 3.20. Primers for reverse transcription were designed to cross intron-exon boundaries and details are given in section 2.1.6.3. These genes which mapped to the OFD1 region between *DXS996* and *DXS7105* were considered to be the best known candidates for OFD1.

FXY/MID1 is a developmental gene which codes for a RING finger protein which would be predicted to be involved in protein-protein interactions (Perry et al, 1998). *FXY/MID1* was shown to be expressed in all tissues examined in 8 and 9 week fetus (Figure 3.20) suggesting the gene could be further examined as a candidate for OFD1.

Figure 3.20
Reverse transcription of candidate genes, FXY, APXL, KAL, GRPR in 8 and 9 week old fetus

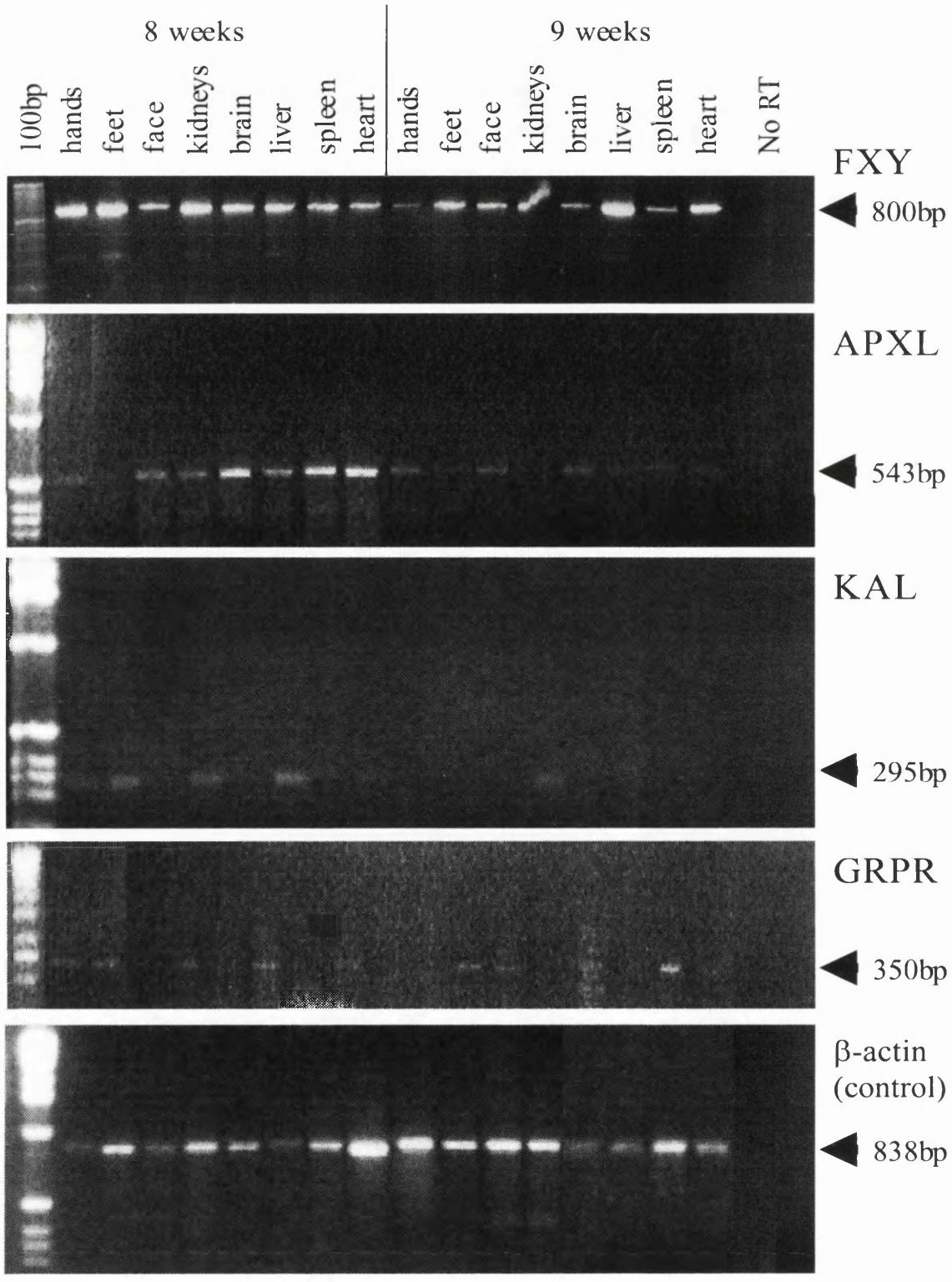

KAL codes for a putative cell adhesion molecule and is the gene responsible for X-linked recessive Kallmann's syndrome (Franco et al, 1991) in which affected males have some similar phenotypic defects to OFD1; midline defects and renal malformations. *KAL* was shown to be expressed in the 8 and 9 week kidney. *KAL* was also expressed in the feet and at 8 weeks but was not expressed in any tissues other than the brain and kidney at 9 weeks (Figure 3.20). KAL expression, by reverse transcription, was detected in some of the tissues in which the gene for OFD1 would be expected.

APXL, shows homology to the *Xenopus laevis APX* gene which codes for a protein which may modulate the activity of amiloride-sensitive sodium channels and in the adult was shown to be expressed in brain, lung, kidney and pancreas (Schiaffino et al, 1995). Expression analysis shows that the gene was expressed ubiquitously in the 8 week human fetus, except in the feet and also in the 9 week hands and face (Figure 3.20).

GRPR, a receptor for gastric releasing peptide (GRP), a growth factor was expressed in all the tissues examined in the 8 week and 9 week fetus suggesting it could be considered as a candidate for OFD1 (Figure 3.20).

3.1.6. Screening of candidate genes using single strand conformation polymorphism analysis with sequencing of changes detected

Eleven genes have been screened for mutations in individuals with OFD1, *APXL*, *KAL, FXY/MID1*, *CLC4* (chloride channel 4), *GRPR, CaBP9K* (calbindin-Dk9), *HCCS* (human holocytochrome c-type synthetase gene), *ARHGAP6* (rho-type GTPase-activating protein gene), *SCML1* (sex comb midge leg like type 1), *STK9* (Serine-threonine kinase type 9) and *RAI2* (mouse retinoic acid-induced

gene in Xp22). The primers used for SSCP were designed within intronic sequence or overlapping within exonic sequence so that the whole of the coding region was examined. The primer details are given in section 2.1.6.2.

APXL

All ten exons of *APXL* were screened in pedigrees 1 and 2 and sporadic cases S1-6. A shift was detected in S3 in exon 3 (Figure 3.21). This shift was also present in the mother of S3 who had no phenotypic features of OFD1 but could have represented a case of incomplete penetrance in OFD1. Sequencing of the shift revealed the single nucleotide substitution C2550T in S3 and her mother which did not alter the amino acid, leucine, coded for and was likely to represent a polymorphism. Furthermore, *APXL* is no longer in the OFD1 region (Gedeon et al, 1999).

CaBP9K

CaBP9K codes for a vitamin D-dependent calcium binding protein which is known to be expressed in the kidney and teeth in rodents (Gross et al, 1990) but only in the intestine in adult humans (Howard et al, 1992). Calbindin-D28K, another calcium binding protein is expressed in the metanephric kidney in development and therefore *CaBP9K* was considered to be a candidate gene for OFD1. All three exons of *CaBP9K* were screened in 5 pedigrees and 15 sporadic patients with OFD1 and no shifts were detected.

GRPR

All three exons of *GRPR* were screened in all 5 pedigrees and 15 sporadic patients and no shifts were detected.

Figure 3.21
SSCP analysis of *APXL* exon 3

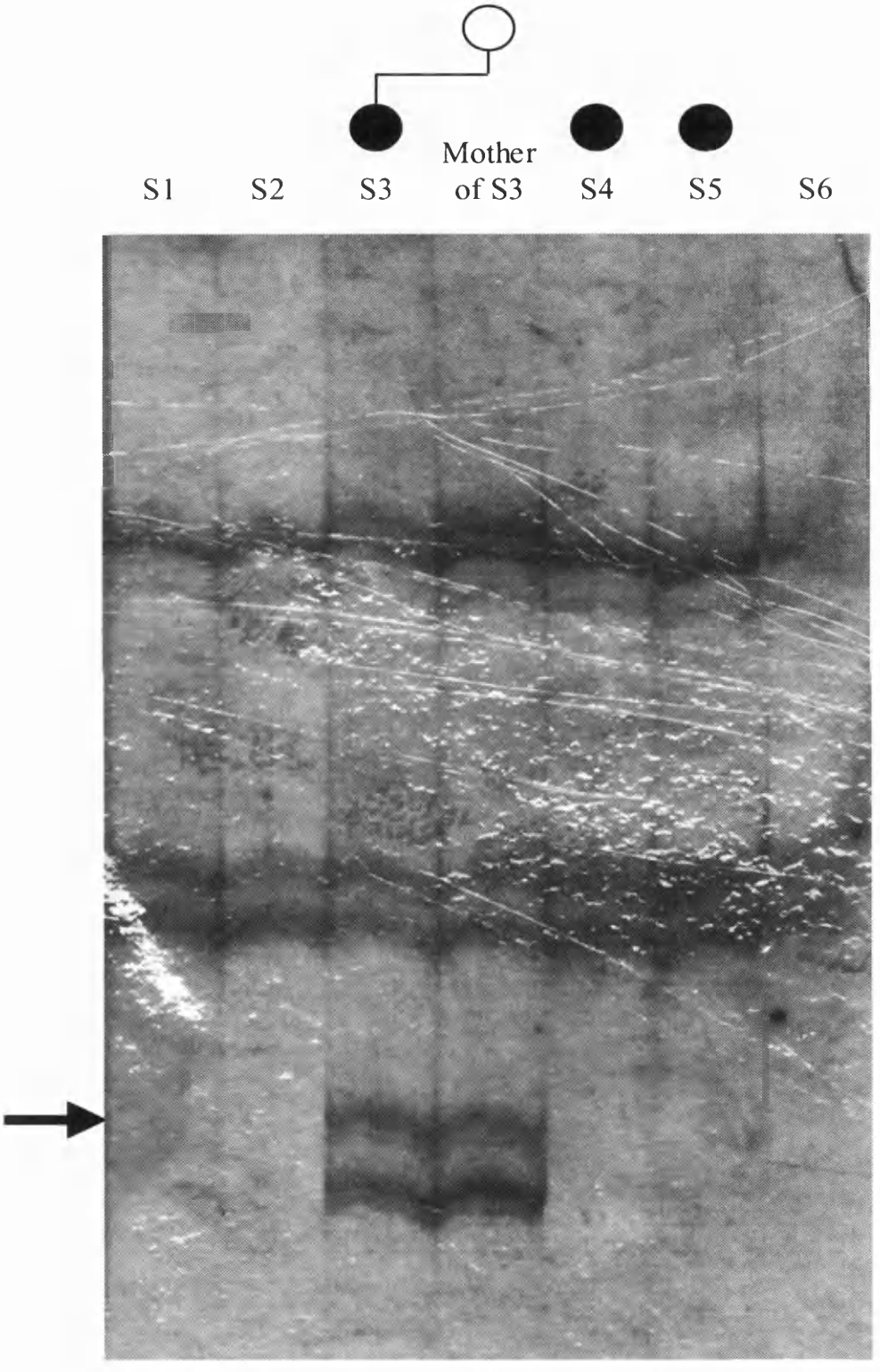

Note: The presence of band shift in S3, which is also present in her unaffected mother

KAL

All fourteen exons were screened in pedigrees 1 and 2 and S1-6. Interestingly, an additional band was noted in normal males in exon 14 (see figure 3.22). This shift has been noted by other investigators and represents the amplification of the non-functional gene with homology to *KAL* on the Y chromosome (Dr V. Duke, London University, London, UK personal communication). No other shifts were detected in *KAL*. *KAL* is no longer in the OFD1 region.

HCCS

HCCS codes for a protein with homology to holocytochrome c-type synthetases which catalyse the covalent addition of a heme group onto c-type cytochromes in the mitochondria. OFD1 is associated with learning difficulties, although not the degenerative neurological features associated with mitochondrial defects and so all seven exons of *HCCS* were screened in pedigrees 1 and 2 and S1-6 and no shifts were detected.

MID1/FXY

The ten exons of *MID1/FXY* were screened by SSCP and no shifts were detected in pedigrees 1 and 2 and sporadic cases S1-15. No shifts were detected and the coding regions of the genes were sequenced by collaborators, Dr B Franco, (TIGEM, Milan, Italy) and Dr J Perry, (ICR, London). Furthermore, *MID1/FXY* is no longer in the OFD1 coding region (Gedeon et al, 1999).

Figure 3.22
SSCP analysis of *KAL* exon 14

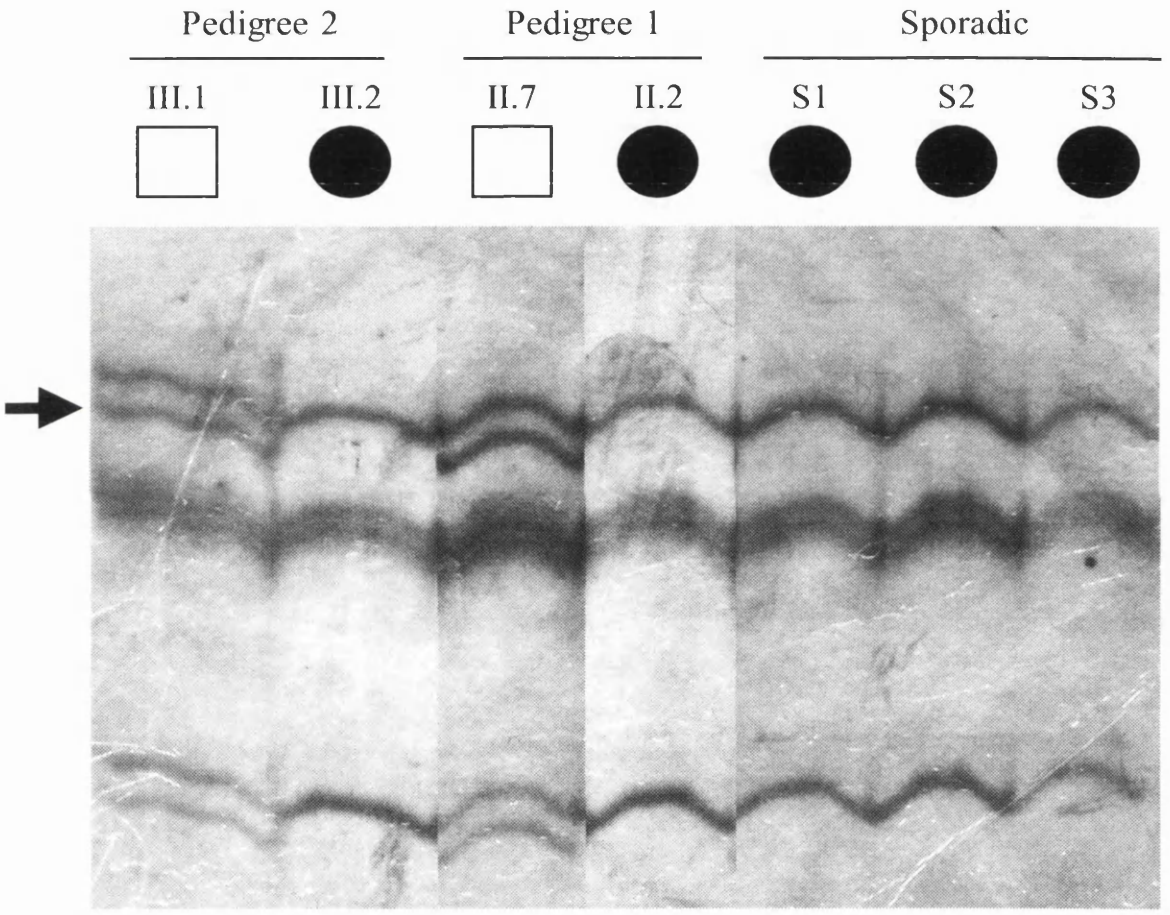

Note: The extra band in normal males III.1, II.7. This is considered to represent amplification of Y chromosome homologue of *KAL*

ARHGAP6

ARHGAP6 (rho-type GTPase-activating protein gene) contains homology to the GTPase-activating (GAP) domain of the rhoGAP family of proteins, which has been implicated in the regulation of actin polymerization at the plasma membrane in several cellular processes. ARHGAP6 is expressed ubiquitously in adult tissue and is a potential candidate for OFD1 (Schaefer et al, 1997). All twelve exons of the gene were screened in pedigrees 1-5 and sporadic cases 1-15. A shift was detected in exon 3 (Figure 3.23) in III.1 in pedigree 1 but not in her affected mother II.2, in sporadic case S2 and normal control individuals. The shift was considered to be a polymorphism and was not sequenced. The coding region of the whole gene was sequenced by collaborator Dr H Zoghbi, (Baylor Institute, Texas, USA) and no mutations have been detected in OFD1 patients.

CLC4

CLC4 shares a high degree of sequence homology with voltage gated chloride channels (van Slegtenhorst et al, 1994) and ion channels have been involved in muscle contraction, neuronal signalling and exocytosis (Hille et al, 1992). In addition, PKD2, one of the genes mutated in ADPKD, is predicted to have ion channel functions (Mochizuki et al, 1996). Hence *CLC4* was considered to be a good candidate for OFD1. All fourteen exons of *CLC4* were screened and a shift was detected in II.2 in pedigree 2 (see figure 3.24). This shift was also present in normal individuals and considered to be a polymorphism so the shift was not sequenced. In addition, *CLC4* is no longer in the candidate region for OFD1 (Gedeon et al, 1999).

Figure 3.23
SSCP analysis of *ARHGAP6* exon 3

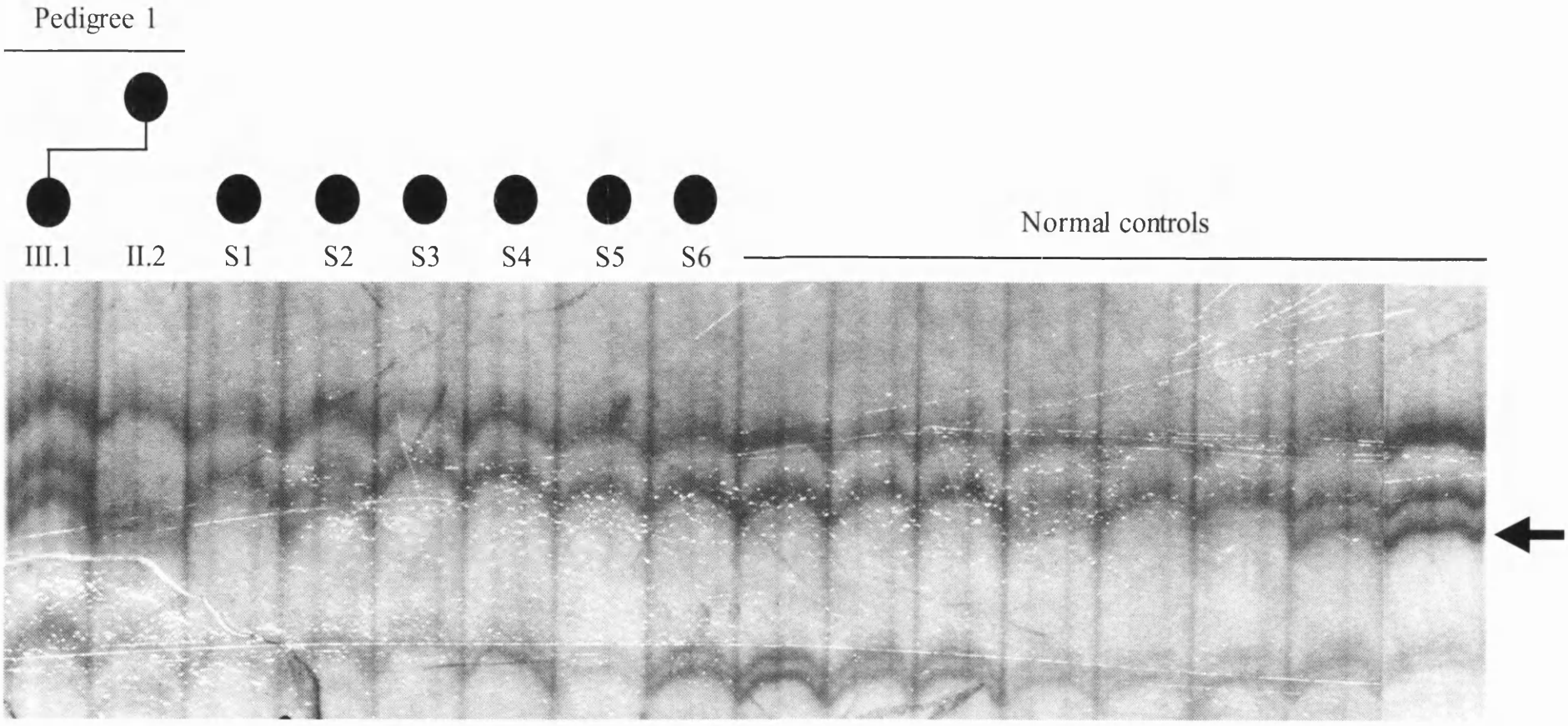

Note: The presence of ◄—— band shift in unaffected individual III.1 (which is not present in her mother II.2) and S2. The band shift is also present in normal control DNA samples

SCML1

SCML1 is ubiquitously expressed in tissues that include the kidney, although it is most markedly expressed in skeletal muscle. *SCML1* contains 2 domains which have homology to *Drosophila* transcriptional repressors of the polycomb group and are considered to have a developmental role in the regulation of homeotic genes (Van de Vosse et al, 1998). The gene has six exons and these were screened in all five pedigrees and 15 sporadic cases of OFD1 and no shifts were detected. In addition, the coding region of the gene was sequenced by collaborator Dr D Trump, (Cambridge University, UK).

STK9

STK9 has homology to serine-threonine kinase genes (Montini et al, 1998) and is expressed in the adult brain, lung and kidney. All twenty exons of the gene were screened in 5 pedigrees with OFD1 and 15 sporadic cases and no shifts were detected. In addition, the entire coding region of the gene was sequenced by collaborator Dr B Franco, (TIGEM, Milan, Italy) and no mutations were found.

RAI2

RAI2 has a single exon and is expressed in brain, lung, kidney and heart in the human fetus and in heart, brain, placenta, lung kidney, pancreas and retina in the adult. The gene has 94% homology with the mouse retinoic acid-induced gene (Walpole et al, 1999). Retinoic acid is involved in early embryonic development including vertebrate AP axis formation and *RAI2* is therefore a good candidate gene for OFD1. No shift was detected in the single exon of *RAI2* in all 5 pedigrees and 15 sporadic patients with OFD1 and the gene was sequenced by Dr D Trump, (Cambridge University, UK).

Figure 3.24
SSCP analysis of *CCLC4* exon 11

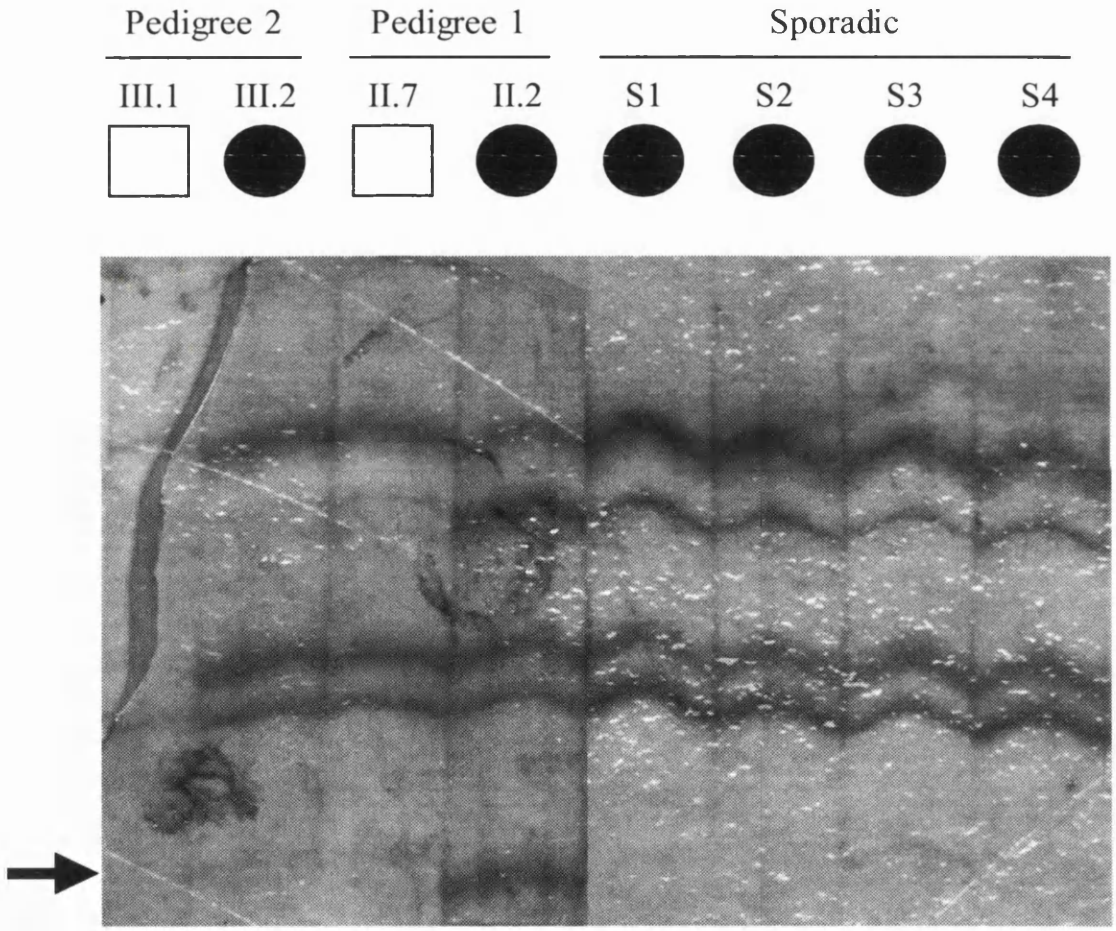

Note: The band shift in II.2 (pedigree 1).
This shift was also present in normal individuals (data not shown).

No mutations have been detected in patients with OFD1 in the eleven genes described using SSCP and sequencing of shifts or sequencing of the entire gene by collaborators. The genes *APXL, CLC4, FXY/MID1* and *KAL* are no longer in the OFD1 critical region.

3.2. Vesicoureteric reflux and reflux nephropathy

3.2.1. Clinical details of pedigrees with VUR

Individuals were classified as affected with VUR if they had VUR demonstrated on a cystogram study and affected with RN if they had RN on an intravenous pyelogram or isotope renogram. All other individuals were classified as unknown. Details of renal function and history of suggestive symptoms were noted but individuals with symptoms such as hypertension and cystitis were not classified as affected.

Initially, seven pedigrees consistent with dominant inheritance were studied (Figures 3.27 – 3.33 inclusive). The clinical details of the pedigrees are given in Tables 3.7- 3.13 inclusive). All the pedigrees are Caucasian in origin. In each family at least one individual had presented with symptomatic renal disease and had been established to have VUR and/or RN by radiological investigations. This prompted enquiry into the rest of the family. Some family members had already been investigated and diagnosed as having these disorders but some affected individuals were discovered by active radiological screening of asymptomatic relatives. The designation of individuals as having VUR or RN or both allowed analysis of different components of the disease. There were no dysmorphic features in any of the pedigrees and no visual problems or deafness. Secondary causes of VUR were excluded and no history was given of abnormal bladder function. A basic chromosomal karyotype was performed on an affected individual in each pedigree and no gross chromosomal aberrations were noted. These seven, dominant type pedigrees were used in the genome wide scan.

In addition, twenty five additional pedigrees have been ascertained and samples collected. Twenty four of these pedigrees are Caucasian in origin and one pedigree is Asian in origin. Details of these pedigrees are given in Table 3.15. When all thirty two pedigrees are considered there are striking differences between the numbers of males and females in the pedigrees. Overall, sixty one females were affected, twenty five with VUR alone, five with RN alone and thirty one with VUR and RN. Only thirty four males were affected, seventeen with VUR alone, two with RN alone and fifteen with VUR and RN giving a total of 34 affected males.

Fourteen affected parents with documented VUR or RN had nineteen children with documented VUR or RN. Thirteen affected mothers had eighteen affected children, nine girls and seven boys. Only one affected father had one affected daughter. It is interesting that there is no proven male to male transmission in any of the pedigrees although there are instances of fathers who might be carriers in a pedigree having affected sons.

Figure 3.25. Key of clinical details used in VUR pedigrees

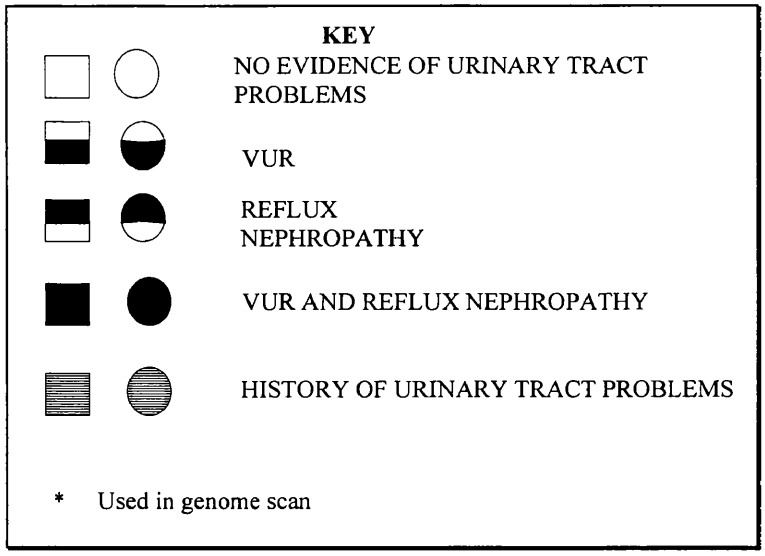

Figure 3.26. Pedigree One VUR

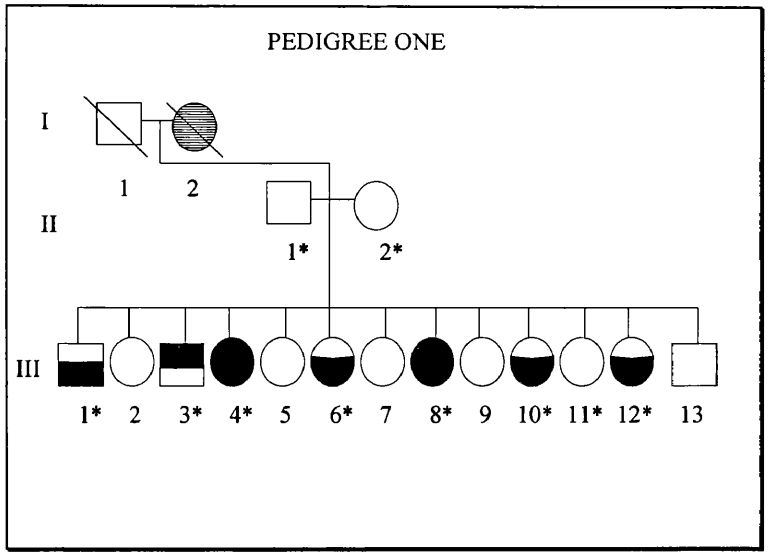

Table 3.8. Clinical details of pedigree one VUR

Individual	VUR on cystogram	RN on isotope renogram or IVP	Renal function	Other
I.1	Not done	Not done	Unkown	Unknown
I.2	Not done	Not done	Unknown	History of scarred kidneys
II.1	Not done	Normal	Unknown	Unknown
II.2	Not done	Normal	Unknown	Unknown
III.1	R VUR	Normal	Normal	Unknown
III.2	Normal	Normal	Normal	Unknown
III.3	Normal	R RN	Normal	Unknown
III.4	R/L VUR	R/L RN	Impaired	Recurrent UTI
III.5	Normal	Normal	Normal	Unknown
III.6	R/L VUR	Normal	Normal	Unknown
III.7	Normal	Normal	Normal	Unknown
III.8	R/L VUR	R/L VUR	Impaired	Recurrent UTI
III.9	Normal	Normal	Normal	Unknown
III.10	R VUR	Normal	Normal	Unknown
III.11	Normal	Normal	Normal	Unknown
III.12	L VUR	Normal	Normal	Unknown
III.13	Normal	Normal	Normal	Unknown

Figure 3.27. Pedigree Two

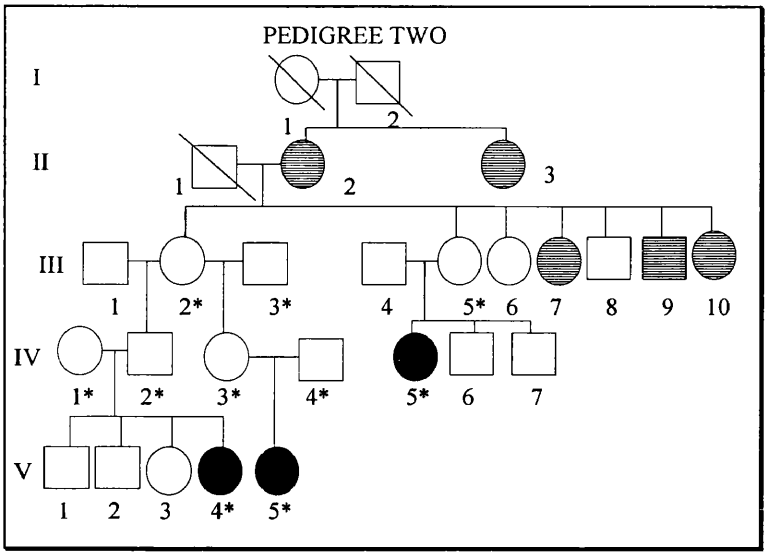

Table 3.9. Clinical details of Pedigree Two (VUR)

Individual/s	VUR on cystogram	RN on isotope renogram or IVP	Renal function	Other
I.1,2	Not done	Not done	Not done	Not known
II.1	Not done	Not done	Not done	Not known
II.2	Not done	Normal	Not known	Recurrent UTI Hypertension
II.3	Not done	Abnormal	Not known	Recurrent UTI Renal vein thrombosis as a neonate
III.1,2,3,4,5,6	Not done	Not done	Not done	Not known
III.7	Not done	Normal	Not known	Recurrent UTI Hypertension
III.8	Not done	Not done	Not done	Not known
III.9	Not done	Normal	Not done	Hypertension
III.10	Not done	Not done	Not done	'Renal problems'
IV.1,2,3,4	Not done	Not done	Not done	Not known
IV.5	R/L VUR	Reflux nephropathy	Not done	Not known
IV.6,7	Not known	Not known	Not known	Not known
V.1,2,3	Not known	Not known	Not known	Not known
V.4	R/L VUR	R/L RN	Not known	Not known
V.5	R/L VUR	R/L RN	Not known	Not known

Figure 3.28. Pedigree Three (VUR)

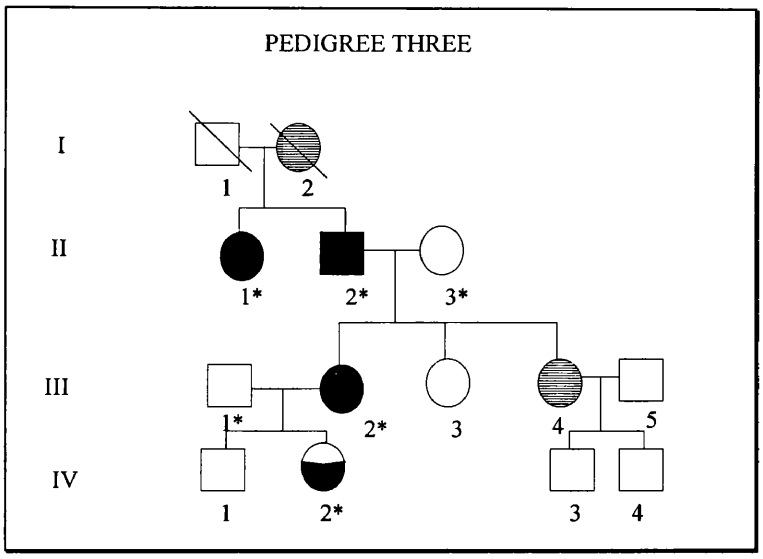

Table 3.10. Clinical details of pedigree Three (VUR)

Individual/s	VUR on cystogram	RN on isotope renogram or IVP	Renal function	Other
I.1	Not known	Not known	Not known	Not known
I.2	Not known	Not known	Not known	'Scarred kidneys and nephrectomy'
II.1	R/L VUR	R/L RN	Not known	Recurrent UTI L nephrectomy
II.2	R/L VUR	R/L RN	Not known	Recurrent UTI
II.3	Not known	Not known	Not known	Not known
III.1	Not known	Not known	Not known	Not known
III.2	L VUR	L RN	Normal	Recurrent UTI L nephrectomy
III.3	Not known	Not known	Not known	Not known
III.4	Not known	Not known	Normal	UTI as an adult
III.5	Not known	Not known	Not known	Not known
IV.1	Not known	Normal	Not known	UTI
IV.2	R VUR	Not known	Not known	Febrile episodes ?UTI
IV.3,4	Not known	Not known	Not known	Not known

Figure 3.29. Pedigree four (VUR)

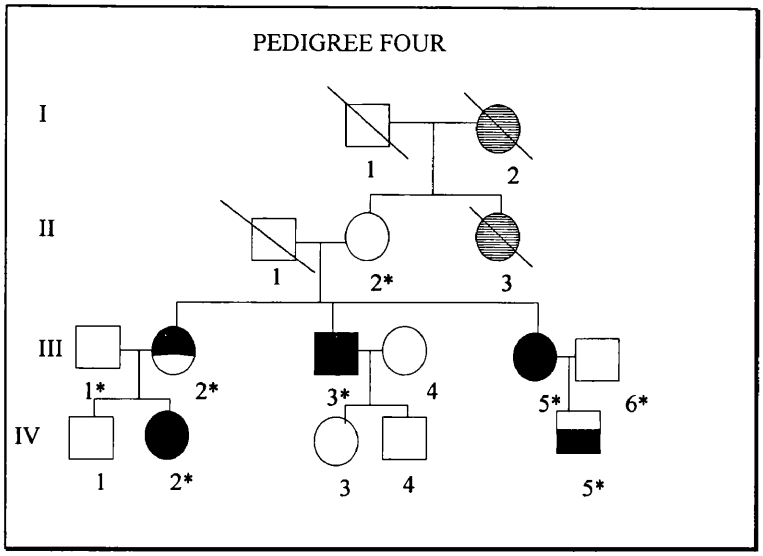

Table 3.11. Clinical details of Pedigree Four (VUR)

Individual/s	VUR on cystogram	RN on isotope renogram or IVP	Renal function	Other
I.1	Not known	Not known	Not known	Not known
I.2	Not known	Not known	Not known	'Single kidney'
II.1	Not known	Not known	Not known	Not known
II.2	Not known	Normal	Not known	Not known
II.3	Not known	Not known	Not known	'Single kidney'
III.1	Not known	Not known	Not known	Not known
III.2	Not known	Single kidney with RN	Not known	Not known
III.3	L VUR	L RN	Not known	Not known
III.4	Not known	Not known	Not known	Not known
III.5	R/L VUR	R/L RN	ESRF Renal transplant	Not known
III.6	Not known	Not known	Not known	Not known
IV.1	Not known	Not known	Not known	Not known
IV.2	R/L VUR	R/L RN	Not known	Not known
IV.3,4	Not known	Not known	Not known	Normal renal ultrasound scans
IV.5	R/L VUR	Normal	Not known	Not known

Figure 3.30. Pedigree Five (VUR)

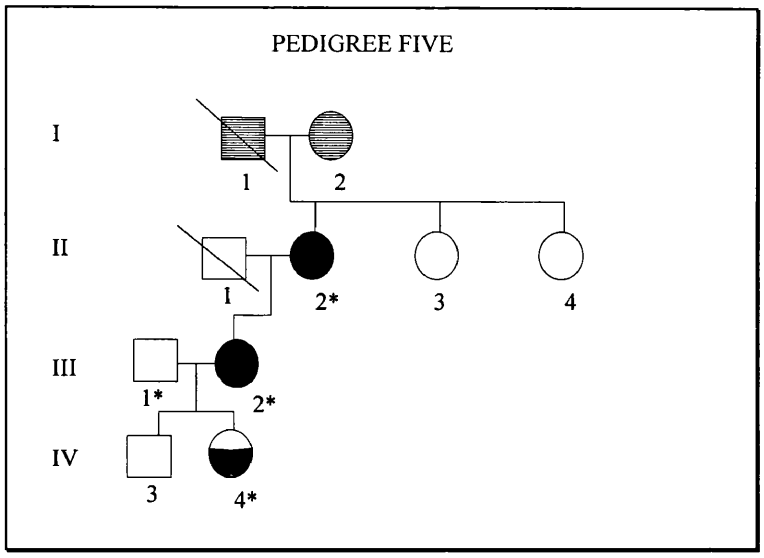

Table 3.12. Table of Clinical details of Pedigree Five (VUR)

Individual/s	VUR on cystogram	RN on isotope renogram or IVP	Renal function	Other
I.1	Not known	Not known	Not known	'Nephritis'
II.2	Not known	Normal	Not known	Recurrent UTI
II.1	Not known	Not known	Not known	Not known
II.2	R/L VUR	R/L RN	ESRF Renal transplant	Recurrent UTI
II.3	Not known	Not known	Not known	UTI as an adult
II.4	Not known	Not known	Not known	Normal renal ultrasound scan
III.1	Not known	Not known	Not known	Not known
III.2	R/L VUR	R/L RN	Not known	Recurrent UTI Bilateral ureteric reimplantation
IV.1	Not known	Not known	Not known	-
IV.2	R VUR	Not known	Not known	Normal renal ultrasound. VUR resolved aged 3 years

Figure 3.31. Pedigree Six (VUR)

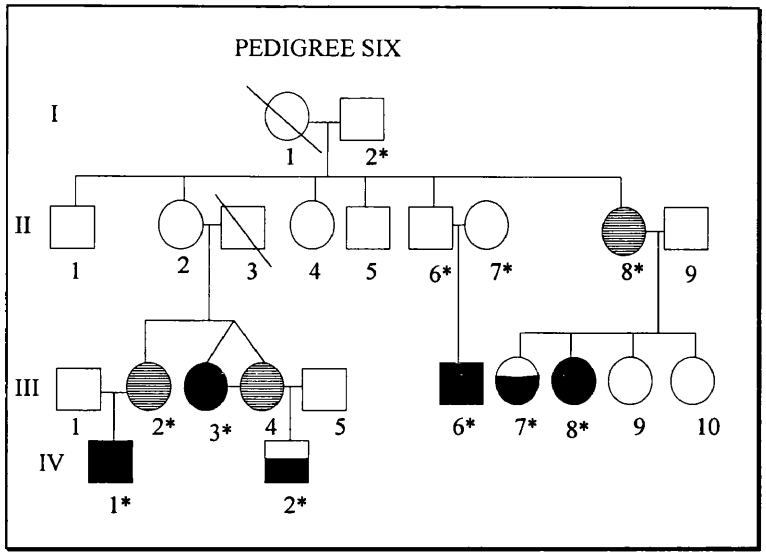

Table 3.13. Table of Clinical details of Pedigree six (VUR)

Individual/s	VUR on cystogram	RN on isotope renogram or IVP	Renal function	Other
I.1,2	Not known	Not known	Not known	Not known
II.1,2,3,4,5,6, 7	Not known	Not known	Not known	Not known
II.8	Not known	Not known	Not known	Recurrent UTI
II.9	Not known	Not known	Not known	Not known
III.1	Not known	Not known	Not known	Not known
III.2	Not known	Not known	Not known	Recurrent UTI
III.3	VUR	R/L RN	CRF	Recurrent UTI
III.4	Not known	Not known	Normal	Small L kidney
III.5	Not known	Not known	Not known	Not known
III.6	R/L VUR	R/L RN	Hypertension	Recurrent UTI R/L Ureteric Reimplantation
III.7	VUR	Not known	Not known	Recurrent UTI
III.8	VUR	R/L RN	CRF	L Ureteric Reimplantation
III.9	Normal	Not known	Not known	UTI
III.10	Not known	Not known	Not known	Not known
IV.1	R/L VUR	R/L RN	Not known	Ureteric Reimplantation
IV.2	L VUR	Not known	Not known	UTI VUR resolved

Figure 3.32. Pedigree Seven (VUR)

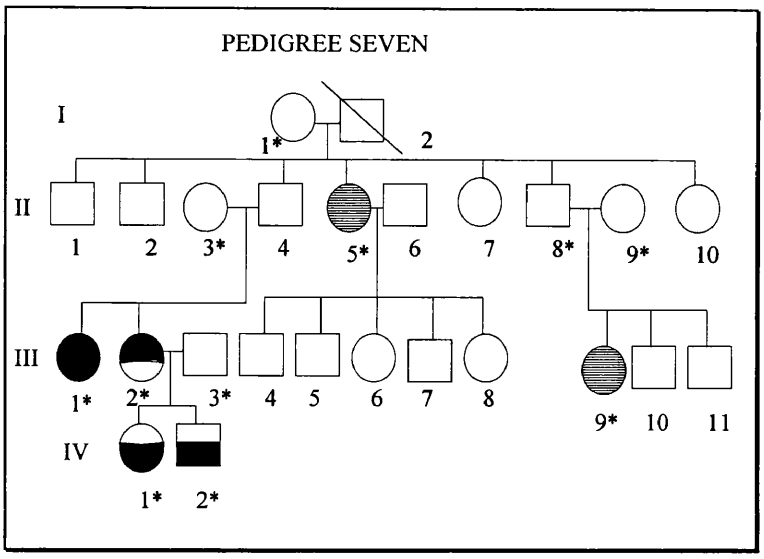

Table 3.14. Clinical details of Pedigree seven (VUR)

Individual/s	VUR on cystogram	RN on isotope renogram or IVP	Renal function	Other
I.1,2	Not known	Not known	Not known	Not known
II.1,2,3,4	Not known	Not known	Not known	Not known
II.5	Not known	Not known	Not known	UTI Nephrectomy for dilated kidney
II.6,7,8,9,10	Not known	Not known	Not known	Not known
III.1	VUR	RN	Not known	Recurrent UTI
III.2	Not known	RN	Not known	UTI
III.3,4,5,6,7,8	Not known	Not known	Not known	Not known
III.9	Not known	Not known	Not known	UTI ?Renal surgery
III.10,11	Not known	Not known	Not known	Not known
IV.1	R/L VUR	Not known	Not known	?Renal surgery
IV.2	VUR	Not known	Not known	VUR resolved spontaneously

Table 3.15. Additional pedigrees with VUR

Affected relatives in pedigree	Number collected
4 siblings	1
Mother and 2 siblings	1
3 siblings	4
2 siblings	11
Mother and child	3
Child, mother and aunt	1
2 siblings and cousin	1
Child, aunt and grandmother	1
3 siblings and mother	1
2 siblings, cousin and mother	1

3.2.2. The results of the genome wide search in VUR and RN

A summary of the results for the genome wide scan in analysis T (i.e. affected individuals have either VUR or RN), analysis V (i.e. affected individuals have VUR only) and analysis R (i.e. affected individuals have RN only) are shown in Tables 3.16, 3.17 and 3.18 respectively and in graphical form in Figure 3.33 and will be referred to throughout this section.

3.2.2.1. Evidence for a major locus on chromsome one

The results of the genome wide non-parametric analysis for analysis T show that the most significant region is on chromosome one between the markers *D1S1631* and *D1S1653* and is a seventeen centimorgan interval. The non-parametric lod score (NPL) is 5.48 and the p value is 0.0002 for this region. This p value is more than 200 times more significant than p=0.05 which is the Lander and Kruglyak (1995) criteria suggestive of linkage but is an order of magnitude less than their stringent criteria for significance, p=0.00002. These results include

fifteen additional markers within the region spaced at less than one centimorgan apart, (*GATA133AOB, D1S239, D1S2651, D1S2726, D1S502, D1S2746, D1S2744, D1S252, D1S514, D1S2696, D1S498, D1S2346, D1S1595, D1S2624*) in addition to the four markers in the genome wide screening panel, *D1S1631, GATA176G01, D1S534 and D1S1653.*

The results of non-parametric analysis V (affected individuals with VUR on cystogram only) show that this region is again the most significant genome wide with an NPL score of 5.35 and a p value of 0.0003. The region is also the most significant in analysis R with an NPL score of 3.91 and a p value of 0.003. The results of chromosome one suggest that VUR and RN are different manifestations of the same phenotype.

Parametric lod scores for the region on chromosome one are based on a genetic model of VUR as a dominant disorder with a gene frequency of 0.01, a penetrance of 75% and a phenocopy rate of 1% and are calculated for conditions of heterogeneity. In analysis T, the lod score is 3.12 with a heterogeneity of 0.78. In analysis V, the lod score is 2.32 with a heterogeneity of 0.71. In analysis R, the lod score is 2.08 with a heterogeneity of 0.82.

Pedigree six has the highest parametric and non-parametric lod scores at this locus (2.16 analysis T, 2.15 analysis V, 1.58 analysis R). Pedigree one has negative lod scores at this locus for two analyses (-0.46 analysis T, -0.65 analysis V) and pedigree two has negative lod scores for all three analyses (-1.08 analysis T, -1.08 analysis V, 1.08 analysis R). The results suggest that there is genetic heterogeneity at this locus on chromosome one.

3.2.2.2. Genetic heterogeneity between families suggests the presence of additional loci on chromosomes three, eight and twenty

As discussed in 3.2.1, pedigrees one and two did not appear to map to the major chromosome one region. In addition, it was clear that pedigree six has a major effect at any locus as this is the largest family in the series. The genome scan was repeated for analysis T without pedigree six and the results are shown in Table 3.19. In pedigree one, the most significant region genome wide is on chromosome three between 117 and 184 cM with a parametric lod score of 1.21 analysis T, 1.03 analysis R and 0.55 analysis V. It is interesting that with the removal of pedigree six the non-parametric and parametric scores improve for this region, NPL 3.79, p value 0.004 and parametric lod score of 1.89.

In pedigree two the most signicant region genome wide was on chromosome eight between 20 and 30 cM with a parametric lod score of 1.32 analysis T, 1.32 analysis V and 1.29 analysis R.

On chromosome twenty, between 45 and 53 cM, a further significant region exists with an NPL 2.92 and a p value of 0.009. The parametric lod score for pedigree six at this locus is –1.74. With the removal of this pedigree the score on chromosome twenty improves with a parametric lod score of 2.90, NPL score of 3.42 and a p value of 0.003.

In addition, with the removal of pedigree six from the analysis the scores the X chromosome (70-84) increase and the scores on chromosome one (149-166cM) decreases.

3.2.2.3. Additional areas with a p value of less than 0.05 in analyses T, V and R.

In analysis T it can be seen that there are 12 additional areas with a p value of less than 0.05 on chromosomes two, three (two regions), eight, nine (two regions), thirteen, twenty (two regions), twenty-two (two regions) and the X chromosome.

In analysis V, there are nine additional areas of which six overlap with the areas found in analysis T. The region on chromosome five appears in analysis V but not T and the two regions on chromosome nine, and one of the regions on chromosomes twenty and twenty one appear in analysis T but not V.

In analysis R, there are nine additional areas of which five overlap with the areas found in analysis T. The regions on chromosome one (13-44cM), chromosome four and chromosome twenty one appear in analysis R but not T and the region on chromosome X appears in analysis T but not R.

The existence of suggestive susceptibility loci in addition to chromosome one and regions that appear only in individuals with VUR or RN raises two questions. First, how many additional loci contribute to VUR and RN in addition to chromosome one. Second, although on chromosome one, it appears that VUR and RN are manifestations of the same genetic disorder, the existence of additional areas in only individuals with VUR or RN raises the question as to whether different genes contribute to VUR or RN separately.

As some of these regions may represent false positives, further data will be required to answer these questions fully.

3.2.2.4. Candidate regions in the genome scan; evidence for the X chromosome but not chromosome 6p or 10q.

Prior to the genome wide scan, a number of regions were considered to be candidates including chromosome 6p (the HLA locus), chromosome 10q (where the genes *PAX2, RET* and *FGFR2* are located) and the X chromosome as discussed in Chapter One. On the X chromosome there is a region barely suggestive of linkage between the markers *GATA144DO4-DXS6800* with a p value of 0.04, NPL score of 1.9 and a parametric lod score of 0.58. This region is also just suggestive of linkage in analysis V but does not reach a suggestive level in analysis R. On chromosomes 6 and 10 no regions reached a suggestive level of linkage and the NPL results for analyses T, V and R across the whole of chromosomes 6 and 10 are shown in Figure 3.33.

Table 3.16. Summary of Genehunter analysis T
Analysis T is affecteds only analysis with 'affected' meaning the presence of reflux nephropathy on an isotope renogram or intravenous pyelogram study and/or the presence of VUR on a cystogram, all other individuals have unknown affected status). Areas with a p value of less than 0.05 are described.

Chromosome	Distance	Markers	Parametric lod score (heterogeneity)	NPL score	P value	Individual pedigrees (Lod)(NPL)(p value) at the position of the maximum p value
One	149-166	*D1S1631 - D1S1653*	3.12 (0.78)	5.48	0.0002	1 (-0.46)(-0.37)(0.70) 2 (-1.08)(-0.51)(0.31) 3 (0.56)(1.77)90.12) 4 (0.85)(2.45)(0.03) 5 (0.27)(1.0)(0.50) 6 (2.16)(9.68)(0.003) 7 (0.56)(1.88)(0.06)
Two	55-68	*D2S1788 - D2S1352*	1.17 (0.31)	3.35	0.005	1 (-0.13)(0.73)(0.11) 2 (-0.86)(-0.44)(0.31) 3 (-0.65)(-0.08)(0.37) 4 (-0.54)(0.30)(0.31) 5 (-0.01)(0.05)(0.50) 6 (1.02)(7.56)(0.003) 7 (0.11)(0.76)(0.25)
Three	37-66	*GATA16 4B08- D3S1768*	2.43 (0.87)	2.95	0.009	1 (-0.45)(-0.37)(0.49) 2 (1.25)(3.68)(0.03) 3 (0.16)(0.29)(0.250 4 (-0.09)(-0.02)(0.37) 5 (0.19)(0.65)(0.50) 6 (1.06)(1.41)(0.04) 7 (-0.19)(-0.49)(0.56)
Three	117-184	*GATA12 8C02- D3S1763*	1.61 (0.98)	3.00	0.008	1 (1.21)(3.89)(0.03) 2 (-0.13)(0.56)(0.31) 3 (-0.15)(-0.19)(0.37) 4 (0.11)(0.97)(0.16) 5 (0.27)(0.97)(0.50) 6 (-0.24)(0.20)(0.21) 7 (0.51)(1.51)(0.06)
Eight	25-29	*D8S1106 - D8S1145*	1.05 (0.45)	2.38	0.02	1 (-0.46)(-0.63)(0.74) 2 (1.32)(4.23)(0.03) 3 (-0.20)(-0.13)(0.37) 4 (0.84)(2.56)(0.03) 5 (0.27)(0.99)(0.50) 6 (-0.85)(-0.39)(0.73) 7 (-0.91)(-0.72)(0.81)
Nine	64-69	*D9S1122 -D9S922*	0.60 (0.34)	2.16	0.03	1 (1.19)(4.47)(0.01) 2 (-1.08)(-0.51)(0.31) 3 (0.52)(1.27)(0.25) 4 (-0.95)(-0.41)(0.46) 5 (0.27)(0.99)(0.50) 6 (-0.74)(0.08)(0.30) 7 (-0.36)(-0.18)(0.37)
Nine	143-145	*ATA59H 06- D9S158*	0.93 (0.48)	1.87	0.04	1 (1.14)(4.09)(0.01) 2 (-0.85)(-0.43)(0.31) 3 (0.44)(1.19)(0.25) 4 (-1.70)(-0.62)(0.62) 5 (0.07)(0.21)(0.50) 6 (0.68)(1.14)(0.07)

						7 (-0.50)(-0.76)(0.81)
Thirteen	90-117	*D13S793 - D13S285*	2.03 (0.99)	2.34	0.02	1 (-0.03)(-0.55)(0.70) 2 (0.81)(1.68)(0.03) 3 (0.31)(0.87)(0.25) 4 (0.72)(1.93)(0.12) 5 (0.04)(0.11)(0.50) 6 (-0.09)(0.38)(0.20) 7 (0.55)(1.76)(0.06)
Twenty	3-35	*D20S103 - D20S470*	2.79 (0.99)	2.75	0.01	1 (-0.37)(-0.40)(0.70) 2 (0.95)(2.15)(0.03) 3 (0.50)(1.47)(0.12) 4 (0.84)(2.15)(0.12) 5 (0.27)(0.98)(0.50) 6 (0.53)(2.56)(0.04) 7 (0.38)(0.94)(0.25)
Twenty	45-53	*D20S477 - D20S481*	1.77 (0.74)	2.92	0.009	1 (1.20)(3.45)(0.04) 2 (0.85)(2.05)(0.04) 3 (0.55)(1.50)(0.12) 4 (-0.61)(-0.66)(0.65) 5 (0.27)(0.99)(0.50) 6 (-1.74)(-0.64)(0.74) 7 (0.54)(1.53)(0.06)
Twenty two	24-25	*GCT10C10- D22S689*	0.91 (0.48)	2.19	0.02	1 (1.11)(3.13)(0.03) 2 (-0.74)(-0.36)(0.31) 3 (0.55)(1.70)(0.12) 4 (-1.17)(-0.67)(0.65) 5 (0.24)(0.87)(0.50) 6 (0.23)(0.68)(0.11) 7 (-0.28)(-0.22)(0.37)
Twenty two	40-44	*D22S685 - D22S445*	1.20 (0.71)	2.04	0.03	1 (-0.28)(-0.30)(0.44) 2 (0.39)(0.99)(0.03) 3 (0.56)(1.76)(0.12) 4 (-1.4)(-0.73)(0.65) 5 (0.26)(0.95)(0.50) 6 (0.78)(2.26)(0.04) 7 (0.30)(0.49)(0.31)
X	70-84	*GATA144D04- DXS6800*	0.58 (0.75)	1.9	0.04	1 (0.01)(1.64)(0.09) 2 (0.43)(0.69)(0.09) 3 (0.50)(1.35)(0.25) 4 (-0.40)(0.39)(0.12) 5 (-0.05)(-0.14)(0.5) 6 (-0.36)(0.04)(0.37) 7 (0.39)(1.06)(0.37)

Table 3.17. Summary of Genehunter analysis V
Analysis V is an affecteds only analysis with 'affected' meaning the presence of VUR on a cystogram study, all other individuals have unknown affected status. Areas with a p value of less than 0.05 are described.

Chromosome	Distance	Markers	Parametric lod score (heterogeneity)	NPL score	P value	Individual pedigrees (Lod)(NPL)(p value) at the position of the maximum p value
One	156-165	*D1S1631* - *D1S1653*	2.77 (0.71)	5.35	0.0003	1 (-0.65)(-0.60)(0.90) 2 (-1.08)(-0.51)(1.0) 3 (0.57)(1.77)(0.12) 4 (0.83)(2.46)(0.06) 6 (2.15)(9.6)(0.003) 7 (0.55)(1.86)(0.125)
Two	53-68	*D2S402-D2S1352*	1.14 (0.30)	3.40	0.04	1 (-0.3)(0.31)(0.21) 2 (-0.86)(-0.44)(0.31) 3 (-0.65)(-0.08)(0.37) 4 (-0.37)(0.91)(0.18) 6 (2.02)(7.56)(0.003) 7 (0.11)(0.75)(0.25)
Three	37-65	*D3S1259* - *D3S1768*	2.15 (0.71)	2.72	0.01	1 (-0.64)(-0.45)(0.49) 2 (0.41)(1.04)(0.03) 3 (0.04)(0.12)(0.25) 4 (-0.04)(0.12)(0.18) 6 (1.73)(4.47)(0.003) 7 (-0.31)(-0.77)(0.62)
Three	158-169	*D3S3023* - *D3S1764*	1.33 (0.99)	2.38	0.01	1 (1.03)(2.84)(0.06) 2 (0.25)(0.81)(0.03) 3 (-0.12)(-0.15)(0.37) 4 (0.11)(1.09)(0.12) 6 (-0.40)(0.17)(0.3) 7 (0.52)(1.72)(0.12)
Five	53-55	*D5S1470* - *D5S1457*	0.22 (0.40)	1.84	0.04	1 (-0.29)(0.46)(0.09) 2 (-0.61)(-0.23)(0.31) 3 (0.56)(1.75)(0.12) 4 (-0.46)(0.51)(0.19) 6 (0.14)(0.81)(0.07) 7 (0.46)(1.42)(0.12)
Eight	20-30	*D8S1130* - *D8S1106*	0.87 (0.38)	1.73	0.04	1 (-0.65)(-0.62)(0.9) 2 (1.32)(4.23)(0.03) 3 (-0.2)(-0.13)(0.37) 4 (0.82)(2.42)(0.06) 6 (-0.85)(-0.39)(0.06) 7 (-0.91)(-0.92)(0.93)
Thirteen	97-117	*D13S779* - *D13S285*	1.75 (0.99)	2.17	0.02	1 (-0.05)(-0.50)(0.61) 2 (1.04)(2.24)(0.03) 3 (0.28)(0.76)(0.25) 4 (0.68)(1.70)(0.12) 6 (-0.07)(0.41)(0.20) 7 (0.51)(1.62)(0.125)
Twenty	4-33	*D20S103* - *D20S604*	2.18 (0.99)	1.96	0.03	1 (-0.55)(-0.44)(0.49) 2 (0.95)(2.15)(0.03) 3 (0.50)(1.45)(0.25) 4 (0.58)(0.86)(0.19) 6 (0.84)(2.56)(0.04) 7 (0.37)(1.17)(0.25)
Twenty-two	38-42	*D20S470* -	0.92 (0.62)	1.69	0.04	1 (-0.48)(-0.52)(0.61) 2 (0.47)(1.08)(0.03)

		D20S477				3 (0.56)(1.77)(0.12) 4 (-1.53)(-0.95)(0.87) 6 (0.73)(2.30)(0.04) 7 (0.31)(0.93)(0.25)
X	38-80	*GATA17 5D03-DXS7132*	0.76 (0.87)	1.91	0.04	1 (-0.15)(1.03)(0.18) 2 (0.27)(0.58)(0.09) 3 (0.56)(1.61)(0.25) 4 (-0.53)(0.10)(0.43) 6 (0.20)(0.52)(0.07) 7 (0.39)(1.21)(0.37)

Table 3.18. Summary of Genehunter analysis R

Analysis R is an affecteds only analysis with 'affected' meaning the presence of reflux nephropathy on an isotope renogram or intravenous pyelogram study, all other individuals have unknown affected status). Areas with a p value of less than 0.05 are described.

Chromosome	Distance	Markers	Parametric lod score (heterogeneity)	NPL score	p value	Individual pedigrees (Lod)(NPL)(p value) at the position of the maximum p value overall
One	13-44	*D1S1612* - *D1S1622*	0.53 (0.57)	1.7	0.04	1 (0.56)(2.45)(0.06) 2 (0.37)(0.97)(0.03) 3 (0.14)(0.27)(0.50) 4 (-0.25)(-0.29)(0.43) 6 (-0.93)(-0.24)(0.39) 7 (0.27)(1.36)(0.25)
One	138-168	*D1S1631* - *D1S1653*	2.08 (0.82)	3.91	0.003	1 (0.56)(2.45)(0.06) 2 (-1.08)(-0.51)(1.0) 3 (0.28)(1.25)(0.25) 4 (0.56)(1.86)(0.06) 6 (1.58)(1.12)(0.01) 7 (0.27)(1.41)(0.25)
Two	61-65	*D2S1788* - *D2S1352*	1.67 (0.84)	1.73	0.04	1 (0.27)(0.82)(0.06) 2 (-0.91)(-0.45)(0.31) 3 (0.25)(0.99)(0.25) 4 (0.54)(1.32)(0.25) 6 (1.12)(2.90)(0.03) 7 (0.21)(1.03)(0.25)
Three	61-65	*D3S3038* - *D3S1768*	1.40 (0.99)	1.7	0.04	1 (0.18)(0.47)(0.43) 2 (1.30)(4.05)(0.03) 3 (0.07)(0.16)(0.5) 4 (0.09)(0.09)(0.37) 6 (0.33)(0.56)(0.45) 7 (-0.42)(-0.97)(0.75)
Three	115-118	*D3S2406* - *D3S2459*	0.77 (0.82)	1.65	0.04	1 (0.31)(0.94)(0.06) 2 (0.53)(0.75)(0.03) 3 (-0.74)(-0.69)(0.75) 4 (0.50)(1.84)(0.06) 6 (-0.13)(0.58)(0.43) 7 (0.21)(0.98)90.25)
Three	157-185	*D3S3023* - *D3S1763*	1.46 (0.99)	2.0	0.02	1 (0.55)(2.32)(0.06) 2 (-0.06)(0.38)(0.31) 3 (-0.37)(-0.61)(0.5) 4 (0.51)(1.47)(0.06) 6 (0.73)(1.24)(0.03) 7 (0.12)(0.51)(0.25)
Four	45-62	*D4S2632* – *D4S3248*	0.67 (0.35)	1.91	0.03	1 (-0.56)(2.44)(0.06) 2 (-1.07)(-0.51)(0.31) 3 (-0.95)(-0.65)(0.75) 4 (-0.78)(-0.21)(0.37) 6 (1.26)(3.92)(0.03) 7 (0.02)(0.08)(0.25)
Eight	20-30	*D8S1130* - *D8S1145*	1.65 (0.83)	2.57	0.008	1 (0.31)(0.99)(0.06) 2 (1.29)(4.01)(0.03) 3 (0.22)(4.39)(0.5) 4 (0.22)(4.39)(0.5) 6 (-0.78)(-0.55)(0.43) 7 (-0.05)(-0.19)(0.75)

Thirteen	94-113	*D13S779 - D13S285*	1.89 (0.99)	2.65	0.007	1 (0.26)(0.76)(0.43) 2 (1.04)(2.24)(0.03) 3 (0.24)(1.02)(0.25) 4 (0.45)(1.66)(0.06) 6 (-0.15)(0.52)(0.43) 7 (0.27)(1.35)(0.25)
Twenty-one	13-24	*D21S1437- GATA129D11*	1.10 (0.71)	3.24	0.03	1 (0.39)(1.36)(0.06) 2 (-0.74)(-0.40)(0.31) 3 (0.53)(0.40)(0.20) 4 (0.23)(0.31)(0.28) 6 (1.08)(2.66)(0.03) 7 (0.18)(0.84)(0.25)

Table 3.19. Summary of Genehunter analysis T excluding pedigree six
This is an affecteds only analysis with 'affected' meaning the presence of reflux nephropathy on an isotope renogram or intravenous pyelogram study and/or the presence of VUR on a cystogram, all other individuals have unknown affected status, excluding pedigree six. Areas with a p value of less than 0.05 are described.

Chromosome	Distance	Markers	Parametric lod score	NPL score	p value
One	152-166	*D1S1631 - D1S1653*	0.7	2.65	0.01
Three	61-65	*GATA16 4B08- D3S1768*	1.01	1.90	0.04
Three	114-177	*GATA12 8C02- D3S1763*	1.89	3.79	0.004
Eight	24-30	*D8S1106 - D8S1145*	0.86	2.57	0.01
Thirteen	96-113	*D13S793 - D13S285*	2.08	2.37	0.02
Twenty	2-36	*D20S103 - D20S470*	1.22	1.57	0.02
Twenty	42-54	*D20S477 - D20S481*	2.90	3.42	0.003
Twenty two	24-28	*GCT10C 10- D22S689*	-0.3	1.9	0.04
X	74-84	*GATA17 5DO3- DXS7132*	0.89	2.04	0.03

Figure 3.33
The results of the NPL scores genome made in analysis V, R and T.
The areas with a suggestive P value of less than 0.05 in analysis T as described in Table 3.16 are highlighted *.

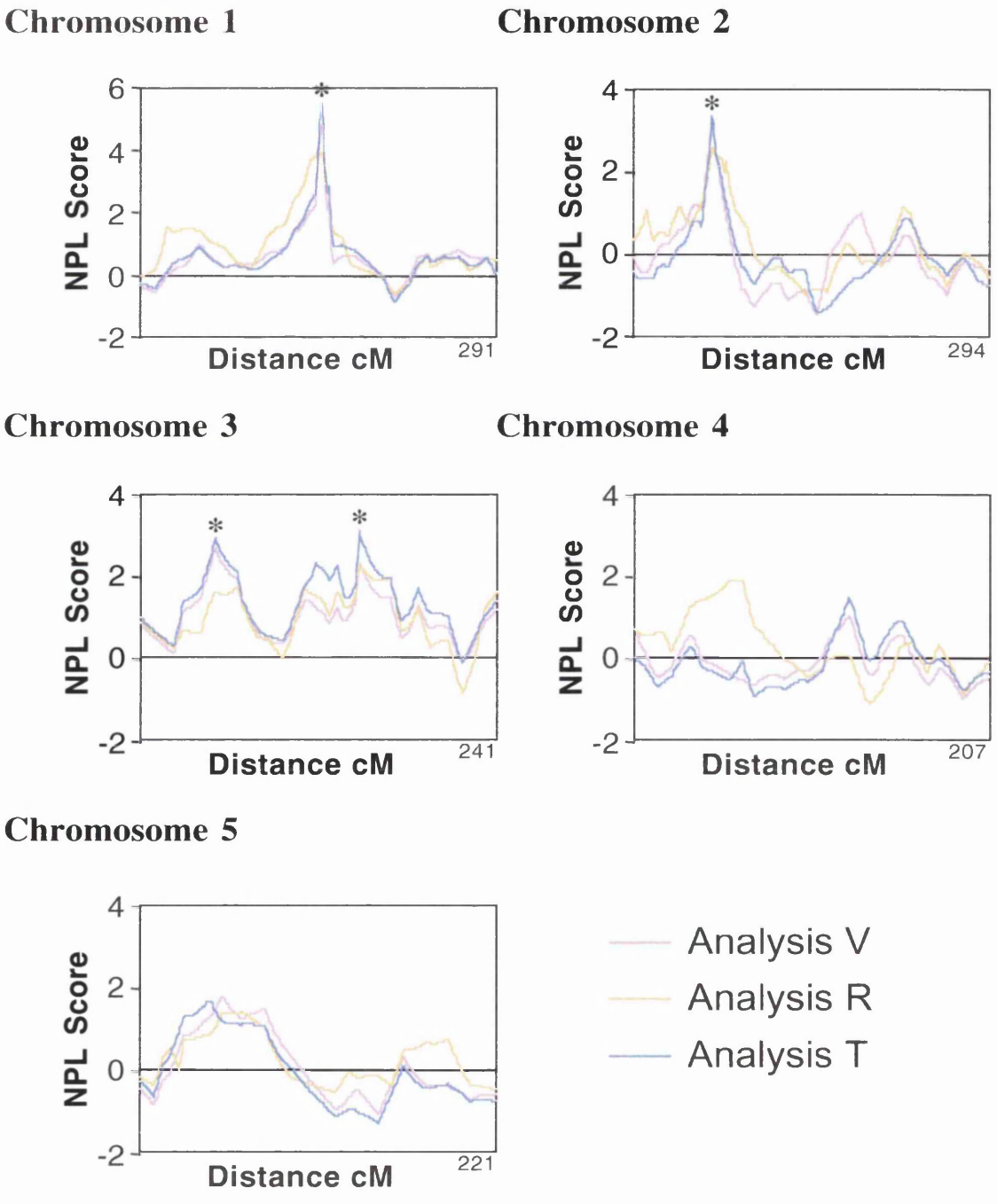

Chromosome 6

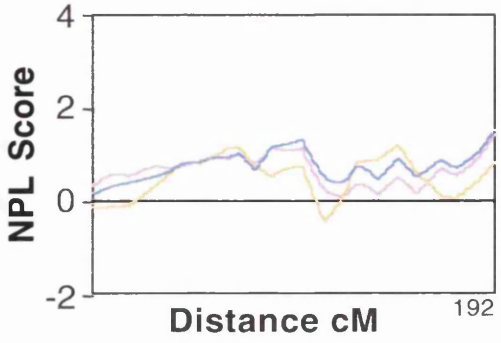

Chromosome 7

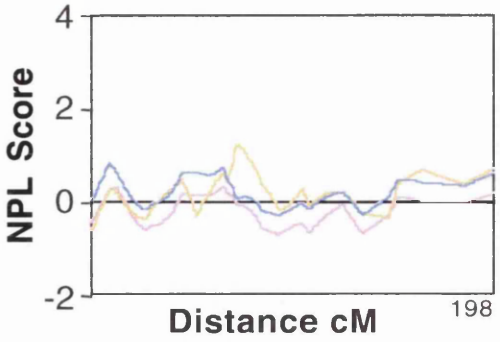

Chromosome 8

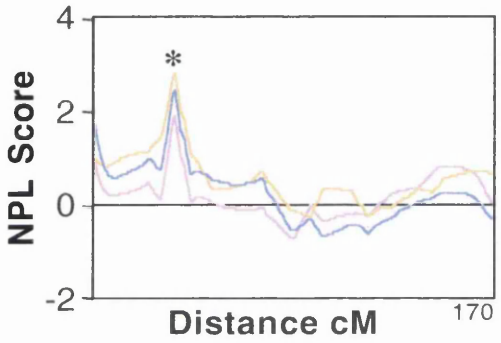

Chromosome 9

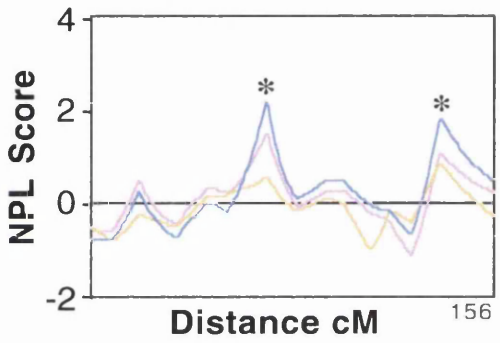

Chromosome 10

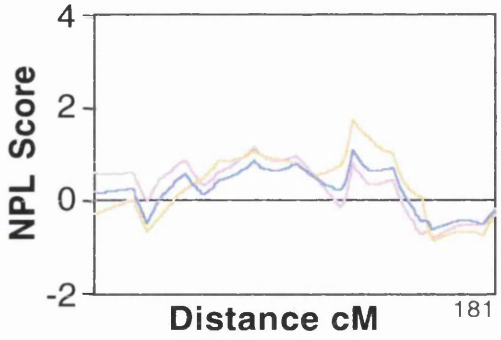

Chromosome 11

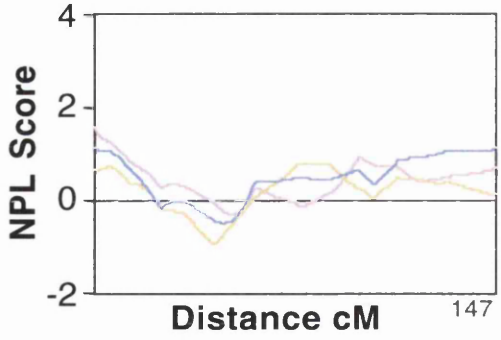

Chromosome 12

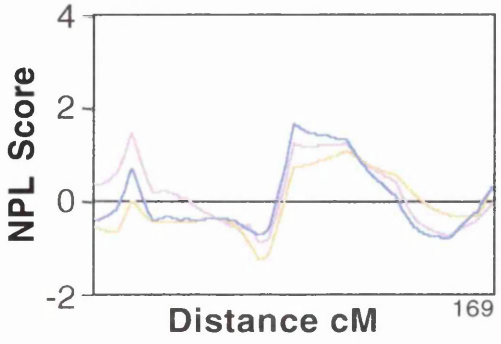

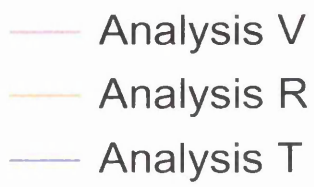

Chromosome 13

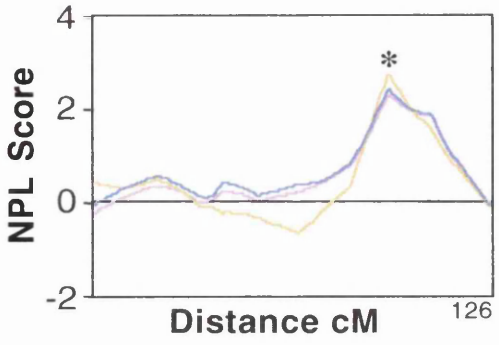

Chromosome 14

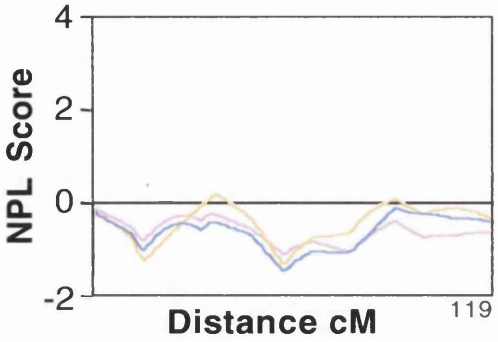

Chromosome 15

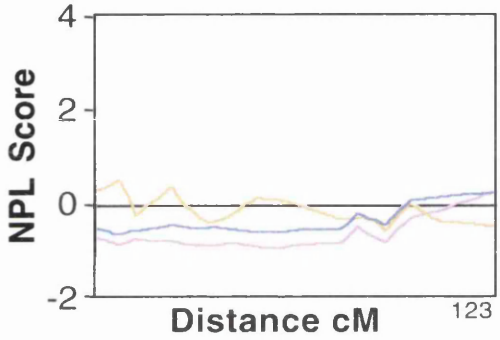

Chromosome 16

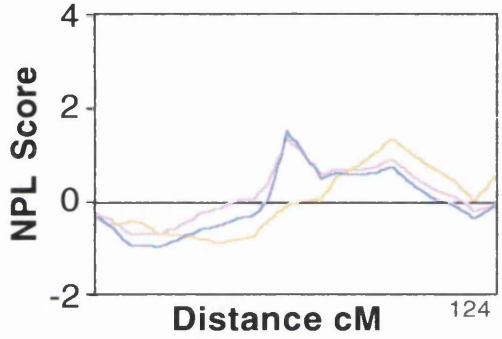

Chromosome 17

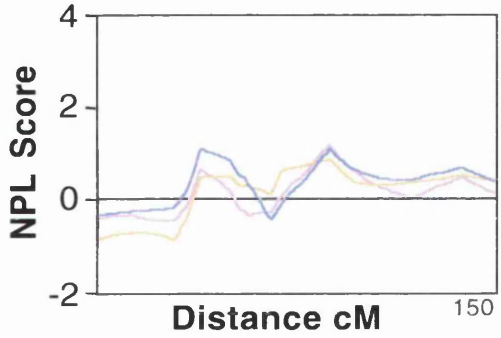

Chromosome 18

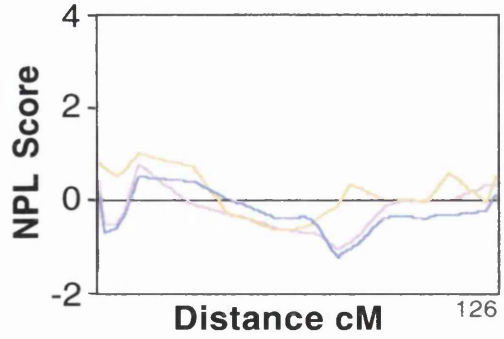

Chromosome 19

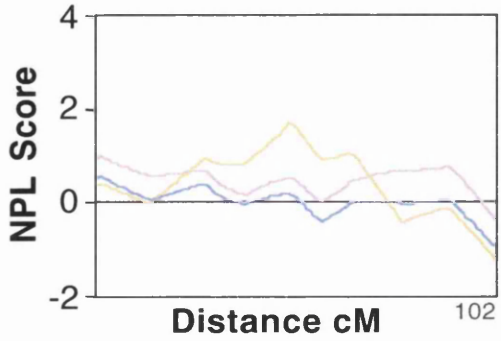

Analysis V
Analysis R
Analysis T

Chromosome 20

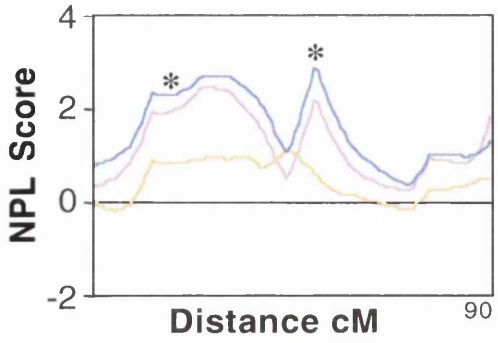

Chromosome 21

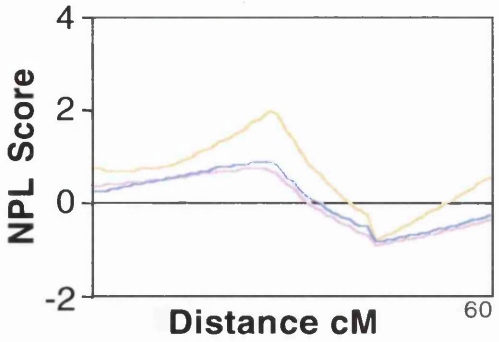

Chromosome 22

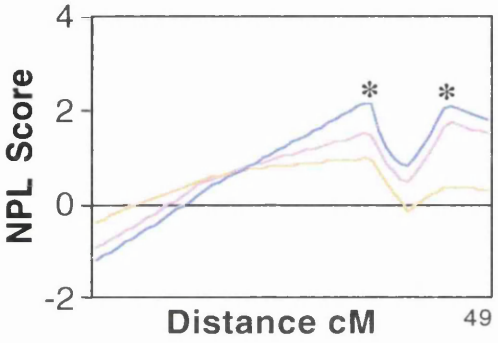

Chromosome x

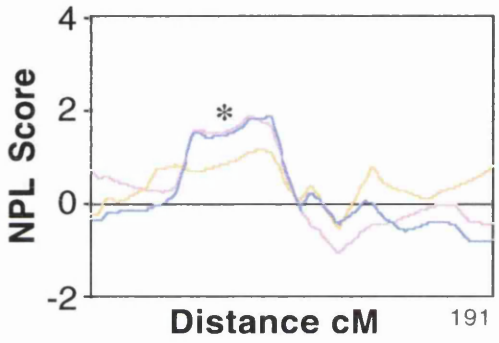

Analysis V
Analysis R
Analysis T

4.1 OFD 1

4.1.1 Proof that OFD1 is an X-linked dominant disorder that maps to Xp22.2-3

The hypothesis at the start of this thesis was that OFD1 was an X-linked dominant, male lethal disorder based on clinical data described by other authors (Doege et al, 1964; Wettke Schaeffer et al, 1983). The pedigree data collected during this thesis supports this hypothesis as the disorder was found almost exclusively in females, apart from pedigree 3 in which an affected male infant died shortly after birth due to cardiac failure associated with a complex congenital cardiac defect. This held true both in sporadic cases and pedigrees and the inheritance of OFD1 appeared to be dominant in the pedigrees collected. In addition, there were multiple miscarriages in affected females in the pedigrees collected in this thesis which is consistent with loss of hemizygous affected males as described by other authors (Wettke Schaeffer et al, 1983).

Various patterns of expression have been found in disorders caused by genes mapping to the X chromosome. Normally, the X-linked inheritance is suggested by the absence of male to male transmission and the observation that males are more severely affected than females. However, in OFD1 the X-linked dominant mode of inheritance of the phenotype would appear to contrast with most cases of X-linked inheritance in which males are typically affected while female carriers are normal or mildly affected e.g. Kallmann's syndrome (Franco et al, 1991). However, it is likely that in OFD1 the normal function of the gene product must

be so important that at least one normal copy in some cells is necessary for survival.

Other examples of X-linked dominant disorders in which the males generally die before birth include incontinentia pigmenti, a skin disorder associated with multiple congenital defects, and focal dermal hypoplasia (the Goltz-Gorlin syndrome) in which hypoplastic skin defects occur in association with digital, dental and ocular abnormalities (Wettke-Schaefer et al, 1983). Incontinentia pigmenti and focal dermal hypoplasia both occur almost exclusively in females and there is an increased rate of miscarriage.

Although clinical data would suggest that OFD1 is an X-linked dominant, male lethal disorder, in order to establish the mode of inheritance of OFD1, a linkage strategy was adopted using microsatellite markers on the X chromosome.

In this thesis OFD1 has been mapped to the short arm of the X chromosome, Xp22.2-22.3, between the telomeric marker *DXS996* and the centromeric marker *DXS7108* with a maximum lod score of 3.32 at $\theta = 0.0$ at *KAL* using an affecteds only analysis. This lod score, being greater than 3.0, is considered to be significant for linkage (Ott, 1991). It is robust to perform an affecteds only analysis in OFD1 using affected females and unaffected males as there is most likely to be too wide a range of phenotype in affected females to be certain whether a female in a pedigree is unaffected.

The presence of a recombination was detected in the middle of the OFD1 region at *DXS7108* (Figure 3.14) in II.6 (an apparently unaffected female). If we assume that II.6 was truly unaffected then it follows that OFD1 maps to the centromeric region between between *DXS7105* and *DXS7108.* Conversely, if II.6 was an asymptomatic carrier of an OFD1 mutation then OFD1 must map to the telomeric

region between *DXS996* and *DXS7108.* In view of this dilemma apparently unaffected females were labelled as unknown analysis leading to OFD1 being described as mapping to the wider region between *DXS996* and *DXS7108.*

The linkage study performed in this thesis has been subsequently confirmed by an analysis using affected females only which has further narrowed the region for OFD1 to between *DXS85* and *DXS7105* (Gedeon et al, 1999). Since *DXS85* is centromeric to *DXS7108*, this data strongly suggests that II.6 in pedigree one is not carrying the OFD1 mutation and hence is truly unaffected.

4.1.2. Deletions and translocations involving Xp22.2-22.3 have assisted in localising disease genes in the OFD1 region

A number of cytogenetic rearrangements are located within the OFD1 region on Xp22 and are summarised in Figure 4.1.

Females with monosomy of Xp which includes the centromeric portion of the OFD1 region have X linked dominant, male lethal disorders in which some clinical features overlap with those of OFD1 and with the clinical features of each other. These syndromes are Aicardi, focal dermal hypoplasia and microopthalmia with linear skin defects (MLS) syndrome.

In Aicardi syndrome (OMIM 304050) affected females have infantile spasms, absence of the corpus callosum and specific chorioretinal defects. In focal dermal hypoplasia (OMIM 305600) affected females have aplastic skin with a linear and asymmetric distribution, microopthalmia, chorioretinal defects, sparse hair, nail dystrophy and oral and skeletal malformations including digital malformations. In the MLS syndrome (OMIM 309801) females have a combination of phenotypic

features including microopthalmia, corneal opacities short stature, absent septum pellucidum and hypoplastic areas of skin.

Individuals with clinical features of Aicardi, Goltz and MLS have been mapped to Xp22 by gross chromosomal aberrations including terminal deletions (Friedman et al, 1988), X/Y translocations (Al-Gazali et al, 1990) and X/autosome translocations (Ropers et al, 1982; Donnenfield et al, 1990). The most centromeric marker deleted in an individual with MLS is *DXS1229* which is centromeric to *DXS85* (Lindsay et al, 1994). It is reasonable to speculate that the gene for OFD1 might lie within the region *DXS85* and *DXS1229.* However, it has not been possible to order the clinical features in Aicardi, focal dermal hypoplasia and MLS syndromes to suggest a contiguous gene defect which would have been useful to sublocalise OFD1 (Figure 4.1).

In males, interstitial deletions including the more telomeric portion of the region cause nullisomy and contiguous gene syndromes occur characterised by the association of up to five of the following diseases: short stature, X linked recessive chondrodysplasia punctata, mental retardation, X-linked ichthyosis due to steroid sulphatase deficiency and Kallmann's syndrome (Figure 4.1). However, since these disorders are distal to *DXS85*, OFD1 no longer maps to the region that contains these genes (Gedeon et al, 1999).

4.1.3. X-inactivation may be important in the expression of phenotype in OFD1

The striking variation in phenotype between affected females in OFD1 with respect to both the dysmorphic features and renal disease was noted. It is reasonable to hypothesise that different mutations of the OFD1 gene could be

responsible for the variation between unrelated affected individuals with OFD1. An example of clear genotype/phenotype correlations exists within the dystrophin gene. Deletions leading to frameshift changes causes an absence of dystrophin production in the more severe Duchenne muscular dystrophy whereas deletions leading to an intact reading frame and production of partially functional dystrophin occurs in the milder Becker muscular dystrophy (Hoffman et al, 1987; Monaco et al, 1988). An example of a poor genotype/phenotype correlation exists in the branchio-oto-renal syndrome in which the severity of the renal disease is unrelated to the mutation in the *EYA1* gene (Abdelhak et al, 1997). However, the phenotype is also variable between affected individuals in an OFD1 pedigree which might be related to differences in genetic background between affected individuals in the pedigree.

Another possibility is that differences in X-inactivation between affected females with OFD1 might play a part in the wide range and asymmetry of phenotype. Non-random X-inactivation has been described in carrier females in the X linked OTC (ornithine transcarboxylase) deficiency. Symptoms can occur in heterozygous female carriers of OTC deficiency and disease activity is correlated with extent to which X-inactivation is skewed in the liver cells of heterozygotes (Rowe et al, 1986; Yorifuji et al, 1998). Of note, the lymphocytes in affected OTC heterozygotes show random X-inactivation. Similarly, as OFD1 affects the kidney, oral cavity, face and digits X-inactivation studies in OFD1 would need to be performed in these tissues, not in lymphocytes to be meaningful.

It is possible to speculate that Aicardi, Golz and MLS phenotypes involve X inactivation. Females with a single X chromosome do not have these defects which suggests that having a single copy of the gene is sufficient to prevent them

Figure 4.1
Summary of the region to which OFD1 maps on Xp22.3-22.3

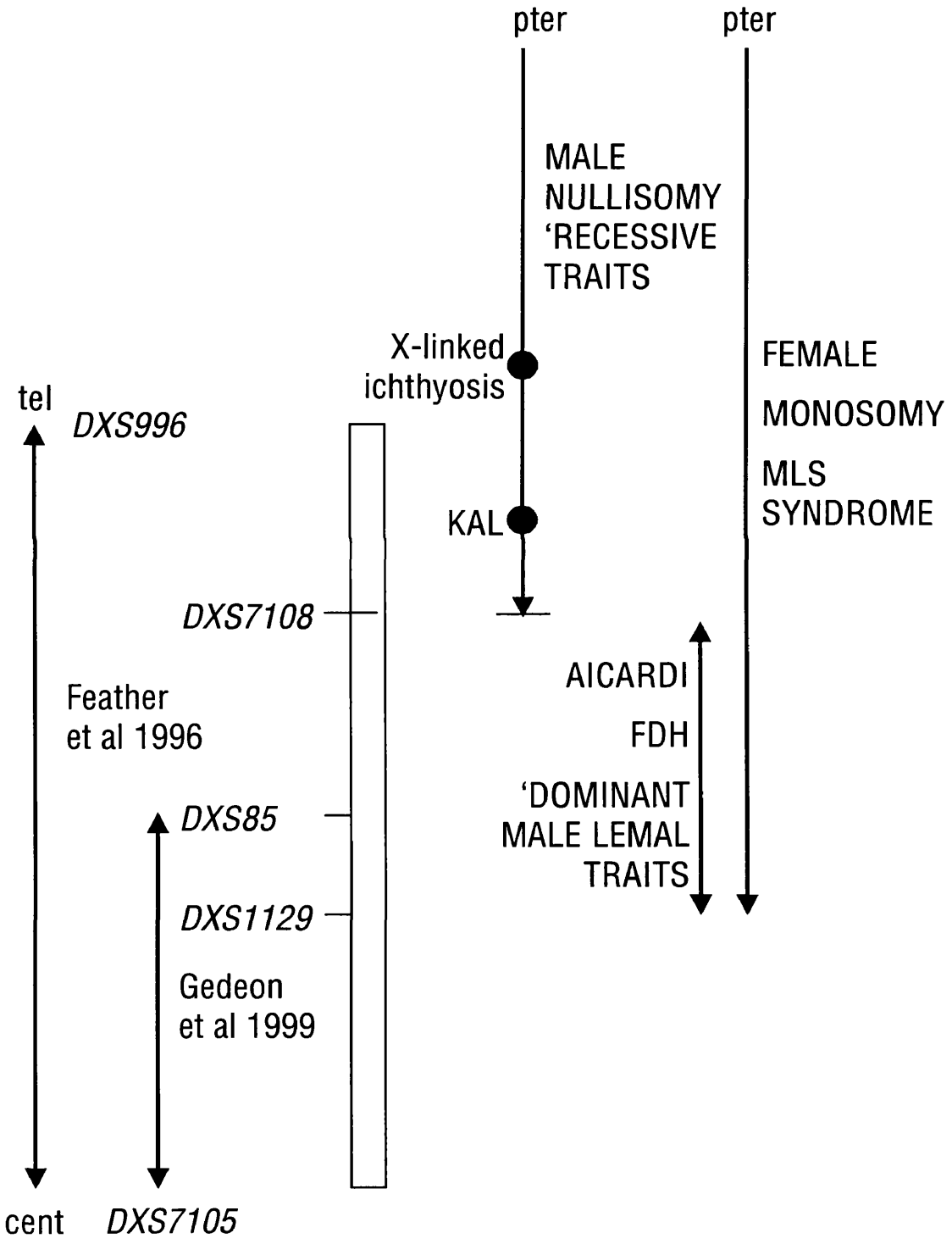

so it seems reasonable to predict that X inactivation plays a role in the expression of Aicardi, Goltz and MLS phenotypes (Ballabio and Andria, 1992). X inactivation studies have been performed in a number of individuals with Aicardi, Golz and MLS syndromes with conflicting results (Ballabio et al, 1992). These studies were performed in lymphocytes which may be misleading as discussed in OTC.

Females with deletions involving Xp22.2-3 do not show any of the recessive diseases described in males and it is suggested that as these genes escape X-inactivation one copy is sufficient to prevent the disease (Ballabio and Andria, 1992).

4.1.4. How robust is the exclusion of candidate genes in the OFD1 region?

How robust was the approach taken to finding the gene in OFD1 within the Xp22.2-3 region? It was not possible to further narrow the region with recombinations in further pedigrees nor were there any gross chromosomal aberrations in OFD1 to pinpoint the gene localisation. A candidate gene approach was therefore taken examining all known genes in the region which would be predicted from knowledge of their function and expression to cause the oral, facial, digital and renal phenotypes of OFD1. Four of the genes examined in the region, *KAL, APXL, CLC4 and FXY/MID1* are no longer in the OFD1 critical region and are therefore excluded (Gedeon et al, 1999).

Single strand conformation polymorphism analysis in a sensitive technique which should detect 70-95% of mutations (Grompe et al, 1993) and with 20 unrelated individuals with OFD1 it is likely, based on the knowledge that there are typically many different mutations in X chromosome genes, such as the gene for Fabry's

(Eng et al, 1994) and OTC (Tuchman et al, 1996) that mutations would be detected by this method. Although this method is not 100% sensitive, it is a rapid and practical method in view of the large number of genes to be examined. In addition, genes have been sequenced by collaborators and found to have no mutations.

However, gross rearrangements of the gene such as deletions and inversions would not be detected by this method and future studies should include Southern blotting to exclude major rearrangements. An example where difficulties in finding mutations in a gene was due to gross rearrangements was in the Factor VIII gene in haemophilia where up to 50% of patients did not have mutations in the coding sequence (Higuchi et al, 1991). This was explained when a messenger RNA defect was found in over 40% of patients due to DNA inversions involving intron 22 of the gene which could be demonstrated on Southern Blotting (Naylor et al, 1992; Naylor et al, 1993).

4.1.5. New insights into the glomerulocystic renal disease in OFD1

There have only been two previous reports of OFD1 renal histology published and both cases were not in proven pedigrees. One was a female who developed renal failure in the second decade (Stapleton et al, 1982) and the other was an XY male neonate with massively dilated kidneys and lung hypoplasia who died hours after birth (Gillerot et al, 1993). Both studies noted a predominance of glomerular cysts as assessed by gross histological appearances. This study confirms this impression in a clearly documented familial case and adds new insights.

The histology perfomed using renal tissue obtained at autopsy from individual I.2 in pedigree one, demonstrated that the majority of cysts were glomerular in origin

as they failed to stain with lectins that bind to proximal and distal tubules and some cysts contained tufts with capillary loops surrounded by cells staining for WT-1, a protein expressed by podocytes in the postnatal kidney. However, a minority of smaller cysts stained with *Arachis hypogaea* lectin, indicating an origin in distal tubules. This observation is important as it suggests that the (as yet unknown) OFD1 gene product plays a biological role in distal as well as glomerular epithelia. Proliferation was detected in approximately 50% of cells within glomerular tufts attached to OFD1 cyst walls. Therefore deregulated proliferation might be important in the genesis of OFD1 renal cysts and it is notable that epithelial hyperproliferation has been implicated in a variety of human and animal models of PKD (Grantham et al, 1992). PAX2 transcription factor protein is barely detectable by immunohistochemistry in mature human kidneys (Winyard et al, 1996) but in this study PAX2 was strongly expressed by epithelia lining distal tubule OFD1 cysts. PAX2 is highly expressed by proliferating distal tubule precursor cells in human fetal kidneys, in cysts of human dysplastic kidneys (Winyard et al, 1996) and in Wilms' tumours (Dressler et al, 1993). Conversely, PAX2 was not expressed in OFD1 glomeruli, suggesting that other factors must drive proliferation in these structures. In future, it would be interesting to examine the histology of other OFD1 patients who have PKD but are not in severe renal failure.

4.1.6. Clinical applications of the results of this thesis

How can the findings in this study advance the clinical management of patients and families with OFD1? Firstly, proving that OFD1 is an X-linked disorder means that predictions can be made about the offspring of affected females with

OFD1; there is a 50% chance that female offspring will be affected whereas the vast majority of male offspring will be normal as affected males will be lost in miscarriages. Males in pedigrees with OFD1 who appear to be unaffected will not be carriers. Linkage studies between *DXS85* and *DXS7105* could be used to as a diagnostic test to establish affected status in an apparently normal female or in the offspring of affected females in a OFD1 pedigree.

Counselling of affected individuals with OFD1 about the implications of polycystic kidney disease is different from ADPKD. A wide range of age of onset and severity of PKD occurs in OFD1 even within pedigrees and current knowledge does not allow prediction of progress of renal disease or the age at which it would be safe to stop screening for PKD in affected individuals with OFD1. In the future it would be useful to follow the renal progress in the cohort of OFD1 individuals collected in this study in order to answer these questions.

Finding the location of OFD1 on the X chromosome can be used to redefine the categorisation of some OFD cases (Table 4.1.). For example the original report of pedigree three used in my study (Goodship et al, 1991) questioned whether the pedigree was OFD1 or OFDII as there is considerable overlap in the clinical features between OFD1 and OFDII. The microsatellite analysis performed in this pedigree shows that affected individuals in pedigree three share the same haplotype across the OFD1 region. Although the pedigree is not large enough to calculate a statistically significant lod score, the results are consistent with pedigree three being classified as OFD1 or being allelic with OFD1. Similarly, it would be interesting to examine pedigrees with OFDVIII (X-linked recessive) (Edwards et al, 1988) to see if OFDVIII is allelic with OFD1. When the gene for OFD1 is known, it will be possible to answer these questions more accurately. In

addition, the gene for OFD1 would be predicted to be related to the genes for the other OFDs which could assist in cloning the as yet unknown genes for other types of OFDs.

4.1.7. Future studies planned in OFD1

4.1.7.1. Isolation of the gene for OFD1

Future studies to find the gene for OFD1 will include continued collaboration with groups whose remit is to isolate all the genes in the OFD1 region as all the known genes have been screened for mutations in OFD1. A subsection of this region is being sequenced at the Sanger Center, Cambridge University and bioinformatic approaches could be taken such as GRAIL to identify novel genes in this region. Additional approaches could involve examining UniGene clusters that map to the OFD1 region.

4.1.7.2. Examination of the *Xpl* mutant as a mouse model of OFD1

The mouse mutant with X-linked dominant polydactyly (*Xpl*) maps to a region of the mouse chromosome that includes the homologous region to which OFD1 maps in humans flanked by the *AMELX* and *APXL* genes in both mice and humans (Sweet et al, 1980; Boyd et al, 1998). Urogenital abnormalities are known to occur in this mouse including hydroureter, hydronephrosis and cystic or absent kidneys (Sweet et al, 1980). The renal cysts in the OFD1 mouse deserve further examination to determine whether they are glomerulocystic, the polycystic renal disease associated with OFD1 as this mutant should be considered a good candidate for the mouse model of OFD1. Future studies should include more accurate mapping of the *Xpl* mouse on the X chromosome as the region to which

the *Xpl* mouse maps also includes a region homologous to the more proximal human Xp11.2 region where the genes SMXC and ALAS2 are located (Blair et al, 1998; Boyd et al, 1998). Backcross mapping experiments in the mouse could be used to more accurately map the *Xpl* mouse and, if it still mapped within the OFD1 region, to substantially narrow the region allowing a positional cloning approach to discovering the *Xpl* gene. Once the mouse gene was discovered, the sequence could be used to find the homologous human gene.

4.2 VUR and RN

4.2.1. Difficulties in ascertainment of clinical data

The diagnoses of VUR and RN in this thesis were made radiologically; VUR being demonstrated in cystogram study and RN being demonstrated on an isotope renogram or intravenous pyelogram. These criteria are stringent but it was important to exclude individuals with vague symptoms of renal disease such as cystitis or hypertension as these would not necessarily be caused by VUR or RN. However, these stringent criteria mean that much information was lost as firstly individuals with no symptoms were reluctant to have radiological investigations and secondly as VUR regresses with age (Tamminen-Mobius et al, 1992) a normal cystogram in an adult does not exclude the presence of VUR when they were younger. For these reasons any individual who did not have VUR or RN demonstrated radiologically was labelled unknown, thereby reducing the potential power of many of the pedigrees collected.

My study is of primary, non-syndromic VUR and attempts were made to ensure that no individual had any dysmorphic features suggestive of a syndrome.

Secondary causes of VUR were excluded through clinical history and investigations previously performed. Affected individuals were questioned about bladder abnormalities but no formal urodynamic studies were performed which might have picked up subtle defects. However, as discussed in section 1.6.3, the true nature of the defect in primary VUR is unknown and suggestions have included abnormal bladder contractility (Koff, 1992) as well as anatomical anomalies at the insertion of the ureter into the bladder.

RN was defined in this study as the presence of an abnormal intravenous pyelogram or isotope renogram. As discussed in section 1.6.4 there are at least three different types of RN. These are focal scarring associated with IRR of infected urine, congenital renal malformations and focal segmental glomerulosclerosis. As no renal histology is available on affected individuals it is not clear which type of RN they have. Therefore, the individuals with RN may represent a heterogeneous group with respect to renal histology.

4.2.2. Is a genome wide search in seven large families a justified approach?

At the commencement of this thesis there were only three potential candidate regions for VUR, chromosome 6, chromosome 10 and the X chromosome as discussed in section 1.6.10. A large number of potential candidate genes exist genome wide and so a systematic genome wide search was a justified approach and could be tackled practically with genome wide panels of microsatellite markers available an access to an automated sequencing facility.

This approach has been used in a number of different disorders including IDDM and inflammatory bowel disease as discussed in section1.6.11. In the case of IDDM genome-wide scans revealed evidence that the HLA locus and the insulin

gene are important in the pathogenesis (Vyse and Todd, 1996). In the case of inflammatory bowel disease genome-wide scans have excluded the HLA locus as playing a role in the pathogenesis and isolated other loci for investigation (Hugot et al, 1996; Ohmen et al, 1996; Satsangi et al, 1996). However, in other diseases this approach has been less successful such as multiple sclerosis in which despite a number of genome scans, no definitive locus or genes have been found (Ebers et al, 1996; Haines et al, 1996; Sawcer et al, 1996).

Our choice of pedigrees to use in the genome wide scan was different from the approach taken in, for example, multiple sclerosis in which large numbers of affected sibling pairs were screened. We did not choose this approach as the pedigrees available to us were much larger and therefore potentially more powerful. Using large dominant-looking pedigrees in the first genome wide scan allowed us to combine a parametric (genetic model dependent) approach which is potentially more powerful unless the model is wrong with a non-parametric approach (genetic model free). A hypothesis at the commencement of the study was that these pedigrees might represent a subset in which a single gene was playing a major role as in the families with early onset of breast cancer as a distinguishing feature which led to the isolation of the *BRCA1* gene (Hall et al, 1990).

4.2.3. To what extent were candidate regions excluded?

At the commencement of this thesis I reasoned that three regions, chromosome 6p, chromosome 10q and the X chromosome, were good candidates to test for VUR and RN. Chromosome 6p was considered to be a good candidate because the HLA region and a hereditary hydronephrosis loci are located there (Groenen et

al, 1998; Izquierdo et al, 1992; Macintosh et al, 1989) and chromosome 10 was considered to be a good region because the genes *PAX2*, *FGFR2* and *RET* are located there (Schuchardt et al, 1994; Wilkie et al, 1996; Sanyanusin et al, 1995). The X chromosome was considered because of the increased incidence of VUR in females generally (Baker et al, 1966) and the presence of a subset of male infants with congenital renal malformations in association with VUR (Yeung et al, 1997).

No region on 6p or 10q had a p value approaching suggestive of linkage ($p = 0.05$). This is not the same as formal exclusion of the regions with a parametric lod score of less than –2 (Ott , 1991). This study is not as accurate as a formal exclusion of the candidate genes such as *PAX2* by mutation screening but the formal exclusion of *PAX2* in other VUR kindreds has been performed by other authors (Choi et al, 1998).

On the X chromosome there was a region barely suggestive of linkage between the markers *GATA144D04* and *DXS6800* with a p value of 0.04, NPL score of 1.9 and a parametric lod score of 0.58 in the combined analysis T. The region is also suggestive of linkage in analysis V but did not reach significance in analysis R. Interestingly, the *AT2R* gene is located in this region and an association between an intronic polymorphism of this gene and renal malformations in male infants has been reported (Nishimura et al, 1999). This area clearly warrants further examination both to examine the role of the *AT2R* association in our group of patients with VUR and to explore the wider region to test whether this polymorphism is in linkage disequilibrium with another candidate gene for VUR.

4.2.4. What positive conclusions can be drawn from the genome scan results?

4.2.4.1. Evidence for a major locus on chromosome one

My study provides strong evidence for a major locus on chromosome one between the markers *D1S1631* and *D1S1653* with a p significance value of 0.0002 and an NPL score of 5.48 in analysis T. Although the p value does not meet the stringent criteria for significant linkage (p = 0.00002) (Lander and Kruglyak, 1995) the p value is more than two hundred times more significant than the criteria suggestive of linkage. In addition, the parametric lod score tested under conditions of heterogeneity is 3.12 which meets conventional criteria of significance (Ott, 1991). The area is again the most significant locus in analysis V and R.

Interesting genes within this region include the glutathione S-transferase (GTSM1). Germline deletion of this gene is associated with an increased risk of bladder cancer (Golka et al, 1997). Another gene is the colony-stimulating factor CSF-1 which is implicated in renal damage (Wada et al, 1997). It is also possible that there might be more than one gene in the same region interacting as, for example, in the fawn hooded rat where two genes controlling susceptibility to hypertension and progression of renal disease (Brown et al, 1996) or in the case of *PKD1* and *TSC2* in which genetic interplay can determine the extent of renal cystic phenotype (Sampson et al, 1997).

4.2.4.2. Genetic heterogeneity

Considerable evidence for genetic heterogeneity exists as pedigrees one and two do not map to the most significant locus on chromosome one. As discussed in section 3.2.2.2. there is evidence for three additional loci for these pedigrees on chromosomes three, eight and twenty and when the genome scan analysis was

repeated with the exclusion of pedigree one the scores on chromosomes three and eight improved.

It is possible that more than one locus exists for VUR as in autosomal dominant polycystic kidney disease in which at least two loci exist (Mochizuki et al, 1996).

4.2.4.3. Is VUR a dominant disorder?

In the pedigrees collected, the mode of inheritance appeared to be dominant. In addition a previous segregation analysis suggested that the inheritance was most likely to be autosomal dominant (Chapman et al, 1985). Overall, VUR is genetically heterogeneous featuring in a number of syndromes with different underlying mutations e.g. the renal-coloboma syndrome. However, the question to be addressed in this thesis was that a subset of families with VUR could have a major effect due to a single gene.

Thirteen different loci have been identified genome wide which at first glance would appear to be similar to results obtained in genome wide scans performed in disorders in which a polygenic mode of inheritance is likely such as IDDM and inflammatory bowel disease. However, in favour of a dominant mode of inheritance is the presence of a major susceptibility locus on chromosome one in pedigree six. It is likely that some of the loci suggestive of linkage are false positives (Lander and Kruglyak, 1995). It remains to be seen whether mutations in a gene on chromosome one can account for the VUR phenotype in a large number of families or whether genes at additional loci contribute also.

4.2.4.4. Are VUR and RN manifestations of the same genetic disorder?

Three separate analyses were performed in the genome scan in order to attempt to answer this question. The pathogenesis of the renal disease could either be due to IRR of infected urine or both the VUR and RN could be manifestations of the same genetically determined defect. In addition, the pedigrees collected were all ascertained because at least one individual had renal disease associated with VUR. Certainly with respect to chromosome one, this region is the most significant in all three analyses suggesting that VUR and RN are manifestations of the same genetic disorder.

However, genome wide the region on chromosome 5 appears only in the VUR analysis and the region on chromosomes four and twenty one appear only in the analysis of RN. Further analysis of these regions should answer the question as to whether additional separate genetic mechanisms operate in VUR and RN. Indentifying the individuals with VUR who are prediposed to RN would be of clear clinical importance.

4.2.5. Clinical applications

This study has made the first steps towards understanding the genetics of VUR and RN. Once the genes underlying this disorder are known it may be possible to develop genetic screening tests initially within known kindreds with VUR but eventually for isolated cases as well. Genetic tests would be invaluable to predict which infants with urinary tract infections are at risk of developing VUR and, more importantly, which are at risk of developing renal disease. Some invasive radiological investigations could be avoided and arrangements could be made to clinically monitor the group who is at risk of renal disease more closely.

4.2.6. Future directions

4.2.6.1. Candidate genes in chromosome one region

Future directions in the VUR study should focus on the most significant locus on chromosome one by testing the region with additional pedigrees with VUR and RN in an attempt to narrow the region further. In addition, candidate genes in the chromosome one region should be tested using the strategies for mutation screening used in OFD1.

4.2.6.2 Testing regions with additional clinical material

Additional pedigrees should be tested against the regions suggestive of linkage in the genome scan which would either provide additional proof of linkage or would show that the areas were false positives.

Table 4.1. OFD Types II-IX. (Adapted from Toriello, 1993)

Type of OFD	Oral Features	Facial Features	Digital Features	Renal Features	Other Features	Mode of inheritance
OFD II (Mohr, 1941)	Arched or cleft palate Oral Frenulae Tongue nodules and clefts	Median cleft lip Bifid nose tip	Clinodactyly Syndactyly Pre- or postaxial polydactly	None reported	Coarse hair Congenital heart defects Por-encephaly Hydro-cephaly	Autosomal recessive
OFD III (Sugarman et al, 1971)	Cleft uvula Tongue nodules and clefts Extra and small teeth	Hyper-telorism Bulbous nose Low set ears	Postaxial polydactyly	None reported	See-saw winking Myoclonic jerks Short sternum Hyper-convex nails	Autosomal recessive
OFD IV Burn et al, 1984)	High arched or cleft palate Lobed tongue Tongue nodules Frenulae	Epicanthal folds Micro-gnathia Low-set ears	Pre- and postaxial polydactyly Brachy-dactyly Clinodactyly Syndactyly	None reported	Por-encephaly Cerebral atrophy Pectus excavatum Hypoplastic tibiae Short stature	Autosomal recessive
OFD V (Thurston, 1909)	Frenulae	Midline cleft lip	Pre- and post axial polydactyly	None reported	None reported	Autosomal recessive
OFD VI (Varadi et al, 1980)	Highly arched/ cleft palate	Hyperteloris m Cleft lip Broad nasal	Pre- and post axial polydactyly Brachy-	Renal agenesis and dysplasia	Congenital heart defects Cerebellar	Autosomal recessive

	Lobed tongue Tongue nodules Frenulae	tip	dactyly Clinodactyly Syndactyly Central polydactyly Poly-syndactyly		anomalies	
OFD VII (Whelan, 1975)	Highly arched/ cleft palate Tongue nodules Oral Frenulae	Hyper-telorism Cleft lip Asymmetry	Clinodactyly	Hydronephrosis	Preauricular skin tag	Autosomal dominant or X-linked dominant
OFD VIII (Edwards et al, 1988)	Lobed tongue Highly arched palate Oral Frenulae Absent teeth Tongue nodules	Median cleft lip Telecanthus Broad/bifid nose	Pre- and postaxial polydactyly	None reported	Tibial and radial defects Hypoplastic epiglottis	X-linked recessive
OFD IX (Gurrieri et al, 1992)	Lobed tongue Tongue Nodules Frenulae	Cleft lip	Brachy-dactyly Syndactyly Bifid toes	None reported	Retinal defects Short stature	Autosomal recessive or X-linked recessive

Abbott GD (1972) Neonatal bacteriuria: a prospective study in 1,460 infants. BMJ 1: 267- 277

Abdelhak S, Kalatzis V, Heilig R et al (1997) A human homologue of the Drosophila eyes absent gene underlies branchio-oto-renal syndrome. Nat Genet 15: 157-164

Ainsworth PJ, Surh L, Coulter-Mackie MB (1991) Diagnostic single strand conformation polymorphism (SSCP): a simplified non-radioisotopic method as applied to a Tay-Sachs B1 variant. Nucleic Acids Res 19: 405-406

Al-Gazali LI, Mueller RF, Caine A et al (1990) Two 46,XX t(X;Y) females with linear skin defects and congential microphthalmia: a new syndrome at Xp22.3. J Med Genet 27: 59-63

Allen G, Harvald B, Shields J (1967) Measures of twin concordance. Acta Genet Stat Med 17: 475-481

Allen TD (1979) Vesicoureteral reflux as a manifestation of dysfunctional voiding. In Hodson J, Kincaid-Smith P eds. Reflux nephropathy. Masson, New York, USA. 171-180

Allen TD (1992) Commentary: voiding dysfunction and reflux. J Urol 148: 1706-

1712

Alpers CE, Seifert RA, Hudkins KL et al (1992) Developmental patterns of PDGF B chain, PDGF receptor and α-actin expression in human glomerulogenesis. Kidney Int 42: 390-399

Amar AD (1972) Familial vesico-ureteral reflux. J Urol 108: 969-979

Ambrose SS (1969) Reflux pyelonephritis in adults secondary to congenital lesions of the ureteral orifice. J Urol 102: 302-312

Arfeen S, Rosborough DR, Luger AM et al (1993) Familial unilateral renal agenesis and focal and segmental glomerulosclerosis. Am J Kidney Dis 21: 663-668

Asscher AW, McLachlan MSF, Jones RV et al (1973) Screening for asymptomatic urinary tract infection in schoolgirls. Lancet 2: 1-4

Askari A, Belman AB (1982) Vesicoureteral reflux in black girls. J Urol 127: 747-757

Atiyeh B, Husmann D, Baum M (1992) Contralateral renal abnormalities in multicystic dysplastic kidney disease. J Paediatr 121: 65-67

Atiyeh B, Husmann D, Baum M (1993) Contralateral renal abnormalities in

patients with renal agenesis and non-cystic renal dysplasia. Paediatr 91: 812-815

Attar R, Quinn F, Winyard PJD et al (1998) Short-term urinary flow impairment deregulates pax-2 expression, proliferation and cell survival in fetal sheep kidneys. Am J Pathol 142: 1225-1235

Atwell JD, Cook PL, Howell CJ et al (1974) Familial incidence of bifid and double ureters. Arch Dis Child 49: 390-393

Atwell JD, Allen NH (1980) The interrelationship between paraureteric divertiula, vesicoureteric reflux and duplication of the pelvicalyceal collecting system: a family study. Br J Urol 52: 269-273

Attwell JD (1985) Familial pelviureteric junction hydronephrosis and its association with a duplex pelvicalyceal system and vesicoureteric reflux. A family study. Br J Urol 57: 365-375

Avner ED, Sweeney WE (1990) Polypeptide growth factors in metanephric growth and segmental nephron differentiation. Paediatr Nephrol 4: 372-377

Avner ED, Sweeney WE Jr, Nelson WJ (1992) Abnormal sodium pump distribution during renal tubulogenesis in congenital murine polycystic kidney disease. Proc Natl Acad Sci USA 89: 7447-7451

Aufderderheide E, Chiquet-Ehrismann R, Ekblom P (1987) Epithelial

mesenchymal interactions in the developing kidney lead to expression of tenascin in the mesenchyme. J Cell Biol 105: 599-608

Bailey RR (1973) The relationship of vesicoureteric reflux to urinary tract infection and chronic pyelonephritis-reflux nephropathy. Clin Nephrol 1: 132-141

Bailey RR, Wallace M (1978) HLA-B12 as a genetic marker for vesicoureteric reflux? BMJ 2: 48-49

Bailey RR (1979) Vesicoureteric reflux in healthy infants and children. In: Hodson J, Kincaid-Smith P eds. Reflux Nephropathy. Masson, New York, USA. 59-61

Bailey RR, Lynn KL, Buttimore AL, Robson RA (1991) End stage reflux nephropathy. In: Bailey RR ed. Second J Hodson Symposium on Reflux Nephropathy. Design Printing Service, Christchurch, New Zealand. 49-60

Baker R, Maxted W, McCrystal H et al (1965) Unpredictable results associated with treatment of 133 children with ureterorenal reflux. J Urol 94: 362-372

Baker R, Maxted DW, Maylath J et al (1966) Relation of age, sex and infection to reflux: data indicating high spontaneous cure rate in paediatric patients. J Urol 95: 27-37

Baker R, Barbaris HT (1976) Comparative results of urological evaluation of

children with initial and recurrent urinary tract infection. J Urol 116: 503-513

Ballabio A, Sebastio G, Carrozzo R et al (1987) Deletions of the steroid sulphatase gene in 'classical' X linked ichthyosis and in X linked ichthyosis associated with Kallmann's syndrome. Hum Genet 77: 338-341

Ballabio A, Andria G (1992) Deletions and translocations involving the distal short arm of the human X chromosome: review and hypotheses. Hum Mol Genet 1: 221-227

Bao Q, Hughes RC (1995) Galectin- 3 expression and effects on cyst enlargement and tubulogenesis in kidney epithelial MDCK cells cultured in three-dimensional matrices in vitro. J Cell Sci108: 2791-2800

Barbaux S, Niaudet P, Gubler MC et al (1997) Donor splice-site mutations in WT-1 are responsible for Frasier syndrome. Nat Genet 17: 467-470

Bard JBH (1990) The cellular and molecular processes of developmental anatomy. In Barlow PW, Bray DB, Green PB and Slakc JMW eds. Morphogenesis. Cambridge University Press, Cambridge, UK

Bard JBH, Ross ASA (1991) LIF, the ES-cell inhibition factor, reversibly blocks nephrogenesis in cultured mouse kidney remnants. Development 113: 193-198

Bard JBH, Woolf AS (1992) Nephrogenesis and the development of renal disease.

Nephrol Dial Transplant 7: 563-572

Bardelli A, Longati P, Albero D et al (1996) HGF receptor associates with the anti-apoptotic protein BAG-1 and prevents cell death. EMBO J 15: 6205-6212

Beck AD (1971) The effect of intrauterine urinary obstruction upon the development of the fetal kidney. J Urol 105: 784-789

Bellairs R, Lear P, Yamada KM et al (1995) Posterior extension of the chick nephric (mesonephric) duct: the role of fibronectin and NCAM polysialic acid. Develop Dynam 202:333-342

Bennett ST, Lucassen AM, Gough SCL (1995) Susceptibility to human type 1 diabetes at *IDDM2* is determined by tandem repeat variation at the insulin gene minisatellite locus. Nat Genet 9: 284-292

Berman D, Maizels M (1982) The role of urinary obstruction in the genesis of renal dysplasia: a model in the chick embryo. J Urol 128: 1091-1100

Bernstein J, Meyer R (1967) Parenchymal maldevelopment of the kidney. Brennemann-Kelley ed. Practice of Paediatrics. Harper and Row, Haggerstown, Maryland. 1-30

Bernstein J (1971) The morphogenesis of renal parencyhymal development (renal dysplasia). Paediatr Clin N Amer 18: 395-407

Bernstein J, Cheng F, Roska J (1981) Glomerular differentiation in metanephric culture. Lab Invest 45: 183-190

Bernstein GT, Mandell J, Lebowtiz RL (1988) Ureteropelvic junction obstruction in the neonate. J Urol 140: 1216-21

Bernstein J (1993) Glomerulocystic kidney disease: nosological considerations. Paediatr Nephrol 7: 464-470

Bernstein J, Risdon RA, Gilbert-Barness E (1996) Renal system. Gilbert-Barness E, ed. Potter's pathology of the fetus and infant. St Louis: Mosby, 863-922

Bialestock D (1965) Studies of renal malformation and pyelonephritis in children with and without associated vesico-ureteral reflux and obstruction. Aus NZ J Surg 35: 120-135

Bladt F, Riethmacher D, Isenmann S et al (1995) Essential role for the c-met receptor in the migration of myogenic precursors into the limb bud. Nature 376: 768-771

Blair HJ, Uweche IC, Barsh GS et al (1998) An integrated genetic and man-mouse comparative map of the DXHS674-Pdha1 region of the mouse X chromosome. Genomics 48: 128-131

Boguski MS, Schuler GD (1995) ESTablishing a human transcript map. Nat Genet 10: 369-371

Bois EH, Feingold J, Benmaiz H et al (1975) Congenital urinary tract malformations: epidemiologic and genetic aspects. Clin Genet 8: 37-47

Booth EJ, Bell TE, McLain C et al (1975) Fetal vesicoureteral reflux. J Urol 113: 258-258

Borden KLB, Freemont PS (1996) The RING finger domain: a recent example of a sequence-structure family. Current Opin Struct Biol 6: 395-401

Bottaro DP, Rubin JS, Faletto DL et al (1991) Identification of the hepatocyte growth factor as the c-met proto-oncogene product. Science 251: 802-804

Boyd Y, Blair HJ, Cunliffe P et al (1998) Encyclopaedia of the mouse genome VII. Mouse chromosome X. Mamm Genome 8: 361-377

Brasier JL, Henske EP (1997) Loss of the polycystic kidney disease (PKD1) region of chromosome 16p13 in renal cyst cells supports a loss of function model for cyst pathogenesis. J Clin Invest 99: 194-199

Bravo R, Frank R, Blundell PA et al (1987) Cyclin/PCNA is the auxillary protein of DNA polymerase-delta. Nature 326: 515-517

Bredin HC, Winchester P, McGovern JH et al (1975) Family study of vesico-ureteral reflux. J Urol 113: 623-633

Brown DM, Provoost AP, Daly MJ et al (1996) Renal disease susceptibility and hypertension are under independent genetic control in the fawn hooded rat. Nat Genet 12: 44-51

Brown NA (1997) Chemical teratogens: hazards, tools and clues. Thorogood P, ed. Embryos, genes and birth defects. Chichester, UK: Wiley. 69-88

Bullock Sl, Fletcher JM, Beddington RP et al (1998) Renal agenesis in mice homozygous for a gene trap mutation in the gene encoding heparan sufate 2-sulfotransferase. Genes Devel 12: 1894-1906

Bunge RC (1954) Further observations with delayed cystograms. J Urol 71: 427-437

Burger RH, Smith C (1971) Hereditary and familial vesico-ureteral reflux. J Urol 92: 845-855

Burger RH (1972) A theory on the transmission of congenital vesico-ureteral reflux. J Urol 108: 249-259

Burn J, Dezeteux C, Hale CM et al (1984) Orofacial digital syndrome with mesomelic limb shortening. J Med Genet 21: 189-192

Cain DR, Griggs D, Lackey DA et al (1974) Familial renal agenesis and total dysplasia. Am J Dis Child 128: 377-380

Calvet JP (1993) Polycystic kidney disease: primary extracellular matrix abnormality or defective cellular differentiation. Kidney Int 43: 101-108

Cale CM, Klein NJ, Morgan G et al (1998) Tumor necrosis factor-α inhibits epithelial differentiation and morphogenesis in the mouse metanephric kidney in vitro. Int J Devel Biol 42: 663-674

Campbell MF (1930) Cystography in infants and childhood. Am J Dis Child 39: 386-396

Cavanaugh JA, Callen DF, Wilson SR et al (1998) Analysis of Australian Crohn disease pedigrees refines the localisation for susceptibility to inflammatory bowel disease on chromosome 16. Ann Hum Genet 62: 291-298

Chalepakis G, Goulding M. Read A et al (1994) Molecular basis of splotch and Waardenburg Pax-3 mutations. Proc Natl Acad Sci USA 91: 3685-3689

Chapman CJ, Bailey RR, Janus ED et al (1985) Vesicoureteral reflux: segregation analysis. Am J Med Genet 20: 577-584

Charlieu JP, Larsson S, Miyagawa K et al (1995) Does the Wilms tumour

suppressor gene, WT1, play roles in both splicing and transcription? J Cell Sci Suppl 19:95-99

Cheng EH, Kirsch DG, Clem RJ (1997) Conversion of Bcl-2 to a bax like death effector by caspases. Science 278:1966-1968

Chevalier RL (1996) Growth factors and apoptosis in neonatal ureteral obstruction. J Am Soc Nephrol 7: 1098-1105

Cho E, Patterson LT, Brookhiser et al (1998) Differential expression and function of cadherin-6 during renal epithelium development. Development 125: 803-812

Cho JH, Nicolae DL, Gold LH et al (1998) Identification of novel susceptibility loci for inflammatory bowel disease on chromosomes 1p, 3q and 4q: evidence for epistasis between 1p and IBD1. Proc Natl Acad Sci 91: 12721-12724

Choi KL, McNoe LA, Fench MC et al (1998) Absence of PAX2 gene mutations in patient with primary familial vesicoureteric reflux. J Med Genet 35: 338-339

Chomczynski P, Sacchi N (1987) Single step method of RNA isolation by acid guanidium thiocyanate-phenol-chloroform extraction. Annal Biochem 162:156-159

Clerget-Darpoux F, Bonaiti-Pellie C, Deschamps I et al (1981) Juvenile insulin-dependent diabetes: a possible susceptibility gene in interaction with HLA. Ann

Hum Genet 45: 199-206

Cohen MM, Kreiborg S (1993) Visceral anomalies in Apert syndrome. Am J Med Genet 45: 758-760

Coles HS, Burne JF, Raff MC (1993) Large scale normal cell death in the developing rat kidney and its reduction by epidermal growth factor. Development 118: 777-784

ConnacherAA, Forsyth CC, Stewart WK (1987) Orofaciodigital syndrome type 1 associated with polycystic kidneys and agenesis of the corpus callosum. J Med Genet 24: 116-122

Connolly LP, Treves ST, Zurakowski D et al (1996) Natural history of vesicoureteral reflux in siblings. J Urol 156: 1805-1807

Connolly LP, Treves St, Connolly SA et al (1997) Vesicoureteral reflux in children: incidence and severity in siblings. J Urol 157: 2287-2290

Conway JJ, Belman B, King LR (1974) Direct and indirect radionuclide cystography. Seminars in Nuclear Medicine 4: 197-207

Conway JJ (1984) Radionuclide cystography. Contrib Nephrology 39:1-12

Coons AH, Leduc EH, Connolly JM (1955) Studies on antibody production. 1. A

method for the histochemical demonstration of specific antibody and its application to the study of the hyperimmune rabbit. J Exp Med 102: 49-60

Coppes MJ, Huff V, Pelletier J (1993) Denys-Drash syndrome: relating a clinical disorder to genetic alterations in the tumor suppressor gene WT1. J Paediatr 123: 673-678

Craig JC, Irwig LM, Christie J et al (1997) Variation in the diagnosis of vesicoureteric reflux using micturating cystourethrography. Paediatr Nephrol 11: 455-459

Curran M, Kaefer M, Treves T, Bauer S, Hardy Hendren H (1998) Sibling reflux in multiple gestation births. Am Soc Urol September Abstract Book: 124

Cussen LS (1967) Dimensions of the normal ureter in infancy and childhood. Invest Urol 5: 164-174

Daikha-Dahame F, Dommergirs M, Narcy F et al (1995) Distribution and ontogenesis of tenascin in normal and cystic human fetal kidneys. Lab Invest 73: 547-557

Daikha-Dahmane F, Dommergues M, Narcy F et al (1997) Development of the human fetal kidney in obstructive uropathy: correlations with ultrasonography and biochemistry. Kidney Int 53: 21-23

Davies J, Lyon M, Garrod D (1995) Sulphated proteoglycan is required for collecting duct growth and branching but not nephron formation during kidney development. Development 121: 1507-1517

Davies JA, Garrod D (1995) Induction of early stages of kidney tubule differentiation by lithium ions. Develop Biol 167:50-60

Davies JL, Kawaguchi Y, Bennett ST et al (1994) A genome wide search for human type 1 diabetes susceptibility genes. Nature 371: 130-136

Davis AP, Witte DP, Hsieh-Li HM et al (1995) Absence of the radius and ulna in mice lacking hoxa-11 and hoxd-11. Nature 375: 791-795

De Chiara TM, Efstriadis A, Robertson EJ (1990) A growth deficiency phenotype in heterozygous mice carrying an insulin-like growth factor II gene disrupted by targeting. Nature 345: 78-80

Debhi M, Pelletier J (1996) PAX-8 mediated activation of the wt1 tumor suppressor gene. EMBO J 15: 4297-4306

de The H, Lavau C, Marchio A et al (1991) The PML-RAR(fusion mRNA generated by t(15;17) translocation in acute promyelocytic anaemia encodes a functionally active RAR. Cell 66: 675-684

DeVargas A, Evans K, Ransley P et al (1978) A family study of vesicoureteral

reflux. J Med Genet 15: 85-95

Diglio MC, Marino B, Formigari R et al (1995) Maternal diabetes causing DiGeorge anomaly and renal agenesis. Am J Med Genet 55: 513-514

Dixon JS, Canning DA, Gearheart JP et al (1994) An immunohistochemical study of the innervation of the ureterovesical junction in infancy and childhood. Br J Urol 73: 292-297

Dixon JS, Yen PYP, Yeung CK et al (1998) The structure and autonomic innervation of the vesico-ureteric junction in cases of primary ureteric reflux. Br J Urol 81: 146-151

Doege T, Thuline H, Priest J et al (1964) Studies of a family with the oral-facial-digital syndrome. NEJM 271: 1073-1080

Donnai D, Kerzin-Storrar L, Harris R (1987) Familial orofaciodigital syndrome type 1 presenting as adult polycystic kidney disease. J Med Genet 24: 84-87

Donnenfield AE, Graham JM, Packer RJ et al (1990) Microopthalmia and chorioretinal lesions in a girl with an Xp22.2-pter deletion and partial 3p trisomy: clinical observations relevant to Aicardi gene localisation. Am J Med Genet 37: 182-186

Dono R, Zeller R (1994) Cell-type specific nuclear translocation of fibroblast

growth factor-2 isoforms during chicken kidney and limb morphogenesis. Develop Biol 163: 316-330

Donnis-Keller H, Dou S, Chi D et al (1993) Mutations in the RET proto-oncogene are associated with MEN2A and FMT-C. Hum Mol Genet 2: 851-856

Dressler GR, Deutsch U, Chowdhury K et al (1990) Pax-2 a new paired box gene and its expression in the developing excretory system. Development 109: 787-795

Dressler GR, Douglas EC (1992) Pax-2 is a DNA-binding protein expressed in embryonic kidney and Wilms tumour. Proc Natl Acad Sci USA 89: 1179-1183

Dressler GR, Wilkinson JE, Rothenpieler UW et al (1993) Deregulation of Pax-2 expression in transgenic mice generates severe kidney abnormalities. Nature 362: 65-67

Drew JH, Acton CM (1976) Radiological findings in newborn infants with urinary tract infection. Arch Dis Child 51: 628-638

Drummond IA, Madden SL, Rohwer-Nutter P et al (1992) Repression of the insulin like growth factor II gene by the Wilms tumour suppressor WT-1. Science 257: 674-678

Dudley AT, Lyons KM, Robertson EJ (1995) A requirement for bone morphogenetic protein-7 during development of the mammalian eye and kidney.

Genes Dev 9: 2795-2807

Duke VM, Winyard PJD, Thorogood P et al (1995) KAL, a gene mutated in Kallmann's syndrome, is expressed in the first trimester of human development. Mol Cell Endocrinol 110: 73-79

Duke V, Quinton R, Gordon I, Bouloux PM, Woolf AS (1998) Proteinuria, hypertension and chronic renal failure in X-linked Kallmann's syndrome, a defined genetic cause of solitary functioning kidney. Nephrol Dial Transplant 13: 1998-2003

Dwoskin JY, Perlmutter AD (1970) Vesicoureteral reflux in children: a computerised review. J Urol 109: 888-898

Dwoskin JY (1976) Sibling uropathology. J Urol 115: 726-736

Dwoskin JY (1979) Ureteropelvic junction obstruction and sibling uropathology. Urol 13: 153-163

Ebers G, Kukay K, Bulman D et al (1996) A full genome search in multiple sclerosis. Nat Genet 13: 472-476

Eccles MR, Wallis LJ, Fidler AE et al (1992) Expression of the PAX2 gene in human fetal kidney and Wilms' tumout. Cell Growth Diff 3: 279-289

Eccles MR, Bailey RR, Abbott GD et al (1996) Unravelling the genetics of vesicoureteric reflux: a common familial disorder. Hum Mol Genet 5: 1425-1429

Edery P, Lyonnet S, Mulligan LM et al (1994) Mutations of the RET proto-oncogene in Hirschprung's disease. Nature 367: 378-380

Edwards M, Mulcahy D, Turner G (1988) X-linked recessive inheritance of an orofaciodigital syndrome with partial expression in females and survival of affected males. Clin Genet 34: 325-332

Ehrich JH, Loirat C, Brunner FP et al (1992) Report on management of renal failure in children in Europe, XII, 1991. Nephrol Dial Transplant 7 supp 2: 36-48

Ekblom P (1981) Formation of basement membranes in the embryonic kidney: an immunohistochemical study. J Cell Biol 91: 1-10

Ekblom P, Lehtonen E, Saxen L, Timpl R (1981) Shift in collagen type as a response to induction of the metanephric mesenchyme. J Cell Biol 89: 276-283

Ekblom P, Klein G, Ekblom M, Sorokin L (1991) Laminin isoforms and their receptors in the developing kidney. Am J Kidney Dis 17: 603-605

Ekblom P, Weller A (1991) Ontogeny of tubulointerstitial cells. Kidney Int 39: 394-500

Ekblom P (1994) Embryology and prenatal development. Holliday MA, Barratt TM , Avner ED eds Paediatric Nephrology, 3rd edition. Williams and Wilkins, Baltimore, Maryland, USA. 2.18

Ekblom P (1996) Extracellular matrix and adhesion molecules in nephrogenesis. Exp Nephrol 4: 92-96

Eldabawi A, Amaku ED, Frank IN (1973) Trilaminar musculature of the submucosal ureter. Anatomy and functional implications. Urology 2: 409-416.

Ellison BS, Taylor D, Van der Wall H et al (1992) Comparison of DMSA scintigraphy with intravenous urography for the detection of renal scarring and its correlation with vesicoureteric reflux. Br J Urol 69: 294-302

Emanuel B, Nachman R, Aronson N, Weiss H (1974) Congenital solitary kidney. A review of 74 cases. J Urol 111:394-397

Eng CM, Resnick-Silverman LA, Niehaus DJ (1993) Nature and frequency of mutations in the alpha-galactosidase A gene that cause Fabry disease. Am J Hum Genet 53: 1186-1197

Erlich HA (1989) Polymerase chain reaction. J Clin Imm 9: 437-447

European Polycystic Kidney Disease Consortium (1994) The polycystic kidney disease 1 gene encodes a 14kb transcript and lies within a duplicated region on

chromosome 16. Cell 77: 881-894

Farrer LA, Cupples LA (1998) Determining the genetic component of a disease. Haines and Pericak-Vance eds. Approaches to Gene Mapping in Complex Human Diseases. Wiley Liss, New York, USA. 93-129

Favor J, Sandulache R, Neuhauser-Klaus A et al (1996) The mouse Pax2(1Neu) mutation is identical to a human PAX2 mutation in a family with renal-coloboma syndrome and results in developmental defects of the ear, brain, eye and kidney. Proc Natl Acad Sci USA 93: 13870-13875

Feather SA, Winyard PJD, Dodd S et al (1996) Oral-facial-digital syndrome type 1 is another dominant polycystic kidney disease: clinical, radiological and histopathological features of a new kindred. Nephrol Dial Transplant 12: 1354-1361

Fedorcsak I, Ehrenberg L (1966) Effects of diethylprocarbonate and methylmethanesulphate on nucleic acids and nucleases. Acta Chem Scand 20: 107-112

Fellows RA, Leonidas JC, Beatty EC Jr (1976) Radiologic features of 'adult type' polycystic kidney disease in the neonate. Paediatr Radiol 4: 87-92

Fejes-Toth G, Naray-Fejes-Toth (1992) Differentiation of renal α-intercalated cells to α-intercalated and principal cells in culture. Proc Nat Acad Sci USA 89:

5487-5491

Ferrero GB, Franco B, Roth EJ et al (1995) An integrated Physical and genetic map of a 35Mb region on chromosome Xp22.3-Xp21.3. Hum Mol Genet 4: 1821-1827

Flack CE, Bellinger MF (1993) The multicystic dysplatic kidney and contralateral vesicoureteral reflux: Protection of the solitary kidney. J Urol 150: 1873-1874

Franco B, Guioli S, Pragliola A et al (1991) A gene deleted in Kallmann's syndrome shares homology with neural cell adhesion and axonal path-finding molecules. Nature 353: 529-536

Frenette PS, Wagner DD (1996a) Adhesion molecules: Part 1. NEJM 334: 1526-1529

Frenette PS, Wagner DD (1996b) Adhesion molecules: Part II: Blood vessels and blood cells. NEJM 335: 43-45

Fried K, Yuval E, Eidelman A et al (1975) Familial primary vesico-ureteral reflux. Clin Genet 7: 144-154

Friedland GW (1979) The voiding cystourethrogram: an unreliable examination. Hodson J, Kincaid Smith P (eds). Reflux Nephropathy. New York, Masson. 91-101

Friedman PA, Rao KW, Teplin SW et al (1988) The MLS syndrome. Am J Hum Genet 43: 50A

Fryns JP, Kleczowska A, Moerman P, Vandenberghe K (1993) Hereditary hydronephrosis and the short arm of chromosome 6. Hum Genet 91: 514-518

Gage JC, Sulik KK (1991) Pathogenesis of ethanol induced hydronephrosis and hydroureter as demonstrated following in vivo exposure of mouse embryos. Teratol 44: 299-312

Gashler AL, Bonthron DT, Madden SL et al (1992) Human platelet derived growth factor A chain is transcriptionally repressed by the Wilms tumor suppressor WT-1. Prc Natl Acad Sci USA 89: 10984-10988

Gattone VH, Lowden DA, Cowley BD (1995) Epidermal growth factor ameliorates autosomal polycystic kidney disease in mice. Devel Biol 169: 504-510

Gearheart JP, Canning DA, Gilpin SA et al (1993) Histological and Histochemical Study of the Vesicoureteric Junction in Infancy and Childhood. Br J Urol 72: 648-654

Gedeon AK, Oley C, Nelson J et al (1999) Gene localization for oral-facial-digital syndrome type 1 (OFD1: MIM 311200) proximal to *DXS85.* Am J Med Genet 82:

352-354

Geng L, Segal Y, Pavlova A et al (1997) Distribution and developmentally regulated expression of murine polycystin. Am J Physiol 272 (4 pt 2): F 451-459

Gibson HM (1949) Ureteral reflux in the normal child. J Urol 62: 4-12

Gilbert SF (1994) Developmental Biology 4th edition. Sunderland, Massachusetts, USA: Sinauer Associates Inc

Gillerot Y, Heimann M, Fourneau C et al (1993) Oral-facial-digital syndrome type 1 in a newborn male. Am J Med Genet 46: 335-383

Goldraich IH, Goldraich NP, Anselmi OE (1983) Comparative study betweeen intravenous urography and DMSA renal scans in the diagnosis of reflux nephropathy in infants and preschoolchildren. Eur J Paediatr 140: 212-

Goodship JA, Platt J, Smith R et al (1991) A male with type 1 oral-facial-digital syndrome. J Med Genet 28: 691-694

Golka K, Reckwitz T, Kempkes M et al (1997) N-acetyltransferase (NAT2) and Glutathione S-Transferase mu (GSTM1) in bladder cancer patients in a highly industrialised area. Int J Occup Environ Health 3: 105-110

Gorlin R, Psaume J (1962) Orodigitofacial dysostosis. A new syndrome. J

Paediatr 61: 520-530

Granata C, Wang Y, Puri P et al (1997) Decreased bcl-2 expression in segmental renal dysplasia suggests a role in its morphogenesis. Br J Urol 80: 140-144

Grantham JJ (1992) Fluid secretion, cellular proliferation and the pathogenesis of renal epithelial cysts. J Am Soc Nephrol 3: 1841-1857

Greenstein RM, Reardon MP, Chan TS et al (1980) An (X;11) translocation in a girl with Duchenne muscular dystrophy. Cytogenet Cell Genet 27: 268

Grignani F et al (1994) Acute promyelocytic leukaemia: from genetics to treatment. Blood 83: 10-25

Grobstein C (1953a) Morphogenetic interaction between embryonic mouse tissues separated by a membrane filter. Nature 172: 869-871

Grobstein C (1953b) Inductive epithelio-mesenchymal interaction in cultured organ rudiments of the mouse. Science 118: 52-55

Grobstien C (1995) Inductive interactions in the development of the mouse metanephros. J Exp Zool 130: 319-340

Groenen PM, Garcia E, Debeer P et al (1996) Structure, sequence and chromosome 19 localisation of human *USF2* and its rearrangement is a patient

with multicystic renal dysplasia. Genomics 38: 141-148

Groenen PM, Vanderlinden G, Devriendt K et al (1998) Rearrangement of the human CDCL5 gene by a t(6;19)(p21;q13.1) in a patient with multicystic renal dysplasia. Genomics 49: 218-229

Grompe M (1993) The rapid detection of unknown mutations in nucleic acids. Nat Genet 5: 111-117

Gross M, Kumar R (1990) Physiology and biochemistry of vitamin D-dependent calcium binding proteins. Am J Physiol 259: 195-209

Gruss P, Walther C (1992) Pax in development. Cell 69: 719-722

Gurrieri F, Sammito V, Ricci B et al (1992) A possible new type of the oral-facial-digital syndrome with retinal abnormalities. Am J Med Genet 42: 789-792

Haines J, Pericak-Vance M, Seboun E et al (1996) A complete genome screen in multiple sclerosis underscores a role for the major histocompatibility complex. Nat Genet 13: 467-471

Hall JM, Lee MK, Newman B et al (1990) Linkage of early-onset familial breast cancer to chromosome 17q21. Science 250: 1684-1689

Hampel N, Levin DR, Gersh I (1975) Bilareral vesico-ureteral reflux with

pyelonephritis in identical twins. Br J Urol 47: 535-537

Hardelin JP, Levilliers J, Blanchard S et al (1993) Heterogeneity in the mutations responsible for X-linked Kallman syndrome. Hum Mol Genet 2: 373-377

Hardman P, Kolatsi M. Winyard PJD et al (1994) Branching out with the ureteric bud. Exp Nephrol 2: 211-219

Hartner A, Strezel B, Reindl N et al (1994) Cytokine induced expression of leukaemia inhibitory factor in renal mesangial cells. Kidney Int 45: 1562-1571

Hatini V, Huh SO, Herzlinger D et al (1996) Essential role of stromal mesenchyme in kidney morphogenesis revealed by targeted disruption of Winged Helix transcription factor BF-2. Genes Devel 10: 1467-1478

Hedgepath CM, Conrad LJ, Zhang J et al (1997) Activation of the Wnt signalling pathway: a molecular mechanism for lithium action. Devel Biol 185: 82-91

Herzlinger D, Koseki C, Mikawa T et al (1992) Metanephric mesenchyme contains multipotent stem cells whose fate is restricted after induction. Development 114: 565-572

Herzlinger D, Qiao J, Cohen D, Ramkrishna N, Brown AM (1994) Induction of kidney epithelial morphogenesis by cells expressing Wnt-1. Devel Biol 166: 815-818

Heale WF (1997) Hereditary vesicoureteric reflux: phenotypic variation and family screening. Paediatr Nephrol 11: 504-50

Heikel PE, Parkkulainen KV' (1966) Vesico-ureteric reflux in children: a classification and results of conservative treatment. Annal Radiol 19: 37-47

Higuchi M, Kazazian HH, Kasch L (1991) Molecular characterisation of severe haemophilia suggests that about half the mutations are not within the coding regions and splice junctions off the factor V111 gene. Proc Natl Sci USA 88: 7405-7415

Hille B (1978) Ionic channels im excitable membranes. Biophys J 22: 283-294

Hinchcliffe SA, Chan YF, Jones L et al (1992) Renal hypoplasia and postnatally acquired cortical loss in children with vesicoureteral reflxux. Paediatr Nephrol 6: 439-446

Hodson CJ, Edwards D (1960) Chronic pyelonephritis and vesicoureteric reflux. Clin Radiol 11: 219-231

Hodson CJ (1967) The radiologiical contribution toward the diagnosis of chronic pyelonephritis. Radiology 88: 857-867

Hodson CJ (1975) The radiological diagnosis of pyelonephritis. Proceedings of

the Royal Society of Medicine 52: 669-679

Hodson CJ, Maling TMJ, Macnamon PJ et al (1975) The pathogenesis of reflux nephropathy (chronic atrophic pyelonephritis). Br J Radiol (suppl) 14: 1-35

Hoffman EP, Brown RH, Kunkel LM (1987) The protein product of the Duchenne muscular dystrophy locus. Cell 51: 919-928

Hofstra RMW, Landsvater RM, Ceccherini I et al (1994) A mutation in the RET proto-oncogene associated with multiple endocrine neoplasia type 2B and sporadic medullary thyroid carcinoma. Nature 367: 375-376

Holthoffer H, Virtanen I, Petersson E et al (1981) Lectins as fluorescent microscopic markerss for saccharides in the human kidney. Lab Invest 45: 391-399

Holthoffer H, Miettinen A, Lehto VP et al (1984) Expression of vimentin and cytokeratin types of intermediate filament proteins in developing and adult human kidneys. Lab Invest 50: 552-559

Houston CS, Optiz JM, Spranger JW et al (1983) The campomelic syndrome: review, report of 17 cases and follow-up on the currently 17-year old boy first reported by Maroteaux et al in 1971. Am J Med Genet 15: 3 –28

Howard A, Legon S, Spurr NK et al (1992) Molecular cloning and chromosomal

assignment of human calbindin-D9K. Biochem Biophys Res Com 185: 663-669

Howie AJ, Smithson N, Rollason TP (1993) Reconsideration of the development of the distal tubule of the human kidney. J Anat 1: 141-147

Hughes J, Ward CJ, Peral B et al (1995) The polycystic kidney disease (PKD1) gene encodes a novel protein with multiple cell recognition domains. Nat Genet 10: 151-160

Hughes-Benzie RM, Pilia G et al (1996) Simpson-Golabi-Behmel syndrome: genotype/phenotype analysis of 18 affected males from 7 unrelated families. Am J Med Genet 66: 227-234

Hugot JP, Laurent-Puig P, Gower-Rousseau C (1996) Mapping of a susceptibility locus for Crohn's disease on chromosome 16. Nature 379: 821-823

Hutch JA (1962) Theory of maturation of the intravesical ureter. J Urol 88: 169-179

Izquierdo L, Porteous M, Paramo PG et al (1992) Evidence for genetic heterogeneity in hereditary hydronephrosis caused by pelviureteric junction obstruction, with one locus assigned to chromosome 6p. Hum Genet 89: 557-560

Jadresic L, Leake J, Gordon I et al (1990) Clinicopathogic review of twelve children with nephropathy, Wilms tumour and genital abnormalities (Drash

syndrome). J Paediatr 117 (5): 717-725

Jequier S, Jequier JC (1989) Reliability of voiding cystourethrography to detect reflux. AJR Am J Roentgenol 153: 807-810

Jena N, Martin-Sesdedos C, mcCue P et al (1997) BMP7 null mutation in mice: developmental defects in skeleton,kidney and eye, Exp Cell Res 230: 28-37

Jerkins GR, Noe HN (1982) Familial vesicoureteric reflux: a prospective study. J Urol 128: 774-777

Jing S, Wen D, Yu Y et al (1996) GDNF-induced activation of the ret protein tyrosine kinase is mediated by GDNFR-alpha, a novel receptor for GDNF. Cell 85: 1113-1124

Jones BW, Headstream JW (1958) Vesico ureteral reflux in children. J. Urol 80: 114-124

Jordanova A, Kalydjieva L, Savov A et al (1997) SSCP analysis: a blind sensitivity trial. Hum Mut 10: 65-70

Kampmeier OF (1926) The metanephros or so called permanent kidney is in part provisional and vestigial. Anat Rec 33: 115-120

Kanwar YS, Liu ZZ, Kumar A et al (1995) Cloning of mouse c-ros renal cDNA,

its role in development and relationship to extracellular matrix glycoproteins. Kidney Int 48: 1646-1659

Karp SL, Ortiz Ardaun A, Lis A et al (1994) Epithelial differentiation of metanephric mesenchymal cells after stimulation with hepatocyte growth factor or embryonic spinal cord. Proc Natl Acad Sci USA 91: 5286-5290

Kelais PP (1971) proper perspective on vesicoureteral reflux. Mayo Clin Proc 46: 807-817

Keller SA, Jones JM, Boyle A et al (1994) Kidney and retinal defects (Krd), a transgene-induce mutation with a deletion of mouse chromosome 19 that includes the Pax2 locus. Genomics 23: 309-320

Kenda RB, Fettich JJ (1992) Vesicoureteric reflux and renal scars in symptomatic siblings of children with reflux. Arch Dis Child 67: 506-508

Kernohan DC, Dodge JA (1969) Further observations on a pedigree of the Oral-Facial-Digital syndrome. Arch Dis Child 44: 729-731

Kerr DNS, Pillai PM (1983) Identical twins with identical vesicoureteric reflux: chronic pyelonephritis in one. BMJ 286: 1245-1246

Kincaid-Smith P (1975) Gomerular lesions in atrophic pyelonephritis and reflux nephropathy. Kidney Int 8: S81-89

Kincaid Smith P, Becker GJ (1978) Reflux nephropathy and chronic atrophic pyelonephritis: a review. J Infect Dis 138: 774-784

Kincaid-Smith P, Becker GJ (1979) Reflux nephropathy in the adult. Hodson CJ, Kincaid-Smith P (eds) Reflux nephropathy. Masson, New York 21-28

King LR, Surian MA, Wendel RM et al (1968) Vesicoureteral reflux; a classification based on cause and the results of treatment. JAMA 203: 169-179

Kjellberg SR, Ericsson NO, Rudhe U (1957) Selected aspects of urinary tract infection. The Lower Urinary tract in Childhood: Some Correlated Clinical and Roengtenologic Observations. Stockholm, Almqvist and Wiksell 182-192

Koff SA (1992) Relationship between dysfunctional voiding and reflux. J Urol 148: 1703-1710

Kolatsi- Joannou M, Moore R, Winyard PJD et al (1997) Expression of HGF/SF and its receptor, MET, suggests roles in human embryonic organogenesis. Paediatr Res 41: 657-665

Koseki C, Herzlinger D, al Awqati Q (1992) Apoptosis in metanephric development. J Cell Biol 119: 1327-1333

Kreidberg JA, Sariola H, Loring JM et al (1993) WT-1 is required for early

kidney development. Cell 74: 679-691

Kreidberg JA, Donovan MJ, Goldstein SL et al (1996) Alpha 3 beta 1 integrin has a crucial role in the kidney and lung organogensis. Development 122: 3537-3547

Kreisberg JI, Ventatachalam MA, Radnik RA et al (1985) Role of mysoin light chain phosphorylation and microtubules in stress fiber morphology in cultured mesangial cells. Am J Physiol 249: F227-235

Kretschmer HL (1916) Cystography. Surgery Gynaecology and Obstetrics. 23: 709-719

Kruglyak L, Daly MJ, Reeve-Daly MP et al (1996) Parametric and nonparametric linkage analysis: a unified multipoint approach. Am J Hum Genet 58: 1347-1363

Kunin CM, Southall I and Paquin A. Jr (1960) Epidemiology of urinary tract infections: pilot study of 3057 school children. NEJM 263: 817-827

Kunin CM, Zacha E, Paquin AJ (1962) Urinary tract infection in school children. Prevalence of bacteriuria and associated urological findings. NEJM 266: 1287-1297

Kunin CM, Deutscher R, Paquin A, Jr (1964) Urinary tract infection in school children: and epidemiologic, clinical and laboratory study. Medicine 43: 91-101

Lai E, Clark KL, Burley SK et al (1993) Hepatocyte nuclear factor 3/fork head or winged helix proteins: a family of transcription factors of diverse biological function. Proc Natl Acad Sci USA 90: 10421-10423

Lalouel JM, Morton NE (1981) Complex segregation analysis with pointers. Hum Hered 31: 312-321

Lander ES, Kruglyak L (1995) Genetic dissection of complex traits: guidelines for interpreting and reporting linkage results. Nat Genet 11: 241-247

Larsen WJ (1993) Human embryology, 1st edition. New York, USA: Churchill Livingstone Inc.

Larsson SH, Charlieu JP, Miyagawa K et al (1995) Subnuclear localization of WT1 in splicing or transcription factor domains is regulated by alternative splicing. Cell 81: 391- 401

Lathrop GM, Lalouel JM (1984) Easy calculations of lod scores and genetic risks on small computers. Am J Hum Genet 36: 460-465

Lebowitz RL, Blickman JG (1983) The coexistence of ureteropelvic junction obstruction and reflux. Am J Roent 140: 231-238

LeBrun DP, Warnke RA, Cleary ML (1993) Expression of bcl-2 in fetal tissues suggests a role in morphogenesis. Am J Pathol 142: 743-753

Lechner MS Dressler GR (1997) The molecular basis of embryonic kidney development. Mech Dev 62: 105-120

Lee BR, Partin AW, Epstein JI et al (1992) A quantitative histological analysis of the dilated ureter of childhood. J Urol 148: 1482-1486

Legouis R, Lievre CA, Leibovici M et al (1993) Expression of the KAL gene in multiple neuronal sites during chicken development. Proc Natl Acad Sci USA 90: 2461-2465

Lembley KV, Kriz W (1991) Anatomy of the renal interstitium. Kidney Int 39: 370-381

Letterio JJ, Geiser AG, Kulkarni AB et al (1994) Maternal rescue of transforming growth factor-beta 1 null mutant mice. Science 264:1936-1938

Leveen P, Pekny, Gebre-Mehdin S, Swolin B et al (1994) Mice deficient for PDGF B show renal, cardiovascular and haematological abnormalities. Genes Dev 8: 1875-1887

Lewy PR, Belman AB (1975) Familial occurrence of non-obstructive , non-infectious vesicoureteral reflux with renal scarring. J Paediatr 86: 851-856

Lich R Jr, Howerton LW Jr, Goode LS et al (1964) The uterovesical junction of

the newborn. J Urol 92: 436-438

Lindenbaum RH, Clarke G, Patel C et al (1979) Muscular dystrophy in an X;1 translocation female suggests that Duchenne locus is on X chromosome short arm. J Med Genet 16 (5): 389-392

Lindsay EA, Grillo A, Ferrero G et al (1994) Microphthalmia with linear skin defects (MLS) syndrome: clinical, cytogenetic and molecular characterisation. Am J Med Genet 49: 229-234

Litt M, Luty JA (1989) A hypervariable microsatellite revealed by in vitro amplification of a dinucleotide repear within the cardiac muscle actin. Am J Hum Genet 44: 397-401

Lo Ten Foe JR, Rooimans MA, Bosnoyan-Collins L et al (1996) Expression cloning of a cDNA for the major Fanconi anaemia gene FAA. Nat Genet 14: 320-323

Liu ZZ, Wada J, Kunar A et al (1996) Comparative role of phototyrosine kinase domains of c-ros and c-ret protooncogenes in metanephric developmentvwith respect to growth factors and matrix morphogens. Dev Biol 178: 133-148

Lombard MN, Grobstein C (1996) Activity in various embryonic and post embryonic sources for induction of kidney tubules. Dev Biol 19: 41-51

Luo G, Hofmann C, Bronckers ALJJ, Sohocki M, Bradley A, Karentsy G (1995) BMP-7 is an inducer of nephrogenesis and is also required for eye development and skeletal patterning. Genes Dev 9: 2808-2820

Lyon RP, Marshall S, Tanagho EA (1969) The ureteral orifice: Its configuration and competency. J Urol 102: 504-509

MacGregor ME, Freeman P (1975) Childhood urinary infection associated with vesicoureteric reflux. QJ Medicine 44: 481-491

Mackie GG, Stephens FD (1975a) Duplex kidneys: a correlation of renal dysplasi with position of the ureteral orifice. J Urol 114: 274-280

Mackie GG, Awang H, Stephens FD (1975b) The ureteric orifice; the embryologic key to radiologic status of duplex kidneys. J Paediatr Surg 10: 473-481

Mackintosh M, Almarhoos G, Heath DA (1989) HLA linkage with familial vesicoureteral reflux and familial pelvi-ureteric junction obstruction. Tissue Antigens 34: 185-189

Maizels M, Smith CK, Firlit CF (1984) The management of children with vesic-ureteral reflux and ureteropelvic junction obstruction. J Urol 131:722-727

Mansour M, Azmy AF, MacKenzie JR (1987) Renal scarring secondary to

vesicoureteral reflux, Critical assessment and grading. Br J Urol 53: 544-554

Mansouri A, Chowdhury K, Gruss P (1998) Follicular cells of the thyroid require Pax8 gene function. Nat Genet 19: 505-514

Mass RL, Zeller R, Woychik RP et al (1990) Disruption of formin-encoding transcripts in two mutant limb deformity alleles. Nature 346: 853-855

Matsell DG, Bennett T, Armstrong RA et al (1997) Insulin-linke growth factor (IGF) and IGF binding protein gene expression in multicystic renal dysplasia. J Am Soc Nephrol 8: 85-94

Matsuno T, Tokunaka S, Koyanagi T (1984) Muscular development in the urinary tract. J Urol 132: 148-152

McConnell MJ, Cunliffe HE, Chua LJ et al (1997) Differential regulation of the human Wilms tumour suppressor gene (WT1) promoter by two isoforms of PAX2. Oncogene 14:2689-2700

McDonald IM, Dumble LJ, Kincaid-Smith PS (1976) HLA-A3, vesicoureteric reflux and analgesic abuse. First International Symposium on HLA and Disease, Paris, Abstract Book. 255

McEnery PT, Stablein MDD, Arbus G et al (1992) Tansplantation in children; A report of the North American Pediatric Renal Transplant Cooperative Study

NEJM 26: 1727-1732

McPhersin E, Carey J, Kramer A et al (1987) Dominantly inherited renal adysplasia. Am J Med Genet 26: 863-872

Meadow SR, White RHR, Johnston NM (1969) Prevalence of symptomless urinary tract disease in Birmingham schoolchildren 1. Pyuria and bacteriuria. BMJ 3: 75-79

Mebust WK, Foret JD (1972) Vesicoureteric reflux in identical twins. J Urol 108: 635-636

Melnick M, Bixler D, Nance WE et al (1976) Familial branchio-oto-renal dysplasia: a new addition to the branchial arch syndromes. Clin Genet 9: 25-34

Mendelsohn C, Lohnes D, Decimo D et al (1994) Function of the retinoic acid receptors (RAR) during development. Development 120: 2749-2771

Merrick MV, Uttler WS, Wild R (1979) A comparision of two techniques of detecting vesicoureteric reflux. Br J Radiol 52: 792-795

Middleton GW, Howards SS, Gillenwater JY (1975) Sex-linked familial reflux. J Urol 114: 36-46

Miller HC, Caspari EW (1972) Ureteral reflux as a genetic trait. JAMA 220: 6-20

Mobley DF (1973) Familial vesicouretric reflux. Urology 2: 514-525

Mochizuki T, Wu G, Hyashi T et al (1996) PKD2, a gene for polycystic kidney disease that encodes an integral membrane protein. Science 272: 1339-1342

Mohr OL (1941) A hereditary sublethal syndrome in man. Nor Vidensk Akad Oslo 1 Mat Naturv Klasse 14: 3-18

Monaco AP, Bertelson CJ, Liechti-Gallati S et al (1988) An explanation for phenotypic differences between patient bearing partial deletions of DMD locus. Genomics 2: 90-95

Montesano R, Schaller G, Orci L (1991) Induction of epithelial tubular morphogenesis in vitro by fibroblast –derived solube factors. Cell 66: 697-711

Montini E, Andolfi G, Caruso A et al (1998) Identification and characterisation of a novel serine-threonine kinase gene from the Xp22 region. Genomics 51: 427-433

Moore KL (1988) The developing human. Clinically orientated embryology. Philadelphia, Pennysylvania, USA: WB Saunders

Moore MW, Klein RD, Farinas I et al (1996) Renal and neuronal abnormalities in mice lacking GDNF. Nature 382: 76-79

Morham SG, Langenbach R, Loftin CD et al (1995) Prostaglandin synthase 2 gene disruption causes severe renal pathology in the mouse. Cell 83: 473-482

Morton NE (1955) Sequential tests for the detection of linkage. Am J Hum Genet 7: 277-318

Mulcahy JJ, Kelalis PP, Stickler GB et al (1970) Familial vesico-ureteral reflux. J Urol 104: 762-772

Mulligan LM, Kwok JBJ, Healey CS et al (1993) Germ-line mutations of the RET proto-oncogene in multiple endocrine neoplasia type 2A. Nature 363: 458-460

Mugrauer G, Ekblom P (1991) Contrasting expression patterns of three members of the myc family of protooncogenes in the developing adult mouse kidney. J Cell Biol 112: 13-25

Muller U, Wang D, Denda S et al (1997) Integrin alpha8beta1 is critically important for epithelial-mesenchymal interactions during kidney morphogenesis. Cell 88: 603-613

Murray JC, Beutow KH, Weber JL et al (1994) A comprehensive human linkage map with centimorgan density. Co-operative Human Linkage Centre (CHLC). Science 265: 2049-2055

Murugasu B, Cole BR, Hawkins EP et al (1991) Familial renal adysplasia. Am J Kidney Dis 18: 490-494

Nakayama K, Negishi I, Kuida K et al (1994) Targeted disruption of Bcl-2 alpha beta in mice: occurrence of gray hair, polycystic kidney disease and lymphocytopenia. Proc Natl Acad Sci USA 91: 3700-3704

Nasrallah PF, Nara S, Crawford J (1982) Clinical applications of nuclear cystography. J Urol 128: 550-553

Naylor JA, Green PM, Rizza CR et al (1992) Factor V111 gene explains all cases of haemophilia A. Lancet 340: 1066-1076

Naylor JA, Brinke A, Hassock S et al (1993) Characteristic mRNA abnormality found in half the patients with severe haemophilia A is due to large DNA inversions. Hum Mol Genet 2: 1773-1783

Nishimura H, Yerkes E, Hohenfellner K et al (1999) Role of the Angiotensin Type 2 receptor gene in congenital anomalies of the kidney and urinary tract, CAKUT, of mice and men. Mol Cell 3: 2-10

Noakes PG, Miner JH, Gautam M et al (1995) The renal glomerulus of mice lacking s-laminin/laminin b2: nephrosis despite molecular compensation by laminin b1. Nat Genet 10: 400-406

Noe HN, Wyatt RJ, Peeden JN Jr et al (1992a) The transmissionof vesicoureteral reflux form parent to child. J Urol 148: 1869-1871

Noe HN (1992b) The long term results of prospective sibling reflux screening. J Urol 148: 1739-1742

Novack DV, Korsmeyer SJ (1994) Bcl-2 protein expression during murine development. Am J Pathol 145: 61-73

Novak RW, Robinson HB (1994) Coincident DiGeorge anomaly and renal agenesis and its relation to maternal diabetes. Am J Med Genet 50: 311-312

Ohmen JD, Yang HY, Yamamoto KK et al (1996) Susceptibiliy loci for inflammatory bowel disease on chromosome 16 has a role in Crohn's disease but not in ulcerative colitis. Hum Mol Genet 5: 1679-1683

Orita M, Iwahana H, Kanazawa H et al (1989) Detection of polymorphisms of human DNA by gel electrophoresis as single-strand conformation polymorphisms. Proc Natl Acad Sci USA 86:2766-2770

Orr-Utreger A, Givol D, Yayon A et al (1991) Developmental expression of two murine fibroblast growth factor receptors, flg and bek. Development 113: 1419-1434

Ott J. (1991) Analysis of Human Genetic Linkage (revised edition). The John

Hopkins University Press, Baltimore and London

Ozen S, Alikasifoglu M, Tuncbilek E et al (1997) Polymorphisms in angiotensin convertin enzyme gene and reflux nephropathy: a genetic predispostion to scar formation. Nephrol Dial Transplant 12: 2031-2032

Pachnis V, Mankoo B, Costantini F (1993) Expression of the c-ret proto-oncogene during mouse embyrogenesis. Development 119: 1005-1017

Park WJ, Theda C, Maestri NE et al (1995) Analysis of phenotypic features and FGFR2 mutations in Apert syndrome. Am J Hum Genet 57: 321-328

Parkes M, Satsangi J, Lathrop GM et al (1996) Susceptibility loci in inflammatory bowel disease. Lancet 348: 1588-1568

Parsons V, Patel HR, Stodell A et al (1974) Symptoms by questionnaire and signs by dipstream culture of urtianry tract infection in schoolgirls of south east London. Clin Nephrol 2: 179-189

Perantoni AO, Dove LF, Karanova I (1995)) Basic fibroblast growth factor can mediate the early inductive events in renal development. Proc Natl Acad Sci USA 92: 4696-4700

Perry J, Feather S, Smith A et al (1998) The human FXY gene is located within Xp22.3: implications for evolution of the mammalian X chromosome. Hum Mol

Genet 7: 299-305

Peters PC, Johnson DE, Jackson JH Jr (1967) The incidence of vesicoureteral reflux in the premature child. J Urol 97: 259-260

Peters CA (1997) Obstruction of the fetal urinary tract. J Am Soc Nephrol 8: 653-663

Petit C, Levilliers J, Rouyer F et al (1990) Isolation of sequences from Xp22.3 and deletion mapping using sex chromosome rearrangements from human X-Y interchange sex reversals. Genomics 6: 651-658

Phelps DE, Dressler GR (1996) Identification of novel Pax-2 binding sites by chromatin precipitation. J Biol Chem 271: 7978-7985

Pichel JG, Shen L, Sheng HZ et al (1996) Defects in the innervation and kidney development in mice lacking GDNF. Nature 382: 73-76

Pilia G, Hughes-Benzie RM, MacKenzie A et al (1996) Mutations in GPC3, a glypican gene cause the Simpson-Golabi-Behmel overgrowth syndrome. Nat Genet 12: 241-247

Plachov D, Chowdhury K, Walther C et al (1990) Pax8, a murine paired box gene expresssed in the developing excretory system and thyroid gland. Development 110: 643-651

Pochaczevsky R, Naysan P, Ratner H (1974) Congenital non-obstructive hydronephrosis and bilateral vesicoureteral reflux in identical twins. Am J Roentgen 120: 398-401

Poirier F, Timmons PM, Chan CT et al (1992) Expression of the L14 lectin during mouse embyogenesis and suggests multiple roles during pre-and post-implantation development. Development 115: 143-155

Poleev A, Fickenscher H, Mundlos S et al (1992) PAX8, a human paired box gene: isolation and expression in developing thyroid, kidney and Wilms'tumours. Development 116: 611-623

Potter EL (1972) Normal and abnormal development of the kidney. Chicago, Illinois: Year Book Medical Publishers

Powell-Braxton L, Hollingshead P, Warburton C et al (1993) IGF-1 is required for normal embryonic growth in mice. Genes Dev 7: 2609-2617

Pritchard-Jones K, Fleming S, Davidson D et al (1990). The candidate Wilms' tumour gene is involved in genitourinary development. Nature 346: 194-197

Qian F, Watnick TJ, Onuchic LF et al (1996) The molecular basis of focal cyst formation in human autosomal dominant polycystic kidney disease type 1. Cell 87: 979-987

Qian F, Germino F, Cai Y et al (1997) PKD1 interacts with PKD2 through a probable coiled-coil domain. Nat Genet 16: 179-183

Qiao J, Cohen D, Herzlinger D (1995) The metanephric blastema differentiates into collecting system and nephron epithelia in vitro. Development 121: 3207-3214

Quaderi NA, Schweiger S, Gaudenz K et al (1997) Opitz G/BBB syndrome, a defect of midline development, is due to mutations in a new RING finger gene on Xp22. Nat Genet 17: 285-291

Rahilly MA, Fleming S (1992) Differential expression of integrin alpha chains by renal epithelial cells. J Pathol 167: 327-334

Ransley PG, Risdon RA (1975a) Renal papillary morphology and intrarenal reflux in the young pig. Urol Res 3: 105-109

Ransley PG, Risdon RA (1975b) Renal papillary morphology in infants and young children. Urol Res 3: 111-113

Ransley PG (1978a) Vesicoureteric reflux: continuing surgical dilemma. Urology 12: 246-256

Ransley PG, Risdon RA (1978b) Reflux and renal scarring. Br J Radiol (supp) 14:

Ransley PG, Risdon RA (1979) The pathogenesis of reflux nephropathy. Contrib Nephrol 16: 90-97

Ransley PG, Risdon RA (1981) Reflux nephropathy: effects of antimicrobial therapy on the evoolution of the early pyelonephritic scar. Kidney Int 20: 733-742

Ransley PG, Risdon RA, Godley ML (1984) High pressure sterile reflux and renal scarring: and experimental study in the pig and minipig. In Hodson CJ, Heptinstall RH, Winberg J eds. Contributions to nephrology vol 39. Karger, Basel. 164-168

Reddy BA, Kloc M, Etkin L (1991) The cloning and characterisation of a maternally expressed novel zinc finger phosphoprotein (xnf) in Xenopus laevis. Devel Biol 148: 107-116

Redman JF (1976) Vesicoureteral reflux in twins. J Urol 116: 792-793

Risdon RA (1971a) Renal dysplasia. I. Clinicopathological study of 76 cases. J Clin Pathol 24: 57-65

Risdon RA (1971b) Renal dysplasia. II. A necropsy study of 41 cases. J Clin Pathol 24: 65-71

Risdon RA, Young LW, Chrispin (1975) Renal hypoplasia and dysplasia. A

radiological and pathological correlation. Paediatr Radiol 3: 213-225

Risdon RA, Yeung CK, Ransley PG (1993) Reflux nephropathy in children submitted to unilateral nephrectomy: a clinicopathological study. Clin Nephrol 40: 308-315

Rogers SA, Ryan G, Hammerman MR (1991) Insulin-like growth factors I and II are produced in the metanephros and are required for growth and development in vitro. J Cell Biol 113: 1447-1453

Rolleston GL, Shannon FT, Uttley WLF (1970) Relationship of infantile vesiocoureteric reflux to renal damage. BMJ 1: 430-440

Rolleston GL, Maling TMJ, Hodson CJ (1974) Intrarenal reflux and the scarred kidney. Arch Dis Child 49: 531-539

Romeo G, Ronchetto P, Luo Y et al (1994) Point mutations affecting the tyrosine kinase domain of the RET proto-oncogene in Hirschprung's disease. Nature 367: 377-378

Roodhoft AM, Birnholz JC, Homes LB (1984) Familial nature of congenital absence and severe dysgenesis of both kidneys. NEJM 310: 1341-1345

Ropers HH, Zuffardi O, Bianchi E et al (1982) Agenesis of the corpus callosum,

ocular and skeletal abnormalities (X-linked dominant Aicardi's syndrome) in a girl with a balanced X/3 translocation. Hum Genet 61: 364-368

Ross DG, Travers H (1975) Infantile presentation of adult type polycystic kidney disease in a large kindred. J Paediatr 87: 760-763

Rothenpieler UW, Dressler GR (1993) Pax-2 is required for mesenchyme to epithelium conversion during kidney development. Development 119: 711-720

Rothenpieler UW (1996) Roles of Pax genes in nephrogenesis. Exp Nephrol 4: 86-91

Rothman KJ, Moore LL, Singer MR et al (1995) Teratogenicity of high vitamin A intake. NEJM 333: 1369-1373

Rousseau F, Bonaventure J, Legeai-Mallet L et al (1994) Mutations in the gene encoding fibroblast growth factor receptor-3 in achondroplasia. Nature 37: 252-254

Rowe PC, Newman SL, Brusilow SW (1986) Natural history of symptomatic partial ornithine transcarbamylase deficiency. NEJM 314: 514-547

Ruess A, Pruzansky S, Lis E et al (1962) The oral-facial-digital syndrome: A multiple congential condition of females with associated chromosomal abnormalities. Pediatr 29: 985-994

Ruoslahti E, Ymaguchi Y (1991) Proteoglycans as modulators of growth factor actvities. Cell 64: 867-869

Rupprecht HD, Drummond IA, Madden SL et al (1994) The Wilms' tumour suppressor WT-1 is negatively autoregulated. J Biol Chem 269: 6198-6206

Ryan G, Steele-Perkins V, Morris JF et al (1995) Repression of Pax-2 by WT-1 during normal kidney development. Development 121: 867-875

Saga Y, Yagi T, Ikawa Y et al (1992) Mice develop normally without tenascin. Genes Dev 6: 1821-1831

Sainio K, Hellstedt P, Kredber JA et al (1997) Differential regulation of two sets of mesonephric tubules by WT-1. Development 124: 1293-1299

Salinas C, Pai G, Vera C et al (1991) Variability of expression of the orofaciodigital syndrome type 1 in black females: six cases. Am J Med Genet 38: 574-582

Sampson JA (1903) Ascending renal infection with special reference to the reflux of urine from the bladder into the ureters as an aetiological factor in its causation and maintenance. Bull John Hopkins Hospital 14: 334-337

Sampson JR, Maheshwar MM, Aspinwall R et al (1997) Renal cystic disease in

tuberous sclerosis: role of the polycystic kidney disease 1 gene. Am J Hum Genet 61: 843-851

Sanchez MP, Silos-Santiago I, Frisen J et al (1996) Renal agenesis and absence of enteric neurones in mice lacking GDNF. Nature 382: 70-73

Santos OF, Nigam SK (1993) HGF- induced tubulogenesis and branching of epithelial cells is modulated by extracellular matrix and TGF-beta. Dev Biol 160: 293-302

Santos OF, Barros EJG, Yang XM et al (1994) Involvement of hepatocyte growth factor in kidney development. Dev Biol 163: 525-529

Sanyanusin P, Schimmenti LA, McNoe LA et al (1995) Mutations of the PAX2 gene in a family with optic nerve colobomas, renal anomalies and vesicoureteral reflux. Nat Genet 9: 358-364

Sariola H, Aufderheide E, Bernhard H et al (1988a) Antibodies to cell surface ganglioside GD3 perturb inductive epithelial mesenchymal interactions. Cell 54: 235-245

Sariola H, Holm K, Henke-Fahle S (1988b) Early innervation of the metanephric kidney. Development 104: 589-599

Sariola H, Ekblom P, Henke-Fahle (1989) Embryonic neurons as in vitro inducers

of differentiation of nephrogenic mesenchyme. Dev Biol 132: 271-281

Satsangi J, Parkes M, Louis E et al (1996) Two stage genome wide search in inflammatory bowel disease provides evidence for loci on chromosomes 3, 7 and 12. Nature Genet 14: 199-202

Sauer CG, Gehrig A, Warneke-Wittstock R et al (1997) Positional cloning of the gene associated with X-linked juvenile retinoschisis. Nat Genet 17: 164-170

Savage DCL, Wilson MI, Ross EM and Fee WM (1969) Asymptomatic bacteriuria in girl entrants to Dundee Primary Schools. BMJ 3: 75-79

Savage DCL, Wilson MI, McHardy M et al (1973) Covert bacteriuria of childhood. A clinical and epidemiological study. Arch Dis Child 48: 8-18

Sawcer S, Jones H, Feakes R et al (1996) A genome screen in multiple sclerosis reveals susceptibility loci on chromosome 6p21 and 17q22. Nature Genet 13: 464-468

Saxen L (1987) Organogenesis of the kidney. Cambridge University Press, Cambridge UK

Schaefer L, Prakash S, Zoghbi HY (1997) Cloning an characterisation of a novel rho-type GTPase-activating protein gene (ARHGAP6) from the region for microopthalmia with linear skin defects. Genomics 46: 268-277

Schiaffino VV, Bassi MT, Rugarli EI et al (1995) Cloning of the Xenopus laevis APX gene from the ocular albinism type 1 critical region. Hum Mol Genet 4: 373-382

Schimmenti LA, Pierpoint ME, Carpenter BL et al (1995) Autosomal dominant optic nerve colobomas, vesicoureteral reflux and renal anomalies. Am J Med Genet 59: 204-208

Schimmenti LA, Cunliffe HE, Mc Noe LA et al (1997) Further delineation of renal-coloboma syndrome in patients with extreme variability of phenotype and identical PAX2 mutations. Am J Hum Genet 60: 869-878

Schmid P, Schulz WA, Hameister H (1989) Dynamic expression of the myc protooncogene in mid gestation mouse embryos. Science 243: 226-229

Schmidt C, Bladt F, Groedecke S et al (1995) Scatter factor/hepatocyte growth factor is essential for liver development. Nature 373: 699-702

Schmidt JD, Hawtrey CE, Flocks RH et al (1972) Vesico-ureteral reflux, An inherited lesion. JAMA 220: 821-831

Schuchardt A, D'Agati V, Larsson-Blomberg L et al (1994) Defects in the kidney and nervous system in mice lacking the tyrosine kinase receptor Ret. Nature 367: 380-383

Scolari F, Valzorio B, Carli I et al (1997) Oral-facial-digital syndrome type 1: an unusual cause of hereditary cystic kidney disease. Nephrol Dial Transplant 12: 1247-1250

Scott JES, Swallow V, Coutlhard MG et al (1997) Screening of newborn babies for familial ureteric reflux. Lancet 350: 396-400

Shefelbine SE, Khorana S, Schultx PN (1998) Mutational analysis of the GDNF/RET-GDNFR alpha signalling complex in a kindred with vesicoureteric reflux. Hum Genet 102: 474-478

Smellie JM, Rigden SPA, Prescod NP (1995) Urinary tract infection: a comparison of four methods of investigation. Arch Dis Child 72: 247-237

Sonnenberg E, Meyer D, Weidner KM et al (1993) Scatter factor/ hepatocyte growth factor and its receptor, the c-met tyrosine kinase, can mediate a signal exchange between mesenchyme and epithelia during mouse development. J Cell Biol 123: 223-235

Sengar DPS, Rashid A, Wolfish NM (1978) Histocompatibility antigens and urinary tract abnormalities. BMJ 1: 1146 -1156

Sengar DPS, Rashid A, Wolfish NM (1979) Familial urinary tract anomalies: association with the major histocompatiblity complex in man. J Urol 121: 194-199

Shawlot W, Behringer RR (1995) Requirement for Lim 1 in head-organiser function. Nature 374: 425-430

Shull MM, Ormsby I, Kier AB et al (1992) Targeted disruption of the mouse transforming growth factor-beta 1 gene results in multifocal inflammatory disease. Nature 359: 693-699

Simpson JL, German J (1970) Familial urinary tract anomalies. JAMA 212: 2264-2274

Sirota L, Hertz M, Laufer J et al (1986) Familial vesicoureteral reflux: a study of 16 families. Urol Radiol 8: 22-24

Skoog S, Belman AB (1991) Primary vesiocoureteric reflux in the black child. Paediatr 87: 538-543

Smellie JM, Pursell R, Prescod N et al (1973) Relation ship between serum antibody titre and radiological findings in children with urinary tract infection. Brumfitt W, Asscher AW eds. Urinary Tract Infection: Proceedings of the Second National Symposium held in London, March 1972. London, Oxford University Press. 31-51

Smellie JM, Normand ICS (1975) Bacteriuria, reflux and renal scarring. Arch Dis Child 50: 581-585

Smellie JM, Edwards D, Hunter N et al (1975) Vesico-reteric reflux and renal scarring. Kidney Int 4: 65-75

Smellie JM, Normand ICS (1979) Reflux nephropathy in childhood. Hodson CJ, Kincaid-Smith P eds. Reflux nephropathy. Masson, New York. 21-28

Smellie JM, Ransley PG, Normand ICS et al (1985) Development of new renal scars: a collaborative study. BMJ 2: 1957-1960

Smellie JA, Rigden SPA, Prescod NP (1995) Urinary tract infection in childhood: a comparison of four methods of investigation. Ach Dis Child 72: 247-253

Sonnenberg E, Godecke A, Walter B et al (1991) Transient and locally restricted expression of the ros 1 protooncogene during mouse development. EMBO J 10: 3693-3702

Sonnenberg E, Meyer D, Weidner KM et al (1993) Scatter factor/hepatocyte growth factor and its receptor, the c-met receptor tyrosine kinase, can mediate a signal exchange between mesenchyme and eipthelia during mouse development. J Cell Biol 123: 223-235

Sonnenberg-Riethmacher E, Walter B et al (1996) The c-ros receptor tyrosine kinase receptor controls regionalisation and differentiation of epithelial cells in the epididymis Genes Dev 10:1184-1193

Sorenson CM, Rogers SA, Korsmeyer SJ et al (1995) Fulminant metanephric apoptosis and abnormal kidney development in bcl-2 deficient mice. Am J Physiol 268: F73-81

Sorenson CM, Padanilam BJ, Hammerman M (1996) Abnormal post-partum renal development and cystogenesis in the bcl-2 (-/-) mouse. Am J Physiol 271: F184-183

Soriano P (1994) Abnormal kidney development and haematological disorders in PDGF beta-receptor mutant mice. Genes Dev 8: 1888-1896

Sorokin L, Ekblom P (1991) Development of tubular and glomerular cells of the kidney. Kidney Int 41: 657-664

Spielman RS, Baker L, Zymijewski CM (1980) Gene dosage and susceptibility to insulin-dependent diabetes. Ann Hum Genet 44: 135-150

Spielman RS, McGinnis R, Ewens W (1993) Transmission test for linkage disequilibrium: the insulin gene region and insulin-dependent diabetes mellitus (IDDM). Am J Hum Genet 52: 506-516

Stanton BR, Perkins AS, Tessarollo L et al (1992) Loss of N-myc function results in embryonic lethality and failure of the epithelial component of the embryo to develop. Genes Dev 6: 2235-2247

Stapleton FB, Bernstein J, Koh G et al (1982) Cystic kidneys in a patient with oral-facial-digital syndrome type 1. Am J Kidney Dis 1: 288-293

Stark K, Vassileva G, McMahon AP (1994) Epithelial transformation of metanephric mesenchyme in the developing kidney regulated by Wnt-4. Nature 372: 679-683

Stephens FD, Joske RA, Simmons RT (1955) Megaureter with vesicoureteric reflux in twins. Aust NZ J Surg 24: 192-195

Stephens FD, Lenaghan D (1962) The anatomical basis and dynamics of vesicoureteral reflux. J Urol 87: 669-679

Strife JL, Souza AS, Kirks DR et al (1993) Multicystic dysplastic kidney in children: US follow-up. Radiology 186: 785-788

Sugarman GI, Kutakia M, Menkes J (1971) See-saw winking in a familial oral-facial-digital syndrome. Clin Genet 2: 248-254

Suzuka I, Daidoji H, Matsuoka M et al (1989) Gene for proliferating-cell nuclear antigen (DNA polymerase delta auxiliary protein) is present in both mammalian and higher plant genomes. Proc Natl Acad Sci, USA 86: 3189-3193

Sweet HO, Lane PW (1980) X-linked polydactyly (Xpl), a new mutation in the

mouse. J Hered 71: 207-209

Tamminen-Mobius T, Brunier E, Ebel KD et al (1992) Cessation of vesicoureteral reflux for 5 years in infants and children allocated to medical treatment. The International Reflux Study in children; European branch. J Urol 148: 1662-1666

Tanagho EA, Guthrie TH, Lyon RP (1969) The intravesical ureter in primary reflux. J Urol 101: 824-832

Tassabehji M, Read AP, Newton VE et al (1993) Mutations in the Pax3 gene causing Waardenburg syndrome type 1 and 2, Nat Genet 3: 26-30

Terwilliger JD and Ott J (1994) Handbook of human genetic linkage. John Hopkins University Press, Baltimore, USA

Thiery J-P, Duband J-L, Rutushauser U et al (1982) Cell adhesion molecules in early chick embryogenesis. Proc Natl Sci USA 79: 6737-6741

Thomas DFM, Agarwal M, Laidin AZ et al (1982) Pelviureteric obstruction in infancy and childhooe. A review of 117 patients. Br J Urol 54: 204-208

Thorner P, Bernstein J, Landing BH (1995) Kidney and lower urinary tract. Reed GB, Claireaux AE, Cockburn F, eds. Diseases of the fetus and newborn. 2nd Ed. London: Chapman and Hall Medical. 609-691

Threadgill DW, Dlugosz AA, Hansen LA et al (1995) targeted disruption of the mouse EGF receptor. Effect of genetic background on mutant phenotype. Science 269: 230-234

Thurston CO (1909) A case of median hare-lip associated with other malformations. Lancet ii: 996-997

Tobenkin MI (1964) Hereditary vesico-ureteral reflux. Southern Med J 57: 139-149

Toriello H (1988) Heterogeneity and variability in the Oral-Facial-Digital Syndromes. Am J Med Genet 4: 149-159

Toriello HV (1993) Oral-facial-digital syndromes, 1992. Clin Dysmorph 2: 95-105

Torres VE, Velosa JA, Holley KE et al (1980a) The progression of vesicoureteral reflux nephropathy. Ann Intern Med 92: 776-784

Torres VE, Moore SB, Kurtz SB et al (1980b) In search of a marker for genetic susceptiblity to reflux nephropathy. Clin Nephrol 14: 217-227

Torres M, Gomez-Pardo E, Dressler GR et al (1995) Pax-2 controls multiple steps of urogenital development. Development 121: 4057-4065

Torrey TW (1954) The early development of the human nephros. Contrib Embryol 239: 175-197

Towers PR, Woolf AS, Hardman P (1998) Glial cell line-derived neurotrophic factor stimulates ureteric bud outgrowth and enhances survival of ureteric bud cells in vitro. Exp Nephrol 6: 337-351

Treanor JJS, Goodman L, de Sauvage F et al (1996) Characterisation of a multicomponent receptor for GDNF. Nature 382: 80-83

Tuchman M (1993) Mutations and polymorphisms in the human ornithine transcarbamylase gene. Hum Mutat 2: 174-178

Tullus K, Fituri O, Burman LG et al (1994) Interleukin-6 and interleukin 8 in the urine of children with acute pyelonephritis. Paediatr Nephrol 8: 280-284

Uehara Y, Minowa O, Mori C et al (1995) Placental defect and embryonic lethality in mice lacking hepatocyte growth factor/scatter factor. Nature 373: 702-705

Uehling DT, Vlach RM, Pauli RM et al (1992) Vesicoureteric reflux in Sibships. Br J Urol 69: 534-537

Unsworth B, Grobstein C (1970) Induction of kidney tubules in mouse metanephrogenic mesenchyme by various embryonic mesenchymal tissues. Dev

Biol 21: 547-556

Vainio S, Lehtonen E, Jalkanen M et al (1989) Epithelial-mesenchymal interactions regulate the stage specific expression of a cell surface proteoglycan, syndecan, in the developing kidney. Dev Biol 134: 382-391

Van den Abbeele, Treves ST, Lebowitz Rl et al (1987) Vesicoureteral reflux in asymptomatic siblings of patients with known reflux: radionuclide cystography. Pediatr 79: 147-153

Van de Vosse E, Walpole SM, Nicolaou A et al (1998) Characterisation of SCML1, a new gene in Xp22, with homology to developmental polycomb genes. Genomics 49: 96-102

Van Heynignen V (1994) One gene-four syndromes. Nature 367: 319-320

Van Sletgenhorst MA, Bassi MT, Borsani G (1994) A gene from the Xp22.3 region shares homology with voltage-gated chloride channels. Hum Mol Genet 3: 547-552

Varadi V, Szabo L, Papp Z (1980) Syndrome of polydactyly, cleft lip/palate or lingual lump, and psychomotor retardation in endogamic Gypsies. J Med Genet 17: 119-122

Vega QC, Worby CA, Lechner MS et al (1996) Glial cell line-derived

neurotrophic factor activates the receptor tyrosine kinase RET and promotes kidney morphogenesis. Proc Natl Acad Sci USA 93: 10657-10661

Veis DJ, Sorenson CM, Shutter JR et al (1994) Bcl-2-deficient mice demonstrate fulminant lymphoid apoptosis, polycystic kidneys and hypopigmented hair. Cell 75: 229-240

Verani R, Walker P, Silva FG (1989) Renal cystic disease of infancy: results of histochemical studies. Paediatr Nephrol 3: 37-42

Vestweber D, Kemler R, Ekblom P (1985) Cell-adhesion molecule uvormorulin during kidney development. Dev Biol 112: 213-221

Vyse TJ, Todd JA (1996) Genetic analysis of autoimmune disease. Cell 85: 311-318

Wada T, Naito T, Griffiths RC et al (1997) Systemic autoimmune nephritogenic components include CSF-1 and TNF-alpha. Kidney Int 52: 934-941

Wagner T, Wirth J, Meyer J et al (1994) Autosomal sex reversal and campomelic dysplasia are caused by mutations in and around the SRY-related gene SOX9. Cell 79: 1111-1120

Wahrman J, Berant M, Jacobs J et al (1966) The oral-facial-digital syndrome: A male lethal condition in a boy with 47XXY chromosome. Paediatr 37: 812-821

Waldeyer W (1882) Ureterscheide, Verhandl. Anat Gesellech 6: 259-261

Wallace DMA, Rothwell DL, Williams DI (1978) The long term follow-up of surgically treated vesico-ureteric reflux. Br J Urol 50: 479-484

Walpole SM, Hiriyana KT, Nicolaou A et al (1999) Identification and characterisation of the human homologue (RAI2) of a mouse retinoic acid-induced gene in Xp22. Genomics 55: 275-283

Wang Z-Y, Madden SL, Deuel TF et al (1992) The Wilms' tumour gene product WT-1 represses the transcription of the platelet derived growth factor A-chain gene. J Biol Chem 267: 21999-22002

Warady BA, Hebert D, Sullivan EK et al (1997) Renal transplantation, chronic dialysis and chronic renal insufficiency in children and adolescents. The 1995 Annual Report of the North American Pediatric Renal Transplant Cooperative Study. Pediatr Nephrol 11: 49-64

Weber JL, May PE (1989) Abundant class of human polymorphisms which can be typed using the polymerase chain reaction. Am J Hum Genet 44: 388-396

Wellling LW, Welling DJ (1988) Theoretical models of cyst formation and growth. Scanning Microsc 2: 1097-1102

Werner H, Rauscher FJ, Sukhatme VP et al (1994) Transcriptional repression of the insulin-like growth factor 1 receptor (IGF-1-R) gene by the tumor suppressor WT-1 involves binding to sequences both upstream and downstream of the IGF-1-R gene transcript start site. J Biol Chem 269: 12577-12582

Wettke-Schafer R, Kantner G (1983) X-linked dominant inherited diseases with lethality in hemizygous males. Hum Genet 64: 1-23

Whelan DT (1975) The oro-facial-digital syndrome. Clin Genet 8: 205-212

Wickramisinghe SF, Stephens FD (1977) Paraureteral diverticula: Associated renal morphology and embryogenesis. J Urol 14: 381-385

Wienecke R, Konig A, DeClue (1995) Identification of tuberin, the tuberous sclerosis-2 product. Tuberin possesses specific Rap1GAP activity. J Biol Chem 270: 16409-16414

Wilkie AO, Slaney SF, Oldridge M et al (1995) Apert syndrome results from localized mutations of FGFR2 and is allelic with Crouzon syndrome. Nat Genet 9: 165-172

Wilson PD, Sherwood AC, Palla K et al (1991) Reversed polarity of Na(+)-K(+)-ATPase: mislocation to apical plasma membrances in polycystic kidney disease epithelia. Am J Physiol 260: F 420-430

Wilson PD, Hreniuk D, Gabow PA (1992) Abnormal extracellulr matrix and excessive growth of human adult polycytic kidney disease epithelia. J Cell Physiol 150 (2): 360-369

Winnearls CG, Hind CR (1983) Indentical twins with vesicoureterci reflux. Br Med J Clin Res Ed 286: 1245-1246

Winter RM, Baraitser M (1998) The London Dysmorphology Database. Oxford University Press, Oxford UK

Winyard PJD, Nauta J, Lirenman DS et al (1996a) Deregulation of cell survival in cystic and dysplastic renal development. Kidney Int 49: 135-146

Winyard PJD, Risdon RA, Sams VR et al (1996b) The PAX2 transcription factor is expressed in cystic and hyperproliferative dysplastic epithelia in human kidney malformations. J Clin Invest 98: 451-459

Winyard PJD, Bao Q, Hughes RC et al (1997) Epithelial galecting-3 during human nephrogenesis and childhood cystic diseases. J Am Soc Nephrol 8: 1647-1657

Woolf AS (1995a) Clinical impact and biological basis of renal malformations. Semin Nephrol 15: 361-371

Woolf AS, Kolatsi-Joannou M, Hardman P et al (1995b). Roles of hepatocyte

growth factor/scatter factor and the Met receptor in the early development of the metanephros. J Cell Biol 128: 171-184

Woolf AS, Cale CM (1997) Roles of growth factors in renal development. Curr Op Nephrol Hypert 6: 10-14

Woolf AS, Winyard PJD (1998) Advances in the cell biology and genetics of human kidney malformations. J Am Soc Nephrol 9: 1114-1125

Wyllie AH, Kerr JFR, Currie AR (1980) Cell death: the significance of apoptosis. Int Rev Cytol 68: 251-306

Yeung CK, Godley ML, Dhillon HK (1997) The characteristics of primary vesico-ureteric reflux in male and female infants with pre-natal hydronephrosis. Br J Urol 80: 319-327

Yorifuji T, Muroi J, Uematsu A (1998) X-inactivation pattern in the liver of a manifesting female with ornithine transcarbamylase deficiency (OTC). Clin Genet 54: 349-353

Zhang P. Liegeois NJ, Wong C et al (1997) Altered cell differentiation and proliferation in mice lacking p57KIP2 indicates a role in Beckwith-Wiedemann syndrome. Nature 387: 151-158

Zimmerman SW, Uehling DT, Burkholder PM (1973) Vesicoureteral reflux

nephropathy: evidence for immunologically mediated glomerular injury. Urology 2: 534-542

Nephrol Dial Transplant (1997) 12: 1354–1361

Nephrology
Dialysis
Transplantation

Original Article

Oral-facial-digital syndrome type 1 is another dominant polycystic kidney disease: clinical, radiological and histopathological features of a new kindred

S. A. Feather[1,2], P. J. D Winyard[2,3], S. Dodd[4] and A. S. Woolf[2,3]

Molecular Genetics, [2]Nephrourology, and [3]Developmental Biology Units, Institute of Child Health; [4]Department of Morbid Anatomy, Royal London Hospital, London

Abstract

Background. Oral-facial-digital syndrome type 1 (OFD1) is a rare disorder comprising malformations of the face, oral cavity, hands, and feet. Polycystic kidney disease (PKD) is a more recently recognized feature of the syndrome.

Subjects and methods. We now report on the clinical, radiological and histopathological features of an OFD1 and PKD kindred with five affected members in three subsequent generations.

Results. All patients were female and had accompanying PKD as assessed by ultrasound scans. The plasma creatinine was normal in three, but PKD caused end-stage renal failure in two of these individuals in the second and fifth decades. A histochemical analysis of renal tissue from one affected member of this kindred demonstrated a predominantly glomerulocystic kidney disease with a minor population of cysts derived from distal tubules as assessed by staining with *Arachis hypogaea* lectin. Cyst epithelia had a high level of mitosis as assessed by staining with antisera to proliferating cell nuclear antigen, and distal cysts overexpressed PAX2 protein, a potentially oncogenic transcription factor. We detected multiple pancreatic cysts in one member affected by OFD1 although there were no symptoms of pancreatic disease; this constitutes a novel radiological feature of the syndrome.

Conclusions. This kindred illustrates the inheritance pattern of OFD1 and its accompanying PKD. Although the renal disease superficially resembles ADPKD with macroscopic cysts and a dominant inheritance pattern, histology shows a predominance of glomerular cysts and the syndrome is X-linked, with affected males dying before birth. The recognition of the accompanying dysmorphic features is the key to a diagnosis of OFD1 in a female child or adult who presents with PKD.

Correspondence and offprint requests to: Dr Sally Feather, Molecular Genetics Unit, Institute of Child Health, 30 Guilford Street, London WC1 1EH, UK.

Key words: end-stage renal failure; histopathology; oral-facial-digital syndrome type 1; polycystic kidney disease; radiology; X-linked dominant disease

Introduction

The genetic causes of polycystic kidney disease (PKD), which are associated with macroscopic renal cysts, include the autosomal dominant PKDs [1,2], tuberous sclerosis [3,4], von Hippel-Lindau disease [5,6], and a recently recognized contiguous gene defect comprising deletions of PKD1 and TSC2 [7]. Other inherited disorders are associated with renal cysts which are generally microscopic, and these entities include autosomal recessive PKD, juvenile nephronophthisis, and medullary cystic disease [8,9]. In this report we wish to draw attention to the PKD associated with a rare disorder called the oral-facial-digital syndrome type 1 (OFD1; previously called orodigitofacial dysostosis or the Papillon-Leage-Psaume syndrome) [10,11].

Individuals affected by OFD1 have characteristic malformations of the face, oral cavity, hands, and feet but these signs may be relatively mild, especially since some of these defects are often surgically corrected in childhood [10,11]. The associated kidney disease superficially resembles ADPKD because of the presence of multiple macroscopic renal cysts and a dominant inheritance pattern [12–16]. Histological analysis of OFD1 kidneys, however, demonstrates a predominance of glomerular cysts, whereas this appearance is rare in ADPKD [13]. Moreover, a closer inspection of kindreds with OFD1 suggests that the mode of inheritance is X-linked dominant, in contrast to the ADPKDs which are autosomal dominant diseases [1,2]. Furthermore, OFD1 is almost exclusively diagnosed in females because males carrying OFD1 mutations die *in utero*, usually in first or second trimester [12,17]. These observations have major implications for genetic counselling of OFD1 patients with PKD who may be

investigated and treated in either paediatric or adult nephrology units. In the current report we describe the clinical, radiological and histopathological features of a three-generation kindred with OFD1 and PKD affecting five females, two of whom have required renal replacement therapy.

Subjects and methods

Subjects

The three-generation family which included five females affected by OFD1 and PKD (e.g. I-2; II-2 and II-4; III-1 and III-2) is depicted in Figure 1. After the diagnosis of polycystic kidney disease in I-2, renal ultrasound were performed in her five children (II-2, II-4, II-6, II-8 and II-9) and, when II-2 and II-4 were found to be affected, their own children (III-1, III-2, III-3 and III-4) had renal ultrasound scans. In those individuals found to have renal cysts, the liver and pancreas were imaged to detect possible cystic involvement.

Histochemistry

Chemicals were obtained from Sigma (Poole, Dorset, UK) unless otherwise stated. Directly after autopsy, PKD kidneys from individual I-2 (see Figure 1) were fixed in 4% paraformaldehyde and embedded in paraffin wax. Sections (10 μm) were placed on glass slides and were dewaxed through Histo-Clear (National Diagnostics, Atlanta, USA) twice for 10 min, followed by dehydration through 100% ethyl alcohol twice for 5 min and then stepwise through 95%, 90%, 75%, 50% and 30% alcohol for 3 min each. They were further processed for immunohistochemistry [18]. After washing in phosphate-buffered saline (PBS, pH 7.4) for 5 min and tap water for 10 min, they were immersed in citric-acid buffer (2.1 g/l, pH 6.0) and boiled in a microwave for 8 min. They were allowed to cool, washed in tap water and PBS, then incubated in 3% hydrogen peroxide for 15 min to quench endogenous peroxidase activity. Non-specific antibody binding was blocked by preincubation of the slides with fetal calf serum (10% volume/volume in PBS). Primary antibodies were rabbit polyclonal antibody raised against amino acids 188–385 in the carboxyterminal domain of PAX2 used as previously described [18]; a rabbit polyclonal IgG fraction raised against an epitope in the carboxyterminus of human WT1 protein (C-19: Santa Cruz Biotechnology, Inc., CA, USA) used as previously described [18]; mouse monoclonal antibody to proliferating cell nuclear antigen (PCNA Ab-1; Oncogene Science Inc., Cambridge, MA, USA) used as previously described [18]. PCNA is a DNA-polymerase δ-associated protein expressed at high levels during S phase [19]. Primary antibodies were detected using a streptavidin biotin peroxidase system (Dako, ABC Kit) followed by diamino benzidine. Sections were counterstained with 0.5% methyl green for 10 min and washed three times with water and butanol, once in Histo-Clear for 10 min, and mounted in DPX (BDH, Poole, UK). They were examined on a Zeiss Axiophot microscope (Carl Zeiss, 7082 Oberkochen, Germany).

Lectin staining was performed as follows. After washing in PBS for 5 min, sections were incubated in propidium iodide (PI) with RNase A in PBS at 37°C for 30 min, and then counterstained with FITC-conjugated *Tetragonolobus lotus* (pea asparagus) or *Arachis hypogaea* (peanut) lectins exactly as described [20]. These lectins bind to proximal tubules and distal segments (distal tubule and collecting ducts) respectively [21]. Sections were mounted in Citifluor™ (Chemical Labs, University of Kent, Canterbury, Kent, UK) and examined under fluorescence (wavelength 488 nm for FITC and 568 nm for PI) on a Leica confocal laser scanning microscope (Aristoplan-Leica, Heidelberg, Germany).

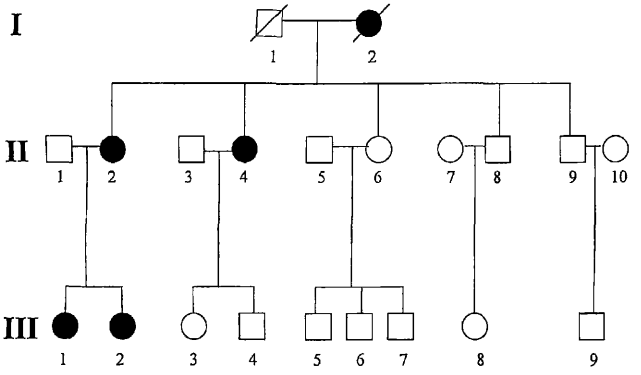

Fig. 1. Family tree of OFD1 kindred. The three generations are designated I, II and III while individual members in each generation are designated I-1, II-2 etc. Female heterozygotes affected by OFD1 are indicted by filled circles. I-2 is the index case who required dialysis and transplantation and who subsequently died. Note the pattern of inheritance is consistant with an X-linked dominant disease which is prenatally lethal in male fetuses who carry the OFD1 mutation.

Results

Clinical and radiological features of the affected members are summarized in Table 1, renal histology of I-2 is shown in Figures 2 and 3, and selected dysmorphic and ultrasonographic features of certain individuals are depicted in Figure 4.

The index case (I-2; Figure 1), presented in her fifth decade with end-stage renal failure. She had a pseudocleft of the upper lip, a broad nasal bridge, and an asymmetrical face, characteristic features of OFD1. Ultrasound scan detected multiple bilateral renal cysts consistent with a diagnosis of PKD. She required dialysis and renal transplantation but subsequently died from a myocardial infarction.

At autopsy her kidneys were polycystic with cysts <1 cm in diameter. Cysts were not noted in other organs. As expected for an 'end-stage' kidney, there was marked fibrosis between cysts (Figure 2A and B). Most cysts were lined by flat epithelial cells and were enclosed by fibrotic walls. In approximately 5–10% of such structures in any single section, a glomerular tuft was seen to be attached to the cyst lining (Figure 2A and B). A subset of nuclei in these tufts stained with antibody to WT1 (Figure 2C), consistent with identities as podocytes [18], and many tufts within cysts contained open capillary loops. Other glomeruli had mildly dilated Bowman's spaces and a minor population of glomerular tufts were sclerosed. Up to 50% of the nuclei in the tufts of cystic glomeruli stained with antibody to PCNA (Figure 2D), suggesting prolifera-

Table 1. Clinical and radiological features of affected individuals.

Case	I-2	II-2	II-4	III-1	III-2
Sex	female	female	female	female	female
Age at diagnosis	5th decade	3rd decade	3rd decade	15 years	13 years
Renal ultrasound	Bilateral polycystic kidneys	Unilateral polycystic kidney	Bilateral polycystic kidneys	Bilateral polycystic kidneys	Bilateral polycystic kidneys
Renal status	End-stage renal failure; renal transplant	Normal plasma cretinine	Plasma creatinine 104 μM	End-stage renal failure	Plasma creatinine 54 μM
Facial features	Pseudocleft upper lip; broad nasal bridge asymmetrical face	Pseudocleft upper lip; broad nasal bridge asymmetrical face	Pseudocleft upper lip; broad nasal bridge asymmetrical face	Pseudocleft upper lip; broad nasal bridge asymmetrical face	Pseudocleft upper lip; broad nasal bridge asymmetrical face
Oral features	Not documented	Tongue hamartoma	Tethered tongue cleft palate	High arched palate oral frenulae; absent lateral incisors	High arched palate tethered and cleft tongue
Digital features	Not documented	Not documented	Soft-tissue syndactyly; middle and index finger left hand; left hallux varus and duplication	Brachydactyly left index finger and 4th toes	Brachydactyly 4th toes
Other features	Learning difficulties	Learning difficulties 2nd timester miscarriages	Learning difficulties	Learning difficulties pancreatic cysts	Learning difficulties

tion. The majority (>90%) of cysts failed to stain with either FITC-conjugated *Tetragonolobus lotus* and *Arachis hypogaea* lectins (Figure 3A), consistent with a glomerular origin. Mildly dilated tubules of up to 100–200 μm were also noted (Figure 2G and H). These stained with *Arachis hypogaea* lectin (Figure 3B) and never contained glomerular tufts, suggesting a distal tubule rather than a glomerular origin. The epithelial cells which lined the distal tubule cysts stained with PAX2 antibody (Figure 2G and H). Glomerular cysts did not express PAX2 (Figure 2E and G), while dilated distal tubules showed no immunoreactivity with WT1 antibody (data not shown). Up to 50% of nuclei in dilated distal tubules stained with PCNA antibody (data not shown).

After presentation of the index case, her family were assessed clinically and by ultrasound scanning (Table 1). Two (II-2 and II-4) of her three daughters had dysmorphic features of OFD1 and two granddaughters (III-1 and III-2) were similarly affected. Dysmorphic features included tongue tethering by frenulae, abnormal dentition and digital abnormalities (Table 1 and Figure 4A–D). No live-born males in this kindred were affected by OFD1 (Figure 1) but there was a family history of miscarriages in OFD1 individuals I-2, II-2, and II-4. The inheritance pattern in this kindred is consistent with an X-linked dominant pattern in which female heterozygotes exhibit the clinical syndrome whereas males who carry a single, mutated gene die before birth. As well as the dysmorphic features, mild to moderate learning difficulties were prominent in this OFD1 kindred.

All affected members had PKD as assessed by ultrasound scans, although renal lengths were within normal limits and the contours were not irregular. Renal cysts were <1 cm across (Figure 4E) and were bilateral in all but II-2. At initial assessment at 15 years, III-1 was found to be in chronic renal failure, but the other three affected members (II-2, II-4, and III-2) had normal plasma creatinine levels. Within 2 years of diagnosis III-1 required treatment with chronic ambulatory peritoneal dialysis and she is awaiting transplantation. We also detected multiple pancreatic cysts (<5 cm) in this individual (Figure 4F) although she reported no symptoms of pancreatic disease. Ultrasound scans did not detect pancreatic cysts in other OFD1 individuals.

Discussion

OFD1 is a rare syndrome, occurring in approximately 1/250,000 live births [10,11,17]. The dysmorphology of OFD1 is characteristic, with facial features which include frontal bossing, facial asymmetry, hypertelorism (widely spaced eyes), a broadened nasal bridge, and facial milia. Oral features include pseudoclefting of the upper lip, cleft palate and tongue, high arched palate, tethering of the tongue (ankyloglossia) by frenu-

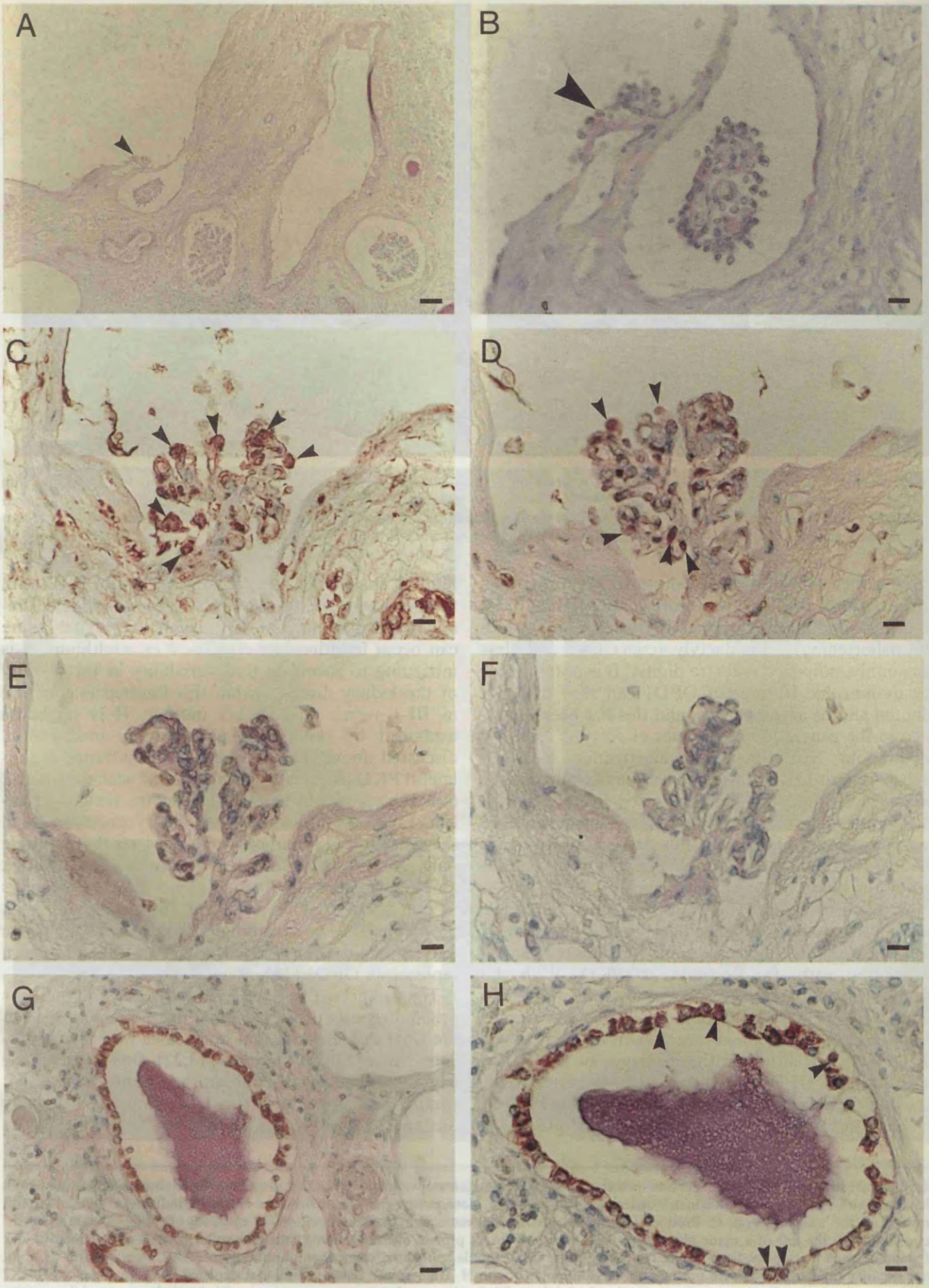
A
B
C
D
E
F
G
H

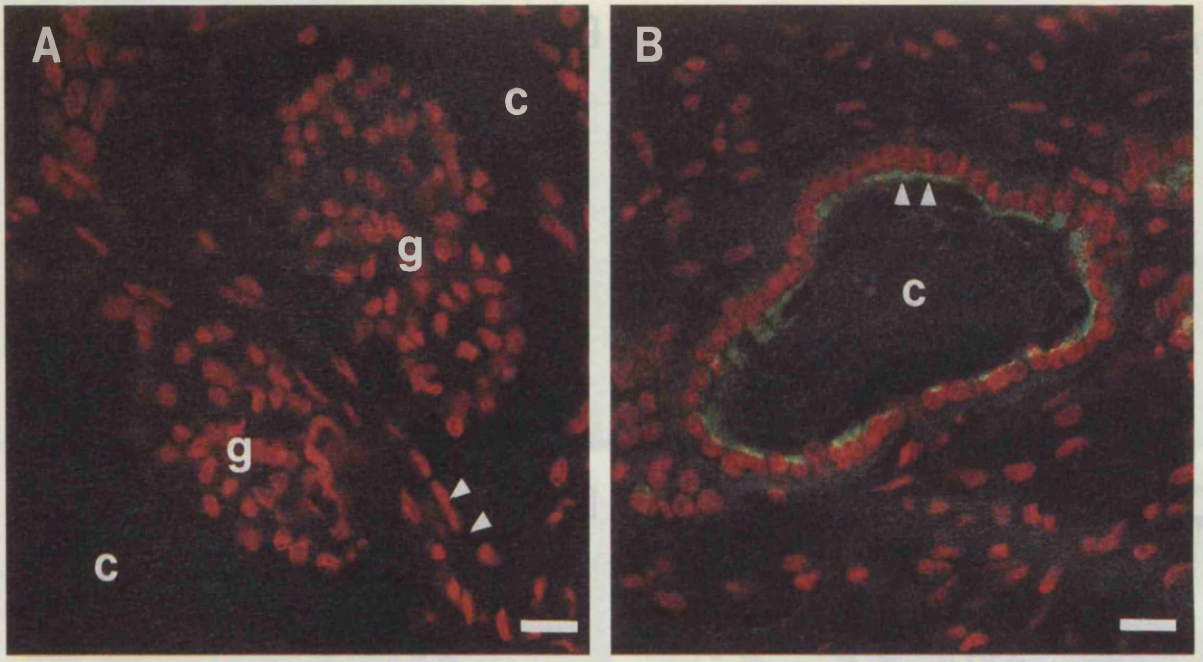

Fig. 3. Lectin histochemistry in OFD1 kidney. A. Parietal epithelia (arrowheads) of two glomerular cysts (c) showed no reactivity with FITC-conjugated *Arachis hypogaea* lectin. Glomerular tufts are also indicated (g). Lack of staining was also noted with *Tetragonolobus lotus* lectin (not shown). B. Epithelial cells (arrowheads) lining a dilated tubule stained positively with FITC-conjugated *Arachis hypogaea lectin* (green), suggesting a distal tubule origin. All nuclei are stained red with PI. Bars are 20 μm.

lae, together with abnormal dentition. Malformations of the digits of the hands are more common than those of the feet and include syndactyly (fusion), brachydactyly (shortening), clinodactyly (curvature) and, less commonly, polydactyly (extra digits). It is notable that the dysmorphic features of OFD1 can vary within a kindred and be asymmetrical, and this has been attributed to the generation of mosaics of somatic cells due to random X chromosome inactivation early in embryogenesis [11,17]. Central nervous system disease occurs in 40% of individuals affected by OFD1 with mental retardation, hydrocephalus, and agenesis of the corpus callosum [11,15]. In this respect it is of note that mild to moderate learning difficulties were prominent in our kindred.

An association with PKD was first noted by Doege and colleagues in a member of a large OFD1 family [12]. Clearly, this single case could have been a chance association with, for example, ADPKD. With the increasing use of high-definition renal ultrasound scanning, however, it has become increasingly apparent that PKD is a common accompanying feature of OFD1 [13–16], although the incidence of PKD in a large series of OFD1 patients has yet to be reported. The kidneys may be of normal length, as in the kindred in the current report, or palpably enlarged [15]. Our kindred showed a complete concordance of PKD with the dysmorphic features of the syndrome, and additionally the family demonstrates that end-stage renal failure can occur in either late childhood or adulthood. It is intriguing to speculate that variability in the severity of the kidney disease within this kindred (e.g. severe in III-1 *versus* mild in her mother, II-2) might be explained by random X chromosome inactivation, discussed above. Furthermore, the occurrence of unilateral PKD as detected by ultrasound scanning of II-2 (see Table 1) might be explained by the same mechanism. Liver cysts have been previously documented in the syndrome [13] and our study suggests that multiple pancreatic cysts are another feature of OFD1, albeit an inconstant one, occurring in 1/5 affected members in our kindred. While OFD1 is the commonest of a group of eight oral-facial-digital syndromes which have overlapping dysmorphic features, PKD has only been reported in OFD1 [11].

To our knowledge there have only been two previous original reports of OFD1 renal histology published in the English literature, and both cases were not apparently part of OFD1 kindreds [13,22]. One was a female who developed renal failure in the second decade [13], while the other was an XY male neonate with massively dilated kidneys and lung hypoplasia who died hours

Fig. 2. Renal histology of case I-2. A. Low-power view of a PKD organ showing cysts of varied diameters. B. Higher power demonstrates glomeruli with mildly dilated Bowman's spaces as well as larger glomerular cysts. The arrows in A and B indicate a glomerular tuft arrached to the wall of a cyst. C. Prodocytes (arrowheads) in a glomerular cysts stained with WT1 antibody. D. PCNA-staining nuclei (arrowheads) in the tuft of a cystic glomerulus. E. Absence of PAX2 protein nuclear staining in a glomerular cyst. F. Represintative lack of staining when first antibodies are omitted. G. A cystic distal tubule epithelium stained with antibody to PAX2; two cysts on the right were negative for PAX2 and were presumably of glomerular origin. H. High-power view of distal cyst depicted in G. In some cells PAX2 staining is clearly localized to nuclei (arrowheads). All nuclei in the panel were counterstained with methyl green, while positive immunohistochemical signals appear brown. Bars are 60 μm in A, 15 μm in B and G, and 10 μm other frames.

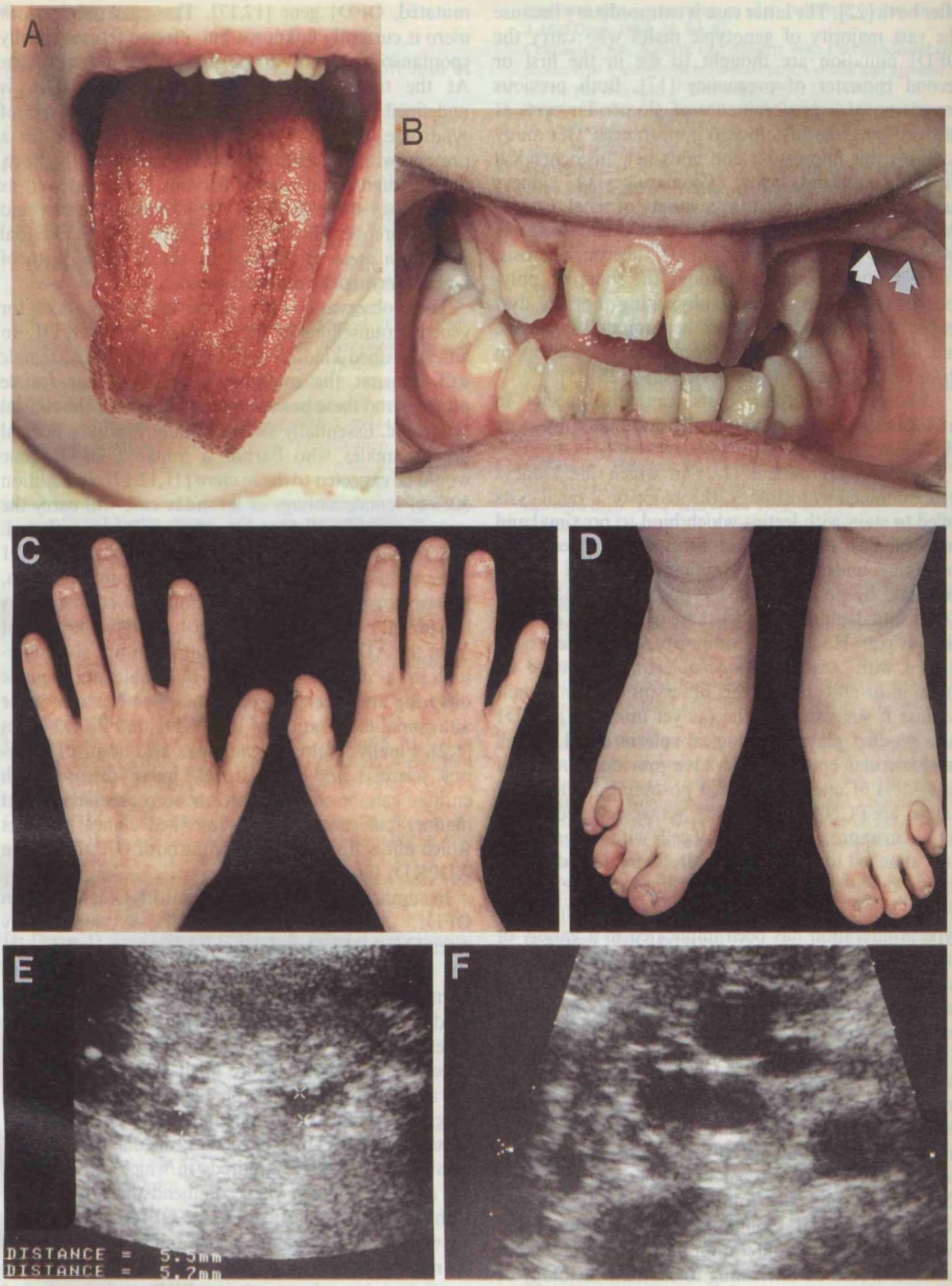

Fig. 4. Dysmorphic and radiological features of the OFD1 kindred. A. Individual III-1 had marked dysmorphic features: note the irregular clefting of the tongue. B. An oral frenulum (arrow) and abnormal dentition (missing lateral inscisors) if III-1. C. Shortened index finger (brachydactyly) in left hand of III-1. D. Bilateral dysmorphic toes (brachydactyly of 4th digits) of III-1. Note the pitting oedema of this teenage patient, who was treated with peritoneal dialysis. E. Ultrasound scan of kidney of III-2 detected cysts of up to 5 mm in diameter. F. Ultrasound scan of III-1 showing a polycystic pancreas.

after birth [22]. The latter case is extraordinary because the vast majority of genotypic males who carry the OFD1 mutation are thought to die in the first or second trimester of pregnancy [17]. Both previous reports noted a predominance of glomerular cysts as assessed by gross histological appearances. Our study confirms this impression and adds new histochemical insights, discussed below. Glomerulocystic kidneys have been found to occur in a variety of renal diseases including non-syndromic glomerulocystic diseases (which may be sporadic or familial), tuberous sclerosis, brachymesomelia-renal syndrome, the short rib polydactyly syndromes, Jeune asphyxiating thoracic dystrophy syndromes, Zellweger hepatorenal syndrome and familial juvenile nephronophthisis, as well as in trisomies 9, 13 and 18 [for reviews, see 23–25].

Although glomerular cysts can also occur in ADPKD, the histology is usually dominated by cysts of tubular origin [23–24].

In our OFD1 patient (I-2) in which the kidneys were examined by histology, the majority of renal cysts failed to stain with lectins which bind to proximal and distal tubules, and some contained tufts with capillary loops surrounded by cells staining for WT1, a protein expressed by podocytes in the postnatal kidney [18]. These data demonstrate that these cysts are of glomerular origin. However, a minority of smaller cysts stained with *Arachis hypogaea* lectin, indicating an origin in distal tubules. This observation is important because it suggests that the (as yet unknown) OFD1 gene product plays a biological role in distal as well as glomerular epithelia. We have previously reported that $<1\%$ of nuclei in normal postnatal glomeruli or tubules are PCNA positive [18], yet we detected proliferation in approximately 50% of cells within glomerular tufts attached to OFD1 cyst walls. Deregulated proliferation might therefore be important in the genesis of OFD1 renal cysts, and it is notable that epithelial hyperproliferation has been implicated in a variety of human and animal models of PKD [26]. We previously reported that the PAX2 transcription factor protein is barely detectable by immunohistochemistry in mature human kidneys [18], but in this study we found that PAX2 was strongly expressed by epithelia lining distal tubule OFD1 cysts. PAX2 is highly expressed by proliferating distal tubule precursor cells in human fetal kidneys, in cysts of human dysplastic kidneys [18] and in Wilms' tumours [27]; furthermore, overexpression of PAX2 causes renal cysts in transgenic mice [28]. Conversely, we found that PAX2 was not expressed in OFD1 glomeruli, suggesting that other factors must drive proliferation in those structures. In future, it would be interesting to examine histology of other OFD1 patients who have PKD but are not in severe renal failure.

Approximately 75% of OFD1 cases are sporadic and these occur almost exclusively in females [10–12,17]. The remaining cases are familial and these too are essentially limited to females. The most likely form of inheritance has been considered to be X-linked dominant with prenatal death of males carrying a single, mutated, OFD1 gene [12,17]. The cause of death *in utero* is currently unknown but affected fetuses usually spontaneously abort in the first or second trimester. At the time of writing, the specific mutation is undefined but, based on the clinical phenotype of syndrome, the wild-type gene is likely to code for a protein which affects the development of the face, mouth, digits, and central nervous system as well as the biology of epithelia in the kidney, pancreas, and liver. Moreover, the OFD1 gene appears to be essential for life *in utero* as assessed by the *in utero* death of males carrying the mutated gene.

These observations have important implications for genetic counselling of PKD patients with OFD1. In an established kindred with OFD1, an affected female will transmit the mutation to 50% of her female progeny and these heterozygotes will exhibit the clinical syndrome. Essentially all live-born boys will be normal because males who harbor a mutated OFD1 gene would be expected to die *in utero* [11,12,17]. In addition 50% of female siblings of an index case will carry the mutation, while all living brothers will be unaffected. The probability that an individual with sporadic OFD1 will produce affected offspring is currently unknown, but we suggest such patients should be counselled as in familial cases. This outlook is clearly very different from the ADPKDs in which mutations are also inherited in a dominant manner but male and female offspring are affected in equal measure because of the autosomal localization of the PKD1 and PKD2 genes [1,2]. Finally, multiple renal cysts also occur in tuberous sclerosis and von Hippel-Lindau disease; both entities can be inherited in an autosomal dominant manner but each has well-described clinical features which allow discrimination from both OFD1 and the ADPKDs [3–6].

In summary, clinically significant PKD can occur in OFD1. Although the renal disease superficially resembles ADPKD with macroscopic cysts and dominant inheritance, OFD1 PKD kidneys are usually of normal size and contour, the renal histology shows a predominance of glomerular cysts, and the specific inheritance pattern is X-linked with practically all affected males dying before birth. The recognition of the accompanying dysmorphic features is the key to a diagnosis of OFD1 in a female child or adult who presents with PKD. In particular, the diagnosis should be suspected in PKD kindreds in which only females are affected. Finally, we recommend that all children with the dysmorphic features of OFD1 are followed up with renal ultrasound scans and simple measures of renal function (e.g. blood pressure and plasma creatinine) in order to detect PKD and its clinical consequences.

Acknowledgements. SF and PJDW are supported by Training Fellowships from Action Research. We thank Profs R. Winter and S. Malcolm for helpful discussions and also Ms Jennifer Allison, Dr S. Roy, Dr M. Dillon, and all the other nursing staff and medical staff who attended members of the family described in this report.

Note added in proof

We have recently mapped OFD1 to the short arm of the X chromosome [29].

References

1. European Polycystic Kidney Disease Consortium. The polycystic kidney disease 1 gene encodes a 14 kb transcript and lies within a duplicated region on chromosome 16. *Cell* 1994; 77: 881–894
2. Mochizuki T, Wu G, Hayashi T *et al.* PKD2, a gene for polycystic kidney disease that encodes an integral membrane protein. *Science* 1996; 272: 133–1342
3. European Chromosome 16 Tuberous Sclerosis Consortium. Identification and characterisation of the tuberous sclerosis gene on chromosome 16. *Cell* 1993; 75: 1305–1315
4. Zimmerhackl LB, Rehm M, Kaufmehl K, Kurlemann G, Brandis M. Renal involvement in tuberous sclerosis complex: a retrospective survey. *Pediatr Nephrol* 1994; 8: 451–457
5. Latif F, Kalman T, Gnarra J *et al.* Identification of the von Hippel–Lindau disease tumor suppressor gene. *Science* 1993; 260: 1317–1320
6. Chauveau D, Duvic C, Chretien Y *et al.* Renal involvement in von Hippel-Lindau disease. *Kidney Int* 1996; 50: 944–951
7. Brook-Carter PT, Peral B *et al.* Deletion of the TSC2 and PKD1 genes associated with severe infantile polycystic kidney disease: a contiguous gene syndrome. *Nature Genet* 1994; 8: 328–332
8. Zerres K, Mucher G, Bachner L *et al.* Mapping of the gene for autosomal recessive polycystic kidney disease (ARPKD) to chromosome 6p21-cen. *Nature Genet* 1994; 7; 429–432
9. Kissane JM. Renal cysts in pediatric patients: a classification and overview. *Pediatr Nephrol* 1990; 4: 69–77
10. Gorlin RJ, Psaume J. Orodigitofacial dysostosis – a new syndrome. *J Pediatr* 1962; 61: 520–530
11. Branchial Arch and Oro-acral disorders. In: Gorlin RJ, Cohen MM, Levin LS. (eds). *Syndromes of the Head and Neck*. Third edn.. Oxford Monographs on Medical Genetics No. 19. Oxford University Press, New York, 1990; 676–686
12. Doege TC, Thuline HC, Preist JH, Norby DE, Bryant JS. Studies of a family with the oral-facial-digital syndrome. *N Engl J Med* 1964; 271: 1073–1080
13. Stapleton FB, Bernstein J, Koh G, Roy S III, Wilroy RS. Cystic kidneys in a patient with oral-facial-digital syndrome, type 1. *Am J Kidney Dis* 1982; 1: 288–293
14. Donnai D, Kerzin-Storrar L, Harris R. Familial orofaciodigital syndrome type 1 presenting as adult polycystic kidney disease. *J Med Genet* 1987; 24: 84–87
15. Connacher AA, Forsyth CC, Stewart WK. Orofaciodigital syndrome type I associated with polycystic kidneys and agenesis of the corpus callosum. *J Med Genet* 1987; 24: 116–122
16. Salinas CF, Pai GS, Vera CL *et al.* Variability of expression of the orofaciodigital syndrome type 1 in black females: six cases. *Am J Med Genet* 1991; 38: 574–582
17. Wettke-Schafer R, Kanter G. X-linked dominant inherited diseases with lethality in heterozygous males. *Hum Genet* 1983; 64: 1–23
18. Winyard PJD, Risdon RA, Sams VR, Dressler GR, Woolf AS. The PAX2 transcription factor is expressed in cystic and hyperproliferative dysplastic epithelia in human kidney malformations. *J Clin Invest* 1996; 98: 451–459
19. Bravo R, Frank R, Blundell PA, MacDonald-Bravo H. Cyclin/PCNA is the auxillary protein of DNA polymerase-delta. *Nature (London)* 1987; 326: 515–517
20. Winyard PJD, Nauta J, Lirenman DR *et al.* Deregulation of cell survival in cystic and dysplastic renal development. *Kidney Int* 1996; 49: 135–146
21. Verani R, Walker P, Silver FG. Renal cystic disease of infancy: results of histochemical studies. *Pediatr Nephrol* 1989; 3: 37–42
22. Gillerot Y, Heimann M, Fourneau C, Verellen-Dumoulin C, van Maldergem L. Oral-facial-digital syndrome type 1 in a newborn male. *Am J Med Genet* 1993; 46: 335–383
23. Bernstein J, Landing BH. Glomerulocystic kidney disease. In: Spitzer A, Avner E. (eds). *Genetics of Kidney Disorders*. Alan Riss, Inc. 1989; 27–43
24. Bernstein J. Glomerulocystic kidney disease: nosological considerations. *Pediatr Nephrol* 1993; 7: 464–470
25. Craver RD, Ortenberg J, Baliga R. Glomerulocystic disease: unilateral involvement of a horseshoe kidney and in trisomy 18. *Pediatr Nephrol* 1993; 7: 375–378
26. Grantham JJ. Fluid secretion, cellular proliferation, and the pathogenesis of renal epithelial cysts. *J Am Soc Nephrol* 1992; 3: 1841–1857
27. Eccles MR, Wallis LJ, Fidler AE, Spurr NK, Goodfellow PJ, Reeve AE. Expression of the PAX2 gene in human fetal kidney and Wilms' tumor. *Cell Growth Diff* 1992; 3: 279–289
28. Dressler GR, Wilkinson JE, Rothenpieler UW, Patterson LW, Williams-Simons L, Westphal H. Deregulation of Pax-2 expression in transgenic mice generates severe kidney abnormalities. *Nature* 1993; 362: 65–67
29. Feather S, Woolf AS, Donnai D, Malcolm S, Winter R. The oral-facial-digital syndrome type 1, a cause of polycystic disease and associated malformations, maps to Xp22.2–Xp22.3. *Hum Mol Genet* 1997; 6 (in press)

Received for publication: 6.12.96
Accepted in revised form: 21.2.97

Human Molecular Genetics, 1997, Vol. 6, No. 7 1163–1167

The oral–facial–digital syndrome type 1 (OFD1), a cause of polycystic kidney disease and associated malformations, maps to Xp22.2–Xp22.3

Sally A. Feather[1,2,*], Adrian S. Woolf[2,3], Dian Donnai[5], Sue Malcolm[1] and Robin M. Winter[4]

[1]Molecular Genetics Unit, [2]Nephrourology Unit, [3]Developmental Biology and [4]Clinical Genetics Unit, Institute of Child Health, London WC1 1EH, UK and [5]Medical Genetics Unit, St Mary's Hospital, Manchester M13 OJH, UK

Received March 17, 1997; Revised and Accepted April 28, 1997

Key features of the oral–facial–digital syndrome type 1 (OFD1) include malformations of the face, oral cavity and digits. In addition, the clinical phenotype often includes mental retardation and renal functional impairment. Approximately 75% of cases of OFD1 are sporadic, and the condition occurs almost exclusively in females. In familial cases, the most likely mode of inheritance is considered to be X-linked dominant with prenatal lethality in affected males. Therefore, the *OFD1* gene product appears to have widespread importance in organogenesis and is essential for fetal survival. We have studied two kindreds in which the clinical course was dominated by polycystic kidney disease requiring dialysis and transplantation. Using polymorphic chromosome markers spaced at ~10 cM intervals along the X chromosome, we mapped the disease to a region on the short arm of the X chromosome (Xp22.2–Xp22.3) spanning 19.8 cM and flanked by crossovers with the markers *DXS996* and *DX7S105*. There was a maximum lod score of 3.32 in an 'affecteds only' analysis using a marker within the *KAL* gene ($\theta = 0.0$), thereby confirming the location of the gene for OFD1 on the X chromosome. The remainder of the X chromosome was excluded by recombinants in affected individuals. The importance of our findings includes the definitive assignment of this male-lethal disease to the X chromosome and the mapping of a further locus for a human polycystic kidney disease. Furthermore, this mapping study suggests a possible mouse model for OFD1 as the X-linked dominant *Xpl* mutant, in which polydactyly and renal cystic disease occurs, maps to the homologous region of the mouse X chromosome.

INTRODUCTION

In 1962, Gorlin and Psaume defined a syndrome characterized by malformation of the face, oral cavity and digits (1). They called this orofaciodigital dysosotosis, a disorder which subsequently has been renamed the oral–facial–digital syndrome type 1 (OFD1: OMIM 311200) (2). The incidence of OFD1 is estimated to be 1 in 250 000 live births, and it occurs in diverse racial backgrounds (3). Dysmorphic features affecting the head are described as 'remarkably characteristic' (2) and include facial asymmetry, frontal bossing, hypertelorism, micrognathia, broadened nasal bridge and facial milia. Lesions of the mouth include median pseudoclefting of the upper lip (45%), clefts of the palate (>80%) and tongue (30%), as well as lingual hamartomata and oral frenulae. Thickened alveolar ridges and abnormal dentition, including absent lateral incisors, are further characteristics of the syndrome. The digital abnormalities, which affect the hands (50–70%) more often than the feet (25%), include syndactyly, brachydactyly, clinodactyly and, more rarely, pre- or post-axial polydactyly. These clinical features overlap with those reported in the other seven oral–facial–digital syndromes (2).

The central nervous system may also be involved in as many as 40% of cases of OFD1, with reports of mental retardation, hydrocephalus, cerebellar anomalies, porencephaly and agenesis of the corpus callosum (4). In recent years, with the introduction of high definition renal ultrasound scanning, it has been realized that polycystic kidney disease is commonly associated with OFD1 (4–6). In fact, renal failure necessitating dialysis and transplantation in either childhood or adulthood can dominate the clinical course of this disease (6).

Approximately 75% of cases of OFD1 are sporadic. The condition occurs almost exclusively in females. In familial cases, the most likely mode of inheritance is considered to be X-linked dominant with prenatal lethality in affected males (7,8). This hypothesis is supported by the high incidence of miscarriage of male fetuses and the ratio of 2:1 females to males in reported sibships. Phenotypic variability is often found in affected females within a family, and this might be explained by different degrees of somatic mosaicism resulting from random X chromosome inactivation. A case of a liveborn OFD1 male (XY) with massively enlarged polycystic kidneys has been reported, but death occurred within 4 h due to pulmonary hypoplasia (9). Furthermore, a case of Klinefelter syndrome (XXY) has been reported with OFD1, with a phenotype very similar to that of affected females (10). There have been no genetic studies to date which definitively link the syndrome to the X chromosome. An alternative hypothesis would be that OFD1 is a sex-limited

*To whom correspondence should be addressed. Tel: + 44 171 242 9789 ext. 2222; Fax: +44 171 831 0488; Email: sfeather@hgmp.mrc.ac.uk

autosomal dominant disease. In this context, an early report of insertion of an extra segment in chromosome 1 (11) has yet to be substantiated by modern cytogenetic techniques. With regard to the other oral–facial–digital syndromes, most are autosomal recessive but it has been suggested that type VIII is X-linked recessive (2).

In the current study of two OFD1 families with pronounced polycystic kidney disease, we map the locus for the syndrome to a 19.8 cM region on the short arm of the X chromosome between the markers *DXS996* and *DXS7105*. The importance of our new findings include the definitive assignment of this male-lethal disease to the X chromosome as well as the mapping of a further locus for human polycystic kidney disease.

Table 1. Two point linkage analysis for nine markers in order from *DXS996* to *DXS7105*

Marker	Recombination fractions (θ)						
	0.0	0.01	0.05	0.1	0.2	0.3	0.4
DXS996	–∞	0.16	0.68	0.76	0.62	0.39	0.19
	–∞	0.24	0.30	0.41	0.36	0.25	0.14
KAL	–∞	1.90	2.34	2.29	1.85	1.25	0.60
	3.32	3.25	2.97	2.61	1.89	1.19	0.54
DXS1223	**2.67**	2.62	2.43	2.18	1.66	1.11	0.54
	2.32	2.27	2.09	1.86	1.40	0.94	0.47
DXS8051	1.83	1.81	1.73	1.61	1.32	0.96	0.51
	2.24	2.20	2.03	1.82	1.40	0.96	0.49
DXS7108	–∞	–0.30	0.51	0.82	0.92	0.71	0.37
	2.13	2.11	2.02	1.83	1.37	0.86	0.37
DXS8022	**2.52**	2.50	2.41	2.24	1.79	1.23	0.59
	2.84	2.79	2.60	2.35	1.80	1.19	0.55
DXS987	1.05	1.06	1.08	1.06	0.94	0.71	0.40
	1.49	1.48	1.40	1.29	1.02	0.71	0.37
DXS8036	1.76	1.74	1.67	1.54	1.19	0.75	0.29
	2.32	2.27	2.10	1.87	1.38	0.84	0.32
DXS7105	–∞	0.20	0.78	0.93	0.87	0.62	0.28
	–∞	–0.00	0.58	0.72	0.68	0.47	0.20

For each marker, the upper line of figures indicates the two-point lod score for all family members using 100% penetrance, and the lower line indicates the score for affected females and unaffected males only. The maximum lod scores are highlighted in bold in each case.

RESULTS

A G-banded karyotype performed on an affected individual in each family showed no gross chromosomal aberrations.

Two-point linkage analysis of the two kindreds (see Fig. 1) using 100% penetrance gave a maximum two-point lod score of 2.67 at θ = 0.0 with the marker *DXS1223* and a slightly lower lod score (2.52 at θ = 0.0) with the more proximal marker *DXS8022* (see Table 1). An 'affecteds only' analysis (12) gave a maximum lod of 3.32 at θ = 0.0 with *KAL* and a lod of 2.84 at θ = 0.0 with *DXS8022*. The higher lod score in the 'affecteds only' analysis was due to the elimination of individual II-6 in family 1 from the analysis. Although apparently phenotypically normal, she could represent a case of incomplete penetrance, as could individual II-5 from family 2, as has been described in other families (13). An 'affecteds only' multipoint analysis gave a maximum lod score of 3.56 at θ = 0 at *KAL* and but also a lod score of 3.56 between *DXS987* and *DXS8036*. Other markers on the X chromosome (*DXS6807*, *DXS989*, *DXS1068*, *DXS6810*, *DXS1003*, *DXS6800*, *DXS6789*, *DXS6799*, *DXS6797*, *DXS6804*, *DXS1001*, *DXS1047*, *GATA31E08* and *DXS1193*) gave consistently negative lod scores due to recombinations in affected individuals.The critical region that is most likely to contain the gene is between markers *DXS996* and *DXS7105* and spans 19.8 cM.

DISCUSSION

In this study, we have established linkage of OFD1 to the short arm of the X chromosome. This result is consistent with OFD1 being an X-linked dominant disorder with lethality in hemizygous males. Linkage studies of other families with OFD1 are now required to test whether this syndrome is genetically homogeneous and to narrow down the critical region. The OFD1 critical region defined by our linkage study is a 19.8 cM interval (14).

This interval, between *DXS996* and *DXS7105*, is shared by affected individuals in family 1. This is the only region on the X chromosome shared by affected individuals in this family. Affected individuals in family 2 also share this region, but the limits are wider than those defined by family 1. Individual II-6 in family 1 would define the telomeric limit of this region with a recombination at marker *DXS7108*. This female superficially has none of the features of her sisters, II-2 and II-4, but has a history of miscarriage and has three normal sons all of whom have inherited the unaffected haplotype from individual I-1 for this region. These findings and the highly variable phenotypic expression of OFD1 in females noted both in our kindreds and in others in the literature (13) suggest that it is not possible to be certain about the unaffected status of females. The two-point analysis was therefore repeated using unaffected males and affected females only. There is also a possible crossover within the critical region in individual II-5 in family 2. However, as this individual is 'unaffected' and the haplotypes in her affected mother have to be inferred, the data cannot be reliably used to narrow down the candidate region.

The prior evidence that the gene might be X-linked (a lack of unaffected males and a 2:1 ratio in the offspring of affected females), combined with the significant lod scores obtained in this study, makes it highly likely that the gene is localized to distal Xp. This region contains genes already implicated in known diseases such as steroid sulphatase deficiency and amelogenesis imperfecta (14).The biology of these gene products, together with the phenotypes of established human mutations, must make them extremely unlikely candidates for the *OFD1* gene.

KAL, a gene mutated in X-linked Kallmann's syndrome, is also located in this region, and encodes a secreted molecule thought to be important in signalling between cells (15). Affected males have infertility due to hypogonadotrophic hypogonadism, anosmia due to failure of development of the olfactory bulbs and variable renal agenesis. *KAL* mutations in this syndrome are mainly predicted to cause loss of function (16). The external features of Kallmann's syndrome are clearly different from those of OFD1. However, the expression patterns of KAL in human and chick development, i.e. the kidney, the limb bud and central nervous system, would be consistent with the clinical features of

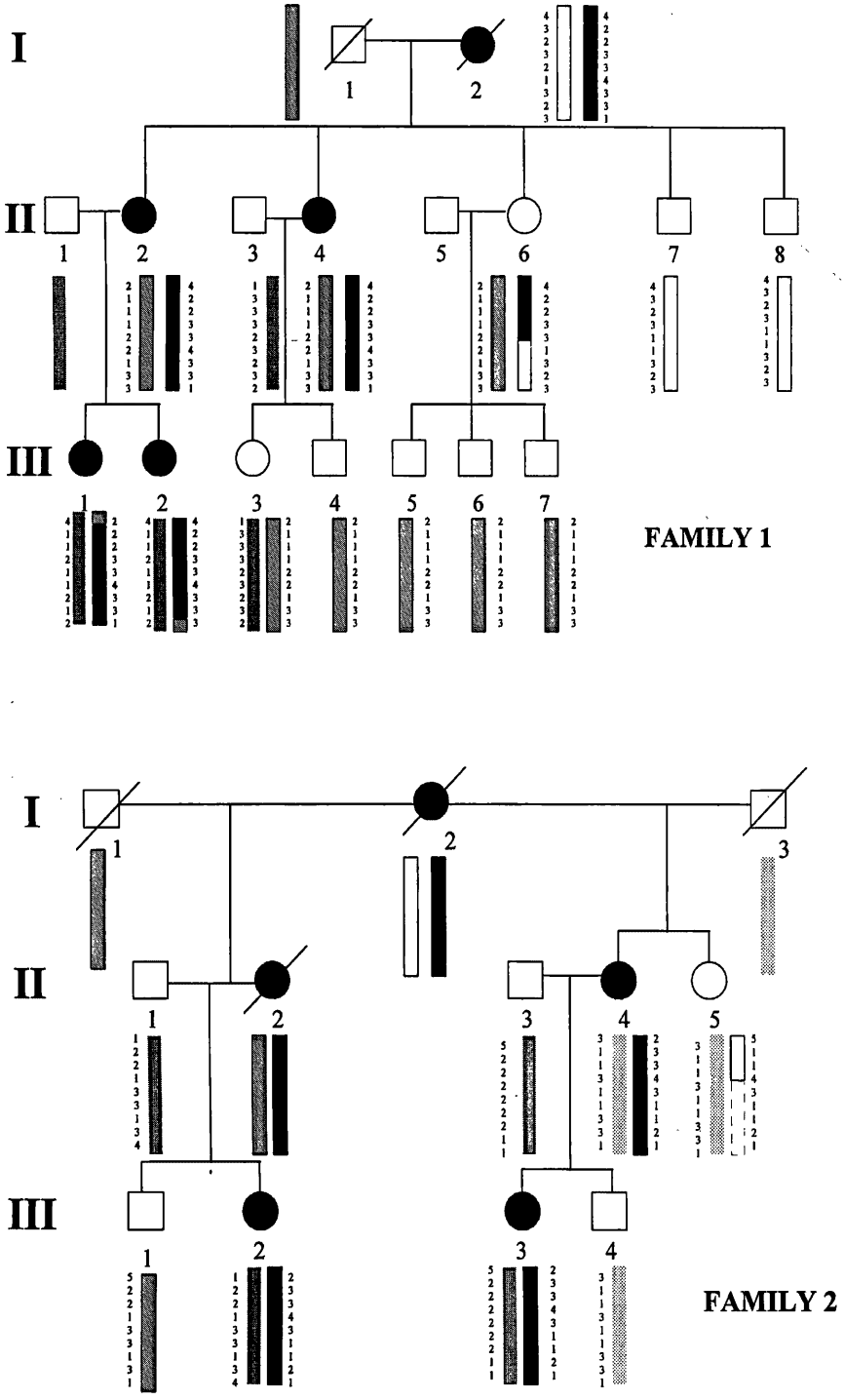

Figure 1. Family trees used in the analysis. The shaded circles represent affected individuals. The order of markers displayed is *DXS996*, *KAL*, *DXS1223*, *DXS8051*, *DXS7108*, *DXS8022*, *DXS987*, *DXS8036* and *DXS7105*. The bars indicate the most likely haplotypes. The affected haplotype is indicated by the solid black bars and the unaffected haplotype by the solid white bars. In family 1, the haplotype of I-1 is indicated by the diagonal shaded bars. In family 2, the haplotype of I-1 is indicated by diagonal shaded bars and I-3 by light grey bars. In family 2, the haplotype of II-5, which could either be affected or unaffected, is indicated by a dotted outline. In both families, additional male haplotypes that have been introduced are indicated by the dark grey bars.

OFD1 (17,18). It is conceivable that different mutations in *KAL*, causing, for example, a gain in function, might generate an OFD1 phenotype.

Genes in the critical region which are not yet implicated in human genetic diseases are the voltage-gated chloride channel 4 (*CLCN4*) (19) and *Xenopus laevis*-like apical protein (*APXL*) (20). We suggest that both of these are candidates for the OFD1 gene. CLCN4 is a voltage-gated chloride channel which is highly conserved in evolution and which is known to be expressed in skeletal muscle, brain and heart (19) and, of note, mutations in another chloride channel gene *CLCN5* cause renal diseases; X-linked recessive nephrolithiasis and hypophosphataemic rickets (21). APXL, *Xenopus laevis*-like apical protein, is implicated in amiloride-sensitive sodium channel activity (20),

which is of interest as the protein encoded by the *PKD2* gene, a gene mutated in autosomal dominant polycystic kidney disease, has homology on database searching with voltage-gated sodium and calcium channels (22). APXL is expressed in melanoma cells, brain, placenta, lung, kidney and pancreas. The *APXL* gene has been excluded as a candidate for optic atrophy which maps to this region (20). Further studies are underway to examine these and other genes for mutations in OFD1 cases.

The mouse mutant with X-linked dominant polydactyly *(Xpl)* maps to the region of the mouse X chromosome that is homologous with the region defined in this study for OFD1 (23). Urogenital malformations are known to occur in this mouse, and include hydroureter, hydronephrosis and cystic or absent kidneys (23). The renal cysts in the *Xpl* mouse deserve further examination to determine whether they are glomerulocystic, the polycystic renal disease associated with OFD1 (24), as this mutant should be considered to be a good candidate for the mouse model of OFD1.

MATERIALS AND METHODS

Family descriptions

Two families with OFD1 were used for linkage analysis. Family 1 (Fig. 1) consisted of five affected females (I-2, II-2, II-4, III-1 and III-2) all with classical features of OFD1 and also polycystic kidney disease as assessed by ultrasound scanning. There was a strong family history of miscarriage. Two cases required treatment with dialysis (I-2 and III-2). The full clinical details, radiology and renal histology of this kindred are described elsewhere (6). I-2 died of a myocardial infarction after renal transplantion, and samples of kidney tissue taken at autopsy were used as the source of DNA (see DNA studies, below). The other relatives were clinically unaffected; they had no dysmorphic features, and renal ultrasound scans in individuals II-6, II-7, II-8 and III-3 were normal. Individual II-6 (kindred 1) has had a miscarriage. Family 2 (Fig. 1) examined in this study has been described previously (5) and contains five affected females, three of whom were alive.

DNA studies

DNA was extracted from peripheral blood lymphocytes by standard techniques and from the pathological specimen by first dissolving the paraffin wax with xylene (Merck Ltd, Poole, UK) (25). DNA was amplified using the polymerase chain reaction (PCR) using primers flanking microsatellite polymorphisms. The first set of microsatellite markers which were used spanned the X chromosome at an average spacing of 10–20 cM (Research Genetics, Huntsville, USA). Additional markers for finer mapping were selected from the Genethon map (www.genethon.fr) (26). The PCR reaction mix consisted of 250 ng of genomic DNA, 50 pmol of each primer, 1.5 M Tris (pH 8.3), 1.5 mM $MgCl_2$, 50 mM KCl, 0.2 mM dGTP, dATP, dTTP and 0.02 mM dCTP, 1 µl [^{32}P]dCTP (3000 Ci/mmol)/ml of reaction mix and 1 U *Taq* polymerase [Bioline (UK) Ltd, London, UK] in a final volume of 25 µl. Conditions for thermal cycling consisted of denaturation at 94°C for 5 min, followed by 30 cycles at 94°C for 1 min, 55°C for 1 min and 72°C for 1 min, and a final extension step of 72°C for 10 min. The products were separated electrophoretically on 6% acrylamide–7 M urea denaturing gels at 65 W for 2–3 h. Dried gels were exposed to X-ray film (X-Omat, Kodak, Rochester, USA) for 12–24 h.

Linkage studies

Genotypes were recorded manually. A gene frequency of 1 in 500 000 was used with an X-linked dominant mode of inheritance. The disease was assumed to be 100% penetrant in males in view of the lethality in hemizygous males reported in the literature and the incidence of miscarriage in the kindreds used in this study. As stated in the Results, the analysis was performed with and without 'unaffected females' in view of the highly variable phenotype (13). Marker allele frequencies were obtained from the Genome Database (www.gdb.org). The genetic distances between markers were obtained from the Genethon map. Two-point and multipoint linkage analysis were performed using the MLINK and LINKMAP programme of the LINKAGE package (27).

ACKNOWLEDGEMENTS

We would like to acknowledge all the clinicians who have been involved in the care of the families, especially Dr L. Rees, Dr S. Roy and Dr M.J. Dillon, and the families for taking part in this study. S.A.F. is a Research Training Fellow supported by Action Research.

REFERENCES

1. Gorlin, R. and Psaume, J. (1962) Orodigitofacial dysostosis. A new syndrome. *J. Paediatr.*, **61**, 520–530.
2. Toriello, H.V. (1993) Oral–facial–digital syndromes, 1992. *Clin. Dysmorph.*, **2**, 95–105.
3. Salinas, C., Pai, G., Vera, C., Milutinovich, J., Hagerty, R., Cooper, J. and Cagna, D. (1991) Variability of expression of the orofaciodigital syndrome type 1 in black females: six cases. *Am. J. Med. Genet.*, **38**, 574–582.
4. Connacher, A.A., Forsyth, C.C. and Stewart, W.K. (1987) Orofaciodigital syndrome type 1 associated with polycystic kidneys and agenesis of the corpus callosum. *J. Med. Genet.*, **24**, 116–122.
5. Donnai, D., Kerzin-Storrar, L. and Harris, R. (1987) Familial orofaciodigital syndrome type 1 presenting as adult polycystic kidney disease. *J. Med. Genet.*, **24**, 84–87.
6. Feather, S.A., Winyard, P.J.D., Dodd, S. and Woolf, A.S. (1996) Oral–facial–digital syndrome type 1 is another dominant polycystic kidney disease: clinical, radiological and histopathological features of a new kindred. *Nephrol., Dial. Transplant.*, in press.
7. Doege, T., Thuline, H., Priest, J., Norby, D. and Bryant, J. (1964) Studies of a family with the oral–facial–digital syndrome. *N. Engl. J. Med.*, **271**, 1073–1080.
8. Wettke-Schafer, R. and Kantner, G. (1983) X-linked dominant inherited diseases with lethality in hemizygous males. *Hum. Genet.*, **64**,1–23.
9. Gillerot, Y., Heimann, M., Fourneau, C., Verellen-Dumoulin, C. and Van Maldergem, L. (1993) Oral–facial–digital syndrome type 1 in a newborn male. *Am. J. Med. Genet.*, **46**, 335–383.
10. Wahrman, J., Berant, M., Jacobs, J., Aviad, I. and Ben-Hur, N. (1966) The oral–facial–digital syndrome: a male lethal condition in a boy with 47XXY chromosome. *Paediatrics*, **37**, 812–821.
11. Ruess, A., Pruzansky, S., Lis, E. and Patau, K. (1962) The oral–facial–digital syndrome: a multiple congential condition of females with associated chromosomal abnormalities. *Pediatrics*, **29**, 985–994.
12. Ott, J. (1991) *Analysis of Human Genetic Linkage*, revised edn. The Johns Hopkins University Press, Baltimore and London.
13. Toriello, H. (1988) Heterogeneity and variability in the oral–facial–digital syndromes. *Am. J. Med. Genet.*, Suppl. **4**, 149–159.

14. Ferrero, G.B., Franco, B., Roth, E.J., Firulli, B.A., Borsani, G., Delmas-Mata, J., Weissenbach, J., Halley, G., Schlessinger, D., Chinault, A.C., Zoghbi, H.Y., Nelson, D.L. and Ballabio, A. (1995) An integrated physical and genetic map of a 35 Mb region on chromosome Xp22.3–Xp21.3. *Hum. Mol. Genet.*, **4**, 1821–1827.
15. Franco, B., Guioli, S., Pragliola, A., Incerti, B., Bardoni, B., Tonlorenzi, R., Carrozzo, R., Maestrini, E., Pieretti, M., Taillon-Miller, P., Brown, C.J., Willard, H.F., Lawrence, C., Persico, M.G., Camerino, G. and Ballabio, A. (1991) A gene deleted in Kallmann's syndrome shares homology with neural cell adhesion and axonal path-finding molecules. *Nature*, **353**, 529–536.
16. Quinton, R., Duke, V.M., de Zoysa, P.A., Platts, A.D., Valentine, A., Kendall, B., Pickman, S., Kirk, J.M.W., Besser, G.M., Jacobs, H.S. and Bouloux, P.M.G. (1996) The neuroradiology of Kallmann's syndrome, a genotypic and phenotypic analysis. *J. Clin. Endocrinol. Metab.*, **81**, 3010–3017.
17. Duke, V.M., Winyard, P.J.D., Thorogood, P., Soothill, P., Bouloux, P.M.G. and Woolf, A.S. (1995) *KAL*, a gene mutated in Kallman's syndrome, is expressed in the first trimester of human development. *Mol. Cell. Endocrinol.*, **110**, 73–79.
18. Legouis, R., Hardelin, J.P., Levilliers, J., Claverie, J.M., Compain, S., Wunderle, V., Millasseau, P., Le Paslier, D., Cohen, D., Caterina, D., Bouguerleret, L., Delamarre-Van de Waal, H., Lutfalla, G., Weissenbach, J. and Petit, C. (1991) The candidate gene for the X-linked Kallmann's syndrome encodes a protein related to adhesion mlecules. *Cell*, **67**, 423–435.
19. Van Slegtenhorst, M.A., Bassi, M.T., Borasni, G., Wapenaar, M.C., Ferrero, G.B., de Conciliis, L., Rugarli, E.I., Grillo, A., Franco, B., Zoghbi, H.Y. and Ballabio, A. (1994) A gene from the Xp22.3 region shares homology with voltage gated chloride channels. *Hum. Mol. Genet.*, **3**, 547–552.
20. Schiaffino, M.V., Bassi, M.T., Rugarli, E.I., Chapman, V. and Ballabio, A. (1995) Cloning of a human homologue of the *Xenopus laevis APX* gene from the ocular albinism type 1 critical region. *Hum. Mol. Genet.*, **4**, 373–382.
21. Fisher, S.E., Van Baker, I., Lloyd, S.E., Pearce, S.H.S., Thakker, R.V. and Craig, I.W. (1995) Cloning and characterisation of *CLCN5*, the human kidney chloride channel gene implicated in Dent's disease (an X-linked hereditary nephrolithiasis. *Genomics*, **29**, 598–606.
22. Mochizuki, T., Wu, G. and Hayashi, T. (1996) *PKD2*, a gene for polycystic kidney disease encodes an integral membrane protein. *Science*, **272**, 1333–1342.
23. Sweet, H.O. and Lane, P.W. (1980) X-linked polydactyly (*Xpl*), a new mutation in the mouse. *J. Hered.*, **7**, 207–209.
24. Stapleton, F.B., Bernstein, J., Koh, G., Roy, S.,III and Wilroy, R.S. (1982) Cystic kidneys in a patient with the oral–facial–digital syndrome type1. *Am. J. Kidney Dis.*, **1**, 288–293.
25. Jackson, D.P., Hayden, J.D. and Quirke, P (1993) Extraction of nucleic acid from fresh and archival material. In McPherson, M.J., Quirke, P. and Taylor, G.R. (eds), *PCR: A Practical Approach*. Oxford University Press, Oxford, pp. 29–50.
26. Dib, C., Faure, S., Fizames, C., Samson, D., Drouot, N., Vignal, A., Millasseau, P., Marc, S., Hazan, J., Seboun, E., Lathrop, M., Gyapay, G., Morissette, J. and Weissenbach,J. (1996) A comprehensive genetic map of the human genome based on 5,264 microsatellites. *Nature*, **380**, 1–129.
27. Terwilliger, J.D. and Ott, J. (1994) *Handbook of Human Genetic Linkage*. The Johns Hopkins University Press. Baltimore and London.

Human Molecular Genetics, 1998, Vol. 7, No. 2 299–305

The human *FXY* gene is located within Xp22.3: implications for evolution of the mammalian X chromosome

Jo Perry[1], Sally Feather[3], Alice Smith[1], Steve Palmer[1,+] and Alan Ashworth[1,2,*]

[1]CRC Centre for Cell and Molecular Biology and [2]Section of Gene Function and Regulation, Chester Beatty Laboratories, The Institute of Cancer Research, Fulham Road, London SW3 6JB, UK and [3]Molecular Genetics Unit, Institute of Child Health, London WC1 1EH, UK

Received October 8, 1997; Revised and Accepted November 4, 1997

DDBJ/EMBL/GenBank accession no. AF035360

It has been proposed that the pseudoautosomal region of mammals has evolved by sequential addition of autosomal material onto the X and Y chromosomes followed by movement of the pseudoautosomal boundary to create X-unique regions. We have previously described a gene, *Fxy*, that spans the pseudoautosomal boundary in mice such that the first three exons of the gene are located on the X chromosome, but the remainder of the gene is located on both X and Y chromosomes. Therefore, this gene might be in a state of transition between pseudoautosomal and X-unique locations. In support of this theory we show here that the human *FXY* gene is located in Xp22.3 in humans, proximal to the pseudoautosomal boundary.

INTRODUCTION

The sex chromosomes of eutherian mammals, although heteromorphic in both size and gene content, are thought to have evolved from a pair of homologous chromosomes (1). A small region of identity, known as the pseudoautosomal region (PAR), exists between the X and Y chromosomes (2,3) and is thought to be a remnant of these ancestral sex chromosomes. During male meiosis the X and Y chromosomes pair and recombine along their PARs, thus ensuring correct chromosomal segregation (2). One significant consequence of the sequence identity of the PAR between the X and Y chromosomes is that genes located within this part of the genome escape X inactivation in females so as to maintain the dosage of genes relative to that of XY males (2,3).

The mouse and human PARs appear to be of distinct evolutionary origin. Of a number of genes that have been mapped to the PAR in humans, those that have been mapped in the mouse are all located on autosomes (4–7). However, some of the genes located on the human X chromosome proximal to the pseudoautosomal boundary are located near or within the PAR in mice. The *Steroid Sulphatase* gene (*Sts*) is located within the PAR in mice and has been shown to escape X chromosome inactivation in females (8). However, the human *STS* gene is located just proximal of the human pseudoautosomal boundary in Xp22.3 (9). The escape from X inactivation of the human *STS* gene and the presence of *STS*-related sequences on the Y chromosome are thought to be remnants of its previous PAR location (9). The human enamel protein gene *Amelogenin* (*AMELX*), located in Xp22.3 proximal to *STS* (10), also has related sequences present on the Y chromosome. In mice linkage between *Amelogenin*, which is X-unique in mice, and *Sts* has been preserved, although some other rearrangements have occurred (11–13).

The gene content of mammalian X chromosomes is highly conserved, as predicted by Ohno (1). However, the order of these genes with respect to each other has changed dramatically between species. This conservation of the X chromosome is also found, to a certain extent, in metatherian and prototherian mammals. The marsupial and much of the monotreme X chromosomes are thought to be equivalent to the long arm of the human X chromosome, Xq, and thus the marsupial X chromosome may represent an ancestral X chromosome (14,15). However, genes located on the short arm, Xp, of the human X chromosome are located in two autosomal clusters in both monotremes and marsupials, suggesting that human Xp, including the PAR, was originally autosomal and is a relatively recent addition to the eutherian X chromosome (14).

The 'addition–attrition' theory (16) proposes that divergence of the mammalian X and Y chromosomes has occurred through cyclical addition of autosomal segments onto the PAR of either the X or Y chromosome. The autosomal addition is then recombined onto its partner, resulting in an enlarged PAR. Meanwhile the male-determining Y chromosome undergoes a series of rearrangements and deletions, reducing its homology with the X chromosome and gradually decreasing the size of the PAR as genes within this region lose their homologous Y chromosome partner and become X-unique (16). The change in location of the *STS* gene from its presumed original pseudoautosomal location to Xp22, proximal to the PAR, in humans has been presented as evidence for the addition–attrition theory. Recently we have identified a novel gene, *Fxy* (finger on X and Y), which spans the mouse pseudoautosomal boundary on the X chromosome (17). The first three exons of the gene are located on the X chromosome, whereas the 3′ exons of the gene are located on both the X and Y chromosomes. We proposed that the gene is at an

*To whom correspondence should be addressed. Tel: +44 171 352 8133; Fax: +44 171 352 3299; Email: alana@icr.ac.uk
+Present address: The Walter and Eliza Hall Institute of Medical Research, Post Office, Royal Melbourne Hospital, Melbourne, Victoria 3050, Australia

intermediate stage in evolving from a pseudoautosomal location to one that is X-unique. Here we demonstrate that the human *FXY* gene is located within Xp22.3, proximal to the human pseudoautosomal boundary. This finding provides further evidence for the addition–attrition theory and we discuss the implications for evolution of the eutherian X chromosome and PAR.

RESULTS

Cloning of human *FXY* cDNA

PCR primers derived from mouse *Fxy* exon 3 were used to amplify a 90 bp fragment from human genomic DNA. Sequence analysis confirmed high sequence similarity to the mouse *Fxy* gene. This 90 bp fragment was used to screen a human full-term placenta cDNA library in pCDM8 by colony hybridization. One positive clone was isolated, sequenced and found to contain nt 747–1100 of the human *FXY* cDNA sequence. Simultaneously, database searching using the mouse *Fxy* sequence revealed a number of overlapping ESTs in the GenBank expressed sequence database (dbEST) covering the 3′ coding region and 3′-untranslated region (UTR) of the human *FXY* gene (Unigene accession no. WI-12892). The 5′ coding portion of human *FXY* was obtained by PCR using a combination of mouse and human *FXY* primers on cDNA synthesized from human placental RNA. Finally, the 5′-UTR was obtained using a modified 5′-RACE procedure.

FXY is a member of the RING finger gene family

The compiled *FXY* cDNA contig consisted of 3334 bp and included an open reading frame of 2001 bp. An in-frame termination codon present 51 bp upsteam of the potential initiating methionine suggested that we had cloned the entire coding potential of the *FXY* gene (GenBank accession no. AF035360). The human *FXY* cDNA encodes a 667 amino acid protein which shows very high (95%) identity to the protein encoded by the mouse *Fxy* gene (Fig. 1a).

FXY is a member of the rapidly growing family of RING finger genes which are characterized by the presence of an N-terminal C_3HC_4 zinc binding domain (18; Fig. 1b). *FXY* also contains four additional domains; two potential zinc binding B box domains and a leucine coiled coil domain characteristic of a subgroup of this family, the 'RING–B box–coiled coil' (RBCC) subgroup (19), as well as a C-terminal domain conserved in several proteins (Fig. 1b). FXY contains two types of B box motif; the first (a B1 box) is thought to be related to the B box motif through a common ancestor (19) and the second is a typical B box binding domain seen in the majority of the members of the RBCC subgroup. Overall, FXY is most similar to nuclear phosphoprotein xnf7 from *Xenopus laevis* (20) and a human estrogen-responsive finger protein, EFP (21).

Genomic structure of the *FXY* gene

To investigate the genomic organization of *FXY* we screened a human X chromosome Charon 35 phage library with PCR primers derived from the *FXY* cDNA sequence. The *FXY* gene consists of 10 exons, with the first intron located in the 5′-UTR and the potential translation initiating methionine codon located within exon 2 (Fig. 2). The largest exon of the gene, exon 2, encodes one third of the FXY protein and also contains the RING, B1 and B box domains. The coiled coil domain is located in exons 3 and 4 and the C-terminal domain is encoded by exons 9 and 10. Not all of the splice junctions in the mouse gene have been isolated but all of those that have are conserved between the human and the mouse gene. Long range PCR with human genomic DNA as template was used to estimate the size of the introns of the *FXY* gene. These results indicated that the *FXY* gene spans at least 80 kb.

Comparison of the DNA sequences of human and mouse *FXY* cDNA shows that the genes are highly conserved. However, if the sequence identity in the coding region is plotted exon by exon it is clear that the 5′ exons are, in general, more conserved than the 3′ exons (Fig. 2b). This might reflect a more stringent requirement for conservation of particular amino acids in the N-terminus of the encoded protein. Alternatively, this might be due to the pseudoautosomal location of the 3′-region of the *Fxy* gene. Exons IV–X of the mouse gene are located in the PAR and other genes in this region are known to evolve rapidly (22).

Expression of the *FXY* gene

We used hybridization analysis and RT-PCR to investigate the expression pattern of the human *FXY* gene. A fragment of the 5′-end of *FXY* cDNA encompassing exons 2–4 was hybridized to a northern blot containing poly(A)$^+$ RNAs isolated from human adult tissues. A major RNA species of 7.4 kb and two minor RNAs of 4.3 and 2.6 kb were detected in all the tissues analysed (Fig. 3). The *FXY* cDNA contig that we characterized was 3334 bp in length. The multiple transcripts that we observed might be the result of alternative splicing or might arise through the use of alternative polyadenylation sites. However, the presence of an in-frame termination codon upstream of the potential initiating methionine and the similarity to the mouse *Fxy* gene strongly suggests that we have isolated the entire coding region of the gene. RT-PCR analysis was used to examine expression of the *FXY* gene during human foetal development. *FXY* was found to be expressed in several tissues of 8 and 9 week human foetuses (data not shown). Although this analysis is non-quantitative, it demonstrates that *FXY* is widely expressed.

FXY maps to Xp22.3

Southern blot hybridization analysis of male and female human genomic DNA demonstrated that *FXY* was probably X linked; this was suggested by a comparison of the signal obtained from DNA derived from the two sexes (Fig. 4). We have found no evidence of male-specific fragments, suggesting that *FXY*-related sequences are not present on the human Y chromosome.

To locate the human *FXY* gene more precisely in the genome, PCR primers derived from exon 2 were used to screen the Genebridge 4 radiation hybrid mapping panel. This consists of 93 cell lines segregating fragments of human chromosomes on a rodent cell background (23). Analysis of these data indicated that *FXY* mapped within 6.4 cR (1 cR = 250 kb; 24) of the marker *DXS1223* on the short arm of the X chromosome within Xp22.3. These data were confirmed by mapping of an EST present in the Unigene database encompassing the 3′-end of *FXY*. This EST also mapped to Xp22.3, in agreement with our radiation hybrid data. We have also placed *FXY* on two YAC contigs which span the region, the CEPH-Genethon integrated YAC contig (25) and a 35 Mb YAC contig that spans Xp22.3–Xp21.3 (26). PCR with primers specific for *FXY* on YAC DNAs from these contigs mapped the gene to a number of YACs from both contigs (Fig. 5).

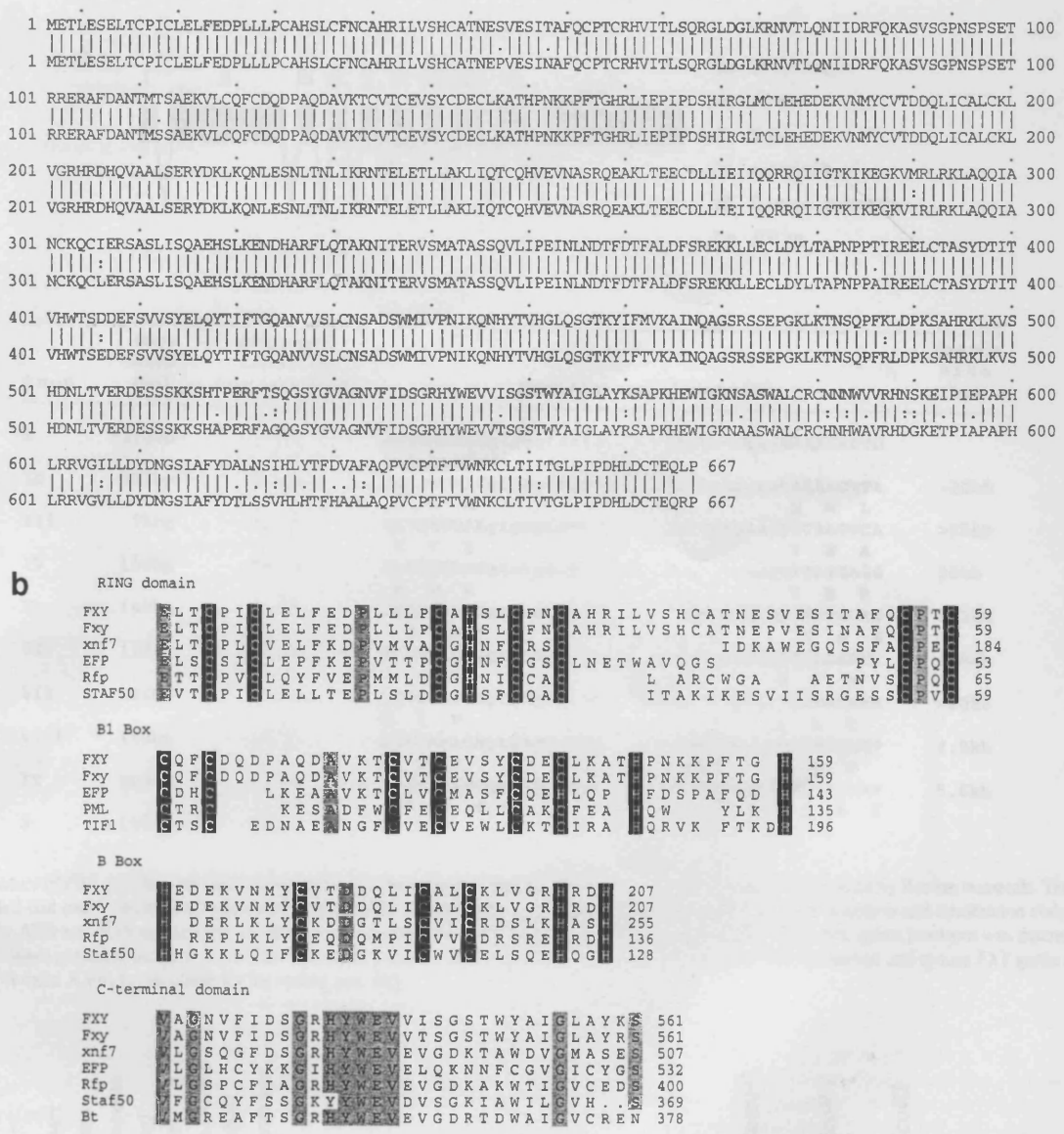

Figure 1. Amino acid sequence of the human FXY protein. (**a**) Comparison of human and mouse FXY proteins. The human FXY sequence (top) is aligned with the mouse Fxy protein (bottom). Sequences were aligned using the BESTFIT program of the GCG suite of programs (Daresbury Computing Group). Similarities between amino acids as determined by the scoring matrix in the program are illustrated as follows. |, identical amino acids; :, non-identical amino acid pairs having matrix scores >0.5; ., non-identical amino acids having a positive score <0.5. (**b**) Alignment of FXY with other members of the RBCC family. Residues important for zinc binding in the RING, B1 and B box domains are boxed in black. Other identical residues are boxed in grey. Sequences were aligned using the PILEUP and PRETTYBOX programs of the GCG suite of programs (Daresbury Computing Group). The following proteins are shown: Fxy (17); xnf7 (20); EFP (21); Rfp (35); Staf50 (36); TIF1 (37); Bt (29).

Comparison of markers known to be present on these YACs allowed us to delimit the position of *FXY* to a location between the *STS* markers *DXS7108* and *DXS6848*. The gene is flanked by two previously characterized genes, *AMELX* and *CLCN4* (10,27).

DISCUSSION

The PAR has unique properties in mammalian genomes due to its function in ensuring proper pairing and segregation of the sex chromosomes at meiosis (2,3). This function is complicated by the location of genes within the PAR. These genes are present in two identical expressed copies in males and in females are found to escape X chromosome inactivation. Whether this is a property of the genes themselves or a property of the PAR globally is not known. The PAR appears to be organized very differently in the two species, humans and mice, in which it has been characterized: no gene has been identified which is pseudoautosomal in both species. Despite this, a region proximal to the pseudoautosomal boundary in humans, Xp22.3, shows evidence of a pseudoautosomal location at some time in the past. Here we have characterized a human gene, *FXY*, that is located in Xp22.3, while in the mouse this gene spans the pseudoautosomal boundary (17).

The human *FXY* gene encodes a 667 amino acid protein which contains several regions of sequence similarity to previously characterized RING finger proteins (Fig. 1b). This is seen not only over the RING domains of these proteins but also within

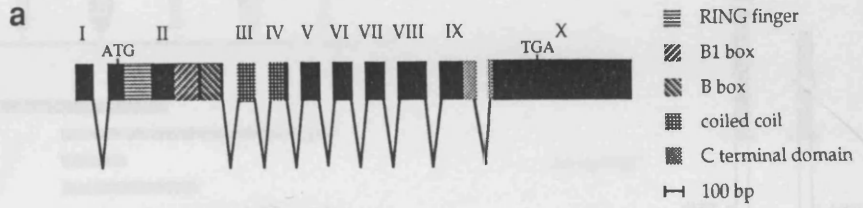

b

Exon	Exon size (bp)	Sequence Identity (mouse/human)	Exon/intron junctions	Intron size (bp)
I	~190bp		AGTCCATTGgtgggtattc.....ttgtttccagGAAACACTG	
II	717bp	93.5%	AAATTGAAGgttagtccga.....ttttgaacagCAAAACTTA K L K Q N L	>20kb
III	96bp	93.7%	CATGTTGAAgtgagtatct.....tatcctgtagGTCAATGCA H V E V N A	>20kb
IV	108bp	89.7%	GAAGGGAAGgtatgatttc.....ttgtttcaagGTGATGAGG E G K V M R	20kb
V	149bp	85.8%	CACCGAGAGgtgaatgcag.....tgcattacagAGTCTCCAT T E R V S M	8.2kb
VI	128bp	93.7%	ACCTTACAGgtattgtctt.....acccccacagCTCCCAACC Y L T A P N	4.8kb
VII	144bp	90.1%	ACGTCGTTAgtgagtatct.....ggctttgcagGTCTGTGTA N V V S L C	>20kb
VIII	162bp	88.9%	AGACAAACAgtaagtgctg.....ttgttttcagGCCAACCAT K T N S Q P	4.8kb
IX	208bp	80.7%	AAGCACATGgtaagcaact.....gtttccgcagGTATGCCAT S T W Y A I	5.6kb
X	>1592bp	80.9%		

Figure 2. Gene structure of *FXY*. (**a**) Diagrammatic representation of the exon structure of *FXY*. *FXY* consists of 10 exons designated by Roman numerals. The RING, B1 box, B box, coiled coil and C-terminal domains are represented by shaded boxes and described in the key. The putative initiation and termination codon of the gene are indicated by ATG and TGA respectively. (**b**) Intron/exon structure of *FXY*. The position and sequence of the exon/intron splice junctions was determined by analysing genomic clones spanning the gene. Exons are indicated by Roman numerals. The percentage identity between the human and mouse *FXY* genes for each exon is indicated. For exon X this is calculated for the coding part only.

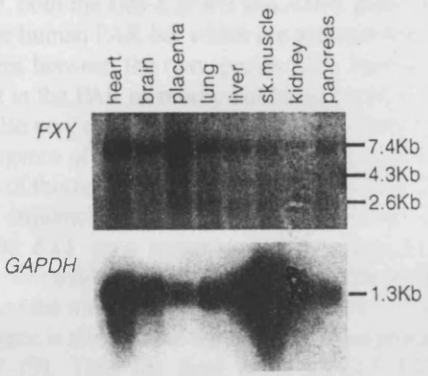

Figure 3. Expression of *FXY* in adult and fetal tissues. Northern analysis of *FXY* expression. A multiple tissue northern blot hybridized with (i) a 5′ fragment of the *FXY* cDNA and (ii) a *GAPDH* control as described in Materials and Methods. The transcript sizes are estimated from markers.

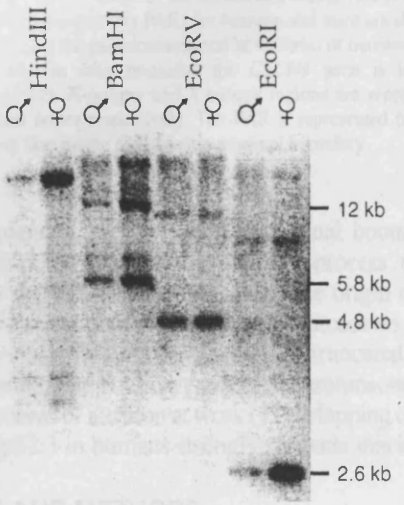

Figure 4. *FXY* is X-linked in humans. Southern hybridization of male and female human genomic DNA digested with restriction enzymes and hybridized with an 800 bp fragment of the *FXY* cDNA. The hybridization intensity ratio of 2:1 between female and male DNA suggests X linkage of *FXY* in humans. Reprobing of the blot with a probe derived from an autosomal gene confirmed that equal amounts of DNA were loaded.

other domains that are common to this family. RBCC domains have recently been shown to be involved in protein–protein interactions through the coiled coil domain, with the B box domain also being necessary for this interaction (28). There is also evidence that the RING finger and B box domains may be involved in subcellular compartmentalization (28). The RBCC domains of mouse and human *FXY* are completely conserved, suggesting a crucial role for these domains in the function of *FXY*.

An additional C-terminal domain common to some of the RING finger family is also present in *FXY*, but little is known about its

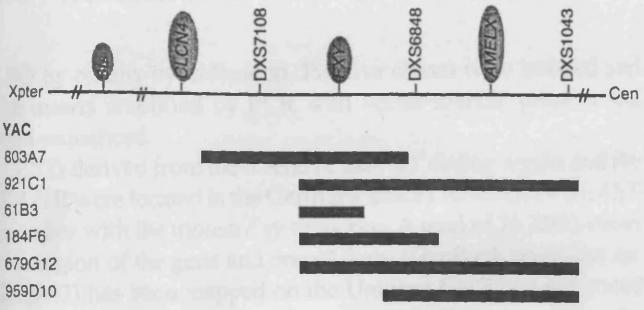

Figure 5. *FXY* maps to Xp22.3. Schematic representation of the position of *FXY* and other markers on the human X chromosome and the location of various YACs used in the mapping of *FXY*. Grey boxes represent YACs from the CEPH YAC and mega-YAC libraries. Genes from the surrounding region (within grey ovals) and other markers are indicated.

function. This domain is also present in the Butyrophilin protein, a milk fat globule membrane protein, although this protein does not contain any of the other RING finger domains (29). The C-terminal domain also appears to be almost completely conserved between the mouse and the human proteins. Despite the presence in FXY of these multiple domains it is difficult to assign a function to the protein, as members of the RING finger family of proteins have such diverse cellular roles.

FXY shows very high sequence similarity to the mouse *Fxy* gene at both the DNA and protein levels, suggesting that both have similar roles *in vivo*. Although overall highly conserved, the 3′-part of the gene appears to be less highly conserved that the 5′-part (Fig. 2b). This may correspond to a greater level of divergence of the part of the mouse gene (exons IV–X) present in the PAR. Several lines of evidence suggest a much higher rate of divergence of genes that are present in the PAR than genes that are present in the unique part of the X chromsome or on autosomes. For example, both the *GM-CSFRα* and *Il3Rα* genes, which are present in the human PAR but which are autosomal in mice, are very divergent between the two species (22). Similarly, the *Sts* gene present in the PAR of mouse but located within Xp22.3 of humans, is also very divergent (8). Thus it seems possible that the greater divergence of the 3′-part of the mouse *Fxy* gene is due to the presence of this region of the gene within the PAR. This could be tested by sequencing *FXY* from other mammalian species.

The human *FXY* gene maps to Xp22.3, distal to *AMELX*, providing further evidence for a conservation between this region in humans and the mouse distal X chromosome (13; Fig. 6). The human *STS* gene is also located within Xp22.3 just proximal to the human PAR (9). Thus the gene order *AMELX–FXY–STS* is conserved between humans and mice. A gene encoding a chloride channel, *CLCN4*, is located distal to *FXY* in humans (27) and this gene is absent from the X chromosome in laboratory mice, being located on chromosome 7 (11,12; Fig. 6). However, the *CLCN4* gene is located on the X chromosome in *Mus spretus*, suggesting that the ancestral gene order was probably *AMELX–FXY–CLCN4–STS* and that this cluster of genes might have been pseudoautosomal at some time.

It has been suggested that the PAR in mammals is evolving by the addition of autosomal segments to the PAR together with progressive loss of material from the Y chromosome PAR (16). In this 'addition–attrition' hypothesis the site of attrition is the point at which the homologous PAR diverges into X- and

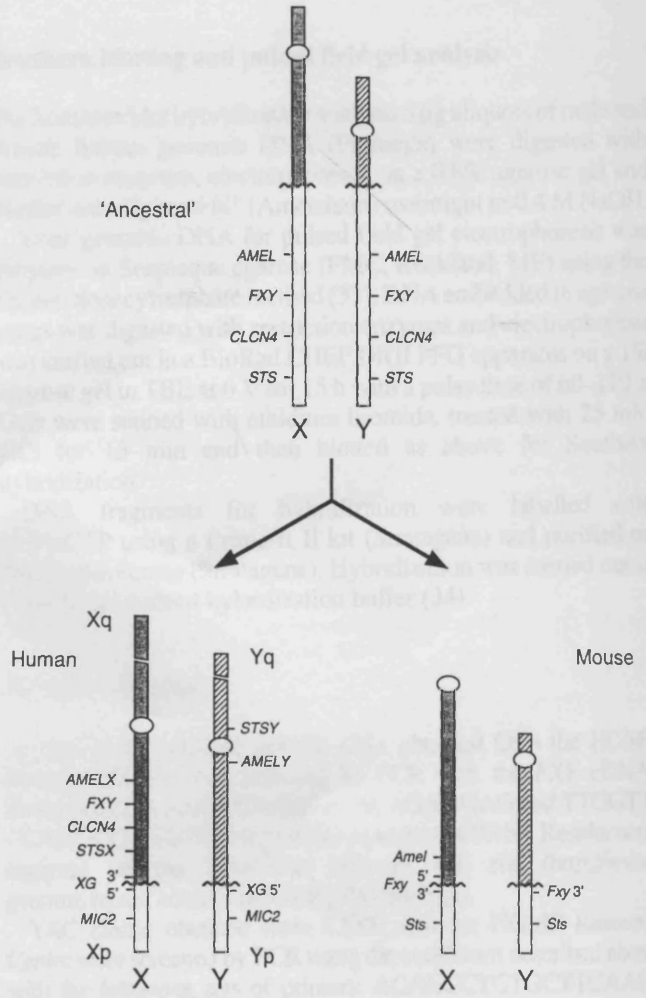

Figure 6. Model for the evolution of the human and mouse PARs. A possible ancestral PAR and the present day PARs for humans and mice are shown. The *XG* and *Fxy* genes span the pseudoautosomal boundaries of humans and mice respectively (17,38). In *Mus musculus* the *CLCN4* gene is located on chromosome 7 (11,12). X-unique and Y-unique regions are represented by shaded and hatched boxes respectively. The PAR is represented by an open white box. A wavy line marks the pseudoautosomal boundary.

Y-specific sequences, i.e. the pseudoautosomal boundary. The action of attrition is part of the ongoing process that, it is suggested, has degraded the Y PAR since the origin of the sex chromosomes from a pair of homologous autosomes (16). We suggested previously that the presence of the truncated *Fxy* gene at the pseudoautosomal boundary on the Y chromosome of mice revealed the process of attrition at work (17). Mapping of the *FXY* gene within Xp22.3 in humans strongly supports this idea.

MATERIALS AND METHODS

Cloning of human *FXY* cDNA and genomic DNA

Primers derived from mouse *Fxy* exon 3 (CAACATGTTGACA AGTTTGG and ACTTGGAGAGTAATCTCACC) were used to amplify a 90 bp fragment from human genomic DNA using PCR conditions of 30 cycles of: 94°C, 30 s; 52°C, 30 s; 72°C, 1 min. This fragment was used to screen a human full-term placenta cDNA library in pCDM8 (HGMP Resource Centre, Hinxton,

UK) by colony hybridization. Positive clones were isolated and the inserts amplified by PCR with vector-specific primers and then sequenced.

ESTs derived from the 3′-end of the *FXY* coding region and the 3′-UTR were located in the GenBank dbEST database by BLAST searches with the mouse *Fxy* sequence. A total of 23 ESTs cover this region of the gene and one of these (GenBank accession no. Z40343) has been mapped on the Unigene-Genethon integrated map of the human X chromosome (Unigene web site: http://www.ncbi.nlm.nih.gov/Unigene/index.html, accession no. WI-12892). Most of the remaining coding cDNA was obtained by PCR on human placenta cDNA with the following primers: the mouse *Fxy* primer GAAACACTGGAGTCGGAGCT and the human *FXY* primer TTGGTTCCAATAATCTGTCG amplify the 5′-portion of the gene from the initiation codon to exon 4; AAGCCAAATTGACAGAGGAG and CCTGAACCTTACTG-TTCCCC amplify nt 862–2138 of the human cDNA. The 5′-UTR of the cDNA was isolated using a modified 5′-RACE procedure based on the template switching capacity of reverse transcriptase (A.Ashworth, unpublished results).

A human X chromosome λ Charon 35 phage library (ATCC) was screened by hybridization with probes derived from each of the 10 exons. Intron/exon boundaries were amplified either by long range PCR (Boehringer Expand Long Template PCR kit) using vector- and exon-specific primers or by subcloning λ DNA digested with various restriction enzymes into pBluescript.

Automated DNA sequencing was performed by cycle sequencing with Applied Biosystems Taq FS containing Dye Terminators and analysed on an Applied Biosystems 377 sequencer.

Expression analysis

A human multiple tissue northern blot (Clontech) was hybridized according to the manufacturer's instructions with an 800 bp cDNA fragment spanning exons 2–4, produced by PCR with the primers ACAGCCTCTGCTTCAACTGC and TTGGTTCCAATAATC-TGTCG corresponding to nt 166–935 of the human cDNA sequence. After removal of this probe the northern blot was rehybridized with a 1 kb fragment of *Gapdh* cDNA (30) as a loading control.

Human tissues were provided by the Institute of Child Health from embryonic and foetal collections made under local research ethical committee permission. Three normal foetuses were collected from chemically induced and surgically induced terminations performed at 8–9 weeks after fertilization as described (31). The stage of gestation was determined by standard criteria based on examination of external morphology (32). Total RNA was extracted from freshly dissected human foetal tissues using TRI Reagent (Molecular Research Centre Inc.) and used to synthesize cDNA with M-MLV reverse transcription enzyme (Gibco) according to the manufacturer's instructions. To investigate expression of *FXY* RT-PCR, with the same primers used to produce the 800 bp fragment described above, was used to amplify *FXY* from human foetal cDNA with 30 cycles of the following PCR conditions: 94°C, 1 min; 52°C, 1 min; 72°C, 1 min.

Southern blotting and pulsed field gel analysis

For Southern blot hybridization analysis 5 μg aliquots of male and female human genomic DNA (Promega) were digested with restriction enzymes, electrophoresed on a 0.8% agarose gel and blotted onto Hybond N^+ (Amersham) overnight in 0.4 M NaOH.

Yeast genomic DNA for pulsed field gel electrophoresis was prepared in Seaplaque agarose (FMC, Rockland, ME) using the lithium dodecylsulphate method (33). DNA embedded in agarose plugs was digested with restriction enzymes and electrophoresis was carried out in a BioRad CHEF DRII PFG apparatus on a 1% agarose gel in TBE at 6 V for 15 h with a pulse time of 60–120 s. Gels were stained with ethidium bromide, treated with 25 mM HCl for 15 min and then blotted as above for Southern hybridization.

DNA fragments for hybridization were labelled with [^{32}P]dCTP using a Prime-It II kit (Stratagene) and purified on NucTrap columns (Stratagene). Hybridization was carried out in Church and Gilbert hybridization buffer (34).

Physical mapping

A panel of 93 radiation hybrids (23), obtained from the HGMP Resource Centre, was screened by PCR with the *FXY* cDNA-derived primers AAGCCAAATTGACAGAGGAG and TTGGTT-CCAATAATCTGTCG to produce a product of 73 bp. Results were analysed on the Whitehead Institute web site (http://www.genome.wi.mit.edu/cgi-bin/contig/rhmapper.pl).

YAC clones obtained from CEPH and the HGMP Resource Centre were screened by PCR using the conditions described above with the following sets of primers: ACAGCCTCTGCTTCAAC-TGC and TCACTCAAAGCTGCCACCTG derived from exon 2; AAGCCAAATTGACAGAGGAG and TTGGTTCCAATAATC-TGTCG derived from exon 4; ATTTGGACTGCACAGAGCAG and CCTGAACCTTACTGTTCCCC derived from exon 10.

REFERENCES

1. Ohno, S. (1967) *Sex Chromosomes and Sex-Linked Genes*. Springer-Verlag, Berlin.
2. Burgoyne, P.S. (1982) Genetic homology and crossing over in the X and Y chromosomes of mammals. *Hum. Genet.*, **61**, 85–90.
3. Ellis, N. and Goodfellow, P.N. (1989) The mammalian pseudoautosomal region. *Trends Genet.*, **5**, 406–410.
4. Disteche, C.M., Brannan, C.I., Larsen, A., Adler, D.A., Schorderet, D.F., Gearing, D., Copeland, N.G., Jenkins, N.A. and Park, L.S. (1992) The human pseudoautosomal GM-CSF receptor alpha subunit gene is autosomal in mouse. *Nature Genet.*, **1**, 333–336.
5. Miyajima, I., Levitt, L., Hara, T., Bedell, M.A., Copeland, N.G., Jenkins, N.A. and Miyajima, A. (1995) The murine interleukin-3 receptor alpha subunit gene: chromosomal localization, genomic structure, and promoter function. *Blood*, **85**, 1246–1253.
6. Rao, E., Weiss, B., Fukami, M., Rump, A., Niesler, B., Mertz, A., Muroya, K., Binder, G., Kirsch, S., Winkelmann, M., Nordsiek, G., Heinrich, U., Breuning, M.H., Ranke, M.B., Rosenthal, A., Ogata, T. and Rappold, G.A. (1997) Pseudoautosomal deletions encompassing a novel homeobox gene cause growth failure in idiopathic short stature and Turner syndrome. *Nature Genet.*, **16**, 54–63.
7. Ellison, J.W., Wardak, Z., Young, M.F., Robey, P.G., Laig-Webster, M. and Chiong, W. (1997) PHOG, a candidate gene for involvement in the short stature of Turner syndrome. *Hum. Mol. Genet.*, **6**, 1341–1347.
8. Salido, E.C., Li, X.M., Yen, P.H., Martin, N., Mohandas, T.K. and Shapiro, L.J. (1996) Cloning and expression of the mouse pseudoautosomal steroid sulphatase gene (Sts). *Nature Genet.*, **13**, 83–86.

9. Yen, P.H., Allen, E., Marsh, B., Mohandas, T., Wang, N., Taggart, R.T. and Shapiro, L.J. (1987) Cloning and expression of steroid sulfatase cDNA and the frequent occurrence of deletions in STS deficiency: implications for X–Y interchange. *Cell*, **49**, 443–454.
10. Salido, E.C., Yen, P.H., Koprivnikar, K., Yu, L.C. and Shapiro, L.J. (1992) The human enamel protein gene amelogenin is expressed from both the X and the Y chromosomes. *Am. J. Hum. Genet.*, **50**, 303–316.
11. Palmer, S., Perry, J. and Ashworth, A. (1995) A contravention of Ohno's law in mice. *Nature Genet.*, **10**, 472–476.
12. Rugarli, E.I., Adler, D.A., Borsani, G., Tsuchiya, K., Franco, B., Hauge, X., Disteche, C., Chapman, V. and Ballabio, A. (1995) Different chromosomal localization of the *Clcn4* gene in *Mus spretus* and C57BL/6J mice. *Nature Genet.*, **10**, 466–471.
13. Dinulos, M.B., Bassi, M.T., Rugarli, E.I., Chapman, V., Ballabio, A. and Disteche, C.M. (1996) A new region of conservation is defined between human and mouse X chromosomes. *Genomics*, **35**, 244–247.
14. Graves, J.A. and Watson, J.M. (1991) Mammalian sex chromosomes: evolution of organization and function. *Chromosoma*, **101**, 63–68.
15. Graves, J.A.M., Cooper, D.W., McKenzie, L.M., Hope, R.M. and Watson, J.M. (1993) Genetic maps of marsupial and monotreme mammals. In O'Brien, S.J. (ed.), *Genetic Maps. Locus Maps of Complex Genomes*. Cold Spring Harbor Laboratory Press, Cold Spring Harbor, NY, pp. 282–289.
16. Graves, J.A. (1995) The origin and function of the mammalian Y chromosome and Y-borne genes—an evolving understanding. *BioEssays*, **17**, 311–320.
17. Palmer, S., Perry, J., Kipling, D. and Ashworth, A. (1997) A gene spans the pseudoautosomal boundary in mice. *Proc. Natl Acad. Sci. USA*, **94**, 12030–12035.
18. Saurin, A.J., Borden, K.L., Boddy, M.N. and Freemont, P.S. (1996) Does this have a familiar RING? *Trends Biochem. Sci.*, **21**, 208–214.
19. Reddy, B.A., Etkin, L.D. and Freemont, P.S. (1992) A novel zinc finger coiled-coil domain in a family of nuclear proteins. *Trends Biochem. Sci.*, **17**, 344–345.
20. Reddy, B.A., Kloc, M. and Etkin, L. (1991) The cloning and characterization of a maternally expressed novel zinc finger nuclear phosphoprotein (xnf7) in *Xenopus laevis*. *Dev. Biol.*, **148**, 107–116.
21. Inoue, S., Orimo, A., Hosoi, T., Kondo, S., Toyoshima, H., Kondo, T., Ikegami, A., Ouchi, Y., Orimo, H. and Muramatsu, M. (1993) Genomic binding-site cloning reveals an estrogen-responsive gene that encodes a RING finger protein. *Proc. Natl Acad. Sci. USA*, **90**, 11117–11121.
22. Ellison, J.W., Li, X., Francke, U. and Shapiro, L.J. (1996) Rapid evolution of human pseudoautosomal genes and their mouse homologs. *Mammalian Genome*, **7**, 25–30.
23. Gyapay, G., Schmitt, K., Fizames, C., Jones, H., Vega-Czarny, N., Spillett, D., Muselet, D., Prud'Homme, J.F., Dib, C., Auffray, C., Morissette, J., Weissenbach, J. and Goodfellow, P.N. (1996) A radiation hybrid map of the human genome. *Hum. Mol. Genet.*, **5**, 339–346.
24. Hudson, T.J. *et al.* (1995) An STS-based map of the human genome. *Science*, **270**, 1945–1954.
25. Gyapay, G., Morissette, J., Vignal, A., Dib, C., Fizames, C., Millasseau, P., Marc, S., Bernardi, G., Lathrop, M. and Weissenbach, J. (1994) The 1993–94 Genethon human genetic linkage map. *Nature Genet.*, **7**, 246–339.
26. Ferrero, G.B. *et al.* (1995) An integrated physical and genetic map of a 35 Mb region on chromosome Xp22.3–Xp21.3. *Hum. Mol. Genet.*, **4**, 1821–1827.
27. van Slegtenhorst, M.A. *et al.* (1994) A gene from the Xp22.3 region shares homology with voltage-gated chloride channels. *Hum. Mol. Genet.*, **3**, 547–552.
28. Cao, T., Borden, K.L., Freemont, P.S. and Etkin, L.D. (1997) Involvement of the rfp tripartite motif in protein–protein interactions and subcellular distribution. *J. Cell Sci.*, **110**, 1563–1571.
29. Jack, L.J. and Mather, I.H. (1990) Cloning and analysis of cDNA encoding bovine butyrophilin, an apical glycoprotein expressed in mammary tissue and secreted in association with the milk-fat globule membrane during lactation. *J. Biol. Chem.*, **265**, 14481–14486.
30. Sabath, D.E., Broome, H.E. and Prystowsky, M.B. (1990) Glyceraldehyde-3-phosphate dehydrogenase mRNA is a major interleukin 2-induced transcript in a cloned T-helper lymphocyte. *Gene*, **91**, 185–191.
31. Duke, V.M., Winyard, P.J., Thorogood, P., Soothill, P., Bouloux, P.M. and Woolf, A.S. (1995) KAL, a gene mutated in Kallmann's syndrome, is expressed in the first trimester of human development. *Mol. Cell. Endocrinol.*, **110**, 73–79.
32. Larsen, W.J. (1993) *Development of the Urogenital System*. Churchill Livingstone, Edinburgh, UK, pp. 235–279.
33. Anand, R., Ogilvie, D.J., Butler, R., Riley, J.H., Finniear, R.S., Powell, S.J., Smith, J.C. and Markham, A.F. (1991) A yeast artificial chromosome contig encompassing the cystic fibrosis locus. *Genomics*, **9**, 124–130.
34. Church, G.M. and Gilbert, W. (1984) Genomic sequencing. *Proc. Natl Acad. Sci. USA*, **81**, 1991–1995.
35. Takahashi, M. and Cooper, G.M. (1987) *ret* transforming gene encodes a fusion protein homologous to tyrosine kinases. *Mol. Cell. Biol.*, **7**, 1378–1385.
36. Tissot, C. and Mechti, N. (1995) Molecular cloning of a new interferon-induced factor that represses human immunodeficiency virus type I long terminal repeat expression. *J. Biol. Chem.*, **270**, 14891–14898.
37. LeDouarin, B., Zechel, C., Garnier, J.M., Lutz, Y., Tora, L., Pierrat, P., Heery, D., Gronemeyer, H., Chambon, P. and Losson, R. (1995) The N-terminal part of TIF1, a putative mediator of the ligand-dependent activation function (AF-2) of nuclear receptors, is fused to B-raf in the oncogenic protein T18. *EMBO J.*, **14**, 2020–2033.
38. Ellis, N.A., Ye, T.Z., Patton, S., German, J., Goodfellow, P.N. and Weller, P. (1994) Cloning of PDBX, a MIC2-related gene that spans the pseudoautosomal boundary on chromosome Xp. *Nature Genet.* **6**, 394–400.

Vesicoureteric reflux: all in the genes?

Report of a meeting of physicians at the Hospital for Sick Children, Great Ormond Street, London

Vesicoureteric reflux (retrograde passage of urine from the bladder into the ureter) can be secondary to bladder outlet obstruction or to a neuropathic bladder. However, most occurrences are due to a primary anatomical defect in the junction of the ureter and the bladder. Primary vesicoureteric reflux is usually found during investigation of urinary tract infection in children, but screening shows that it is present in 1–2% of symptom-free children. Moreover, it is often inherited in an autosomal dominant manner, making it one of the commonest of inherited disorders. Mutations of a transcription factor gene which controls prenatal development of the kidney and urinary tract have been found in a rare syndrome which includes vesicoureteric reflux. Vesicoureteric reflux is associated with pyelonephritis, renal scarring, hypertension and renal failure and these associations may be prevented by medical treatment. Early screening for this reflux is recommended in families with other affected members.

Case-presentation

(S Feather)

A 5-year-old girl first presented in 1975 with an 18-month history of recurrent urinary tract infections. She was hypertensive. A micturating cystourethrogram indicated bilateral vesicoureteric reflux (VUR), and an intravenous urogram showed a small left kidney and bilateral cortical defects suggestive of pyelonephritic scars. Her glomerular filtration rate (GFR) was low (60/mL min^{-1} 1·73 m^{-2}; 80–120). She was treated with antihypertensive medications and prophylactic antibiotics.

By age 9 years her GRF had fallen to 30 mL/min^{-1} 1·73 m^{-2}). This decrease was attributed to further scarring of the renal parenchyma from recurrent pyelonephritis, which occurred despite antibiotics. Her blood pressure on antihypertensive treatment was controlled to within the normal limits for age, and no proteinuria was evident on dip-stick testing, so hypertension or glomerular scarring were unlikely explanations for the progressive renal failure. She underwent bilateral ureteric reimplantations and a subsequent micturating cystourethrogram showed no VUR.

Periodic reviews to age 24 years showed no further pyelonephritis; she had normal blood pressure on antihypertensives and her renal function was stable.

Our index case (figure 1, sibling 8) had 12 siblings. VUR and reflux nephropathy had already been diagnosed in an older sister (sibling 4) during investigation of a urinary tract infection at another hospital. The other 11 siblings, aged 1–15 years, were screened by micturating cystourethrography, and VUR was found in four (numbers 1, 6, 10, and 12). An older brother, at age 12 years, had cortical defects on ^{99m}Technetium-dimercaptosuccinic acid (DMSA) isotope renography (sibling 3); although these defects were consistent with a diagnosis of reflux nephropathy, VUR was absent on a mictruating cystourethrogram, and we surmise that VUR had regressed. Two of these siblings (3 and 10) had no history of urinary tract infection. All siblings with VUR were treated with prophylactic antibiotics, and none developed hypertension or renal impairment. The parents had no history of renal disease and their DMSA isotope renograms were normal; micturating cystourethrography was not done. The paternal grandmother died of uraemia and hypertension at age 61, but a primary renal diagnosis was not made. If we assume the grandmother also had VUR with nephropathy, the inheritance of this kindred is consistent with an autosomal dominant disorder with variable expression, as discussed below.

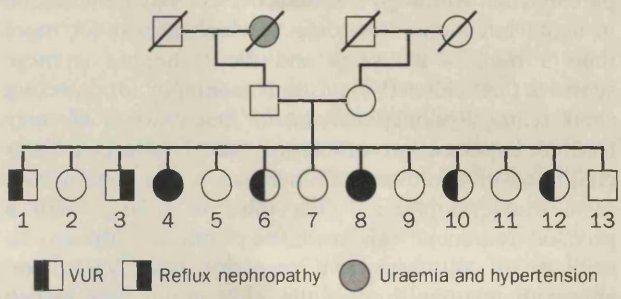

Figure 1: **Family tree**
Numbers under indiviudals refer to siblings discussed in the case history.

Radiological aspects of VUR

(I Gordon)

VUR is the retrograde passage of urine from the bladder into the ureter and in some cases the renal pelvis, calyces, and collecting ducts.[1] VUR can be secondary to high bladder pressure due to anatomical defects or lesions of the urethra (eg, urethral valves), or due to neurological

Lancet 1996; **348:** 725–28

Nephro-urology and Molecular Genetics Units (S Feather MRCP), **and Developmental Biology Unit** (A S Woolf MD), **Institute of Child Health, London WC1N 1EH, UK; Departments of Radiology** (I Gordon FRCR), **and Histopathology** (Prof R A Risdon FRCPath), **Hospital for Sick Children, London; and Department of Paediatric Nephrology, Cardiff Royal Infirmary, Cardiff** (K Verrier Jones FRCP)
Chairman of Grand Round: Professor Albert Aynsley-Green FRCP
Correspondence to: Dr Sally Feather

pathology (ie, neurogenic bladder). In primary VUR there is an anatomical defect at the junction of the ureter with the bladder.

The detection of VUR before toilet training requires that either a micturating cystouretherogram or a direct isotope cystogram be obtained, either of which require a bladder catheter. The radiation burden of a micturating cystourethrogram is an order of magnitude higher than that for an isotopic test. Micturating cystourethrography is the preferred initial investigation for a male child so that urethral defects causing secondary VUR can also be visualised. The direct isotope cystogram may be undertaken in girls and in follow-up of young boys.

If the child has been toilet-trained an indirect cystogram can be performed. This test follows excretion and passage of isotope through the urinary tract: it is physiological and does not require insertion of a bladder catheter.

The short-term variability of VUR is well recognised and does not seem to depend on either time of day or volume of urine voided. Additionally, VUR can regress during childhood. Reflux nephropathy describes renal scarring associated with VUR. DMSA renography is an isotopic technique which visualises functional parenchyma. Although transient defects may be observed in acute infections, new defects which persist for more than 3 months are scars and the technique is more sensitive than either IVU or ultrasonography for detecting small scars.[2] Pyelonephritis in the first years of life may lead to hypertension or chronic renal failure in later childhood or adulthood. Primary VUR can coexist with renal maldevelopment.[3] One third of infants with a prenatal hydronephrosis in whom, postnatally, there is no evidence of an obstructive uropathy, have VUR, and approximately one third of the VUR group have kidney malformations. If urinary tract infection occurs during the first year of life then there is a 70% risk of renal parenchymal disease occurring. Beyond this age development of macroscopic kidney scars after urinary tract infection is less common.[3]

Histopathology of VUR

(R A Risdon)

Reflux nephropathy describes renal scarring that may accompany VUR. It has been related to the extension of reflux into the renal collecting ducts (intrarenal reflux) which may cause scarring by its hydrodynamic effects alone or, in the presence of urinary tract infection, by allowing ingress of organisms into the renal parenchyma.[4,5] VUR has been diagnosed with increasing frequency in infants by fetal ultrasonography, showing hydronephrosis, and micturating cystourethrography soon after birth. VUR thus identified is more common in boys; reflux is often gross and bilateral; renal insufficiency is present at diagnosis in 20–30%, and the kidneys are small with smooth contours rather than segmentally scarred.[6] The evidence is compelling that kidney damage in these patients occurs before birth.

We conducted a histopathological survey involving children with gross primary VUR submitted to unilateral nephrectomy at the Hospital for Sick Children, London, between 1980 and 1992.[7] The indication for nephrectomy was little or no function of the affected kidney. Clinical data showed the remarkable male predominance (34 male, eight female). Segmental scarring was present in all

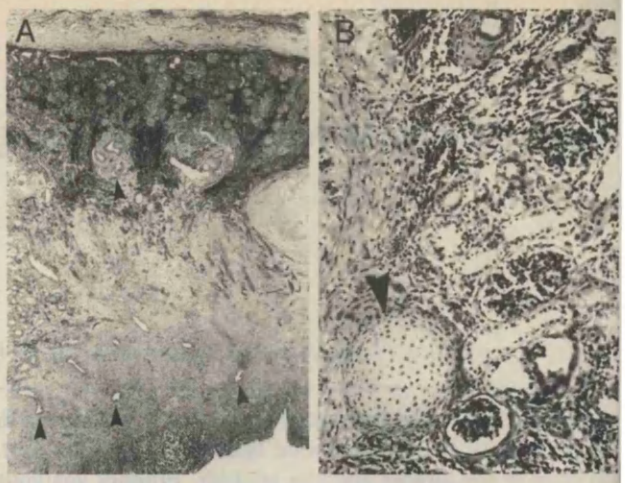

Figure 2: **Renal dysplasia associated with VUR**
Histology of a non-functioning kidney from a boy with VUR. **A** shows many dysplastic tubule malformations (arrowheads); **B** shows diagnostic metaplastic cartilage (arrowhead).

the girls and in 80% of the boys. In addition, there was evidence of kidney maldevelopment (renal dysplasia) in most of the boys (figure 2). Therefore, the renal damage associated with VUR ranges from the scarring acquired through intrarenal reflux and infection, to abnormal differentiation of the fetal kidney associated with intrauterine VUR. The renal dysplasia could be a direct harmful effect of prenatal reflux, or both the dysplasia and the reflux could be caused before birth by other processes.

Developmental biology of urinary tract malformations

(A S Woolf)

Renal development is orchestrated by the expression of transcription factors, growth/survival factors, and adhesion molecules. Mutations of genes encoding all classes of these molecules cause urinary tract malformations in mice.[8] The transcription factor proteins bind to and regulate the expression of other genes. One family of these proteins contains the paired DNA-binding domain and is encoded by the *PAX* genes, which show remarkable homology across evolution.[9] (*PAX* stands for 'paired box'. 'Paired' refers to the original member of the gene family which controls the development of paired segments in fruit fly embryos, and 'box' refers to a highly conserved part of the gene which encodes a protein sequence that binds to DNA.) Thus, *Drosophila PAX* genes control embryonic fruit-fly patterning (body segmentation) and cell specification (determination of the eye), while a zebrafish *PAX* gene controls retinal proliferation. Studies in mice show that *PAX* genes regulate the development of brain, eyes, lymphoid system, musculature, neural crest, and vertebrae. Human mutations of *PAX*-3 cause Waardenburg syndrome (white forelock, deafness and facial dysmorphism) and *PAX*-6 mutations cause aniridia, an eye malformation.[10]

The *PAX*-2 gene is expressed in the metanephros, the precursor of the adult kidney, in cell lineages that are forming nephrons, and also in those that are destined to differentiate into the ureter, renal pelvis and branching collecting duct system.[11,12] This gene is implicated in the genetic basis of VUR and the relation of VUR to kidney malformations. The ablation of a single *PAX*-2 allele in "knock-out" mice (animals in which a specific gene has

been replaced with a segment of non-coding DNA by the technique of homologous recombination, so that the original gene is functionally "knocked-out") causes impaired metanephric growth and fewer nephrons than normal, as well as megaureter, a finding consistent with gross VUR.[11,12] Of note, these animals are blind because of maldevelopment of the retina, another site of embryonic *PAX*-2 expression.[11] Thus, in mice this transcription factor is essential for growth of the prenatal urinary tract and eye. In contrast, the overexpression of *PAX*-2 is associated with renal epithelial overgrowth and the formation of cysts;[13,14] in that setting it acts like an oncogene.

Human genetics of VUR

(S Feather)

PAX-2 mutations also occur in humans, arising de novo or being inherited in an autosomal dominant manner.[15,16] These heterozygous mutations of the paired or octapeptide domains most likely result in haploinsufficiency—ie, a partial lack of functional protein. The mutations are associated with a syndrome involving eye malformations (optic nerve colobomas), VUR, and small, malformed kidneys. This genetic renal-coloboma syndrome in humans is therefore strikingly similar to the mouse *PAX*-2 mutations described above and can be added to a growing list in which human renal and urinary tract malformations are caused by defined mutations (panel).

What evidence is there that isolated primary VUR might have a genetic basis? This disorder often affects more than one family member[17] and there seems to be an autosomal-dominant pattern of inheritance. Thus, about 30% of the siblings of index cases are found to have VUR when screened by micturating cystourethrography before the age of 2 years,[18,19] whereas there is a risk of about 1 in 100 for VUR in children of individuals already known to have the condition.[20] Other screening studies have shown that VUR affects 1 to 2% of young children and, although we do not know whether all these cases are familial, VUR is probably one of the commonest genetic disorders to affect humans. We are assessing the family presented here for *PAX*-2 mutations by single-strand conformation polymorphism and DNA sequencing. VUR, however, may be genetically heterogeneous and a formal linkage approach may be required to analyse this family and the many other families seen at our institute.

Counselling for VUR

(K Verrier Jones)

VUR is usually diagnosed during the investigation of urinary tract infections. These infections in infants do not give rise to classic symptoms and signs seen in adults (such as dysuria, frequency, urgency) but are associated with non-specific signs such as fever, screaming, malaise, and failure to thrive.

The diagnosis is easily missed unless suspicion is high. When VUR is suggested by prenatal hydronephrosis,[21] the newborn infant should be given prophylactic antibiotics until definitive radiological studies have established whether VUR is present. Trimethoprim and nitrofurantoin are not licensed for use in neonates but have been used extensively without problems, provided jaundice is absent.

There are two aspects to consider when VUR is diagnosed in a child; first, the management of the index case, and second, the genetic and clinical implications for present and future family members. The kidneys are most at risk for scarring in the first years of life.[22,23] The risk of urinary tract infection is reduced by prophylactic antibiotics[24] and that risk of renal scarring can probably be reduced by prevention or early detection and prompt treatment of infection.[25] Antireflux surgery offers no improvement in outcome over medical strategies. Families who have experienced serious acute illness or hypertension and renal failure usually welcome the opportunity to have radiological screening of symptom-free siblings, and they are highly motivated to take prophylactic treatment.[26] Since reflux tends to improve or even disappear with time, it is impossible to be sure that an older sibling with negative radiological findings did not have VUR as an infant. Probably the older boy in figure 1 (sibling 3) is one such individual, because renal scarring was present in the absence of VUR. In future, the finding of a reflux gene may facilitate diagnosis in such individuals. Similar considerations apply to parents of index cases: here, we doubt whether the detection of VUR is of any clinical benefit because it is very unusual for urinary tract infections to cause renal scars in adults. Hence, the parents of the index case discussed here were not subjected to definitive radiological tests for VUR.

Panel: **Genetic basis of human kidney malformations**

Defined mutations

Renal-coloboma syndrome—VUR, renal hypoplasia, and colobomas (mutation of a transcription factor); autosomal dominant.[15,16]

Kallmann's syndrome—anosmia, infertility, and renal agenesis (mutation of a putative matrix molecule); X-linked.[27]

Zellweger syndrome—includes renal cystic dyplasia (mutation of a peroxisomal protein); autosomal recessive.[28]

Undefined mutations

Primary VUR—autosomal dominant.[17,20,21]

Branchio-oto-renal syndrome—neck cysts, deafness, kidney malformation; autosomal dominant.[29]

Isolated renal adyplasia—(ie, either incomplete differentiation of kidney, or tiny rudiment); autosomal dominant.[30]

Conclusion

Isolated primary VUR is an autosomal dominant disorder with incomplete penetrance and variable expression: the genetic defect or defects are unknown. Rarely, VUR can be inherited as part of a syndrome—eg, with optic nerve colobomas. In these cases mutations of *PAX*-2 have been defined. The long-term prognosis of primary VUR is determined by the presence and severity of associated renal disease, which is a spectrum of renal maldevelopment and pyelonephritic scarring. Given the high familial incidence of primary VUR, screening of young siblings of index cases is recommended. However, long-term follow-up studies are required to find out whether treatment of children with symptomless VUR detected by screening will reduce long-term morbidity

S F is supported by a training fellowship from Action Research, Vincent House, Horsham, West Sussex RH12 2DP, UK

References

1 Rushton B. Vesico-ureteral reflux and renal scarring. In: Holliday MA, Barrett TM, Avner ED, eds. *Paediatric Nephrology* (3rd ed) Baltimore: Williams and Wilkins, 1994: 963–86.

2 Elison BS, Taylor D, Van der Wall H, et al. Comparison of DMSA scintigraphy with intravenous urography for the detection of renal scarring and its correlation with vesicoureteric reflux. *Br J Urol* 1992; **69:** 294–302.
3 Gordon AC, Thomas DFM, Arthur RJ, Irving HC, Smith SEW. Prenatally diagnosed reflux: a follow-up study. *Br J Urol* 1990; **65:** 407–12.
4 Ransley PG, Risdon RA. Reflux and renal scarring. *Br J Radiol* 1978; suppl 14: 1–35.
5 Ransley PG, Risdon RA, Godley ML. High pressure sterile vesicoureteric reflux and renal scarring: an experimental study in the pig and minipig. In: Hodson CJ, Heptinstall RH, Winberg J, eds. *Contrib Nephrol* 1984; **39:** 320–43.
6 Rosenberg AR. Vesico-ureteric reflux and antenatal sonography. In: Bailer RR, ed. Proceedings of the 2nd C J Hodson symposium on reflux nephropathy. Christchurch: Design Printing Services, 1991: 1–2.
7 Risdon RA, Yueng CK, Ransley PG. Reflux nephropathy in children submitted to unilateral nephrectomy: a clinicopathological study. *Clin Nephrol* 1993; **40:** 308–14.
8 Woolf AS. Clinical impact and biological basis of kidney malformations. *Semin Nephrol* 1995; **15:** 361–72.
9 Gruss P, Walther C. Pax in development. *Cell* 1992; **69:** 719–22.
10 Read AP. Pax genes-*paired* feet in three camps. *Nature Genet* 1995; **5:** 333–34.
11 Keller SA, Jones JM, Boyle A, et al. Kidney and retinal defects (*Krd*), a transgene-induced mutation with a deletion of mouse chromosome 19 that includes the *Pax2* locus. *Genomics* 1994; **23:** 309–20.
12 Torres M, Gomex-Pardo E, Dressler GR, Gruss P. *Pax*-2 controls multiple steps of urogenital development. *Development* 1995; **121:** 4057–65.
13 Dressler GR, Wilkinson JE, Rothenpieler UW, Patterson LT, Williams-Simons L, Westphal H. Deregulation of *PAX*-2 expression in transgenic mice generates severe kidney abnormalities. *Nature* 1993; **362:** 65–67.
14 Winyard PJD, Risdon RA, Sams VR, Dressler GR, Woolf AS. The PAX2 transcription factor is expressed in cystic and hyperproliferative dysplastic epithelia in human kidney malformations. *J Clin Invest* (in press).
15 Sanyanusin P, Schimmenti LA, McNoe LA, et al. Mutations of the PAX2 gene in a family with optic nerve colobomas, renal anomalies and vesicoureteral reflux. *Nature Genet* 1995; **9:** 358–64.
16 Sanyanusin P, McNoe LA, Sullivan MJ, Weaver RG, Eccles MR. Mutation of *PAX2* in two siblings with renal-coloboma syndrome. *Hum Mol Genet* 1995; **4:** 2183–84.
17 Bailey RR. Vesico-ureteric reflux and reflux nephropathy. *Kidney Int* 1993; **44** (suppl 42): S80–85.
18 Noe HN. The long-term results of prospective sibling reflux screening. *J Urol* 1992; **148:** 1739–42.
19 Kenda RB, Fettich JJ. Vesicoureteric reflux and renal scars in symptomatic siblings of children with reflux. *Arch Dis Child* 1992; **6** 506–08.
20 Noe HN, Wyatt RJ, Peeden JN Jr, Rivas ML. The transmission of vesicoureteric reflux from parent to child. *J Urol* 1992; **148:** 1869–
21 Marra G, Barbieri G, Moioli C, Assael BM, Grumieri G, Caccamo ML. Mild fetal hydronephrosis indicating vesicoureteric reflux. *Arc Dis Child* 1994; **70:** F147–50.
22 Winberg J, Anderson HJ, Bergstrom T, Jacobson N, Larson H, Lincoln K. Epidemiology of symptomatic urinary tract infection in childhood. *Acta Paediatr Scand* 1974; **63** (suppl 252): 1.
23 Berg U, Johansson SB. Age as a main determinant of renal functio damage in urinary tract infection. *Arch Dis Child* 1983; **12:** 963–69.
24 Smellie JM, Katz G, Gruneberg RN. Controlled trial of prophylact treatment in childhood urinary tract infection. *Lancet* 1978; ii: 175–78.
25 Winberg J. Management of primary vesico-ureteric reflux in children—operation ineffective in preventing progressive renal damage. *Infect Immunol* 1994; **22:** S4–7.
26 Aggarwal VK, Verrier Jones K. Vesicoureteric reflux: screening of degree relatives. *Arch Dis Child* 1989; **64:** 1538–41.
27 Duke V, Winyard PJD, Thorogood PV, Soothill P, Bouloux PMG, Woolf AS. *KAL*, a gene mutated in Kallman's syndrome, is expres in the first trimester of human development. *Cell Mol Endocrinol* 19 **110:** 73–79.
28 Shimozawa N, Tsukamoto T, Suzuki Y, et al. A human gene responsible for Zellweger syndrome that affects peroxisome assemb *Science* 1992; **255:** 1132–34.
29 Heimler A, Lieber E. Branchio-oto-renal syndrome: reduced penetrance and variable expressivity in four generations of a large kindred. *Am J Med Genet* 1986; **25:** 15–27.
30 McPherson E, Carey J, Kramer A. Dominantly inherited renal adysplasia. *Am J Med Genet* 1987; **26:** 836–50.